

Tailoring the aroma of alcohol-free beer

Gernat, D.C.

DOI

[10.4233/uuid:17b768a1-940b-4e8e-80d1-365b89d20f49](https://doi.org/10.4233/uuid:17b768a1-940b-4e8e-80d1-365b89d20f49)

Publication date

2021

Document Version

Final published version

Citation (APA)

Gernat, D. C. (2021). *Tailoring the aroma of alcohol-free beer*. [Dissertation (TU Delft), Delft University of Technology]. <https://doi.org/10.4233/uuid:17b768a1-940b-4e8e-80d1-365b89d20f49>

Important note

To cite this publication, please use the final published version (if applicable).
Please check the document version above.

Copyright

Other than for strictly personal use, it is not permitted to download, forward or distribute the text or part of it, without the consent of the author(s) and/or copyright holder(s), unless the work is under an open content license such as Creative Commons.

Takedown policy

Please contact us and provide details if you believe this document breaches copyrights.
We will remove access to the work immediately and investigate your claim.

Tailoring the aroma of alcohol-free beer

Deborah Casandra Gernat



Tailoring the aroma of alcohol-free beer

Dissertation

For the purpose of obtaining the degree of doctor at Delft University of Technology by authority of the Rector Magnificus prof.dr.ir. T.H.J.J. van der Hagen chair of the Board of Doctorates to be defended publicly on 9th April at 10:00 o'clock.

by

Deborah Casandra GERNAT

Designer in Process Engineering, Delft University of Technology, The Netherlands,

born in Berlin, Germany

This dissertation has been approved by the promotor.

Composition of the doctoral committee:

Rector Magnificus,	chairperson
Assoc. Prof. dr. ir. M. Ottens	Delft University of Technology, promotor
Prof. dr. ir. L.A.M. van der Wielen	Delft University of Technology, promotor
Independent members:	
Prof. dr. E.J.R. Sudhölter	Delft University of Technology
Prof. dr. ir. H.J. Noorman	Delft University of Technology / DSM
Prof. dr. ir. C.G.P.H. Schroen	University of Wageningen
Prof. dr. M.H.M. Eppink	University of Wageningen / Byondis
Other members:	
Dr. E.R. Brouwer	Heineken Supply Chain B.V.

This research was funded by the Heineken Supply Chain B.V.

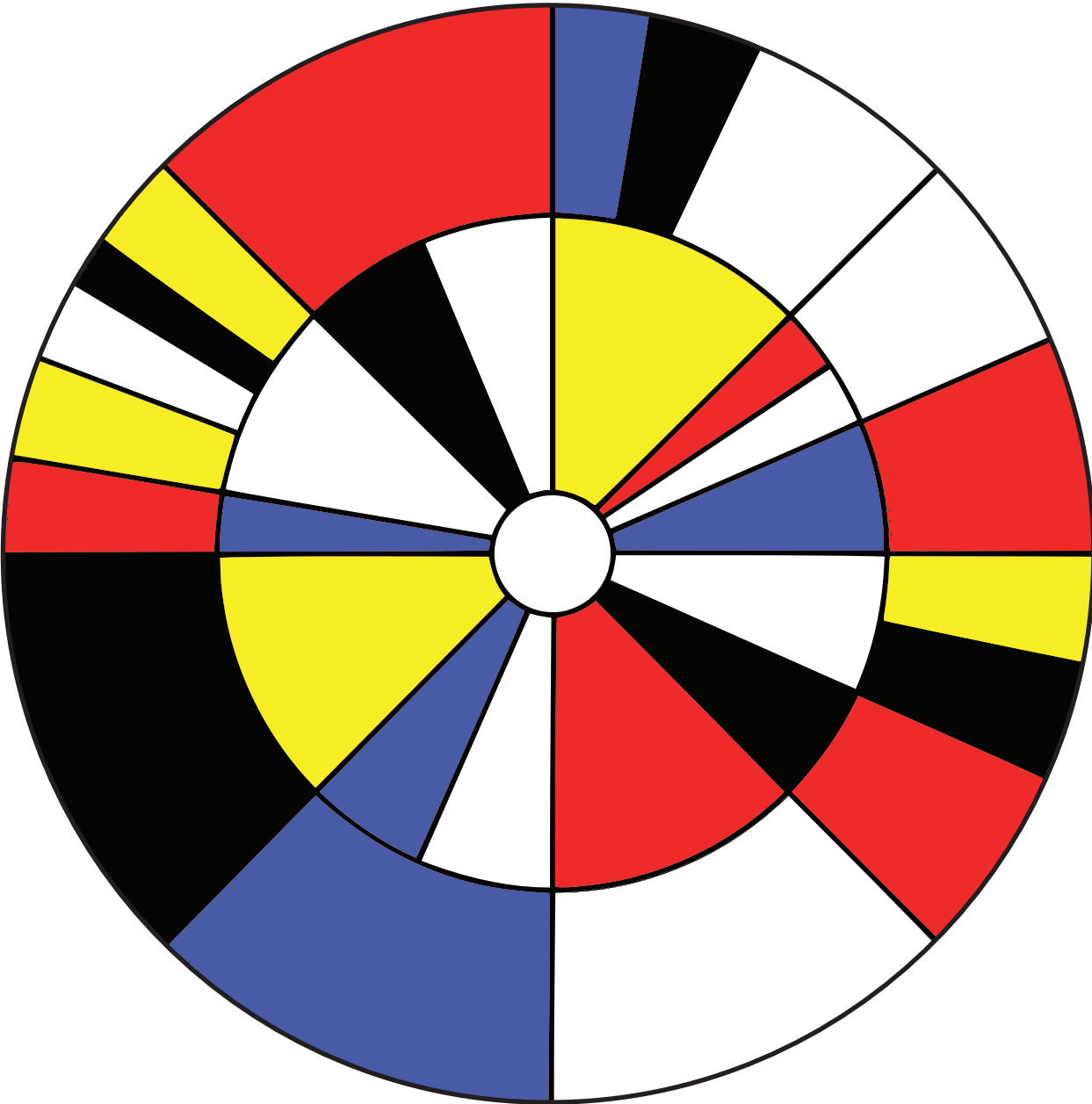
Coverart:	Deborah C. Gernat
Cover:	Ferdinand van Nispen, my-thesis.nl
Lay-out:	Ferdinand van Nispen, my-thesis.nl
Printing:	GVO drukkers en vormgevers, Ede

© 2021 Deborah C. Gernat, The Netherlands

All rights reserved. No part of this publication may be reproduced or transmitted in any form by any means, electronical, or mechanical, including photocopying, recording or otherwise, without the prior written permission of the copyright owner.

Table of Contents

Summary	7
Samenvatting	9
Chapter 1	
Introduction	15
Chapter 2	
Aldehydes as wort off-flavours in alcohol-free beers – origin and control.....	25
Chapter 3	
Simultaneous dealcoholisation and wort-flavour removal in alcohol free beers	67
Chapter 4	
Selective off-flavour reduction by adsorption: A case study in alcohol-free beer	85
Chapter 5	
Flavour-improved alcohol-free beer – quality traits, ageing and sensory perception	117
Chapter 6	
Mass transfer limitations in binderless ZSM-5 zeolite granules during adsorption of flavour compounds from aqueous streams	137
Chapter 7	
Prospect and Challenges for the Production of Flavour-Improved Alcohol-Free Beer	169
Chapter 8	
Conclusion and Outlook	191
Acknowledgments, List of publications & Curriculum Vitae	195
Appendix	203



Summary

The growing group of health-conscious consumers drives the development and sales in the market of low- or non-alcoholic beverages. In particular, sales in alcohol-free beer (AFB) has drastically gained in recent years, giving the incentive to further advance alcohol-free products. This thesis comprises the development of a new technology to produce an alcohol-free beer with an improved flavour, that is, an AFB with a significantly lower concentration in Strecker aldehydes. Despite the fact that Strecker aldehydes are present at trace concentrations of a few micrograms per litre, these compounds are majorly associated with the characteristic wort off-flavour in alcohol-free beer.

In the first stage, the origin of wort flavours is elucidated, and furthermore, the impact of the changed production process in comparison to regular beer and its resulting changes in the product is discussed. The most significant pathways of origin are the Maillard reactions and Strecker degradation, however, many other formation pathways have been suggested. While alcohol-free beers produced through regular fermentation and subsequent dealcoholisation are generally low in wort off-flavour, biologically produced AFBs exhibit a rather strong wortiness. This is because yeast's activity during the fermentation is restricted to prevent alcohol formation, having the side effect that other compounds such as aldehydes are not converted to neutral or characteristic beer flavours. As it is impossible to prevent the formation of wort flavour, selective removal is required to produce an alcohol-free beer with improved flavour profile (balance).

Subsequently, technologies applied to remove aldehydes from aqueous streams are investigated. Mechanisms that can be exploited for such removal are various – from separation based on size or volatility (distillation, pervaporation or membrane filtration) through sorption or conversion – past research has nearly studied all removal techniques available for aldehydes. However, most of the available techniques are not selective enough for a complex matrix such as beer, or not suitable for the application in the food industry. Nonetheless, adsorption is identified as the most promising technique to facilitate selective aldehyde removal.

As a benchmark system, a dealcoholisation plant (spinning cone column) is studied with special focus on wort flavour removal. While volatile aldehydes such as 3-methylbutanal can relatively easily be reduced, methional, having a high boiling point, is not sufficiently separated from the

end-product. Furthermore, due to the impact of heat, and ergo, the continuous formation and evaporation of these flavours, a plateau in their concentration is observed, where no further removal seems possible. This theory is proven by spiking a reactive sugar into the base and forming the mass balance over the system. Hence, in order to achieve a high reduction on high boiling wort flavours, another technology, such as adsorption, is required.

To test, whether a suitable adsorbent can be identified, a wide screening experiment covering three adsorbent types (amine-functionalized polymers, hydrophobic resins and zeolites) and a total of 21 materials is performed. ZSM-5 type zeolites prove to have a superior selectivity as well as a relatively high capacity compared to other adsorbents. The choice of the right pore size and hydrophobicity is crucial for the separation success. Adsorption of the compounds of interest is non-competitive within the design space and robust against small changes in the beer matrix. The process is transferred to pilot scale, where it is shown that the zeolite effectively reduces wort off-flavour while maintaining the original character of the beverage. The reduced wort flavour concentration is also maintained over a period of 4 months ageing. Interestingly, the formation rates of aldehydes related to ageing are similar for the treated and reference product, with the exception of trans-2-nonenal, which is manifold lower in the treated AFB. A trained sensory panel confirms the difference in taste for both, the fresh and the aged product.

In order to upscale this process to industrial scale, also the dynamics of the adsorption process on granular, binderless ZSM-5 zeolite is studied. The homogenous surface diffusion model is employed to regress the intraparticle diffusivity. The so obtained parameters indicate strong intraparticle mass transfer limitations as well as an inverse correlation of the effective diffusion coefficient to the molecules' hydrophobicity. To avoid this process bottleneck, material improvements such as smaller crystal size and smaller granules are recommended.

Finally, all obtained parameters are translated into a unit operation design. With a simple packed-bed operation of crushed particles, the production costs can be as much as 40 % lower than thermal dealcoholisation unit. Nonetheless, several assumptions still need to be verified, such as the material regenerability as well as other non- process-related factors such as material stability and food safety. Concluding, the newly developed technology for selective wort flavour removal in AFB in combination with restricted fermentation represents a great alternative to conventionally produced AFB.

Samenvatting

De groeiende groep gezondheidsbewuste consumenten stimuleert de ontwikkeling en verkoop van alcoholarme of niet-alcoholische dranken. Vooral de verkoop van alcoholvrij bier (AFB) is de laatste jaren drastisch gestegen, wat een stimulans geeft om alcoholvrije producten verder te promoten. Dit proefschrift omvat de ontwikkeling van een nieuwe technologie voor de productie van alcoholvrij bier met een verbeterde smaak, namelijk een AFB met een aanzienlijk lagere concentratie in Strecker-aldehyden. Ondanks het feit dat Strecker-aldehyden in zeer lage concentraties aanwezig zijn (enkele microgrammen per liter), zijn deze verbindingen in belangrijke mate verantwoordelijk voor de kenmerkende onaangename wortige bijmaak (*wort off-flavour*) in alcoholvrij bier.

Als eerste wordt de herkomst van deze wortsmaken opgehelderd. Bovendien wordt de *impact* van het veranderde productieproces voor AFB in vergelijking met gewoon bier besproken en de daaruit voortvloeiende veranderingen in het product. De belangrijkste herkomst van wortsmaken, naast vele andere, blijken Maillard reacties en de Strecker afbraakreactie. Alcoholvrij bier dat geproduceerd wordt door gewone fermentatie waarbij vervolgens de alcohol wordt verwijderd, bevat over het algemeen weinig wort smaak, terwijl biologisch geproduceerd AFB wordt gekenmerkt door een vrij sterke “wortigheid”. Dit ligt aan het feit dat de gistactiviteit tijdens de vergisting beperkt is om de vorming van alcohol te voorkomen, met als neveneffect dat aldehyden niet worden omgezet in meer neutrale dan wel karakteristieke biersmaken. Aangezien het onmogelijk blijkt om de vorming van wort-smaak te voorkomen, is een selectieve verwijdering van deze wort-smaak nodig om een alcoholvrij bier met een verbeterde en evenwichtige smaak te produceren.

Vervolgens worden huidige toegepaste technologieën om aldehyden uit waterige stromen te verwijderen onderzocht. De mechanismen die voor een dergelijke verwijdering kunnen worden gebruikt zijn divers - van scheiding op basis van grootte of vluchtigheid (destillatie, pervaporatie of membraanfiltratie) tot sorptie of conversie. In het verleden zijn bijna alle beschikbare verwijderingstechnieken voor aldehyden wel onderzocht. De meeste beschikbare technieken zijn echter niet selectief genoeg voor een complex mengsel zoals bier, of niet geschikt voor toepassing in de voedingsindustrie. Adsorptie wordt geïdentificeerd als de meest veelbelovende techniek om selectief aldehydes te verwijderen.

Als referentiesysteem wordt een dealcoholisatieinstallatie (*spinning cone column*) onderzocht met speciale aandacht voor de verwijdering van de smaak van het wort. Terwijl vluchtige aldehyden zoals 3-methylbutanal relatief gemakkelijk kunnen worden verwijderd, wordt methional, dat een hoog kookpunt heeft, onvoldoende gescheiden van het eindproduct. Bovendien wordt onder invloed van warmte, de continue vorming en verdamping van deze smaken een concentratieplateau van deze verbindingen waargenomen, waardoor geen verdere verwijdering mogelijk lijkt. Deze hypothese wordt bewezen door een reactief suiker molecuul in het mengsel toe te voegen en een massabalans daarvan over het systeem op te stellen. Om een significante reductie van hoogkokende wortsmaken te bereiken, is dus een andere technologie, zoals adsorptie, nodig.

Daarna wordt een breed *screening*sexperiment uitgevoerd met drie adsorptietypes (aminefunctionele polymeren, hydrofobe harsen en zeolieten) en een totaal van 21 materialen voor het vinden van een geschikt adsorbens. ZSM-5 zeolieten blijken een superieure selectiviteit en een relatief hoge capaciteit te hebben in vergelijking met andere adsorptiemiddelen. De keuze van de juiste poriegrootte en hydrofobiciteit is cruciaal voor een succesvolle scheiding. Adsorptie van de betrokken moleculen blijkt niet competitief binnen de onderzochte experimentele ruimte en is robuust voor kleine veranderingen in het biermengsel. Uitgevoerd op pilotschaal blijkt dat de zeoliet de wortsmaak effectief vermindert, met behoud van het oorspronkelijke karakter van het bier. De verminderde wortsmaak blijft behouden gedurende een periode van 4 maanden. Interessant is verder dat de vorming van aldehyden ten gevolge van veroudering vergelijkbaar is voor het behandelde en het referentieproduct, met uitzondering van trans-2-nonaal, dat in het behandelde AFB veel lager is. Het verschil in smaak wordt bevestigd door een getraind sensorisch panel voor zowel het verse als het verouderde product.

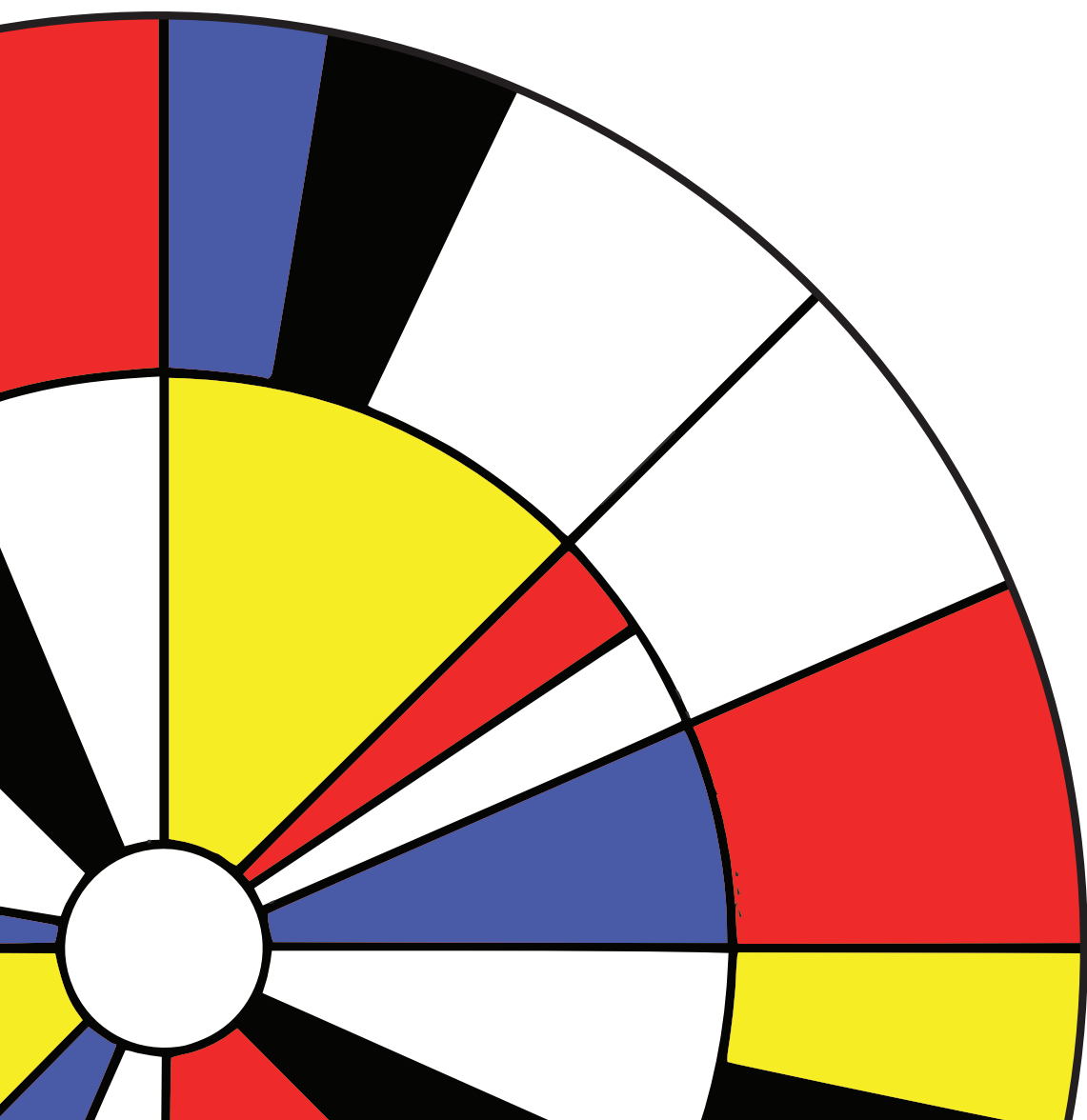
Om dit proces op te schalen naar industriële schaal wordt de dynamiek van het adsorptieproces met bindmiddelvrije ZSM-5 zeoliet korrels bestudeerd. Het homogene oppervlaktediffusiemodel wordt gebruikt om de diffusie in de deeltjes te bepalen. De aldus verkregen parameters wijzen op een sterke beperking van de interne massaoverdracht en een inverse correlatie van de effectieve diffusiecoëfficiënt met de hydrofobiciteit van de moleculen. Om dit knelpunt te omzeilen worden verbeteringen in het zeoliet materiaal voorgesteld, zoals kleinere kristallen en kleinere korrels.

Ten slotte wordt alle verkregen informatie vertaald naar een industrieel procesontwerp. Daaruit volgt dat een eenvoudig gepakt bed van geplette zeoliet deeltjes de productiekosten verlaagt tot 40 % t.o.v. een thermisch dealcoholisatie proces. Niettemin moeten verschillende veronderstellingen nog worden geverifieerd, zoals de regenereerbaarheid van het materiaal en andere niet-proces-gerelateerde factoren zoals de stabiliteit van het materiaal en de voedselveiligheid. Concluderend kan gesteld worden dat deze nieuw ontwikkelde technologie voor selectieve verwijdering van wortsmaak in AFB₁, in combinatie met een beperkte vergisting, een goed alternatief vormt voor conventioneel AFB₁ dat m.b.v. dealcoholisatie wordt geproduceerd.

Für meine Familie

*Es ist nicht genug zu wissen - man muss auch anwenden. Es ist nicht genug zu
wollen - man muss auch tun.*

Johann Wolfgang von Goethe



Chapter 1

1

Introduction

1.1. Background and aim

#dryjanuary, #dryfeb, #soberoctober are promoted throughout social media and an expression of a general development – consumers become more health-conscious and want to reduce their alcohol intake [1, 2]. Moreover, more and more studies show that consumption of alcohol, even in moderation, that is more than seven drinks weekly, can increase the risk for strokes, fatal aneurysms, heart failure and even death [3]. While sold volumes of regular beer have dropped in recent decades, the industry has long realised that the market of the future will look different. Figure 1.1 shows the market development of alcohol-free beer (AFB) of the last 9 years in the Netherlands – since 2010, the sold volume has increased more than fivefold [4]. While the market value in 2016 was estimated at 13.5 billion USD, it is expected to grow to more than 25 billion USD by 2024 [5].

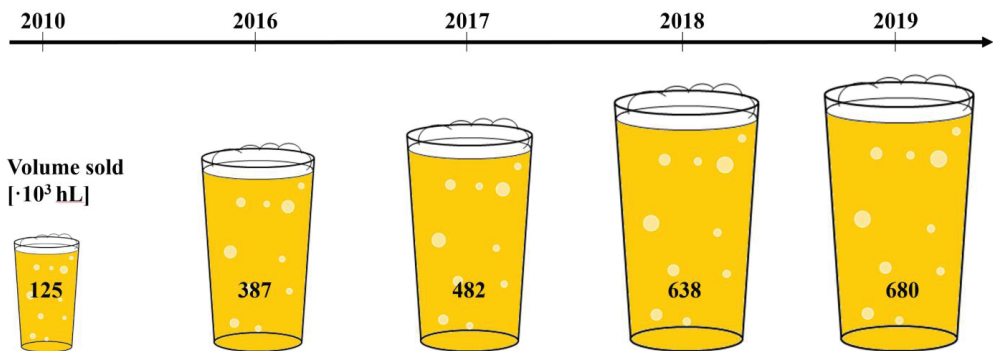


Figure 1.1: Volume of alcohol-free beer sold in the Netherlands between 2010-2019

And indeed, alcohol-free beer has the potential to replace the occasional “after-work-beer”. Recent studies found that the reward reaction of the human brain during consumption is the same, indifferent from the fact a beer contains alcohol or not [6]. However, there is still a clearly perceivable difference between a regular and an AFB [2, 7, 8]. The “taste gap” between regular and alcohol-free products still prevents many consumers from choosing the healthier alternative. According to a national study of Dutch consumers, for 69 % of the population, taste

is the most important factor to choose a beer [9]. As depicted in Figure 1.2 regular beer is characterized by its fruity and floral notes, majorly originating from ester compounds, as well as a well-defined bitterness and a warming mouthfeel from the solvent effect of ethanol. Only very subtle notes of wort flavour are perceivable. On the contrary, AFB exhibits different sensory defects, such as a watery mouthfeel, a high sweetness or intense wort flavour, as a result of their divergent production process [2].

Commercial technologies available for producing AFBs are based on either physical removal of ethanol by thermal separation under vacuum or by membrane technologies. Different equipment is available [7]. Their working principle, characteristic product profile and associated qualitative production costs are compiled in Table 1.1. The advantages of physical dealcoholisation techniques include:

- 3.2 Complete alcohol removal possible
- 3.3 Alcohol can be marketed as a valuable side-product
- 3.4 Continuous and automated operation with a short start-up time
- 3.5 Flexibility with respect to capacity and inlet composition of the feed stream

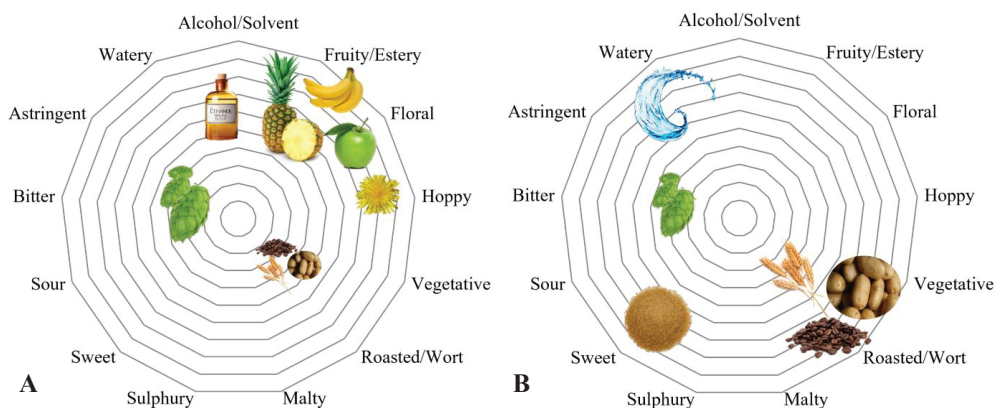


Figure 1.2: Sensory profile of a regular beer (A) and an AFB (B)

Generally, reasonable good quality products are produced through dealcoholisation. However, an incentive to develop new production methods for alcohol-free beer is the fact that physical dealcoholisation methods, require a high initial and high in operational cost due to the high energy requirements. Furthermore, beverages from dealcoholisation can lack body and liveliness and thus appears watery [2, 7]. Biological produced beers, on the contrary, are cheap in production, since no additional investment in equipment is needed and have very low operational costs, as fermentation times are often shorter. Here, ethanol is not removed from

the beverage, but rather its formation is prevented through a reduced metabolism of the yeast. As a result, AFBs produced through these methods exhibit a highly over-pronounced wort flavour, which is not appreciated by consumers, and due to the lack of fruity esters and ethanol as well as the sweetness of the unfermented sugars, it can be even more enhanced by [10-12]. Improving the taste of such biologically produced AFBs has a great potential to reduce costs and the environmental impact on the production of such beverages.

Previous work has identified the major compounds responsible for such wort flavour are aldehydes, in particular, Strecker aldehydes, which are derived from a heat-induced reaction of a reducing sugar and an amino acids [13]. 2- and 3 methylbutanal, methional and 2-methylpropanal, depicted in Figure 1.3 are recognized as the most dominant wort flavours, but other compounds are involved as well [10-12]. For the purpose of this work, also furfural is considered. Although at typical concentrations in AFBs it is not an off-flavour, furfural is a common indicator for heat-induced reactions [14].

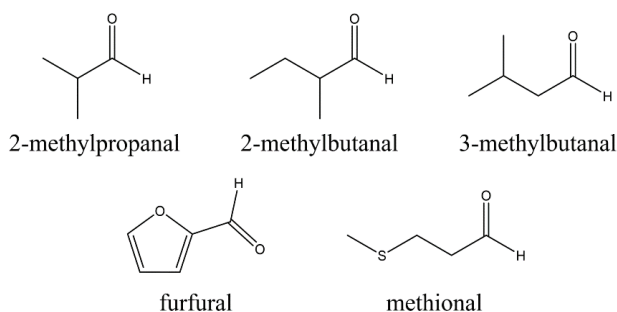


Figure 1.3: Aldehydes associated with wort flavour or heat indicator

It is thus the aim of this work to narrow the taste gap by developing a novel technology to improve the flavour profile of alcohol-free beers and tackle the tricky task of selective wort off-flavour removal to produce a flavour-improved AFB. In the following, an outline on the thesis and its chapter is provided.

1.2. Thesis outline

The **first chapter** briefly introduces the problem of a non-optimal flavour profile in alcohol-free beverages. Hereby, the scope and outline of the thesis are presented. The **second chapter** provides an overview of the current production method(s) and related flavour defects. In particular, the origin and chemical pathways of wort flavour compounds are introduced and the impact of alcohol-free beer composition on the perception of wort off-flavours is treated.

Furthermore, the status-quo in the brewing industry is presented and literature is screened for existing solutions for selective removal techniques. The chapter concludes with the recommendation of suitable separation techniques to facilitate selective off-flavour removal.

Chapter 3 studies exemplarily the spinning cone column as a thermal dealcoholisation system, to simultaneously produce alcohol-free beer and reduce wort flavour. The impact of the stripping rate on the flavour profile (aldehydes, diketones and esters) is presented, as well as the addition of sugar modifiers. The thermal impact on the product is analysed by making the mass balance over the system. The aim is to show, whether thermal methods are suited to reduce the wort flavour.

With the knowledge of **chapter 2 and 3**, an adsorptive capturing step is suggested in **chapter 4** to selectively remove all key wort flavours from alcohol-free beers. Therefore, 3 different types of adsorbents (in total 21 different adsorbents) are screened and the best performing adsorbent type identified. These materials are consequently studied to obtain multicomponent isotherms (mixture amount design). By varying the matrix composition the robustness of the derived model is shown. A proof of principle is provided in **chapter 5** by transferring the process to pilot-scale. The quality traits, sensory perception and ageing behaviour of the flavour-improved beverage are subsequently investigated.

Chapter 6 dives into the topic of mass transfer in complex aqueous media. The main focus is to identify the most suitable mass transfer model and obtain the required parameters (e.g. diffusion coefficients). The diffusivities of the key wort compounds are measured in a model solution, mimicking viscosity, pH and temperature of AFBs. Furthermore, the bottleneck in the mass transfer process is identified with batch uptake experiments.

Table 1.1: Comparison of different production methods for alcohol-free beer with respect to working principle, product quality and production costs

Method	Equipment and working principle	Product quality	Production costs (qualitative)
Thermal dealcoholisation	1. Continuous vacuum rectification system (Schmidt® SIGMATEC Dealcoholisation Systems): Vacuum evaporation by rectification (multistage distillation)	Great loss in flavour and liveliness / Trade-off between ethanol content and flavour loss 4. Degree of flavour loss is dependent on degree of dealcoholisation. 5. The profile of remaining flavours is moreover highly unbalanced. The retained higher alcohols in the product consist of 97 % of 2-phenylethanol [7, 17], which has a characteristic floral odour [18].	8. Medium for very low alcohol concentrations (<0.05 vol. %) due to high initial investment costs and energy consumption [16] [16, 20]
	2. Spinning Cone Column (Flavourtech): Counter-current vacuum steam stripping enhanced by rotation of the inverted cones [15] 3. Falling film evaporator (GEA): Thin film is created by gravity while flowing down downward along steam-heated tube walls at boiling temperature, the liquid stream is partially evaporated under vacuum [16].	6. As vacuum is applied, the impact of thermal stress is considered negligible in literature. Compounds indicative for alteration through thermal stress such as hydroxyl-methyl-furfural or furfural serve as heat indicators [7, 19]. 7. Acetaldehyde-bisulphate can thermally degrade to acetaldehyde [16], creating an off-flavour in the final product.	9. Alcohol can be marketed as a side product
Dealcoholisation through membrane techniques	Reverse osmosis 10. Cross-flow filtration employing semi-permeable membrane 11. Transmembrane pressure > osmotic pressure resulting in separation of ethanol against osmotic pressure. Dialysis 12. Selective diffusion of small molecules through semi-permeable membrane [21]	Loss in aroma and liveliness 13. Less thermal impact on product stream, but small molecules such as CO ₂ , water and flavours also pass through the membrane [22] [23]	14. High for low alcohol concentration 15. Fouling of membranes may increase costs additionally 16. Claimed to be economically unfeasible for product streams with <0.45 vol. % ethanol [24]
Biological: Limited, continuous fermentation with immobilized yeast	17. Immobilized yeast strains are cultivated in specialized reactors under stress conditions, which limit the cell metabolism 18. Only a fraction of the contained sugars is metabolized, resulting in low ethanol concentrations (<0.08 %) [25]	Imbalanced Flavour profile 19. Depending on the fermentation parameters (aeration, residence time, temperature) and the selected yeast strain, the product composition can be controlled [26] 20. Achieving the correct balance of sensory compounds in the short time is still difficult; higher concentrations of diacetyl and aldehydes have been observed, while ester concentrations remain relatively low	21. Low, although specialized equipment and process optimization is required [7] 22. Yeast cells alter over time due to ageing effects, which exacerbates process control [27]
Biological: Cold contact fermentation	23. Wort is pitched with yeast cells at 2-4°C 24. Alcoholic fermentation is suppressed while allowing for (some) metabolic formation of flavour compounds [28]	Worty off-flavours and unbalanced flavour profile 25. Due to the low metabolic activity of the yeast, worty aldehydes such as methional remain above the sensory threshold, resulting in an unbalanced taste experience [28].	26. Low, if carried out in batch [7]

With findings from **chapter 4 and 6**, an overall process model is constructed in **chapter 7**. Having studied the system in detail, a scaled-up unit operation is proposed which circumvents limitations in the mass transfer as much as possible. Thereby, different unit operation configurations are analysed, including simple sludge batch operation to semi-continuous periodic counter-current chromatography.

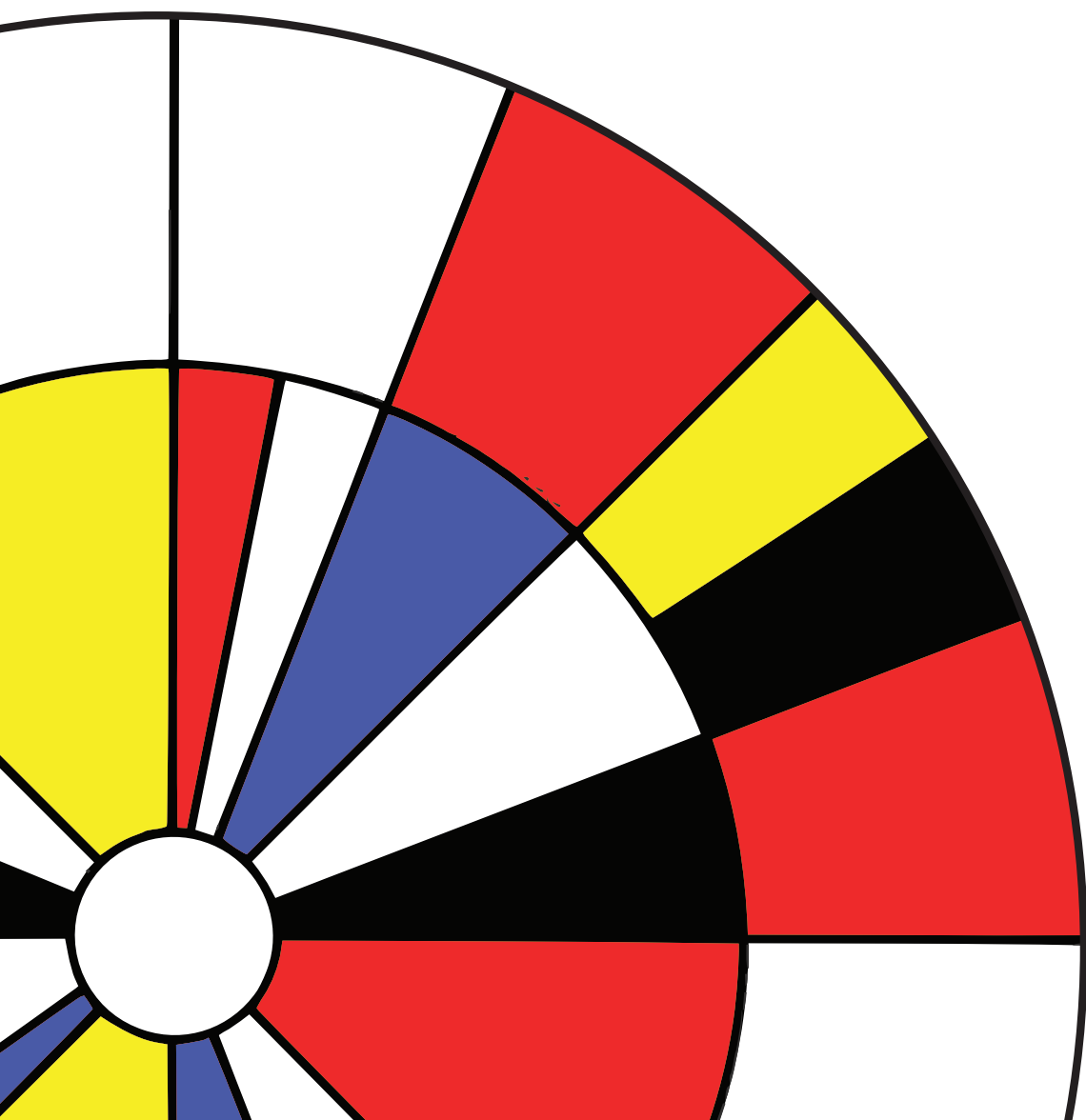
Chapter 8 summarizes the key findings of the thesis, concludes scientific and practical relevance and gives an outlook to future research.

1.3. References

1. Liguori, L., et al., Chapter 12 - Production of Low-Alcohol Beverages: Current Status and Perspectives, in Food Processing for Increased Quality and Consumption, A.M. Grumezescu and A.M. Holban, Editors. 2018, Academic Press. p. 347-382.
2. Blanco, C.A., C. Andres-Iglesias, and O. Montero, Low-alcohol Beers: Flavor Compounds, Defects, and Improvement Strategies. *Crit Rev Food Sci Nutr*, 2016. 56(8): p. 1379-88.
3. Wood, A.M., Kaptoge, S., Butterworth, A.S., Willeit, P., Warnakula, S., Bolton, T. et al, Risk thresholds for alcohol consumption: combined analysis of individual-participant data for 599 912 current drinkers in 83 prospective studies. *The Lancet*, 2018. 391(10129): p. 1513-1523.
4. NederlandseBrouwers, Kerncijfers Nederlandse Brouwers. 2010-2019.
5. Ahuja, K.R., A., Non-alcoholic beer market analysis report 2024. 2019, Global market insights. p. 600.
6. Smeets, P.A.M. and C. de Graaf, Brain Responses to Anticipation and Consumption of Beer with and without Alcohol. *Chemical Senses*, 2018. 44(1): p. 51-60.
7. Brányik, T., et al., A review of methods of low alcohol and alcohol-free beer production. *Journal of Food Engineering*, 2012. 108(4): p. 493-506.
8. Mangindaan, D., K. Khoiruddin, and I.G. Wenten, Beverage dealcoholization processes: Past, present, and future. *Trends in Food Science & Technology*, 2018. 71: p. 36-45.
9. De Jongh, J., Geerlings, N., Tramper, A., Nationaal bieronderzoek 2019, N. Brouwers, Editor. 2019, Ruigrok Net Panel.
10. Piornos, J.A., et al., Orthonasal and retronasal detection thresholds of 26 aroma compounds in a model alcohol-free beer: Effect of threshold calculation method. *Food Res Int*, 2019. 123: p. 317-326.

11. Beal, A.D. and D.S. Mottram, Compounds contributing to the characteristic aroma of malted barley. *Journal of Agricultural and Food Chemistry*, 1994. 42(12): p. 2880-2884.
12. Gijs, L., et al., 3-Methylthiopropionaldehyde as Precursor of Dimethyl Trisulfide in Aged Beers. *Journal of Agricultural and Food Chemistry*, 2000. 48(12): p. 6196-6199.
13. Baert, J.J., et al., On the origin of free and bound staling aldehydes in beer. *J Agric Food Chem*, 2012. 60(46): p. 11449-72.
14. Saison, D., et al., Contribution of staling compounds to the aged flavour of lager beer by studying their flavour thresholds. *Food Chemistry*, 2009. 114(4): p. 1206-1215.
15. Craig, A.J.M., Improved gas-liquid contacting device and method. 1986, Google Patents.
16. Zufall, C. and K. Wackerbauer, Verfahrenstechnische Parameter bei der Entalkoholisierung von Bier mittels Fallstromverdampfung und ihr Einfluss auf die Bierqualität. *Monatsschrift für Brauwissenschaft* 2000. 53(7-8): p. 124-137.
17. Narziss, L., W. Back, and S. Stich, Alcohol removal from beer by countercurrent distillation in combination with rectification (written in German). *Bierwelt* 1993. 133(38): p. 1806-1820.
18. Baker, A.K. and C.F. Ross, Wine finish in red wine: The effect of ethanol and tannin concentration. *Food Quality and Preference*, 2014. 38: p. 65-74.
19. Kern, M., Alcohol removal from beer using continuous vacuum refinement (written in Spanish). *Alimentacion Equipos y Tecnologia*, 1994. 13(5): p. 37-41.
20. Perretti, G. and P. Fantozzi. Brewing process study for high quality low-alcoholic beer. in *EBC Brewing Science Group 10th Technical Meeting*. 2014. Wien.
21. Petkovska, M., I. Leskošek, and V. Nedović, Analysis of Mass Transfer in Beer Diafiltration with Cellulose-Based and Polysulfone Membranes. *Food and Bioproducts Processing*, 1997. 75(4): p. 247-252.
22. Catarino, M., et al., Alcohol Removal From Beer by Reverse Osmosis. *Separation Science and Technology*, 2007. 42(13): p. 3011-3027.
23. Moonen, H. and H.J. Niefind, Alcohol reduction in beer by means of dialysis. *Desalination*, 1982. 41(3): p. 327-335.
24. Pilipovik, M.V. and C. Riverol, Assessing dealcoholization systems based on reverse osmosis. *Journal of Food Engineering*, 2005. 69(4): p. 437-441.
25. Iersel, M.F.M., et al., Continuous production of non-alcohol beer by immobilized yeast at low temperature. *Journal of Industrial Microbiology*, 1995. 14(6): p. 495-501.

26. Lehnert, R.N., Pavel; Macierira, F.; Kurec, M.; Teixeira, J.; Branyik, T., Optimization of Lab-Scale Continuous Alcohol-Free Beer Production. *Czech J. Food Sci.*, 2009. 27(4): p. 267-275.
27. Brányik, T., et al., A Review of Flavour Formation in Continuous Beer Fermentations*. *Journal of the Institute of Brewing*, 2008. 114(1): p. 3-13.
28. Parker, D.K., 6 - Beer: production, sensory characteristics and sensory analysis A2 - Piggott, John, in *Alcoholic Beverages*. 2012, Woodhead Publishing. p. 133-158.



Chapter 2

Aldehydes as wort off-flavours in alcohol-free beers – origin and control

2

Abstract: Although present in concentrations in microgram per litre level, aldehydes, in particular those derived from Strecker degradation, are known to majorly contribute to the undesired wort flavour of alcohol-free beers. In order to improve currently available products, one needs to understand the underlying cause for the over-prevalence and identify leverage points and methods to selectively reduce the aldehydes in alcohol-free beers. This work gives a short overview on relevant flavour active wort flavours identified in alcohol-free beer, and on their involved chemical formation pathways. Consequently, aldehyde removal technologies in general and in brewing industry are presented. Adsorptive removal of off-flavours by aldehyde scavenging groups is already widely exploited in the packaging industry and may achieve reduction of these components to near depletion, depending on the process conditions. Its principles are adaptable to recovering off-flavours before filling. Also, supercritical CO₂ extraction has been successfully applied to separate flavours from food matrices. In brewing, the focus has been set to biologic conversion by restricted fermentation steps, but the reduction of key components of more than 70 % is not achieved. Newer developments focus on thermal separation techniques that not only include non-specific physical dealcoholisation, but also more selective technologies such as pervaporation, where aldehydes are reduced to near depletion. However, for most unit operations selectivity and capacity are not yet investigated. Future research should explore the shortcomings of current techniques and overcome bottlenecks either by developing more specific methods for aldehyde removal and/or a clever combination of unit operations to optimize the separation and process integration.

Published as: Gernat, D.C., Brouwer, E. & Ottens, M. Aldehydes as Wort Off-Flavours in Alcohol-Free Beers—Origin and Control. Food Bioprocess Technol 13, 195–216 (2020).

2.1. Introduction

Current market trends show that consumers are shifting more and more to a health-conscious life-style [1] causing a continuous gain in sales of alternatives such as alcohol-free beers (AFBs) over the past years. As a result, there is a strong interest of the beverage industry in low-alcoholic and alcohol-free products [1, 2]. The definition of alcohol-free and non-alcoholic beers differs significantly between countries. While in the UK only beverages with an alcohol content of less than 0.05 vol.% fall under this category, other European countries such as Germany allow beverages to contain up to 0.5 vol.% of alcohol [3]. In the United States there is a clearer separation between “alcohol-free”, meaning no alcohol contained and “non-alcoholic” beer, where the upper limit is 0.5 vol.% [4]. In this review the term “alcohol-free” is utilized.

Yet, the overall flavour and taste associated with AFBs is not comparable to its alcohol containing equivalent [5]. Market studies conducted in the Netherlands, for instance, show that out of the population of Dutch consumers whom do not consume non-alcoholic beverages, 60% state the sensorial defects as the reason [6]. Constituents of beer are numerous, amongst others it contains higher alcohols, esters, aldehydes, lactones, carboxylic acids and phenols, which contribute to the overall flavour of the drink [7, 8]. In alcohol-free products, worty flavours are often considered over-pronounced. This perception is closely related to an elevated beer aldehyde content and results in an inferior sensory experience compared to a regular drink [3].

The objective of this review is to give an overview on wort off-flavour profiles in AFBs and the underlying formation processes of aldehydes during brewing and downstream processing. Furthermore, aldehydes with the highest impact on taste perception are identified and the influence of the beer matrix constituents on sensory perception evaluated. In the second part of the review, a summary on current general removal technologies and state-of-the art in the brewing industry is given and future research opportunities highlighted.

2.2. Aldehydes as flavour active components in (alcohol-free) beer

2.2.1. Relevant flavour active aldehydes in beer

Flavour profiles of alcoholic and AFBs are complex [9]. A broad outline of most relevant flavour active aldehydes in beer extracted from literature is given in Table 2.1. The list comprises 11 molecules, yet, most persistent and outstanding wort off-flavours are 3-methylbutanal (3-MB), 2-methylbutanal (2-MB) [10] and methional [11], where methional has

with 4.2 ppb the lowest sensory threshold in beer amongst the three [12]. 2-MB is often characterized as malty or almond like, while 3-MB also exhibits a chocolate character.

Table 2.1: Summary of relevant flavour active aldehydes, their sensory threshold in beer [12, 16] and sensory descriptor [12-14, 17, 18]

Name (group)	Threshold [$\mu\text{g/L}$]	Description
Acetaldehyde	1114 -25000	<ul style="list-style-type: none"> Green apple, fruity
2-methylpropanal (Strecker aldehyde)	86 ¹ – 1000	<ul style="list-style-type: none"> Produced through Strecker degradation of valine or oxidative degradation of isohumulones (hops component) Grainy, varnish, fruity
2-methylbutanal (Strecker aldehyde)	45– 1250	<ul style="list-style-type: none"> Produced through Strecker degradation of isoleucine or in presence of oxygen Almond, apple-like, malty
3-methylbutanal (Strecker aldehyde)	56 ¹ – 600	<ul style="list-style-type: none"> Produced through Strecker degradation of leucine or in presence of oxygen Malty, chocolate, cherry, almond
Hexanal (linear aldehyde)	88 -350	<ul style="list-style-type: none"> Product from fatty acid oxidation Green, grassy
Methional (Strecker aldehyde)	4.2 -250	<ul style="list-style-type: none"> Produced through Strecker degradation of methionine Cooked potatoes, warty
Phenyl acetaldehyde (Strecker aldehyde)	105 -1600	<ul style="list-style-type: none"> Produced through Strecker degradation of phenyl alanine Hyacinth, flowery roses
Trans-2-nonenal (linear aldehyde)	0.03 - 0.11	<ul style="list-style-type: none"> Reaction between heptanal and acetaldehyde or auto- / enzymatic oxidation of linoleic Cardboard, papery, cucumber
Benzaldehyde (aromatic aldehyde)	515 – 2000	<ul style="list-style-type: none"> Produced in presence of oxygen Almond, cherry stone
Furfural (heterocyclic aldehyde)	15 000 ¹ -150 000	<ul style="list-style-type: none"> Product of Maillard and caramelisation reaction (heat indicator) Indicator of flavour instability in beer Caramel, bready, cooked meat
5-hydroxy-methyl- furfural (heterocyclic aldehyde)	35784 ¹ -1000000	<ul style="list-style-type: none"> Product of Maillard reaction and caramelisation Bready, caramel

¹ odour threshold

The flavour of methional is related typically to a wort character and the smell of cooked potatoes [12-14]. Often synergistic effects are observed. Currently, it is assumed that the unpleasant taste of AFBs results from the synergic interaction of 2- and 3-MB to sulphur containing degradation products of methional [15].

2.2.2. Chemistry of aldehydes in (alcohol-free) beers

Aldehyde formation in beer involves different substrates and mechanisms and mainly occurs during wort mashing and boiling [15, 19]. The most important pathways are: 1. Oxidation of unsaturated fatty acids by enzymatic oxidation, autoxidation and photo-oxidation, 2. Maillard reactions, 3. Strecker Degradation, 4. Degradation of bitter acids, 5. Aldol condensation, 6. Melanoid-catalysed oxidation of higher alcohols, 7. Secondary autoxidation of aldehydes, 8. Aldehyde secretion by fermenting yeast [13]. Out of these, the most relevant mechanisms for the formation of 2- and 3-MB and methional dominant in alcohol-free products are further explained in the paragraphs below.

Maillard reactions or also called non-enzymatic browning reactions summarize all reactions of amines, amino acids, peptides or proteins with a reducing sugar. The reactions typically take place at temperatures above 50°C and a pH range of 4-7. Therefore, they are usually correlated with the application of heat and visible by a change in colour. Due to the complexity of possible reactions the variety of Maillard products in beer is versatile and their chemical properties divers [20, 21]. The most important aldehydes formed through these reactions in beer production are furfural (FF) and 5-hydroxymethylfurfural (5-HMF), which serve as markers for the heat load impact on the mash, wort and beer [9, 22-24]. Their formation pathways are shown in Figure 2.1. The carbonyl group of an aldose (pentose in case of FF, hexose in case of 5-HMF) reacts with an amine or amino group of an amino acid, peptide or protein to an imine, also called Schiff base. At beer pH (around 4.0 – 5.0) [25], the chemical equilibrium favours the formation of 3-deoxyosone by elimination of a proton and an amine. Ring formation through condensation reaction then results eventually into the typical Maillard products FF (from pentose) and 5-HMF (from hexose) [13, 26].

Strecker degradation is defined as the heat-induced reaction of an α -dicarbonyl or hydroxycarbonyl, such as glyoxal, methylglyoxal, diacetyl or 3-deoxyosone [27, 28], with an amino acid according to the general mechanism outlined in Figure 2.2-A [29]. In the first step of the reaction, an unstable hemiaminal is formed by the nucleophilic addition of the unprotonated amino group to the carbonyl group. The reversible elimination of water and

consequent irreversible decarboxylation results in the formation of an imine zwitter ion. The addition of water yields an amino alcohol, which in turn degrades into an α -ketoamine and the so called “Strecker aldehyde” [13, 30, 31].

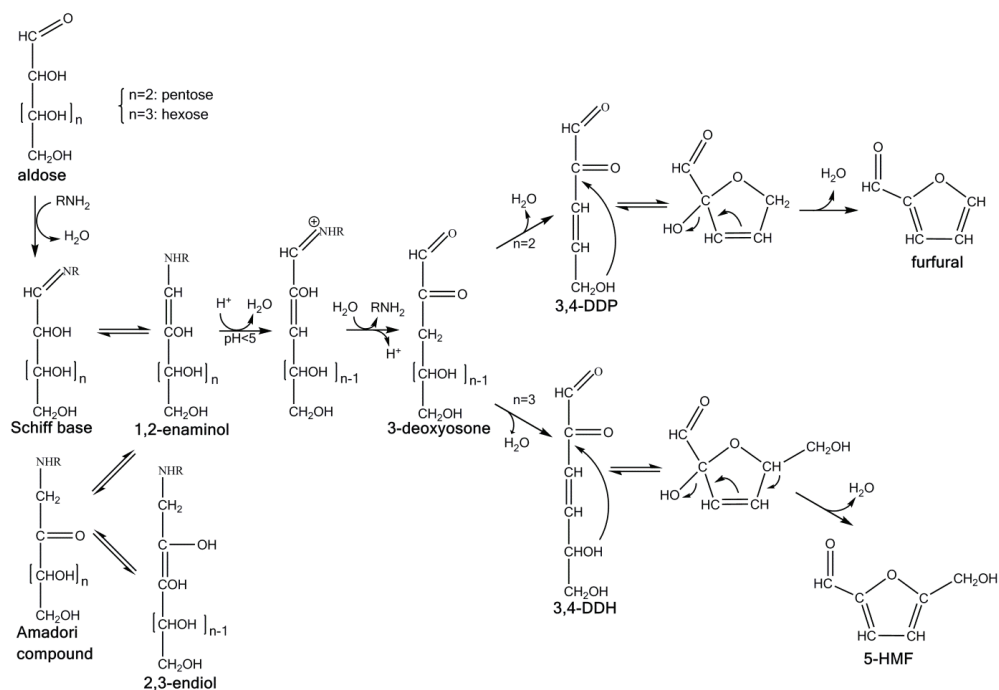


Figure 2.1: Overview on Maillard reactions leading to the formation of FF and 5-HMF [13, 26]

Strecker degradation is generally thought to be related to the chemistry of reducing sugars. During the Maillard reaction the Schiff base can rearrange to the a so-called Amadori product [31-33] as shown in Figure 2.1, which then degrades to the α -dicarbonyl component [21]. However, it has been shown that other reactive carbonyls such as lipid derived carbonyls or quinones from polyphenol oxidation also contribute to the formation of Strecker aldehydes [30, 34-36]. When testing the capacity of 20 phenolic derivatives to form Strecker-type degradation products of phenylalanine and phenylglycine methyl ester, results indicated that polyphenols are potent to induce the reaction in absence of added oxidants [36]. One mechanism proposed for the formation of Strecker aldehydes in presence of reactive carbonyls derived from lipid oxidation is shown in Figure 2.2-B. The reaction is initiated by the formation of an imine from the amino acid and the reactive carbonyl under elimination of water. After consequent decarboxylation due to an electronic rearrangement, the molecule forms a second imine, which then hydrolyses to the Strecker aldehyde. The “by-product” of this reaction in turn is unstable and initiates further reactions with amino acids [37].

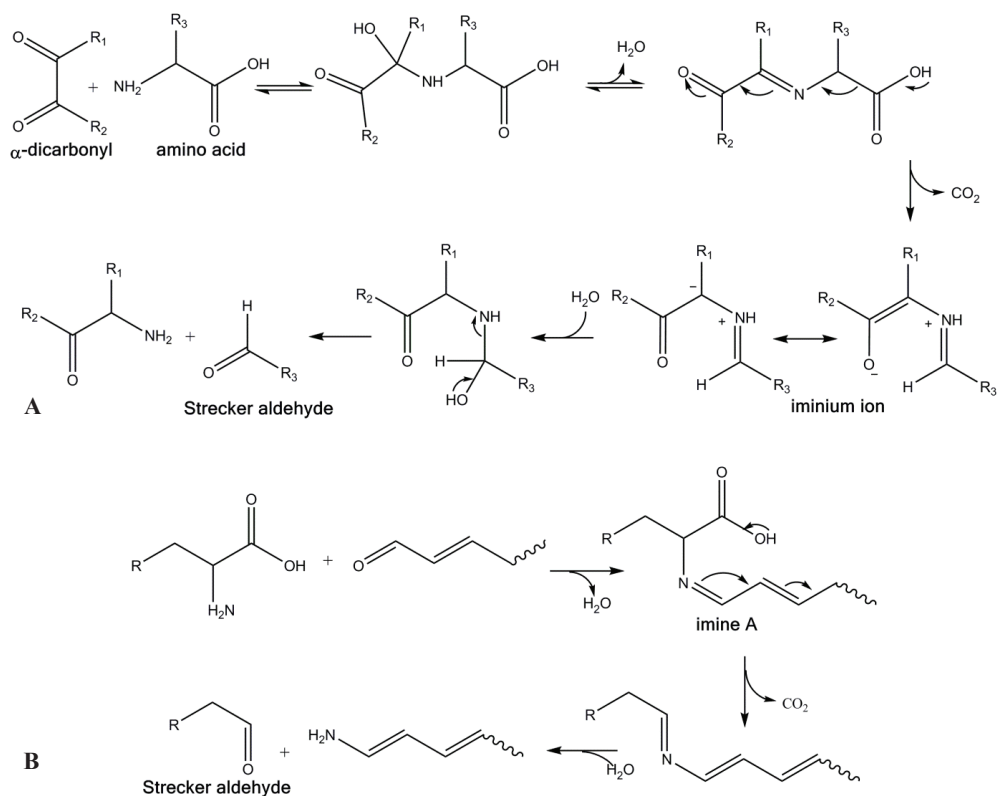


Figure 2.2-A: General formation mechanism of Strecker aldehydes from an amino acid and α -dicarbonyl group [13, 29]; B: Proposed mechanism of formation of Strecker aldehydes from amino acids in presence of lipid-derived reactive carbonyls [37]

The above overview on Strecker aldehyde formation in beer is only a rough insight on involved reactions and pathways. Kinetic modelling of the involved reaction during wort boiling has been attempted, but it is still in its infancy [38].

2.2.3. Origin of aldehyde formation during regular and alcohol-free beer brewing

The common cause of the different composition and hence taste of AFBs is the deviating brewing process of AFBs compared to regular beer. Figure 2.3 provides an overview on the simplified brewing process of regular beer and the related change in aldehyde content in the product. During the brewing process, the most significant change in wort flavour concentration is observed in mashing, fermentation and maturing [39], but some formation of the compounds already occurs during kilning in the malting step [40]. Thereby, the heat subjected to the grains to stop the germination process induces Maillard reactions, caramelisation, Strecker degradation as well as fatty acid oxidation. After malting, the grist is added to the mash mixer

and combined with the brewing liquor. Consequently, a well-defined mashing procedure is followed, where the enzymatic conversion of polysaccharides to short sugars takes place. In parallel, aldehydes are again formed through the head-induced Maillard reactions, caramelisation, Strecker degradation and oxidation of fatty acids. In the following step of wort boiling, the hop is added and contained α -acids are isomerized. Due to the high heat input, the same heat-induced reactions take place, but at the same time, the formed flavours are evaporated and therefore removed from the wort. In the consequent fermentation, yeast metabolizes the fermentable sugars in the wort as well as most aldehydes to their respective alcohol [39, 41]. The final product contains only very small amounts of wort flavour.

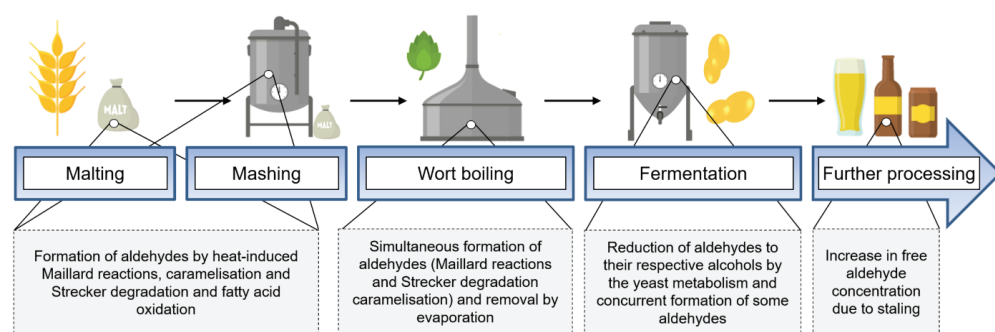
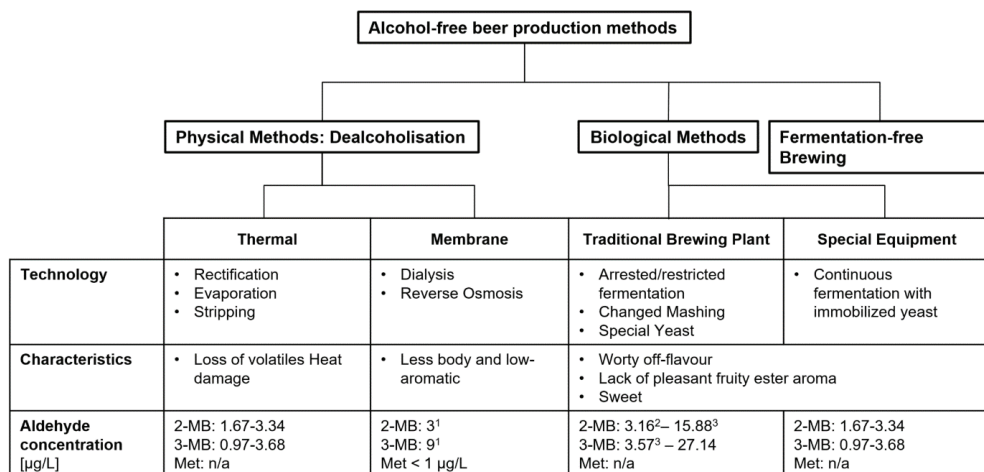


Figure 2.3: Overview on simplified brewing process and the related impact on the aldehyde concentration

For the production of AFBs, several process strategies are pursued. These include biological methods such as fermentation-free brewing, dilution, restricted alcohol fermentation and physical dealcoholisation techniques like thermal or membrane technologies. An overview on employed production technologies and their respective aldehyde levels is given in Figure 2.4 [3, 5].

While physical methods include a regular fermentation and the downstream removal of the produced alcohol, the biological methods follow the strategy of restricting ethanol production during fermentation, allowing for flavour development and off-flavour removal to a certain extend. These fermentations can be carried out in batch or continuous operation. Different practices are under investigation and proposed in the literature. The most common methods include the cold contact procedure, arrested fermentation, the usage of special yeast strains [4] and the reduction of fermentable fractions to non-fermentable fractions by a changed mashing process [42]. Physical methods fall into two categories, which are thermal dealcoholisation methods and membrane-based dealcoholisation technologies. Thermal dealcoholisation

systems include evaporators, rectification units and stripping columns. Membrane-based separations use the principle of dialysis or reverse osmosis, but are currently developing in the newer applications of pervaporation [3] and osmotic distillation [43].



¹close to detection limit of applied technique; ²short fermentation; ³special yeast

Figure 2.4: Schematic classification of AFB production methods adapted from Brányik et al. and Sohrabvandi et al.[3, 5, 44], characteristics [15] and respective levels of relevant aldehydes [14]

As diverse as the production processes known for brewing AFB, are the related organoleptic defects of AFBs [3]. A major problem in dealcoholized beers described in literature is that during the process, not only ethanol is removed, but also aroma compounds, which contribute to the organoleptic characteristics of the beer. Thereby, the ester and higher alcohol content is strongly affected. The highest loss is observed for thermal dealcoholisation techniques, while membrane-based processes have the lowest reduction in volatile aromas compared with the original [3]. Furthermore, if thermal methods of dealcoholisation are applied, alternation by the impact of heat can occur, causing the appearance of heat-induced off-flavours such as 5-HMF or FF. Beverages produced by restricted fermentation or complete elimination of the fermentation process often exhibit an unpleasant taste of sweet wort due to the fact that yeast cannot sufficiently reduce the high aldehyde concentration in the wort at given operating conditions [4]. Other process alternatives such as dealcoholisation by gas desorption [45], extraction with supercritical CO₂ or adsorption with silica gels have been developed, but are of no industrial relevance [44].

2.2.4. Impact of alcohol-free beer composition on the perception of wort off-flavours

At a closer look, the problem is not only the loss of flavour, but also the loss of balance in the flavour profile of the beer [3, 46] and the change in the composition of the beer matrix. Consequently, even if the same exact composition of aroma active compounds in the AFB as in the original could be achieved, the beer would still have an unbalanced taste. This is caused by the change in the thermodynamic properties of the beer matrix [47, 48]. Literature provides thresholds for the perception of worty off-flavours for regular beer. However, it has been proven that these thresholds do not hold for an AFB matrix due to three effects:

- 1) The absence of ethanol as a matrix component increases the polarity of the matrix and hence results in an increased partition coefficient for more nonpolar aldehydes. If compared, the retention of aldehydes in regular beer ranges between 32-39%, while a non-alcoholic beer of 0.5 vol.% could only retain 8-12% of measured aldehydes [3, 49]. Because most flavour molecules are detected by the nose, the taste of a beverage results primarily from its vapour phase [50]. Thus, the increased volatility of aldehyde causes the worty character in AFBs to be over-pronounced, which consequently causes a poor taste experience [15, 49].
- 2) The absence of positive flavours such as esters and higher alcohols in AFB leads to a more pronounced perception of the worty aroma. Fruity esters have been shown to have a significant masking effect for wort flavours in beer, i.e. on addition of an extra amount of 300 ppb isoamyl acetate, the flavour threshold of 2-MB and methional in regular beer increased by 250% and 40%, respectively [12].
- 3) The presence of higher concentrations of monosaccharide sugars typically observed in AFBs causes a “salting out” effect for aldehydes from the beer matrix, which leads to a further increase in the perceived wort flavour. In a sensory evaluation of a model AFB, methional could be detected by 80% of the test panel at concentrations as low as 0.1 ppb [49]. Although this value is not a sensory threshold for AFB, it is an indication for the fact that methional can be perceived at significantly lower concentrations than its sensory threshold of 4.2-250 ppb for regular beer stated in literature [12, 16].

Besides these three factors, other matrix components influence the retention of aldehydes in beer. Studies suggest that polyphenols, such as catechin impact the volatility of esters, but also aldehydes [51, 52]. The decrease in the activity coefficients of isoamyl acetate, ethyl hexanoate and benzaldehyde at a catechin concentration of 10 g/L was observed to be 10-15% [52].

Typically, catechin and epicatechin concentrations in beer are found to be below 10 mg/L [53], but can reach up to 30 mg/L [54]. Hence, in this case the impact of catechin on aldehyde perception is at this concentration insignificant, however, other polyphenols might have a more pronounced effect. Furthermore, it is known that amino acids can readily bind aliphatic aldehydes. In particular cysteine is involved in the formation of thiazolidine carboxylic acids [55, 56]. Baert et al. (2015) showed that aldehydes in beer tend to form adducts with cysteine and bisulphite at beer pH [57, 58]. Consequently, two strategies can be pursued to decrease the perception of worty off-flavours.

2.3. Methods of (selective) aldehyde removal

The complex nature of aldehyde chemistry implies that removing educts such as methionine from the feedstock would decrease the concentration of the corresponding aldehyde to an extent, but will possibly not bring the desired reduction in aldehyde concentration. The following paragraphs will thus rather focus on scouting technologies for the direct removal of aldehydes. When targeting the aldehyde off-flavours the challenge lies in choosing for a high selectivity over other beer constituents thus preserving the natural nutritional value and taste of an AFB [44]. Figure 2.5 shows possible mechanisms to accomplish a selective removal of aldehydes from AFBs.

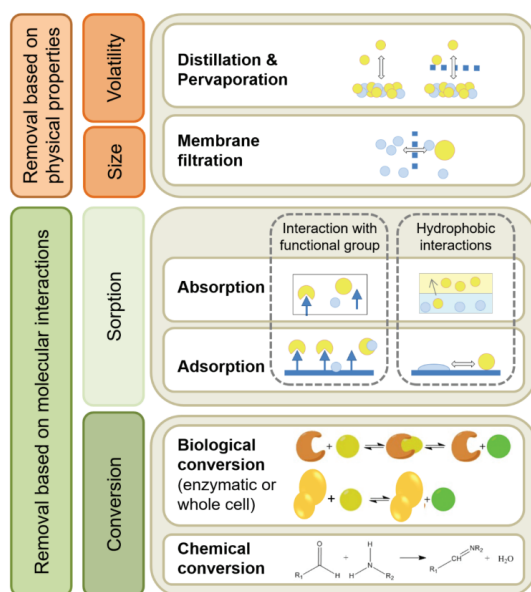


Figure 2.5: Possible mechanisms for the removal of aldehydes from AFBs

The removal can either be based on physical properties of the molecules, such as size and volatility, or based on interactions with other molecules and surfaces, where the selectivity is defined by the specificity of the interaction. Through a thorough study of state-of-the-art in literature, patented technologies for aldehyde removal and the status-quo in brewing industry in this work, technologies making use of the removal mechanisms were compiled as depicted in Figure 2.6 and analysed for their selectivity in the following paragraphs.

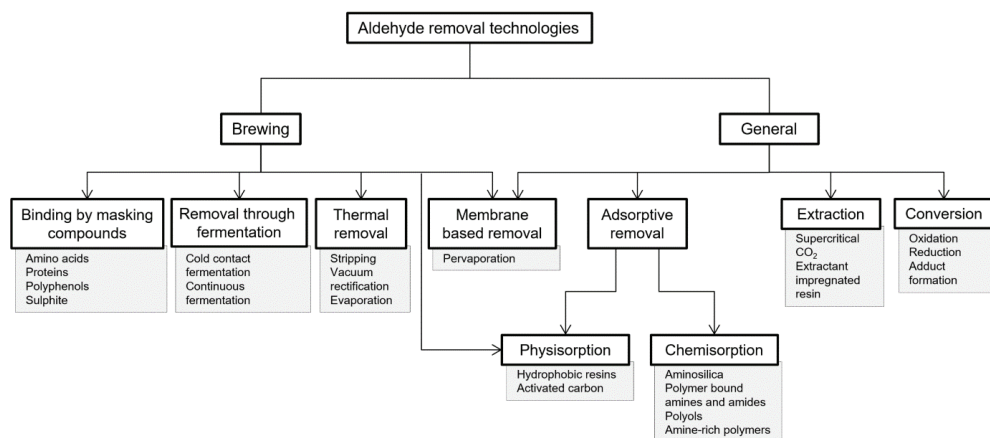


Figure 2.6: Overview on existing removal technologies for aldehydes

2.3.1. General technologies for aldehyde removal

Adsorptive removal: Physisorption on hydrophobic resins and activated carbon

One molecular property often exploited e.g. in pharmaceutical industry for separation of proteins and antibodies is the hydrophobicity of a compound [59]. Since aldehydes such as FF can act as fermentation inhibitors, its removal from biomass hydrolysate by adsorption on the polymeric resins Amberlite XAD-4 and XAD-7 and its desorption by elution with ethanol was studied. Results showed XAD-4 performed superior to XAD-7, which is explained by the higher hydrophobicity of the polystyrene-divinylbenzene copolymer of XAD-4, when compared to the methacrylate backbone of XAD-7. At a temperature of 30°C the FF concentration could be reduced by factor 100-500, from 1-5 g/L to 0,01 g/L and desorption was proven to be feasible with ethanol [60]. In a similar context the removal of FF and HMF from a biomass hydrolysate by Amberlite XAD-8 was measured. After one hour of incubation (8.0 g of resin in 50 ml hydrolysate), the remaining amount of aliphatic acids, HMF, FF, phenols and ketones was determined. The FF concentration was reduced to 35-41% of the initial concentration. The reduction of HMF showed to be dependent on the pH. The reduction was

found to be 20% and 42% at pH 5.5 and 10.0, respectively [61]. This might be due to the fact that the removal of phenols is more efficient at lower pH, leaving less capacity for HMF.

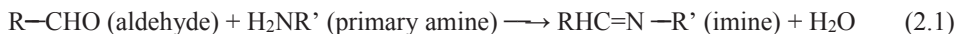
In another lab scale experiment, Amberlite XAD-2 and XAD-4, were compared with the adsorption behaviour of adsorbent manufactured through post-polymerization crosslinking of swollen chloromethylated gel-type and macroreticular copolymers of styrene and divinylbenzene. For the tests, FF uptake from an aqueous solution was studied. The researchers found that the microporous structure of the self-manufactured resin was superior for removing FF at low concentrations (< 2 wt.%), however due to the higher surface area, the macroporous adsorbent XAD-4 was performing more efficiently at higher FF concentrations [62]. The kinetics and impact of several experimental parameters on FF adsorption on activated carbon (AC) in aqueous phase was investigated by Sahu *et al.* (2008). The removal step was found to follow pseudo-second-order kinetics and showed optimal performance at pH 5.9 and an adsorbent dosing of 10 g/L solution. The experimental data could be best characterized by the Redlich-Peterson isotherm model [63].

Hydrophobic resins and AC have also been objective of research for applications in food and beverage industry [64-70]. For instance the selective recovery of key aroma compounds from roasted coffee was investigated for quality optimisation of the final product. FF and ethyl acetate were adsorbed from supercritical CO₂ on AC and the impact of process parameters was studied. The adsorption showed to be dependent on processing temperature and CO₂ density [69]. A similar study was conducted by Canteli *et al.* (2014) to investigate the fixed-bed adsorptive removal of the coffee flavour benzaldehyde from an aqueous solution with granular AC [71]. A comparison of two hydrophobic resins with AC was conducted to test the feasibility of recovering microbiologically produced volatile aroma compounds from off-gas streams during a fermentation. The experiments were carried out at lab- and semi-pilot scale. Major volatiles identified during the experiments were ethanol, acetaldehyde (AcA), ethyl acetate, ethyl propionate and isoamyl acetate. AC, Tenax-TA, and Amberlite XAD-2 were tested to evaluate their suitability for recovering aromas from the gaseous stream. While the AC exhibited poor recovery, the Amberlite XAD-2 resin adsorbed all components present in the headspace. Interestingly, Tenax-TA showed a higher selectivity for AcA over contained esters and ethanol [68]. In a recent study of Müller-Maatsch *et al.* (2019), the removal of glucosinolates and volatiles, e.g. aldehydes, from an anthocyanin-rich extract of red cabbage was investigated. From the studied adsorbent and flocculants (Amberlite XAD 16 HP, polyamide, chitosan, and lignosulfonate), Amberlite, chitosan and lignosulfonate, reduced the

aldehyde content. However, also other molecules such as fatty acids, sulphides, glucosinolates and the isothiocyanates were taken up [72].

Adsorptive removal: Chemisorption on aminated materials

Amine groups are known to form bonds with aldehydes. The so called imine formation shown in equation 2.1 [73] is particularly favoured at pH 4-5 [74], therefore, this system is well applicable to beer or wort feedstock.



Aminosilica resins have been utilized to remove aldehydes from complex mixtures. A study of Drese et al. (2011) tested solid aminosilica adsorbents, namely pore-expanded SBA-15 functionalized with 3-aminopropyltrimethoxysilane, 3-(2-aminoethyl)aminopropyltrimethoxysilane and 3-[2-(2-amino-ethyl)aminoethyl]aminopropyltrimethoxysilane, on a model solution (“bio-oil”) of phenols, cyclohexane, hexanol, aldehydes, ketones and diketones. Light alcohols were not investigated in these experiments as they are considered non-reactive with aliphatic amines. The adsorption showed to be selective for aldehydes and some ketones and the adsorbent capacity increased with primary amines content and increasing temperature [75]. This is expected as imine formation occurs only with primary amines and the reaction is preferred at higher temperature. The selectivity of aldehydes over ketones can be explained by the fact that aldehydes are considerably more reactive than ketones [76]. The reactivity of aldehydes with aminosilica depends strongly on their chemical functionality, but for all tested aldehydes at least moderate removal was achieved. Partial resin regeneration was proven to be feasible by acid hydrolysis of the adsorbent, however, resulted in a significant loss in reactivity [75].

A similar principle is exploited in US patent 7041220 B2 “Method of use for aldehyde removal” in which a solid surface with a primary amine function is used as an adsorbent to remove environmentally hazardous aldehydes such as ortho-phthalaldehyde from waste water streams. Solid surfaces include silica, but also polymer linked systems. Different aldehyde scavengers can be attached to the solid surface. The extended chain length of the amine bearing residual may help to decrease steric hindrance in particular for voluminous aldehydes. On the contrary, if smaller aldehydes are targeted, a short chain length increases the selectivity for low-molecular compounds. Depending on the scavenger properties, different aldehydes are targeted. The patent does not give indications for recycling the adsorption material and furthermore mentions that during the aldehyde removal process, if executed with silica, also other compounds are

removed by means of hydrogen bonding principles or physical filtration mechanisms. Besides attaching scavengers to polymeric backbones, polymeric amino-group rich systems such as chitosan can be made of use for aldehyde removal [73]. Chitosan is a naturally occurring amine-rich polymer generally regarded as safe (GRAS) by the U.S. Food and Drug Administration [77], which has been found to react according to equation 2.1 with aldehydes to form imines [78].

One more application of aminosilica is the improvement of air quality by removing volatile organic compounds such as airborne formaldehyde [79-83]. The first patent was filed by Gesser in 1985 [84, 85], but since then many others have followed [79, 86]. Zhu et al. (2012) functionalized uniform mesoporous silica SBA-15 with N-(2-aminoethyl)-3-aminopropyl]-trimethoxysilane and found the so obtained adsorbent to have a good chemoselectivity for formaldehyde [80]. When systematically investigating the adsorption of airborne aldehydes on aminosilica resins, it was found that the resin capacity was related to the structure of the amine moieties as well as the site density. Primary amines showed to be the most potent aldehyde adsorbent for AcA, hexanal and formaldehyde from air. Aminosilica with a primary amine function showed an around 2-fold higher loading for form- and AcA compared to secondary amine functionalized aminosilica. The capacity for hexanal, however, was only increased by 14%. It is speculated that this can be explained by the slower diffusion of hexanal into the functional material. In the studies performed, it was found that most formaldehyde was adsorbed within the first hour, while AcA and benzaldehyde took more than ten hours [79]. Furthermore, it was observed that there is an optimal amine loading for maximising the (gaseous) formaldehyde adsorption. Medium loaded aminosilica are most effective as at higher loadings steric hindrance is suspected to counteract efficient imine formation [79, 87].

Another potent aldehyde scavenger employed as abatement of indoor pollutants is polyamine polyethylenimine (PEI) [84, 85, 88]. Yet, the compound finds vast application in other fields. PEI is employed in active materials in food packaging in order to enhance food freshness [89]. DuPont patented PEI as an aldehyde scavenger resin in US 5413827, which can be incorporated in the packaging material as cap liner, sticker or package insert. An outer material such as high density polyethylene fibres are permeable for aldehydes at a desired rate and enclose the aldehyde scavenger module. PEI is preferably not heavily branched and has a low percentage in tertiary amines. The molecular structure of the aldehyde scavenger is $H-(CH_2-(CH_2)_n-NH)_m-H$, where n equals most preferably 1 and m is bigger than 100 [89, 90]. The authors do not give an explanation for the underlying mechanisms, but the study of the sorption kinetics of

hexanol performed by DelNobile *et al.* (2002) suggest that “the sorption process of hexanal in the investigated aldehyde scavenger film could be described in terms of the hypothesized “sorption-reaction” mechanism” [91].

The compound is furthermore described as by-product adsorber for oxygen scavenging packaging material systems in US patent 5942297, but the invention also includes other polymeric amines such as polymers and copolymers of allylamine (or diallylamine), vinyl amine and vinyl pyridine and chitosan [92]. In a similar invention (US 6057013) the use of pentaethylene hexamine, triethylene tetraamine, and polyvinyl oxazoline for aldehyde scavenging is patented [93].

Another effective aldehyde scavenger type frequently used in packaging industry is polyamides. Amides are long known to react with aldehydes in a condensation reaction [94-96], but depending on the conditions applied, the reaction of aldehydes with amides can result in numerous products [97]. In order to reduce by-products, in particular AcA, from ozonated water during storage in the bottle, a functional material consisting of a polyester/polyamide blend for lessening the concentration of AcA is described in US patent 6042908 [98]. The mechanism is believed to be the formation of an imine as described in equation 2.1 [89]. A series of aldehyde scavengers was tested for the application of capturing AcA from the gas phase on a beverage bottle. Anthranilamide, anthranilic acid and AC achieved a reduction of up to 98% when compared to the control sample, however, selectivity is not discussed [99].

An effort of producing such a polyamides resin at low-cost to capture aldehydes and ketones was made by de Oliveira *et al.* (2015). The authors synthesized the isoniazid-functionalized resin Amb15-iso by reacting commercially available Amberlyst 15 with isoniazid, which is an antibiotic commonly used in the treatment of tuberculosis. Its performance was tested for acetone and isobutyraldehyde in different solvents. The overall amount of ketone removed increased with increasing polarity of the solvent and the adsorption was hence best in water. The resin showed to be more efficient for the removal of isobutyraldehyde than for acetone, where the maximum removal was 80% after less than 20 min in ethanol and hexane. The trend of increasing removal efficiency with increasing polarity could only partially be reproduced for the aldehyde and water could not be tested as a solvent due to the low miscibility of isobutyraldehyde. The resin was shown to be reusable at least for a second cycle of adsorption [100].

In the field of organic chemistry a separation medium was developed to particularly target aromatic aldehydes, comprising polymer-supported benzylhydrazines to react according to

equation 2.1 [101]. Organic chemists also studied a copoly(styrene-divinylbenzenesulfonylhydrazine) resin containing the chemical functional group of sulphonamides, which was characterized and tested for scavenging aldehydes, ketones and glucose in water. These molecules are presumably bound by forming the corresponding sulfonylhydrazone derivatives. For ketones it was observed that the extend of the reaction depended on the molecular size, ranging from >90% for small ketones to less than 2% for bulky ones such as camphor. The reaction products could be displaced by the addition of pyruvic acid [102]. Polystyrene-based sulfonylhydrazine resin was also proposed as adsorbent to remove impurities from a pharmaceutical product. At a phase ratio of 50 the achieved aldehyde reduction amounted to 85% without adding additional impurity to the product [103].

Similarly, a polystyrene resin functionalized with sulphonamides and pendant oligo(ethyleneimines) was developed to separate aldehydes from hydrocarbon mixtures. Biçak et al. (1996) studied the sorption behaviour of AcA, benzaldehyde and salicylaldehyde on such an oligo(ethyleneimines) polymeric resin, which was found to be second order kinetics. The sorption process is valid for all aromatic aldehydes, however, aliphatic aldehydes, which carry an α -hydrogen can also form aldol products in solution. In the case of aliphatic aldehydes also their aldol products are adsorbed, which limits their recovery. Depending on the amine content of the resin, two different mechanisms for aldehyde scavenging, namely the formation of a Schiff base and five-membered imidazoline rings, are observed as shown in Figure 2.7. The regeneration of the resins by dilute acid solution treatment (aldehydes stay intact) is possible due to good stability of the sulfamide bond towards acid-base hydrolysis. Acetone and alkyl halogenides were observed to interfere in the sorption process [104].

In continuation of this work 1,2-Diaminoethane containing epoxy resins was studied for aldehyde separation. 1,2-Diaminoethane units function as the polymeric analogue of Wanzlick reagent, which forms imidazolines in a condensation reaction. Both studies describe the removal of aldehydes from organic mixtures, using water-miscible solvents such as methanol and dioxane. The sorption is reported to be very slow for unpolar solvents due to the hydrophilicity of the polymer [105].

Adsorptive removal: Chemisorption on polyols functionalized materials

Yet, another example for effective aldehyde elimination by a packaging material is integration of polyols into the polymer material. Aldehydes are converted to an acetal by the reversible nucleophilic addition reaction of the aldehyde (or ketone) with a polyol such as sorbitol,

mannitol or alkoxyated polyols. The formed acetal exhibits a lower volatility than aldehydes and is therefore less detectable in food products [106-108]. The exemplary reaction of valeraldehyde with D-sorbitol is given in Figure 2.8. Suloff (2002) demonstrated in his work that the integration of D-sorbitol into poly(ethylene terephthalate) reduced the total aldehyde content by half during the storage of a model solution of pH 3.6. Furthermore, it was observed that small molecular weight aldehydes were preferred over larger aldehydes [89].

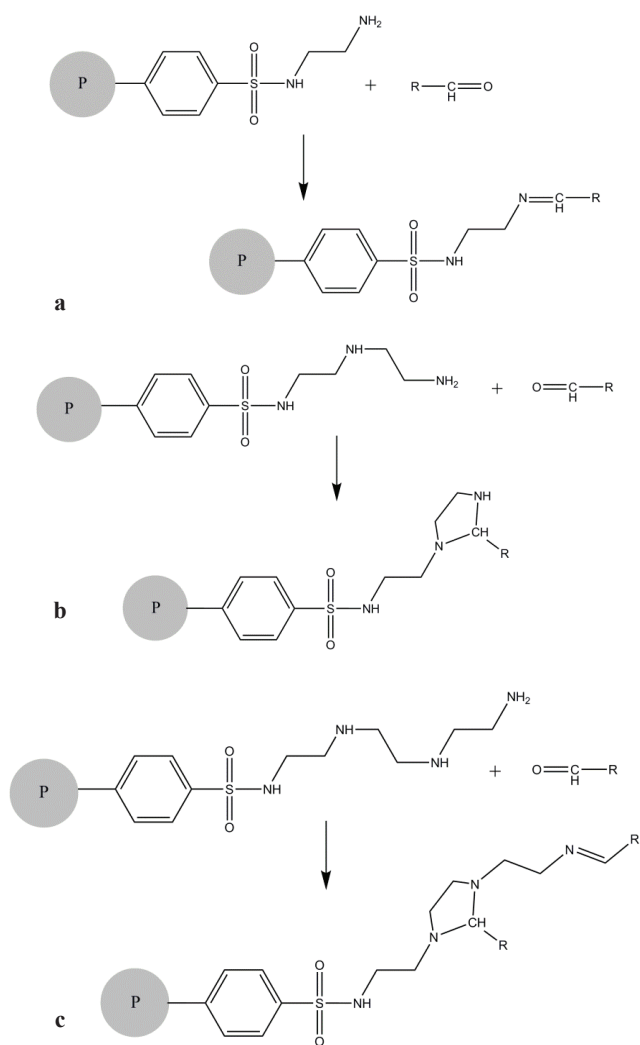


Figure 2.7: Aldehyde binding by three different polymer supported oligo(ethyleneimines); a: sulfamide bond ethylenediamine; b: sulfamide bond diethylenetriamine; c: sulfamide bond triethylenetetramine; adapted from [104]

Adsorption on other materials

Aldehydes have been shown to have a high affinity towards L-cysteine. Therefore, the application of an L-cysteine-containing gel has been proposed for the removal of AcA from indoor air. The researchers found that amongst tested amino acids (glycine, L-lysine, L-methionine, L-cysteine and L-cystine), treating air with L-cysteine resulted in the highest reduction of aldehyde concentration of 91% in comparison to 50 – 64% to water or solutions of other amino acids [109].

Nilvebrant *et al.* (2001) investigated the removal of aliphatic acids, HMF, FF, phenols and ketones on an anion exchanger (AG 1-X8), which was used in its hydroxide form. When compared with other tested resins (XAD-8 and cation exchanger), AG 1-X8 showed a significantly better performance at pH 10. The mechanism for binding of aldehydes is proposed to be hydrophobic interaction. However, when the effect on a glucose solution was tested, the anion exchanger reduced the sugar concentration by 75%. Nonetheless, this effect can be counteracted by addition of inorganic ions such as sulphate [61].

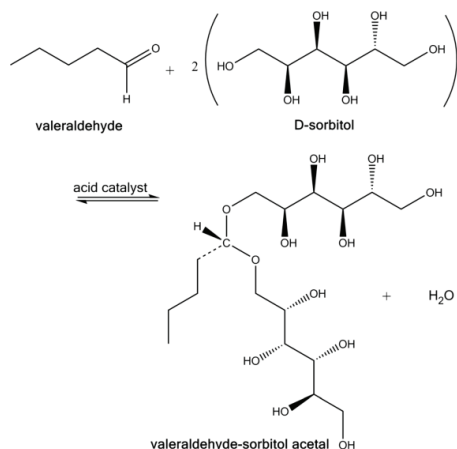


Figure 2.8: Reaction of valeraldehyde with D-sorbitol to the corresponding acetal [89]

Separation by extraction: Supercritical carbon dioxide extraction

In a lab-scale study, the extraction of essential oil from grape bagasse for production of jam was examined [110]. Temperature and fluid density can be used to modify the solubility of components in the extractant and therefore to influence the selectivity of the separation step [111]. While there was no effect of temperature and pressure on the recovered mass of essential oil, the operating conditions influenced the composition of the essential oil. When the

temperature was fixed to 303 K and 15 MPa, hydrocarbons were the dominated compound class in the extract. On increasing the pressure to 25 MPa and decreasing the temperature to 290 K, aldehydes and ketones were identified as the most important molecule class in the oil [110].

Different patents on the purification of vanillin (4-Hydroxy-3-methoxybenzaldehyde) were published. In US patent 4474994 A impurities are removed from the crude vanillin, which is obtained from lignin, lignosulfonates or sulphite cooking liquor, by supercritical CO₂ extraction [112]. A Chinese patent approaches the problem from a different angle by extracting vanillin from the crude mixture with supercritical CO₂ [113].

Lee et al. (2008) investigated the extraction process of fish oil with supercritical carbon dioxide and off-flavour removal from fish viscera. On the contrary of above results, they found that with raising pressure and temperature the recovered quantity was increased. It is also reported that off-flavours such as aldehydes in the remaining powder are significantly reduced after the extraction. For instance n-valeraldehyde was decreased to around 9% of its initial peak area in the analysis. At a closer look however, it is found that the concentration of other aldehydes, such as isovaleraldehyde or propionaldehyde are actually elevated after the extraction [114]. Similar trends were observed by Roh et al., but they were able to nearly completely remove off-flavours from fish oil. For instance, when extracting at 30°C and 20 MPa, butanal and pentanal were not detectable anymore, and the percentual area of propanal was reduced by 99 % (Roh et al. 2006).

Supercritical CO₂ extraction has also been investigated for the dealcoholisation of cider (Medina and Martínez 1997). Although aldehydes were not investigated in this publication, the authors report that flavours are extracted along with the ethanol. More specifically, aroma extraction is favoured at 40°C and 12.5 MPa, while ethanol extraction is more favourable at 40°C and 25.0 MPa. This may be an interesting concept to translate to aldehyde removal from AFBs.

Separation by extraction: Extractant impregnated resin technology

A newer development is the employment of the Extractant Impregnated Resin technology for extraction and thus separation of aldehydes from aqueous streams. Thereby, a porous particle is functionalized by impregnating its pores with extractant as depicted in Figure 2.9. The recovery of benzaldehyde from a model solution was studied by Babić et al. (2006). The highest capacity was achieved with porous adsorbent Amberlite XAD-16 impregnated with Primene®

JM-T. Primene® JM-T is a mixture of isomeric primary aliphatic amines in C18-22 range and was reported to be the most promising extract. The principle of stable formation of a Schiff base is also exploited in this case. Due to the impact on the solubility of benzaldehyde and the amines, increasing the temperature had a positive effect on the separation process [115].

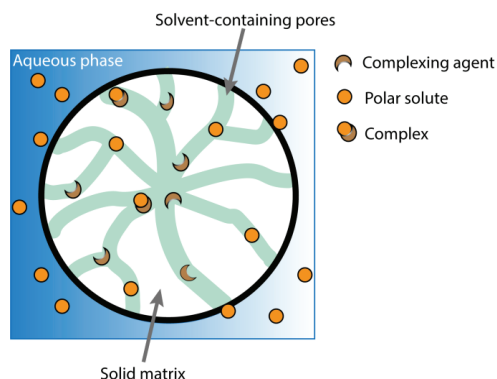


Figure 2.9: Extractant impregnated resin technology [115]

A similar approach was taken by Vidal *et al.* (2012) by functionalizing silica materials with ionic liquids to extract organic acids, amines and aldehydes from atmospheric aerosols [116]. In the past years, ionic liquids, which are composed of bulky non-symmetrical organic cations or different inorganic or organic anions, have gained increasing interest of researchers as a result of their negligible vapour pressure, thermal stability and tuneable viscosity and miscibility with water [117]. The tested ionic liquids, imidazolium, N-methylimidazolium and 1-alkyl-3-(propyl-3-sulfonate) imidazolium showed higher extraction efficiencies for the organic acids due to the fact that anion exchange appears to be the dominant interaction, nonetheless, hydrophobic interaction and hydrogen bonding was also found to contribute [116].

Removal by conversion

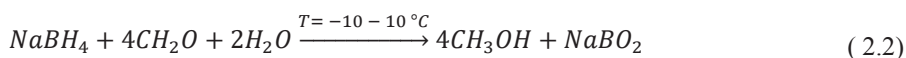
Another strategy to reduce the concentration of aldehydes is to convert them to aroma neutral or positive flavour compounds. In principle the oxidation of aldehydes to the corresponding carboxylic acid or its reduction to an alcohol is possible, which can be further converted to an ester [21, 118]. In nature for instance, alcohol dehydrogenase catalyses the reduction of 3-MB to 3-methylbutanol as the last step of the Ehrlich pathway. This is a very active reaction pathway in yeast, but the reaction is also carried out by lactic acid bacteria at a lower frequency [21, 119-124]. In turn, the conversion of 3-MB to 3-methyl butanoic acid was found to be carried out by aldehyde dehydrogenase in *Staphylococcus xylosus* [21, 125].

In waste water treatment, the removal of odourous aldehydes from drinking water was attempted by employing the UV/H₂O₂ process. Overall, a reduction in aldehyde concentration (e.g. decadienal, hexanal) and the algae-related fishy/grassy smell could be detected by a sensory panel, however, new types of odour were produced (chalky or sweet) [126]. Another technique tested with waste water for the removal of aldehydes and polyphenols is electrocoagulation. Olya *et al.* (2013) showed that a 95% removal of aldehydes could be achieved by immersing a Fe-Fe-electrode combination into the aqueous solution. The suggested mechanism is the formation of metal hydroxides flocs during electrocoagulation and consequent adsorption of aldehyde (polymers) to the floc surface area or direct oxidation of the organic compounds on the anode [127].

Classic organic chemistry has also identified efficient catalysts to accelerate the oxidation /reduction reactions of aldehydes. For the conversion to carboxylic acid, oxidizing agents such as permanganate, bromine, oxone or copper (II) oxide are commonly employed [128, 129]. Since these compounds are strong oxidizing agents, they are not chemoselective and for example also convert alcohols [130]. Typically, the addition of organic solvents is suggested, but examples for the preparation in aqueous solution can also be found. Saadati *et al.* (2016) prepared a nanosized copper (II) oxide embedded in hyper-cross-linked polystyrene to catalyse the aqueous-phase oxidation of aldehydes in water. The optimum reaction conditions were observed at basic pH and 75°C [131]. Another example is the oxidation of HMF to 2,5-furandicarboxylic acid at high pressure conditions (40 bar) and 100°C by active carbon functionalized with platinum and bismuth-platinum catalyst [132]. The catalytic conversion is not only limited to the liquid phase. In the US Patent 7855261 B2 “Aldehyde removal” (2010) a method for removal of a gaseous aldehyde, in particular AcA, is described for the application of removal from tobacco smoke by a filter medium. The filter support material is a polymeric composition containing acetoacetate residues and a metallic oxidizing agent or oxidation catalyst (such as Cu (II)), which oxidized contained aldehydes [133].

The reduction of aldehydes and ketones to primary and secondary alcohols, respectively, is catalysed by complex metal hydrides such as lithium aluminium hydride or sodium borohydride. Generally, these catalysts do not reduce carbon-carbon double or triple bonds, which is advantageous when compared to other reducing agents. However, since lithium aluminium hydride readily reacts with water and alcohols these components need to be eliminated from the reaction mixture and organic solvents employed. Sodium borohydride is more chemoselective and may be used in aqueous or alcoholic solutions. Furthermore, several

agents have been reported to reduce aldehydes more rapidly than ketones, amongst them are sodium triacetoxymethylborohydride or zinc borohydride [129]. The removal of aldehydes by reduction to their alcohol is described in a patent for purification of ethylene oxide. The conversion is achieved by adding sodium or potassium borohydride according to equation 2.2. In this case however, sodium borohydride is not chemoselective and also reacts with ketones to the adequate alcohol [134].



Alternatively to oxidation or reduction, the reaction of glycine and L-tyrosine with n-heptanal has been studied to produce coloured pigments for food applications. In this way carbonyls are removed, while simultaneously unsaturated-polymeric pigments are formed. The experiments suggest that the formed product contains an imine linkage [135]. The strategy of binding aldehydes in the imine form is also employed during the acidic pre-treatment step for the production of ethanol from cellulosic materials for instance, FF and HMF are formed, which are known to inhibit enzymes and microorganisms employed in the fermentation. It was shown that PEI is able to effectively remove these two inhibitory molecules from a simple aqueous solution. Interaction with contained acetic acid was reported to be avoidable by addition of chloride, sulphate or hydroxide ions. The aldehydes could mostly be desorbed from the resin by applying a dilute sulfuric acid solution [136].

Also bisulphite is known to form adducts with aldehydes, methyl ketones, cyclic ketones, α -keto esters, and isocyanates as shown in Figure 2.10. The addition products are readily soluble in water and the reaction is reversible through addition of either acid or base. Formation of addition products is not observed for most ketones, presumably due to steric hindrance [137].

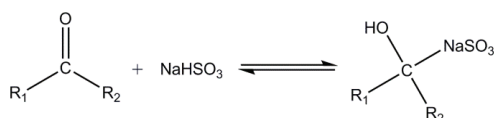


Figure 2.10: Reaction of bisulphate with aldehydes and ketones

This mechanism finds application for the elimination of aldehyde impurities from organic liquids, which are passed through a bed of solid sodium bisulphite particles. The bed can be regenerated by heating to 75 – 120°C. Due to the high solubility of sodium bisulphite (420 g/L) and its addition product this system is only applicable to liquids with a water content less than 10% [138]. Another way of addressing the separation problem was proposed by Boucher et al. (2017). In their work, a liquid-liquid extraction process was developed, where aldehydes

were allowed to react with bisulphite in a water miscible solvent, and then separated from the substrate by addition of a water-immiscible organic solvent [139].

Removal by pervaporation

In food industry, pervaporation has gained attention to separate and concentrate flavour compounds [140]. An example of applying this technique is the concentration of key flavours of soluble coffee by pervaporation. Weschenfelder et al. (2015) investigated the impact of feed flow rate, temperature and permeate pressure on the process performance. While they were able to separate and concentrate flavour compounds from a the industrial solution, optimization is required to achieve the desired aroma profile in the product [141]. An earlier study performed in 2005 successfully recovered key flavour compounds from apple essence, orange aroma and black tea distillate, both, in batch and continuous pervaporation operation. However, the authors state that a significant loss of aromas was observed due to evaporation leakage [142]. Another work focusses on the recovery of pomegranate aroma compounds (e.g. 3-MB) from a model solution. All studied flavours were concentrated. Coupling effects between them were observed that indicate an increased effect at higher aroma concentrations [143]. Nonetheless, quantitative studies are required to understand and describe the coupling phenomena.

2.3.2. Aldehyde removal - State-of-the-art in brewing

Reduction of aldehydes during cold contact fermentations

The principle of producing alcohol-free or low-alcoholic beer via a biological route is to prevent the formation of ethanol during the fermentation step through inhibiting yeast's metabolism. This is achieved by short contact times of the wort with the microorganism at low temperatures of around 2°C. Therefore, this process is often referred to as “cold contact fermentation” (CCF) or “cold contact process”. Despite the low activity of yeast, ester and fusel alcohol production as well as carbonyl reduction can be observed [144]. The effect heat deactivated yeast cells at 0 °C on the aldehyde concentration in wort was studied by Perpète et al. (1999) and compared to the concentration profile of a fermentation with viable yeast at the same conditions [145]. Although an effect of the heat-deactivated yeast on the aldehyde profile is observed, the concentration level decreases only by 10-30%. In contrast, hexanal, as a linear aldehyde, is nearly depleted in the presence of active yeast. Yet, the reduction of the branched Strecker aldehyde, 3-MB, is limited to a maximum of 60-70% of the initial aldehyde concentration found in the raw material. Both, chemical binding and enzymatic reduction are more distinct for linear aldehydes than for branched molecules [145].

Limitations in yeast activity and vitality were initially suspected to be responsible for the restricted reduction of branched Strecker aldehydes. This was, however, disproven during experiments with partially fermented wort. The evolution of 2-MB and 3-MB during CCF was measured. After the initial reduction of the concentration to around 30-40% of the initial concentration, the fermenter was pitched with 2-MB and 3-MB, respectively. The yeast was yet again able to reduce the added aldehydes within 5 hours to the characteristic threshold. Therefore, it is concluded by the authors that the physiological state of the yeast cells cannot be the reason for the insufficient reduction in Strecker aldehydes. To confirm this hypothesis, a second experiment was performed, where the partially fermented wort was pitched with freshly propagated yeast after 5 hours. Once more the same residual concentration was reached. Although the authors conclude that an active yeast is required for Strecker aldehyde reduction, they do not distinguish between intact, but metabolic inactive cell, and viable yeast cells. Heat deactivation most likely leads to disruption or alteration of the cell structure. It therefore remains unclear, if the observed decrease in aldehyde concentration is due to enzymatic or adsorptive reduction.

Nevertheless, these findings could also suggest that aldehyde interaction with wort components might be the reason for the limited degradation of worty off-flavours [146]. As suggested elsewhere, involved components for aldehyde binding are cysteine and sulphite [57, 58].

The hypothesis that sulphite readily binds to aldehydes and interferes in the aldehyde reduction during CCF was experimentally investigated. On adding 10 ppm sulphite to the wort during the fermentation, the reduction of 3-MB and methional was significantly inhibited. However, the concentration of 2-MB was again decreased to its characteristic mark. This difference had not been observed during the fermentation studies. Furthermore, the sulphite concentration during the original fermentation was only at ppb level. Hence, the authors of this work conclude that other wort compounds must be responsible for the binding of aldehydes during CCF [146]. From the study of wine polyphenols it is known, that interactions with aroma substances occur [52]. As polyphenolic compounds also occur in wort, they might be involved in the binding of wort aldehydes. The theory was tested by adding 100 ppm catechin to a CCF of 12° P wort. For 3-MB a clear trend could be observed that is less aldehyde were converted enzymatically, while the trend for 2-MB was less pronounced. The statistical relevance could however be confirmed by a student t-test. The authors hence conclude an involvement of polyphenols in the inhibited aldehyde removal by yeast [146].

On a closer look, it becomes apparent, that yeast is even able to produce aldehydes, such as 3-MB, in the later stage of the CCF. An experiment of Perpète and Collin (2000) with deuterated leucine, a precursor for 3-MB formation, provides evidence that yeast is able to synthesize the aldehyde at such low temperatures. It must be noted, however, that the rate of formation of 3-MB increases over time and a minimum aldehyde concentration can be identified for each process. Therefore, close monitoring of the CCF to avoid elevated aldehyde levels is a key factor [147].

Newer developments in this field aim at increasing the formation of positive flavours or masking molecules in AFBs. A special *Saccharomyces cerevisiae* strain producing increased concentration of organic acids such as lactate and citrate could help to mask the wort flavour features of AFBs [148]. In a study of two 5,5,5-trifluoro-DL-leucine resistant *Saccharomyces pastorianus* strains, spontaneous mutants were able to produce higher levels of isoamyl alcohol and isoamyl acetate when compared to the parental strain. However, levels were still lower than in regular beer and the product had to be diluted to achieve the legally allowed threshold of 0.5 vol.% [149].

Reduction of aldehydes during continuous fermentations of AFBs

Similar to the CCF process immobilized yeast strains are cultivated in specialized reactors under stress conditions, which limit the cell metabolism. Under these conditions only a fraction of the contained sugars is metabolized, resulting in low ethanol concentrations (<0.08%). In absence of oxygen the redox balance is impacted, which enhances reduction of wort aldehydes and intracellular metabolites thus the formation of esters and higher alcohols [150]. Depending on the fermentation parameters (aeration, residence time, temperature) and the selected yeast strain, the product specification can be controlled with respect to ethanol concentration, amount of esters and the ratio of higher alcohols to esters formed. The difficulty lies in achieving the correct balance of sensory compounds in the short time. Higher concentrations of diacetyl and aldehydes have been observed, while ester concentrations remain relatively low [151]. During the fermentation van Iersel *et al.* (2000) found that immobilizing yeast on DEAE-cellulose improves the reducing capacity during the production of AFB [152]. On varying the oxygen transfer rate of a continuous fermentation process it was found that with decreasing oxygen transfer rate, the reduction efficiency of aldehydes could be increased. The reduction in 3-MB was as high as 92% and near to 100% for unbranched aldehydes such as hexanal at an oxygen

transfer rate of 1 mg/L/h. It should be however mentioned that the ethanol concentration was with 0.5 vol.% well above the more conservative definition of an AFB [153].

Reduction of perceived wort flavour by masking components

Literature suggests that besides the enzymatic reduction through yeast, other biomolecules play a role in the removal of aldehydes from wort. A study of Perpète (1999) showed aldehyde concentrations can be reduced by 20-95% if amino acids or industrial wort proteins are added to a model solution. The authors observed that the majority of the chemical binding occurs within the first 30 minutes of the experiment. Presumably, the aldehydes are still contained in the medium, but in a chemically bound form, which is not measured with the analytical method employed. The fact that an increasing temperature decreases the concentration of aldehydes measured in the medium suggests furthermore that the formed chemical bond is based on an endothermic reaction [145]. The impact on other beer constituents was not included in the study and therefore the selectivity for aldehydes is in question.

A similar approach was applied in US patent 280399A1, where the wort flavour of a “beer-like malt beverage” is reduced by adding a terpene (terpinolene) to wort. The authors describe that addition of 0.05-5 ppm terpinolene reduced the perceived strength of wort flavour and improved the overall aroma balance of the product. It should be noted, however, that the methodology of the sensory evaluation is not further specified in the patent and the actual concentration or volatility in key wort flavour compounds was not analysed [154].

Aldehyde removal during dealcoholisation

Despite their mostly high volatility, aldehydes are also found in thermally dealcoholized products. Due to the heat impact heat indicators such as FF are simultaneously formed and evaporated. Generally, the final concentration of aldehydes is lower in fresh AFBs compared to their alcoholic starting beer, but on increasing the operating temperature to 42-48°C, a slight rise in 2-furfural concentration is observed. Processes, where lost flavours are recovered from alcoholic condensates and added back to the AFB have been reported a 2-fold concentration of 2-furfural and γ -nonalacton [44].

A vast study of aldehyde profiles in Czech and Spanish lager beers was performed by Andrés-Inglesias *et al.* (2016). 28 beers, including four AFBs were analysed for defined aldehydes and ketones. The results are depicted in Figure 2.11. Generally, concentrations of aldehydes and ketones are lower, however for some compounds close or in case of trans-non-2-enal above

their respective flavour threshold [14]. This is particularly true, when the matrix effect explained in paragraph 2.2.4 is taken into account. Nonetheless, as the study did not include sensory panels, it is difficult to conclude the perception of off-flavours in the tested AFBs. When comparing AFBs produced by vacuum distillation (see Figure 2.11, beer A and B), with biologically produced AFBs (see Figure 2.11, beer B and C) it is conspicuous that cold contacted fermented beer shows the highest concentration for all compounds, except for diacetyl. Methional, which has a lower vapour pressure and flavour threshold, was not measured although it is the predominant wort flavour in AFBs.

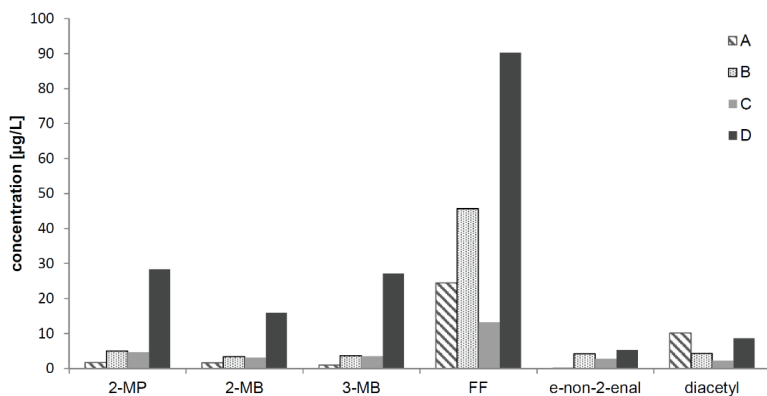


Figure 2.11: Aldehyde concentrations in different AFBs compared to average concentration in lagers adapted from Andrés-Iglesias et al. (2016) [14]

A: Spanish beer (0.01 vol.%), dealcoholized by vacuum distillation; B: Czech beer (0.49 vol.%), dealcoholized by vacuum distillation; C: Czech beer (0.49 vol.%) produced by special yeast strain; D: Czech beer (0.50 vol.%) produced by CCF.

Development in membrane-based technologies

Newer developments can be discovered in the field on membrane based separations. Catarino *et al.* (2011) propose to separate flavours selectively from the beer stream by pervaporation before dealcoholisation by stripping (spinning cone column). This exhibits the advantage that flavours are collected in a stream with a lower ethanol concentration and can be dosed back to the alcohol-free end-product. In the study it is found that AcA can be removed together with esters and higher alcohols prior to entering the stripping equipment [8, 155]. Nonetheless, this process set-up is disadvantageous for aldehyde removal due to the fact that the separation is non-selective and that molecules will be re-formed during the dealcoholisation step. Another approach was followed by Liguori *et al.* (2014). In their work, modified osmotic distillation was employed to dealcoholize beer to an ethanol content < 0.5 vol. %. The total aldehyde

content was decreased from 57.24 to 3.82 mg/L and in particular, 2-MB, 3-MB and Met were reduced by 85, 94 and nearly 100 %, respectively, although the process was not selective for aldehydes only [156].

Removal through adsorptive technologies

The idea of reducing the wort flavour with adsorptive techniques has been described in several patents [157, 158]. In US 2012/0207909 AC is used for batch uptake tests at low temperatures to remove aldehydes. They found that using an amount of 10-30 g_{AC}/kg_{malt grist} is optimal to reduce the wort flavour; if the ratio of AC to wort is increased, this results in an overall decrease in flavour and thus in an insufficient beer taste. Chemical analysis of a production scale batch test at a phase ratio of 18.4 g_{AC}/kg_{wort} showed a reduction of 2-MB from 10.2 to 6.4 µg/L, 3-MB from 29.6 – 20.2 and methional from 19.2 to 10.1 µg/L. A higher removal could be achieved by using a higher phase ratio or a different type of AC [158]. Another approach was taken in US 2012/0207909, where ion-exchange and synthetic resins were studied for reducing the “rough” flavour in alcoholic malt drinks. Both, ion exchange and synthetic resins (XAD7, XAD4) proofed to reduce typical wort flavours in alcoholic beers, even after storing the beer at 30°C for one month. The process is, however, not selective for aldehyde removal, but during the treatment, other molecules such as Maillard components, organic acids and polyphenols are also removed [157].

Methods employed for formation inhibition in regular beer

The formation of Strecker aldehydes during the storage of regular beer is a commonly recognized issue. Besides reducing the oxygen level in the bottled product, several other methods have been developed to reduce or inhibit the formation of wort flavour during storage. As such enzymes, i.e. aldose reductase, have been patented to metabolize 3-deoxyglucosone, which is involved in the Strecker degradation. By converting the precursor, aldehyde formation is circumvented [159]. As it is known, that the main factor contributing to staling are the malt quality and the brewing process itself [19], another approach was taken by Yano et al. (2008). In this study, the effect of treating a part of the wort (second wort, > 10%) during and before the wort boiling process with adsorbents (AC, bentonite, silica gel and PVPP) was investigated. Beers treated with AC resulted in a product with an improved organoleptic taste stability, i.e. a reduced the oxidized flavour of forced aged beer compared to a reference brew. However, since the chemical analysis of the fresh beer showed only a reduction in γ -nonanlacton concentration and other components such as Strecker aldehydes were unaffected, it was postulated that this

difference is not related to a direct wort flavour removal, but rather, the reduction of precursors [160].

2.4. Conclusion and outlook

Aldehyde removal has been a subject of interest for different applications in the past. Due to the limitations of creating a pure product and following traditional approaches, but also obeying to general regulations of food administration, the process development for selective off-flavour removal from AFB has been restricted so far. At this point, applied technologies are either not selective or effective enough to efficiently separate aldehydes from the beer stream. The motivation of creating a healthy and safe beverage alternative that meets the customer's expectation is, however, a key driver for the upcoming market. The aim of such an improvement should be the development of a novel process design that is able to engineer the desired flavour profile to the beer matrix while preserving the product quality.

In this work the chemistry of beer aldehydes with regard to alcohol-free beverages and aldehyde separation processes from industry and research have been compiled. Since aldehyde removal is a focus of interest in many fields and industries, such as biotechnology, packaging or air purification, researcher can benefit from the vast level of knowledge and data available from all disciplines. While not all process concepts presented can be applied for the case of AFB production, many promising technologies are found in literature. Amongst these, adsorptive removal is identified as the most suitable method to specifically target worty off-flavours from aqueous food streams. With regard to the selectivity, the use of hydrophobic resins or amino-modified polystyrenes should be investigated in order to discover the complex interaction of aldehydes, beer matrix components and adsorbents. Going one step further, other materials may be considered such as natural polymers or inorganic adsorbents that have not been investigated for this application, yet.

Reducing sugars, hop acids, hydrophobic flavour components, vitamins, polyphenols and small organic molecules may potentially interfere in the process, thus, it is required to define the product specifications and acceptable losses of nutrients to the separation medium. It is for instance known, that amines and amides as functional aldehyde scavenger also react with organic acids, thus resulting in a reduced selectivity for targeted compounds [92]. Consequently, suitable reaction conditions should be created, which enable a more selective removal of off-flavours. In this approach, a smart process design to circumvent bottlenecks is of uttermost importance. The combination of biological methods for AFB production with a

downstream off-flavour removal unit is one possibility to explore. Potentially, an integrated process of adsorption and physical dealcoholisation depicts an attractive opportunity for quality improvement of AFBs. Future research should furthermore consider the impact of other flavour groups to identify specifically problematic compounds with regard to the perception of alcohol-free beverages.

2.5. Acknowledgements

The authors would like to thank Heineken Supply Chain B.V. for funding this project.

2.6. References

1. Lehnert, R., et al., *Optimisation of lab-scale continuous alcohol-free beer production*. Czech Journal of Food Sciences, 2009. 27(4): p. 267-275.
2. Nederlandse-Brouwers. *Kerncijfers*. 2019; Available from: <https://www.nederlandsebrouwers.nl/biersector/publicaties/kerncijfers-nederlandse-brouwers/>.
3. Brányik, T., et al., *A review of methods of low alcohol and alcohol-free beer production*. Journal of Food Engineering, 2012. 108(4): p. 493-506.
4. Montanari, L., et al., *Chapter 6 - Production of Alcohol-Free Beer*, in *Beer in Health and Disease Prevention*, V.R. Preedy, Editor. 2009, Academic Press: San Diego. p. 61-75.
5. Sohrabvandi, S., et al., *Alcohol-free beer: Methods of production, sensorial defects, and healthful effects*. Food Reviews International, 2010. 26(4): p. 335-352.
6. de Jongh, J., W. Peters, and C. van Teeffelen, *Ruigrok Net Panel*, in *Nationaal Bieronderzoek Nederland*. 2014: Amsterdam.
7. Karlsson, H.O.E. and G. Trägårdh, *Aroma recovery during beverage processing*. Journal of Food Engineering, 1997. 34(2): p. 159-178.
8. Catarino, M., A. Ferreira, and A. Mendes, *Study and optimization of aroma recovery from beer by pervaporation*. Journal of Membrane Science, 2009. 341(1-2): p. 51-59.
9. De Schutter, D.P., et al., *Release and Evaporation of Volatiles during Boiling of Unhopped Wort*. Journal of Agricultural and Food Chemistry, 2008. 56(13): p. 5172-5180.
10. Beal, A.D. and D.S. Mottram, *Compounds contributing to the characteristic aroma of malted barley*. Journal of Agricultural and Food Chemistry, 1994. 42(12): p. 2880-2884.
11. Perpète, P. and S. Collin, *Contribution of 3-methylthiopropionaldehyde to the warty flavor of Alcohol-free beers*. Journal of Agricultural and Food Chemistry, 1999. 47(6): p. 2374-2378.

12. Saison, D., et al., *Contribution of staling compounds to the aged flavour of lager beer by studying their flavour thresholds*. Food Chemistry, 2009. 114(4): p. 1206-1215.
13. Baert, J.J., et al., *On the origin of free and bound staling aldehydes in beer*. J Agric Food Chem, 2012. 60(46): p. 11449-72.
14. Andrés-Iglesias, C., et al., *Comparison of carbonyl profiles from Czech and Spanish lagers: Traditional and modern technology*. LWT - Food Science and Technology, 2016. 66: p. 390-397.
15. Blanco, C.A., C. Andrés-Iglesias, and O. Montero, *Low-alcohol Beers: Flavor Compounds, Defects, and Improvement Strategies*. Critical Reviews in Food Science and Nutrition, 2016. 56(8): p. 1379-1388.
16. Meilgaard, M.C., *Flavor chemistry in beer: Part II: Flavor and flavor threshold of 239 aroma volatiles*. Master Brewers Association of the Americas, 1975. 12: p. 151-168.
17. Chambers Iv, E. and K. Koppel, *Associations of volatile compounds with sensory aroma and flavor: The complex nature of flavor*. Molecules, 2013. 18(5): p. 4887-4905.
18. Kroh, L.W., *Caramelisation in food and beverages*. Food Chemistry, 1994. 51(4): p. 373-379.
19. De Clippeleer, J., et al., *Influence of the Hopping Technology on the Storage-induced Appearance of Staling Aldehydes in Beer*. Journal of the Institute of Brewing, 2010. 116(4): p. 381-398.
20. Saltmarch, M. and T.P. Labuza, *Nonenzymatic browning via the Maillard reaction in foods*. Diabetes, 1982. 31(Suppl. 3II): p. 29-36.
21. Smit, B.A., W.J.M. Engels, and G. Smit, *Branched chain aldehydes: Production and breakdown pathways and relevance for flavour in foods*. Applied Microbiology and Biotechnology, 2009. 81(6): p. 987-999.
22. Pereira, V., et al., *Evolution of 5-hydroxymethylfurfural (HMF) and furfural (F) in fortified wines submitted to overheating conditions*. Food Research International, 2011. 44(1): p. 71-76.
23. Contreras-Calderón, J., E. Guerra-Hernández, and B. García-Villanova, *Indicators of non-enzymatic browning in the evaluation of heat damage of ingredient proteins used in manufactured infant formulas*. European Food Research and Technology, 2008. 227(1): p. 117-124.
24. Carabasa-Giribet, M. and A. Ibarz-Ribas, *Kinetics of colour development in aqueous glucose systems at high temperatures*. Journal of Food Engineering, 2000. 44(3): p. 181-189.
25. Harrison, H.R., et al., *Collaborative determination of the pH of beer and wort*. Journal of the Institute of Brewing, 1998. 104(3): p. 123-126.

26. Vanderhaegen, B., et al., *The chemistry of beer aging – a critical review*. Food Chemistry, 2006. 95(3): p. 357-381.
27. Chuyen, N.V., *Maillard Reaction and Food Processing*, in *Process-Induced Chemical Changes in Process-Induced Chemical Changes in Food*. 1998. p. 213-235.
28. Bravo, A., et al., *Formation of α -Dicarbonyl Compounds in Beer during Storage of Pilsner*. Journal of Agricultural and Food Chemistry, 2008. 56(11): p. 4134-4144.
29. Schonberg, A. and R. Moubacher, *The Strecker Degradation of α -Amino Acids*. Chemical Reviews, 1952. 50(2): p. 261-277.
30. Rizzi, G.P., *The Strecker Degradation of Amino Acids: Newer Avenues for Flavor Formation*. Food Reviews International, 2008. 24(4): p. 416-435.
31. Yaylayan, V.A., *Recent Advances in the Chemistry of Strecker Degradation and Amadori Rearrangement: Implications to Aroma and Color Formation*. Food Science and Technology Research, 2003. 9(1): p. 1-6.
32. Hodge, J.E. and C.E. Rist, *The amadori rearrangement under new conditions and its significance for non-enzymatic browning reactions*. Journal of the American Chemical Society, 1953. 75(2): p. 316-322.
33. Hodge, J.E., *The Amadori Rearrangement*, in *Advances in Carbohydrate Chemistry*. 1955. p. 169-205.
34. Hidalgo, F.J. and R. Zamora, *Strecker-type Degradation Produced by the Lipid Oxidation Products 4,5-Epoxy-2-Alkenals*. Journal of Agricultural and Food Chemistry, 2004. 52(23): p. 7126-7131.
35. Hidalgo, F.J., R.M. Delgado, and R. Zamora, *Intermediate role of α -keto acids in the formation of Strecker aldehydes*. Food Chemistry, 2013. 141(2): p. 1140-1146.
36. Delgado, R.M., R. Zamora, and F.J. Hidalgo, *Contribution of Phenolic Compounds to Food Flavors: Strecker-Type Degradation of Amines and Amino Acids Produced by o- and p-Diphenols*. Journal of Agricultural and Food Chemistry, 2015. 63(1): p. 312-318.
37. Hidalgo, F.J. and R. Zamora, *Amino Acid Degradations Produced by Lipid Oxidation Products*. Crit Rev Food Sci Nutr, 2016. 56(8): p. 1242-52.
38. Huang, Y., J. Tippmann, and T. Becker, *Kinetic studies of main wort flavor compounds and iso- α -acids during wort boiling: a review*. European Food Research and Technology, 2017. 243(9): p. 1485-1495.
39. Briggs, D.E., et al., *Brewing - Science and Practice*. Brewing. 2004: Woodhead Publishing.

40. Yahya, H., R.S.T. Linforth, and D.J. Cook, *Flavour generation during commercial barley and malt roasting operations: A time course study*. Food Chemistry, 2014. 145: p. 378-387.
41. Boulton, C., *Encyclopaedia of Brewing*. 2013: John Wiley & Sons, Ltd.
42. Sieben, R.L. and K.D. Zastrow, *Step mashing process for producing low alcohol beer (US5021246 A)*. 1991, Anheuser-Busch, Incorporated.
43. Russo, P.L., L.; Albanese, D.; Crescitelli, A.; Di Matteo, M., *Investigation of osmotic distillation technique for beer dealcoholization*. Chemical Engineering Transactions, 2013. 32: p. 1735-1740.
44. Müller, M., et al., *Physical Methods for Dealcoholization of Beverage Matrices and their Impact on Quality Attributes*. Chemie-Ingenieur-Technik, 2016. 88(12): p. 1911-1928.
45. Hertel, M., *Verfahren zur Dealkoholisierung von Getränken und zugehörige Vorrichtung (DE112010000824 A5)*. 2011.
46. Narziss, L., W. Back, and S. Stich, *Alcohol removal from beer by countercurrent distillation in combination with rectification (written in German)*. Bierwelt, 1993. 133(38): p. 1806-1820.
47. Conner, J.M., et al., *Headspace concentrations of ethyl esters at different alcoholic strengths*. Journal of the Science of Food and Agriculture, 1998. 77(1): p. 121-126.
48. Philippe, E., et al., *Behavior of Flavor Compounds in Model Food Systems: a Thermodynamic Study*. Journal of Agricultural and Food Chemistry, 2003. 51(5): p. 1393-1398.
49. Perpète, P. and S. Collin, *Influence of beer ethanol content on the wort flavour perception*. Food Chemistry, 2000. 71(3): p. 379-385.
50. Normand, V., S. Avison, and A. Parker, *Modeling the kinetics of flavour release during drinking*. Chem Senses, 2004. 29(3): p. 235-45.
51. Jung, D.-M., J.S. de Ropp, and S.E. Ebeler, *Study of Interactions between Food Phenolics and Aromatic Flavors Using One- and Two-Dimensional 1H NMR Spectroscopy*. Journal of Agricultural and Food Chemistry, 2000. 48(2): p. 407-412.
52. Dufour, C. and C.L. Bayonove, *Interactions between wine polyphenols and aroma substances. An insight at the molecular level*. Journal of Agricultural and Food Chemistry, 1999. 47(2): p. 678-684.
53. Li, H.-J. and M.L. Deinzer, *32 - Proanthocyanidins in Hops A2 - Preedy, Victor R, in Beer in Health and Disease Prevention*. 2009, Academic Press: San Diego. p. 333-348.
54. McGuinness, J.D., et al., *The estimation and significance of catechin and dimeric catechin in beer*. Journal of the Institute of Brewing, 1975. 81(3): p. 237-241.

55. Maier, H.G., *On the sorption of volatile aroma constituents by foods - VII. Aliphatic aldehydes*. Zeitschrift für Lebensmittel-Untersuchung und -Forschung, 1973. 151(6): p. 384-386.
56. Maier, H.G. and R.U. Hartmann, *The adsorption of volatile aroma constituents by foods - VIII. Adsorption of volatile carbonyl compounds by amino acids*. Zeitschrift für Lebensmittel-Untersuchung und -Forschung, 1977. 163(4): p. 251-254.
57. Baert, J.J., et al., *Further elucidation of beer flavor instability: The potential role of cysteine-bound aldehydes*. Journal of the American Society of Brewing Chemists, 2015. 73(3): p. 243-252.
58. Baert, J.J., et al., *Exploring the binding behavior of beer staling aldehydes in model systems*. Journal of the American Society of Brewing Chemists, 2015. 73(1): p. 100-108.
59. Lu, Y., B. Williamson, and R. Gillespie, *Recent advancement in application of hydrophobic interaction chromatography for aggregate removal in industrial purification process*. Curr Pharm Biotechnol, 2009. 10(4): p. 427-33.
60. Weil, J.R., et al., *Removal of fermentation inhibitors formed during pretreatment of biomass by polymeric adsorbents*. Industrial and Engineering Chemistry Research, 2002. 41(24): p. 6132-6138.
61. Nilvebrant, N.-O., et al., *Detoxification of lignocellulose hydrolysates with ion-exchange resins*. Applied Biochemistry and Biotechnology, 2001. 91(1): p. 35-49.
62. Jeřábek, K., L. Hanková, and Z. Prokop, *Post-crosslinked polymer adsorbents and their properties for separation of furfural from aqueous solutions*. Reactive Polymers, 1994. 23(2): p. 107-112.
63. Sahu, A.K., et al., *Adsorption of furfural from aqueous solution onto activated carbon: Kinetic, equilibrium and thermodynamic study*. Separation Science and Technology, 2008. 43(5): p. 1239-1259.
64. Aimoto, U., T. Kobayashi, and S. Adachi, *Temperature Dependence of Retention Factor of Saccharides on Hydrophobic Resin*. Japan Journal of Food Engineering, 2011. 12(4): p. 165-168.
65. Rojas, E.E.G., et al., *Hydrophobic interaction adsorption of hen egg white proteins albumin, conalbumin, and lysozyme*. Journal of Chromatography B: Analytical Technologies in the Biomedical and Life Sciences, 2006. 840(2): p. 85-93.
66. Zhang, Y., et al., *Efficient separation of homologous α -lactalbumin from transgenic bovine milk using optimized hydrophobic interaction chromatography*. Journal of Chromatography A, 2010. 1217(23): p. 3668-3673.
67. Saffarionpour, S., et al., *Selective adsorption of flavor-active components on hydrophobic resins*. Journal of Chromatography A, 2016. 1476: p. 25-34.

68. Medeiros, A.B.P., et al., *Production and recovery of aroma compounds produced by solid-state fermentation using different adsorbents*. Food Technology and Biotechnology, 2006. 44(1): p. 47-51.
69. Lucas, S., et al., *Adsorption isotherms for ethylacetate and furfural on activated carbon from supercritical carbon dioxide*. Fluid Phase Equilibria, 2004. 219(2): p. 171-179.
70. Ottens, M., S. Saffarionpour, and T.R. Noordman, *Method of producing beer having a tailored flavour profile (EP14183788.0)*, in *Patentscope*. 2016, Heineken Supply Chain B.V.
71. Canteli, A.M.D., et al., *Fixed-bed column adsorption of the coffee aroma compound benzaldehyde from aqueous solution onto granular activated carbon from coconut husk*. LWT - Food Science and Technology, 2014. 59(2, Part 1): p. 1025-1032.
72. Müller-Maatsch, J., et al., *Investigation into the removal of glucosinolates and volatiles from anthocyanin-rich extracts of red cabbage*. Food Chemistry, 2019. 278: p. 406-414.
73. Zhu, P., Chen, X., Roberts, C.G., *Method of use for aldehyde removal*, in *Google Patents*. 2006.
74. Neuman, R.C., *Chapter 16: Addition and Substitution Reactions of Carbonyl Compounds*, in *Organic Chemistry*. 2006: University of California Riverside.
75. Drese, J.H., A.D. Talley, and C.W. Jones, *Aminosilica Materials as Adsorbents for the Selective Removal of Aldehydes and Ketones from Simulated Bio-Oil*. ChemSusChem, 2011. 4(3): p. 379-385.
76. Carey, F.A. and R.J. Sundberg, *Addition, Condensation and Substitution Reactions of Carbonyl Compounds*, in *Advanced Organic Chemistry: Part A: Structure and Mechanisms*. 2007, Springer US: Boston, MA. p. 629-711.
77. FDA. *GRAS Notices*. 2002 [cited 2017 13.03.].
78. Monteiro, O.A.C. and C. Airoidi, *Some studies of crosslinking chitosan-glutaraldehyde interaction in a homogeneous system*. International Journal of Biological Macromolecules, 1999. 26(2-3): p. 119-128.
79. Nomura, A. and C.W. Jones, *Amine-Functionalized Porous Silicas as Adsorbents for Aldehyde Abatement*. ACS Applied Materials & Interfaces, 2013. 5(12): p. 5569-5577.
80. Zhu, Y., et al., *Amine-Functionalized SBA-15 with Uniform Morphology and Well-Defined Mesopore Structure for Highly Sensitive Chemosensors To Detect Formaldehyde Vapor*. Langmuir, 2012. 28(20): p. 7843-7850.
81. Lee, Y.G., et al., *Preparation of composite silica particles for the removal of formaldehyde at room temperature*. Journal of Ceramic Processing Research, 2008. 9: p. 302-306.

82. Strommen, M. and H.D. Gesser, *The trapping of indoor air contaminants*. Central European Journal of Chemistry, 2011. 9: p. 404-409.
83. Ewlad-Ahmed, A.M., et al., *Removal of Formaldehyde from Air Using Functionalized Silica Supports*. Environmental Science & Technology, 2012. 46(24): p. 13354-13360.
84. Gesser, H.D., *Abatement of indoor pollutants (US4547350 A)*. 1985.
85. Gesser, H.D., *Removal of aldehydes and acidic gases from indoor air (US4892719 A)*. 1990, Gesser Hyman D.
86. Koller, K.B., Wrenn, S.E., Houck, W.G., Paine, J.P., *Filter for selective removal of gaseous component* P.M. Incorporated, Editor. 1999.
87. Sae-Ung, S. and V. Boonamnuyvitaya, *Direct synthesis and characterization of amine-functionalized mesoporous silica materials and their applications as formaldehyde adsorbents*. Environmental Engineering Science, 2008. 25(10): p. 1477-1485.
88. Gesser, H.D. and S. Fu, *Removal of aldehydes and acidic pollutants from indoor air*. Environmental Science & Technology, 1990. 24(4): p. 495-497.
89. Suloff, E.C., *Sorption behaviour of an aliphatic series of aldehydes in the presence of poly(ethylene terephthalate) blends containing aldehyde scavenging agents*. 2002, Virginia Polytech Institute and State University: Blacksburg, Virginia.
90. Brodie, V. and D.L. Visioli, *Aldehyde scavenging compositions and methods relating thereto (US5413827 A)*. 1995, E. I. Du Pont De Nemours and Company.
91. DelNobile, M.A., et al., *Modeling of Hexanal Sorption Kinetic in an Aldehydes Scavenger Film Intended for Food Packaging Applications*. Journal of Food Science, 2002. 67(7): p. 2687-2691.
92. Speer, D.V., et al., *By-product absorbers for oxygen scavenging systems (US5942297 A)*. 1999.
93. Ching, T.Y., J.L. Goodrich, and K. Katsumoto, *Oxygen scavenging system including a by-product neutralizing material (CA2247985 C)*, in *Chevron Chemical Company Llc*. 2000.
94. Noyes, W.A. and D.B. Forman, *Aldehyde-amide condensation. I. Reactions between aldehydes and acetamide*. Journal of the American Chemical Society, 1933. 55(8): p. 3493-3494.
95. Mehra, R.K. and K.C. Pandya, *The condensation of aldehydes with amides - Part II. The condensation of cinnamaldehyde*. Proceedings of the Indian Academy of Sciences - Section A, 1938. 7(6): p. 376-380.
96. Pandya, K.C. and T.S. Sodhi, *The condensation of aldehydes with amides - Part I. The condensation of salicylaldehyde*. Proceedings of the Indian Academy of Sciences - Section A, 1938. 7(6): p. 361-368.

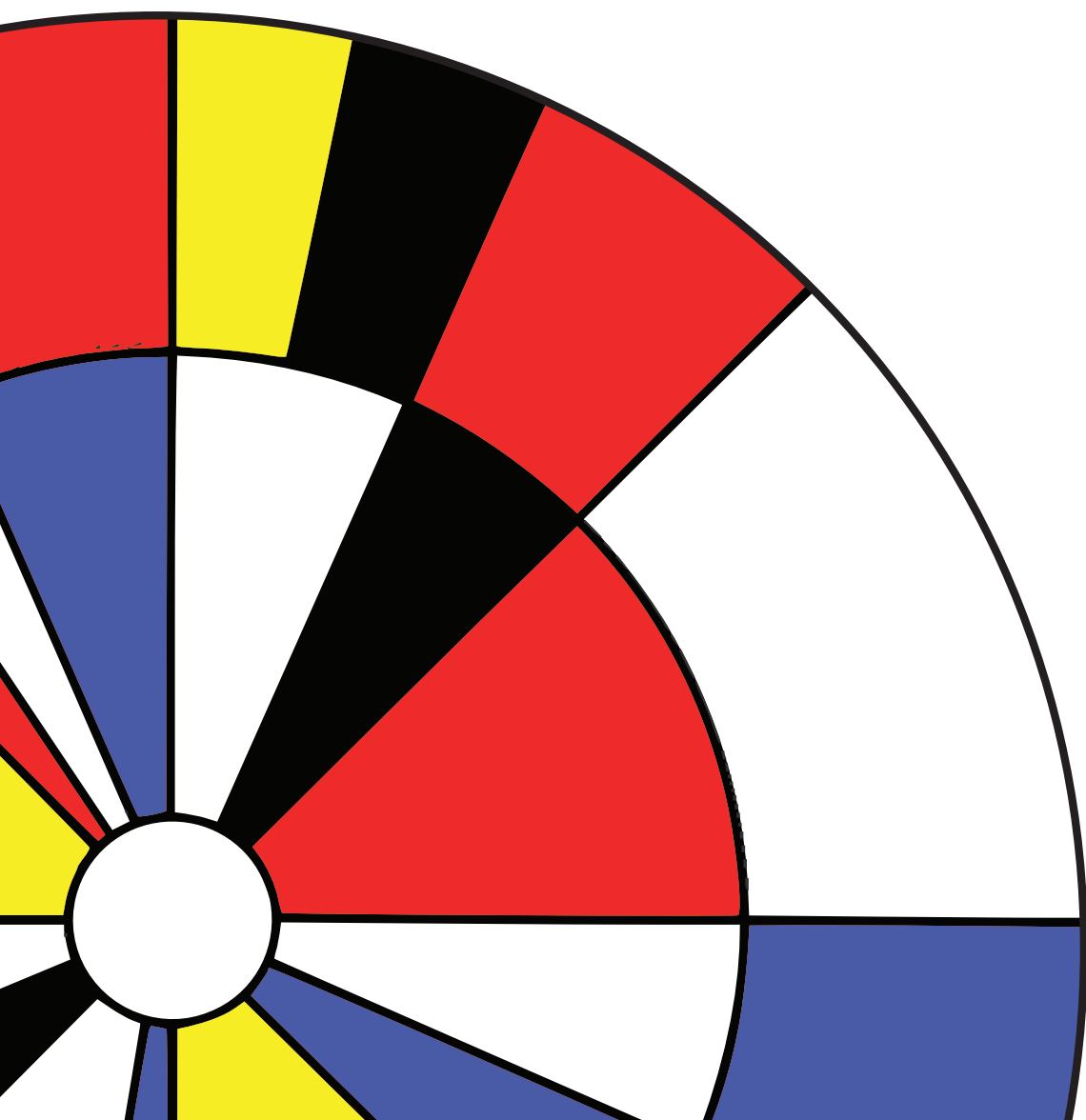
97. Tejedor, D. and F. Garcia-Tellado, *Chemo-differentiating ABB' multicomponent reactions. Privileged building blocks*. Chem Soc Rev, 2007. 36(3): p. 484-91.
98. Long, T.E., et al., *Process for improving the flavor retaining property of polyester/polyamide blend containers for ozonated water (US6042908 A)*. 2000, Eastman Chemical Company.
99. Howell, E. and J.A. Ponasik, *Acetaldehyde scavenging by addition of active scavengers to bottle closures (US20070020418 A1)*. 2008.
100. de Oliveira, A.V.B., et al., *Production of a low-cost scavenger resin to capture aldehydes and ketones in solutions*. Journal of Applied Polymer Science, 2015. 132(29): p. n/a-n/a.
101. Zhu, M., E. Ruijter, and L.A. Wessjohann, *New scavenger resin for the reversible linking and monoprotection of functionalized aromatic aldehydes*. Organic Letters, 2004. 6(22): p. 3921-3924.
102. Emerson, D.W., et al., *Polymer-bound sulfonylhydrazine functionality. Preparation, characterization, and reactions of copoly(styrene-divinylbenzenesulfonylhydrazine)*. The Journal of Organic Chemistry, 1979. 44(25): p. 4634-4640.
103. Welch, C.J., et al., *Selective removal of a pharmaceutical process impurity using a reactive resin*. Journal of Liquid Chromatography and Related Technologies, 2003. 26(12): p. 1959-1968.
104. Biçak, N. and B.F. Şenkal, *Aldehyde separation by polymer-supported oligo(ethyleneimines)*. Journal of Polymer Science Part A: Polymer Chemistry, 1997. 35(14): p. 2857-2864.
105. Biçak, N., et al., *1,2-Diaminoethane-containing epoxy resins for separation of aldehydes*. Reactive and Functional Polymers, 1999. 39(3): p. 197-205.
106. Wiegner, J.P., et al., *Extruded products from polyethylene terephthalate with reduced acetaldehyde content and process of their production (WO2001000724 A1)*. 2001, The Dow Chemical Company.
107. Al-Malaika, S., *Thermoplastic moulding compositions and polymer additives (WO2000066659 A1)*. 2000, Colormatrix Europe Ltd.
108. McNeely, G.W. and A.J. Woodward, *Modified polyethylene terephthalate (US5250333 A)*. 1993, Hoechst Celanese Corporation.
109. Yamashita, K., et al., *Acetaldehyde Removal from Indoor Air through Chemical Absorption Using L-Cysteine*. International Journal of Environmental Research and Public Health, 2010. 7(9): p. 3489-3498.

110. Santos, J.R.D.A.M.G.S.I.N., *Preliminary study of the influence of CO₂ extraction conditions on the ester, aldehyde, ketone and hydrocarbon content of grape bagasses from jam production*. Braz. J. Chem. Eng. [online], 2007. 24(4): p. 637-642.
111. Schroeder, M.A.F., R. A.; Morris, J. B., *The relationship of chemical structure to supercritical-fluid solubility and cosolvent-modifier properties: A literature review*, A.R. Laboratory, Editor. 1995.
112. Makin, E.C., *Purification of vanillin (US4474994 A)*, in *Monsanto Company*. 1984: United States.
113. Changqing L.; Chen C.; Yu, L.G., W.; Xiang, Z.; Yaoxian, L.; Yongxiang, W., *Carbon dioxide supercritical extraction method for vanillic aldehyde or ethyl vanillin raw product*, in *Espacenet*, C.N.P.C.C.J.C.g. Corp, Editor. 2010: China.
114. Lee, M.K., M.S. Uddin, and B.S. Chun, *Off-flavors removal and storage improvement of mackerel viscera by supercritical carbon dioxide extraction*. J Environ Biol, 2008. 29(4): p. 591-7.
115. Babić, K., L. van der Ham, and A. de Haan, *Recovery of benzaldehyde from aqueous streams using extractant impregnated resins*. Reactive and Functional Polymers, 2006. 66(12): p. 1494-1505.
116. Vidal, L., et al., *Ionic liquid-functionalized silica for selective solid-phase extraction of organic acids, amines and aldehydes*. Journal of Chromatography A, 2012. 1226: p. 2-10.
117. Han, D. and K.H. Row, *Recent applications of ionic liquids in separation technology*. Molecules, 2010. 15(4): p. 2405-2426.
118. Velíšek, J., *The chemistry of food*. 2014, Oxford :: Wiley Blackwell.
119. Chen, E.C.H., *Keto acid decarboxylase and alcohol dehydrogenase activities of yeast in relation to the formation of fusel alcohols*. Can Inst Food Sci Techn, 1977. 10: p. 27-30.
120. Hatanaka, A., T. Kajiwarra, and S. Tomohiro, *Purification and properties of alcohol dehydrogenase from Leuconostoc mesenteroides*. Agricultural and Biological Chemistry, 1974. 38(10): p. 1819-1833.
121. Schneider-Bernlöh, H., et al., *Alcohol dehydrogenase from leuconostoc mesenteroides: molecular properties in comparison with the yeast and horse liver enzyme*. International Journal of Biochemistry, 1981. 13(12): p. 1215-1224.
122. Bradshaw, C.W., W. Hummel, and C.H. Wong, *Lactobacillus kefir alcohol dehydrogenase: A useful catalyst for synthesis*. Journal of Organic Chemistry, 1992. 57(5): p. 1532-1536.
123. Arnau, J., et al., *Cloning of the Lactococcus lactis adhE gene, encoding a multifunctional alcohol dehydrogenase, by complementation of a fermentative mutant of Escherichia coli*. Journal of Bacteriology, 1998. 180(12): p. 3049-3055.

124. Temiño, D.M.R.D., W. Hartmeier, and M.B. Ansorge-Schumacher, *Entrapment of the alcohol dehydrogenase from Lactobacillus kefir in polyvinyl alcohol for the synthesis of chiral hydrophobic alcohols in organic solvents*. Enzyme and Microbial Technology, 2005. 36(1): p. 3-9.
125. Beck, H.C., A.M. Hansen, and F.R. Lauritsen, *Metabolite production and kinetics of branched-chain aldehyde oxidation in Staphylococcus xylosus*. Enzyme and Microbial Technology, 2002. 31(1-2): p. 94-101.
126. Jo, C.H. and A.M. Dietrich, *Removal and transformation of odorous aldehydes by UV/H₂O₂*. Journal of Water Supply: Research and Technology-Aqua, 2009. 58(8): p. 580-586.
127. Olya, M.E. and A. Pirkarami, *Electrocoagulation for the removal of phenol and aldehyde contaminants from resin effluent*. Water Sci Technol, 2013. 68(9): p. 1940-9.
128. Haines, A.H., *6 - Oxidation of Carbonyl Compounds*, in *Methods for Oxidation of Organic Compounds*. 1988, Academic Press. p. 241-275.
129. Smith, M.B. and J. March, *Oxidations and Reductions*, in *March's Advanced Organic Chemistry*. 2006, John Wiley & Sons, Inc. p. 1703-1869.
130. Tojo, G. and M. Fernández, *Permanganate*, in *Oxidation of Primary Alcohols to Carboxylic Acids: A Guide to Current Common Practice*. 2007, Springer New York: New York, NY. p. 1-12.
131. Saadati, F., et al., *Preparation and characterization of nanosized copper (II) oxide embedded in hyper-cross-linked polystyrene: Highly efficient catalyst for aqueous-phase oxidation of aldehydes to carboxylic acids*. Catalysis Communications, 2016. 79: p. 26-30.
132. Rass, H.A., N. Essayem, and M. Besson, *Selective aqueous phase oxidation of 5-hydroxymethylfurfural to 2,5-furandicarboxylic acid over Pt/C catalysts: influence of the base and effect of bismuth promotion*. Green Chemistry, 2013. 15: p. 2240-2251.
133. Kuo, T., M.K. Vineyard, and W.C. Liang, *Aldehyde removal (US7855261 B2)*. 2010, Eastman Chemical Company.
134. Randall, D.I., *Removal of aldehydes from ethylene oxide (US3213113 A)*. 1965.
135. Montgomery, M.W. and E.A. Day, *Aldehyde-Amine Condensation Reaction: A Possible Fate of Carbonyls in Foods*. Journal of Food Science, 1965. 30(5): p. 828-832.
136. Carter, B., P.C. Gilcrease, and T.J. Menkhaus, *Removal and recovery of furfural, 5-hydroxymethylfurfural, and acetic acid from aqueous solutions using a soluble polyelectrolyte*. Biotechnology and Bioengineering, 2011. 108(9): p. 2046-2052.
137. Smith, M.B. and J. March, *Addition to Carbon-Hetero Multiple Bonds*, in *March's Advanced Organic Chemistry*. 2006, John Wiley & Sons, Inc. p. 1251-1476.

138. Mameniskis, W. and T. Washall, *Purification of a material containing aldehyde impurities (US3816478 A)*. 1974, Atlantic Richfield Co.
139. Boucher, M.M., et al., *Liquid-Liquid Extraction Protocol for the Removal of Aldehydes and Highly Reactive Ketones from Mixtures*. Organic Process Research & Development, 2017. 21(9): p. 1394-1403.
140. Saffarionpour, S. and M. Ottens, *Recent Advances in Techniques for Flavor Recovery in Liquid Food Processing*. Food Engineering Reviews, 2018. 10(2): p. 81-94.
141. Weschenfelder, T.A., et al., *Concentration of aroma compounds from an industrial solution of soluble coffee by pervaporation process*. Journal of Food Engineering, 2015. 159: p. 57-65.
142. She, M. and S.-T. Hwang, *Recovery of key components from real flavor concentrates by pervaporation*. Journal of Membrane Science, 2006. 279(1): p. 86-93.
143. Raisi, A. and A. Aroujalian, *Aroma compound recovery by hydrophobic pervaporation: The effect of membrane thickness and coupling phenomena*. Separation and Purification Technology, 2011. 82: p. 53-62.
144. Narziss, L., W. Back, and M. Leibhard, *Optimization of biological processes for the production of alcohol-free beer using suitable cultures*. Brauwelt International, 1991. 1: p. 52-57.
145. Perpète, P. and S. Collin, *Fate of the warty flavours in a cold contact fermentation*. Food Chemistry, 1999. 66(3): p. 359-363.
146. Perpète, P. and S. Collin, *How to improve the enzymatic warty flavour reduction in a cold contact fermentation*. Food Chemistry, 2000. 70(4): p. 457-462.
147. Perpète, P. and S. Collin, *Evidence of Strecker Aldehyde Excretion by Yeast in Cold Contact Fermentations*. Journal of Agricultural and Food Chemistry, 2000. 48(6): p. 2384-2386.
148. Selecký, R., D. Šmogrovičová, and P. Sulo, *Beer with reduced ethanol content produced using Saccharomyces cerevisiae yeasts deficient in various tricarboxylic acid cycle enzymes*. Journal of the Institute of Brewing, 2008. 114(2): p. 97-101.
149. Strejc, J., et al., *Production of alcohol-free beer with elevated amounts of flavouring compounds using lager yeast mutants*. Journal of the Institute of Brewing, 2013. 119(3): p. 149-155.
150. van Iersel, M.F.M., et al., *Continuous production of non-alcohol beer by immobilized yeast at low temperature*. Journal of Industrial Microbiology, 1995. 14(6): p. 495-501.
151. Lehnert, R., *Optimization of Lab-Scale Continuous Alcohol-Free Beer Production*. Czech J. Food Sci., 2009. 27(4): p. 267-275.

152. Van Iersel, M.F.M., et al., *Influence of yeast immobilization on fermentation and aldehyde reduction during the production of alcohol-free beer*. Enzyme and Microbial Technology, 2000. 26(8): p. 602-607.
153. Lehnert, R., et al., *Effect of oxygen supply on flavor formation during continuous alcohol-free beer production: A model study*. Journal of the American Society of Brewing Chemists, 2008. 66(4): p. 233-238.
154. Murakami, A., et al., *Malt beverage having reduced wort off-flavor and process for production thereof*, in *Patentscope*, K.B.K. KAISHA, Editor. 2013: United States.
155. Catarino, M. and A. Mendes, *Non-alcoholic beer - A new industrial process*. Separation and Purification Technology, 2011. 79(3): p. 342-351.
156. Liguori, L., et al., *Production and characterization of alcohol-free beer by membrane process*. Food and Bioproducts Processing, 2015. 94: p. 158-168.
157. Shimizu, C.T., M., *Process for producing malt alcoholic drink*, in *Patentscope*, S.B. Limited, Editor. 2003.
158. Itakura, T., Ota, T., Owa, Y., *Unfermented beer-flavored malt beverage having reduced unpleasant wort flavor and method for producing the same*, in *FreePatentsOnline*, K. Beer, Editor. 2012.
159. Bravo, A.S., Beatriz; Rangel-Aldao, Rafael, *EP0773285B1: Method for producing an alcohol-containing fermented malt beverage with stabilized flavour*. 2002.
160. Yano, M., W. Back, and M. Krottenthaler, *The Impact of Low Heat Load and Activated Carbon Treatment of Second Wort on Beer Taste and Flavour Stability*. Journal of the Institute of Brewing, 2008. 114(4): p. 357-364.



Chapter 3

Simultaneous dealcoholisation and wort-flavour removal in alcohol free beers

Abstract The volume of alcohol-free beers (AFBs) sold is steadily growing, yet, sensory deficiencies such as the over-perception of wort flavour still is a reoccurring issue. Hence, the impact of thermal dealcoholisation with a vacuum stripping unit (spinning cone column) on the volatiles profile was investigated with particular focus on Strecker aldehydes, generally regarded to be responsible for wort flavour in beers. Base beers or wort were subjected to different strip rates and the volatile profile was quantified. Bases with initially high levels in aldehydes and diketones showed an exponential decline in concentration of low boiling flavours. However, methional, the most outstanding wort flavour depicted a different behaviour i.e. a linear decrease in concentration with increasing strip rate, due to its high boiling point. On the contrary, base beers with initially low concentrations did not show a decrease in aforementioned compounds. An explanation is the simultaneous formation of aldehydes and diketones due to the heat impact during dealcoholisation. Consequently, a dealcoholisation batch spiked with reactive monosaccharides was performed. Furfural formation was found, proving the heat impact during the operation. In conclusion, thermal dealcoholisation can facilitate wort flavour removal, however, if the complete depletion of high boiling wort flavours is desired, other unit operations such as pervaporation or adsorption are recommended.

3.1. Introduction

Recent market developments have triggered an interest of the beverage industry in low and non-alcoholic alternatives to regular beer [1, 2]. Nevertheless, existing production processes result in alcohol-free drinks with altered flavour profiles and therefore often in a poor organoleptic experience [3]. Previous work has been focussed on different technologies to produce alcohol-free beer (AFB) that on the one hand completely eliminate the presence of ethanol from the beer, but on the other hand retain positive flavours e.g. esters and higher alcohols, to preserve the beer's original character and taste [1, 4]. Fruity esters and higher alcohols contributing to the characteristic flavour profile and mouthfeel of beers, originate from the yeast metabolism [5] and are comparatively stable [6].

Volatiles that are found in AFB, however, are not limited to esters and higher alcohols, but originate from numerous chemical pathways and vary vastly in flavour: For instance, diketones, such as diacetyl and 2,3-pentanedione have a buttery or caramel odour [7], furfural (FF), which originates from caramelization, is a common heat indicator and is described as bready [8]. At elevated concentration levels or changed beer composition, some compounds become overpronounced and are perceived as off-flavours. AFBs often exhibit an overly prominent wort flavour [9], which has been reported to be caused by so-called Strecker aldehydes [10, 11], produced from the reaction of a reactive dicarbonyl with an amino acid [12].

To current knowledge, the most dominant wort off-flavours are 2-methylbutanal (2-MB), 3-methylbutanal (3-MB) [10] and methional (MT) [11]. 2-MB's odour is described as malty or almond like, while 3-MB also has a chocolate note to it. MT exhibits a wort character and has the smell of cooked potatoes [8]. With around 0.5 µg/L, MT has the lowest detection threshold in alcohol-free beer amongst the three [7]. Moreover, synergistic effects can occur [13-15]. Most studies address the reduction of these compounds in biologically produced AFBs through increased yeast activity or addition of masking compounds [11, 16-21], but fewer studies take into account wort off-flavours in thermally treated products. Some data on the concentration of Strecker aldehydes in the final product of dealcoholized beers are reported [1, 14, 22, 23], though, a systematic study of the impact of thermal dealcoholisation on the wort flavour profile is yet missing.

The prerequisite to improve the existing processes is, however, to study and understand the current state-of-the-art available technology, such as the spinning cone column dealcoholisation unit. Hence, the objective of this manuscript is to show the effect of thermal treatment on the

volatiles profile of resulting alcohol-free beers with special focus on wort off-flavour concentration as well as the overall product quality for different bases.

3.2. Materials and Methods

3.2.1. Chemicals

All aqueous solutions were prepared with Milli-Q grade water (Merck Millipore, United States) or absolute ethanol of analytical grade (VWR International BV, The Netherlands). O-(2,3,4,5,6-pentafluorobenzyl)-hydroxylamine (PFBOA) was purchased from Fluka (United States). All other chemicals were purchased from Sigma Aldrich (The Netherlands).

3.2.2. Feedstocks

To test the effect of stripping with different bases, three different feedstocks, specified in Table 3.1, were brewed prior to the trials and stored at 2°C until used. The inlet concentration of relevant volatiles is summarized in Table 3.2. In order to assess the thermal impact during dealcoholisation, an additional test with base 2 was performed, where a sugar solution was added to the base beer increasing the concentration of glucose, maltose, maltotriose and ribose by 2.0, 24.7, 10.1, and 5.0 g/L, respectively.

Table 3.1: Specification of original extract, alcohol and iso- α -acids content in wort and two beer bases

Parameter	Wort	Base 1	Base 2
Original extract [°P]	13.9	12.3	11.3
Total fermentable sugars [g/L]	95.8	40.2	3.1
Ethanol [% v/v]	<0.06	2.93	4.89
Color [EBC]	12.8	9.6	7.4
Total iso- α -acids [mg/L]	29.8	22.8	18.2

3.2.3. Dealcoholisation with SCC

All experiments were carried out with the spinning cone column SCC 1000 (Flavourtech, Australia). The spinning cone column (SCC) is a vacuum distillation unit that strips out volatiles by direct, counter-current stripping with steam. The feed stream is pre-heated to the operational temperature (typically 42-45°C); degassing is not required. Then, the liquid is forced through a series of spinning cones, forming a thin film and hence large surface area to create a high mass

transfer efficiency. This effect is supported by fins placed along the flow path to create turbulence.

Table 3.2: Volatiles concentration in wort and two beer bases

Compound	Wort	Base 1	Base 2
	Concentration [$\mu\text{g/L}$]		
Diacetyl	38.3	19.8	7.4
2,3-pentanedione	19.1	13.3	9.4
2-methylpropanal	64.0	26.9	2.1
2-methylbutanal	61.6	25.3	1.1
3-methylbutanal	155.3	65.1	5.0
Furfural	923.8	373.1	6.0
Methional	245.0	99.0	1.6
Compound	Concentration [mg/L]		
	Wort	Base 1	Base 2
Acetaldehyde	0.9	3.3	4.9
Ethyl acetate	0.3	14.9	24.7
Isoamyl acetate	<0.05	2.2	3.6
Amyl alcohols	<1.1	32.0	53.3

The amount of steam that is fed to the spinning column determines the degree of dealcoholisation and hence the ethanol concentration in the product and the distillate stream. It is expressed as the strip rate applied, which can be calculated from condensate and feed flow according to equation 3.1.

$$\text{Strip rate}[\%] = \frac{\text{Condensate flow } [\frac{\text{kg}}{\text{h}}]}{\text{Feed flow } [\frac{\text{kg}}{\text{h}}]} \quad (3.1)$$

A schematic drawing of the system is given in Figure 3.1. Due to the defined pathway through the unit, the residence time of the liquid is short (~20 s). If flavour recovery is desired, the process can be conducted in two passes, the first one being the “flavour” strip at a strip rate of 2 % and the second one being the dealcoholisation step at a strip rate of 30 %. The flavours stripped out in the first stage can be reintroduced to the base, depending on the preferred ethanol and aroma levels [24].

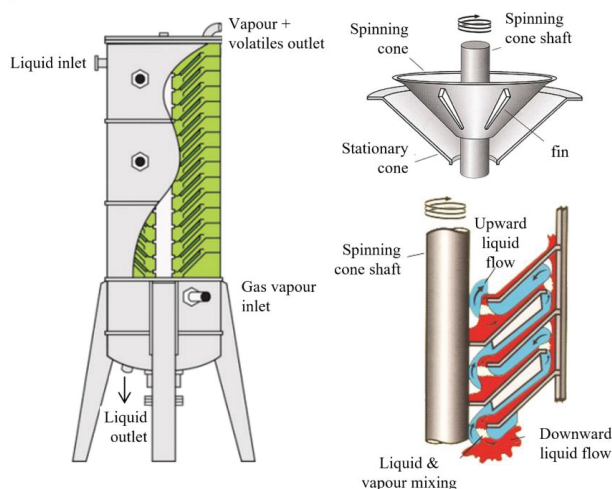


Figure 3.1: Schematic drawing of the SCC of Flavourtech [24]

An overview of all performed test is given in Table 3.3. Due to the large scale of the experiment, the each setting was carried out only once. Each feedstock was fed to the dealcoholisation unit from the top and counter-currently contacted with food-grade steam at an operational temperature of 42-45°C, a vacuum pressure of 0.11 bar and a rotational speed of the cones of 350 rpm. The flow rate varied between 150 – 400 L/h, depending on the feed stream. The feed stream was pre-heated, so that there was no temperature off-set, when entering the column.

Table 3.3: Overview on performed tests with the SCC

Fed Base	External stripping rate
Wort ^a	2 passes:
Base 1	- flavour strip at 2 %
Base 2	- dealcoholisation at 30 %
Base 2 + ribose solution (56 g/L)	
Wort	3.5 %
Wort	5.0 %
Wort	30.0 %
Base 2	2.0 %
Base 2	3.5 %
Base 2	5.0 %
Base 2	30.0 %

^a Although the wort does not contain alcohol, it will also be subjected to the same dealcoholisation conditions so that the impact of the SCC technology on removal of wort off-flavours can be assessed

3.2.4. Analysis of volatile aldehydes

To analyse aldehydes, an adapted method of Vesely *et al.* [25] was employed using headspace solid-phase micro-extraction (HS-SPME) in a GC-MS (Agilent 7890A and 5975C MSD) and

a 30 m x 0.25 mm x 0.25 μm VF17MS column. In order to increase the selectivity for aldehydes, the compounds were derivatized with O-(2,3,4,5,6-pentafluorobenzyl)-hydroxylamine. The carrier gas, helium, was used at a flow rate of 1 mL/min. Calibration was carried out with internal standard addition, so that matrix effects were taken into account [26].

3.2.5. Analysis of esters and higher alcohols

Ethyl acetate, isoamyl acetate, isoamyl alcohol and acetaldehyde were measured by headspace gas chromatography (7820A, Agilent Technologies, The Netherlands) equipped with a flame ionization detector (7890B, Agilent Technologies, The Netherlands) according EBC method 9.39 [27]. A polar capillary narrow bore column (DBWaxETR, 60 m * 0.32 mm ID, 1 μm fused silica) was used for separation and 4-heptanon and 1-butanol were added to each sample as internal standard to increase the accuracy.

To quantify phenethyl alcohol, ethyl decanoate and ethyl dodecanoate, samples were prepared by stir bar sorptive extraction (SBSE) for one hour with a preconditioned PDMS coated stir bar (Twister from Gerstel, United States). In order to account for matrix effects an internal standard was added. After the extraction, the bar was removed, rinsed with distilled water, carefully dried and placed into an open-ended glass tube for analysis in the Agilent (United States) 7890B gas chromatograph equipped with a 50 m x 0.25 mm x 0.25 μm DB-5MS Ultra inert column (Agilent 22-555-2UI). The target compounds were detected with a mass spectrometer (Agilent 5977A) in electron ionization scan mode.

3.2.6. Analysis of diketones

Diketones are measured with an adapted method of Ruehle et al. [28] by headspace gas chromatography (7820A, Agilent Technologies, The Netherlands) equipped with a fused silica WCOT CP Sil CB wide bore column (50 m x 0.53 mm x 1 μm). The separated compounds are detected with an electron capture detector and 2,3-hexanedione was used as internal standard to increase accuracy.

3.2.7. Statistical analysis

The standard deviation of the sample σ and the standard error σ_m^2 were calculated as described in equation 3.2 and 3.3, respectively [29]. All plots in the results section show the standard deviation of the analytical measurement. For aldehydes, the standard deviation was calculated from duplicates, while for diketones, esters, and higher alcohols, the measurement was carried

out with a single measurement and the standard deviation was calculated beforehand from the statistical deviation of 30 samples. During each measurement, two control samples were included, to ensure that the measurement was within the previously determined interval. For the deviation in the flow, a relative error of 5.5 % was assumed, characteristic for centrifugal pumps [30]. The propagated error σ_{mQ} was calculated as described elsewhere [29].

$$\sigma = \sqrt{\frac{1}{(n-1)} \sum_{i=1}^n (x_i - \bar{x})^2} \quad (3.2)$$

$$\sigma_m = \frac{\sigma}{\sqrt{n}} \quad (3.3)$$

3.3. Results

3.3.1. Impact of strip rate on volatile aroma profile

From literature, it is known that volatile components, which contribute to the flavour of beer, are nearly depleted during dealcoholisation. Usually, this is an unwanted effect as it results in a bland product, lacking the characteristic fruitiness of a regular beer [3]. In the case of wort flavours, however, a removal from the non-alcoholic product is regarded as beneficial because their concentration in AFBs is usually higher and due to the lack of ethanol and esters, they are over-perceived. Therefore, the effect of the strip rate on the aldehyde concentration in the final product was studied.

The first feedstock investigated is regular wort. Figure 3.2 A depicts the effect of the applied strip rate during stripping with the SCC on the absolute concentration in dominant Strecker aldehydes. On the one hand, a significant reduction of the volatile aldehydes, 2- and 3-methylbutanal, is observed in the range of 3.5-5.0 % strip rate. After passing wort two times through the unit, the residual concentration of 2-MB and 3-MB ranges between 3.3 and 11.9 $\mu\text{g/L}$, respectively. This means a reduction of 92-95 % compared to the initial aldehyde content. On the other hand, methional shows a relatively different behaviour as such that the initial reduction in concentration is less pronounced and an almost linear decrease is measured. This is attributable to the higher boiling point and the more hydrophilic character of methional, which makes it more difficult to remove the compound by thermal methods. At the highest strip rate of 32 % (two passes), methional's concentration is 96.9 $\mu\text{g/L}$ or 60 % of the initial amount. This means that due to the low sensory threshold of methional, it is still perceivable in the end-product.

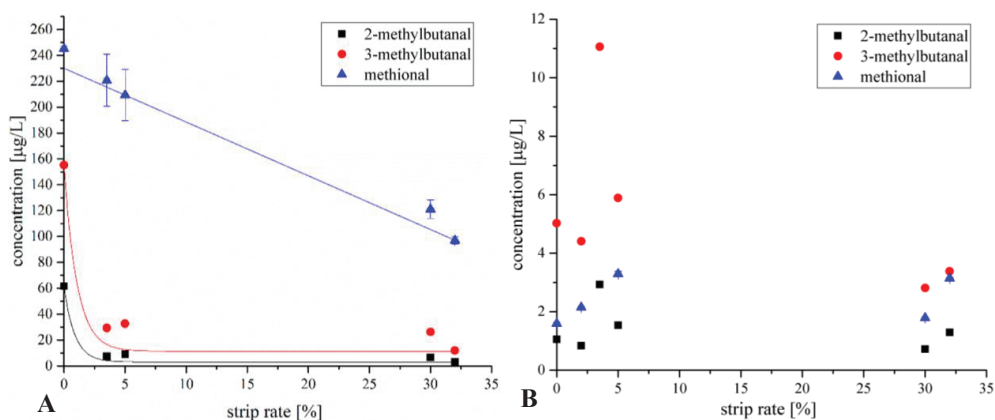


Figure 3.2: Concentration of 2-methylbutanal, 3-methylbutanal and methional in (A) thermally treated wort and (B) dealcoholized beer (AFB 2) in dependency of the strip rate

The second feedstock, which was investigated, is a regular beer. The concentration of Strecker aldehydes versus the (external) strip rate is plotted in Figure 3.2 B. There is no clear trend observed for either of the molecules. Instead, a parallel process of evaporation and formation appears to be involved, which could explain the variation in the product concentration. Whether this formation is through release from a bound state or through Strecker degradation is not known. However, there seems to be a lower limit to which the compounds are removed.

Diketones are flavour active molecules, which have been reduced by the yeast to a concentration level in $\mu\text{g/L}$ level during the fermentation. Nonetheless, if their concentration exceeds the acceptable threshold, the perception of an off-flavour may be the result [31]. They can also act as educts to react with amino acids to Strecker aldehydes [32]. Similar to the Strecker aldehydes, diketone concentrations were measured for each strip rate applied as depicted in Figure 3.3 for wort as feedstock (A) and dealcoholized regular beer (B).

When stripping wort at lower strip rates the level of diketones is initially reduced. At strip rates higher than 5 %, it appears that the concentration slowly approaches a plateau. The lowest level achieved for 2,3-pentanedione is 5.7 $\mu\text{g/L}$ and 8.8 $\mu\text{g/L}$ for diacetyl to 30 % and 23 % of their initial concentration, respectively. On the contrary, for the case of beer as feedstock dealcoholisation causes a slight increase in both compounds e.g. 24 % for 2,3-pentanedione and approximately 58 % for diacetyl. It is interesting to note that the final concentration of both compounds is slightly higher in AFB 2 than in the thermally treated wort, although initially the level in wort was much higher. For diacetyl, this might be because the concentration of α -acetolactate in fermented beer is higher and diacetyl is liberated during the application of heat [31].

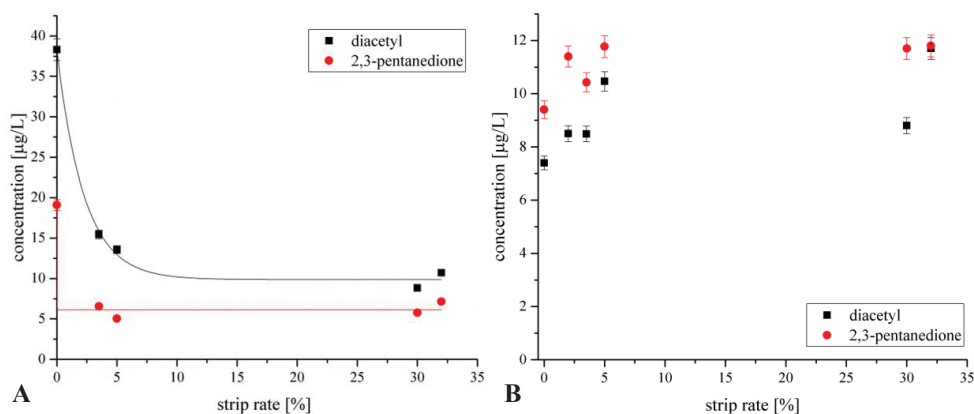


Figure 3.3: Concentration of diacetyl and 2,3-pentanedione in dependency of the strip rate in the SCC system; A) in wort (Apparent extract 7.2°P); B) in dealcoholized beer (AFB 2)

The above results show that despite the mild operation conditions under vacuum and the short residence time, the heat introduced to the system has an effect on the product flavour profile. For instance, diacetyl, 2,3-pentanedione and methional are found to be measurable and even increased in concentration, but have been found below the detection limit when produced with a membrane dealcoholisation technique at 10°C [22].

Similarly, the impact of the strip rate on the concentration in the end-product was measured for volatile components present at higher concentration (mg/L level) as shown in Figure 3.4. While the concentration of the esters ethyl acetate (EA) and isoamyl acetate (IAA) is depleted completely after applying a 2 % strip rate, acetaldehyde (AceA) is initially decreased, but then reaches a plateau as observed before for other aldehydes and diketones.

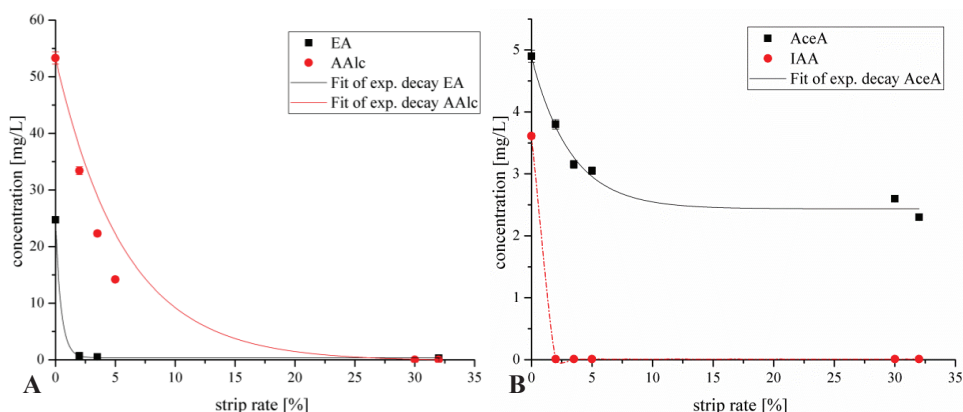


Figure 3.4: A) Concentration ethyl acetate and amyl alcohols B) Concentration of acetaldehyde and isoamyl acetate in dealcoholized beer (AFB 2) in dependency of the strip rate

The amyl alcohols (AAlc) show a slightly different behaviour: the energy, i.e. the strip rate required to remove them completely is distinctly higher, although their boiling points are in a similar range to IAA. Since these are more polar compounds, their vapour pressure is lower and it takes more energy to strip them off the liquid.

When analysing the volatile profile of the final products (flavour stripped at 2 % and dealcoholized by applying a 30 % strip rate), as shown in Table 3.4, the above taken observations are confirmed; higher levels of aldehydes and diketones are stripped from both the wort base and base 1, retaining a residual level of volatiles in the product. Methional and furfural's concentrations are also decreased, but to a lesser extent than the more volatile aldehydes 2-MP, 2-MB and 3-MB. A complete depletion of wort flavours is not achievable, which is particularly true for base 2.

Table 3.4: Concentration (\pm standard deviation from analysis) of aldehydes and diketones in inlet and outlet streams of the SCC

Base Concentration	Wort		AFB 1		AFB2	
	Inlet	Outlet	Inlet	Outlet	Inlet	Outlet
DA [$\mu\text{g/L}$]	38.3 ± 1.3	10.7 ± 0.4	19.8 ± 0.7	7.5 ± 0.3	7.4 ± 0.3	11.7 ± 0.4
PenD [$\mu\text{g/L}$]	19.1 ± 0.7	7.1 ± 0.3	13.3 ± 0.5	8.3 ± 0.3	9.4 ± 0.3	11.8 ± 0.4
AceA [mg/L]	0.9 ± 0.0	0.7 ± 0.0	3.3 ± 0.1	1.1 ± 0.0	4.9 ± 0.1	2.3 ± 0.1
2-MP [$\mu\text{g/L}$]	64.0 ± 0.0	4.3 ± 0.0	26.9 ± 0.0	2.7 ± 0.0	2.1 ± 0.0	2.6 ± 0.0
2-MB [$\mu\text{g/L}$]	61.6 ± 0.0	3.3 ± 0.0	25.3 ± 0.0	1.5 ± 0.0	1.1 ± 0.0	1.3 ± 0.0
3-MB [$\mu\text{g/L}$]	155.3 ± 0.0	11.9 ± 0.0	65.1 ± 0.0	14.9 ± 0.4	5.0 ± 0.0	3.4 ± 0.0
FF [$\mu\text{g/L}$]	923.8 ± 149.7	91.3 ± 1.3	373.1 ± 60.5	41.8 ± 1.6	6.0 ± 0.0	4.8 ± 0.0
MT [$\mu\text{g/L}$]	245 ± 0.0	96.9 ± 0.01	99 ± 0.1	59.9 ± 2.3	1.6 ± 0.0	3.1 ± 0.0

To have a closer look at the ester profile in the product, the composition of esters is illustrated for base 1 (regular beer) and AFB 2 in Figure 3.5. The ester and higher alcohol profile of dealcoholized products is completely distorted. Initially, isoamyl alcohol, ethyl acetate, phenethyl alcohol and ethyl decanoate are the major contributors to the measurable flavour profile. Additionally, there are lower concentrated esters such as isoamyl acetate and ethyl dodecanoate. After dealcoholisation only compounds with a high boiling point are retained. Hence, the major constituent of the flavour profile is phenethyl alcohol. Other originally contained constituents are depleted. As already suspected from Figure 18, this elucidates that esters and higher alcohols are, in contrary to aldehydes and diketones, not formed throughout the process, but only depleted until they appear below their detection limit.

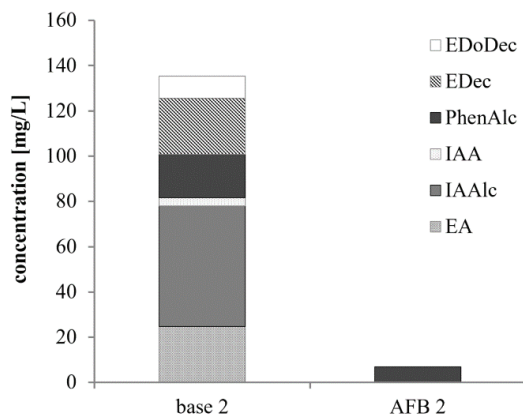


Figure 3.5: Ester and higher alcohol profile of base 2 before and after dealcoholisation with the SCC unit

EA: ethyl acetate; IAAlc: isoamyl alcohol; IAA: isoamyl acetate; PhenAlc: phenethyl alcohol; EDec: ethyl Decanoate; EDoDec: ethyl dodecanoate

3.3.2. Impact of heat and mass balance on overall system

In order to prove that the overall formation of aldehydes and diketones during the thermal dealcoholisation is caused by heat-induced Maillard reactions, an experiment was carried out where base 2 was spiked with glucose, maltose, maltotriose and ribose with 2.0, 24.7, 10.1, and 5.0 g/L, respectively. Ribose is a reactive pentose that serves as a precursor in the heat-induced reaction to furfural [33]. The ribose containing feedstock was dealcoholized at standard conditions and samples of the aroma condensate, distillate and product were analysed. Then, the mass balance over the system was formulated and visualized in Figure 3.6. If a compound is neither formed, nor depleted, the relative increase is equal to zero. A negative number indicates a loss during the operation e.g. loss via the vacuum pump or reaction to another molecule. A positive value means a compound was formed during the process. It is very clear that furfural is formed during the operation and shows an increase of more than 20 times compared to the inlet stream. Most of the furfural is found in the distillate, which is why the impact of pasteurization can be excluded in this case. This clearly indicates that heat induced reactions are accelerated during dealcoholisation. Furthermore, methional is found to increase, which results from the increase in reactive α -dicarbonyl compound derived from ribose and glucose via the Amadori product [34]. In the case of 2-methylpropanal, 2- and 3- methylbutanal, it is suspected that a major amount is lost to the environment via the vacuum pump and thus the formation cannot be traced back by the mass balance. Nonetheless, the concentration of heat indicator furfural in the product diluted to the final specifications amounts to only 9.9 $\mu\text{g/L}$

(13.7 µg/L undiluted). Hence, furfural is not expected to have an impact on the product taste. This was confirmed by a trained sensory panel: Despite the formation of furfural, off-flavours describing a caramelized or burnt taste were not detected (data provided in appendix, Figure 3.7).



Figure 3.6: Relative increase of aldehydes and diketones during dealcoholisation of Glucose/Ribose-mix obtained from mass balance

3.4. Conclusion

This work comprises a systematic study of the impact of thermal dealcoholisation on the volatile composition of AFBs. Through the thermal dealcoholisation of studied beer bases, Strecker aldehydes 2-MB and 3-MB were significantly reduced by up to 92-95 %, where the extent of the reduction depended on the applied strip rate. The concentration of highly volatile molecules was independent of the starting concentration. As an exception, the separation of methional proved to be difficult, due to the compound's low volatility. Since it exhibits a low flavour threshold, this may cause overly worty products. For the case of dealcoholized regular beer, thermal aldehyde removal is not an effective option, since the simultaneous formation during the evaporation process determines the lower reachable concentration limit in the end-product. Closing the mass balance over the system, it was also found that despite the vacuum conditions, heat indicators such as furfural were formed during dealcoholisation. This is, however, irrelevant for the product taste, since the sensory threshold of these compounds is relatively high. It is concluded that for AFBs with a higher wort flavour content, thermal dealcoholisation is a good technology to reduce wort flavour perception. For future research, new technologies should be investigated to enable a selective and complete removal of wort flavour to further optimize the aroma profile of AFBs.

3.5. Acknowledgement

The authors would like to thank Heineken Supply Chain B.V. for the funding provided for this project and the opportunity to carry out the pilot scale tests at their facilities. We also like to thank to Jan-Pieter van Kempen for facilitating the tests, Phil Riley and Fábio da Silva for the technical support to run the SCC unit and Fred Olierook for his knowledge on the analytical equipment.

3.6. References

1. Müller, M., et al., Physikalische Verfahren zur Entalkoholisierung verschiedener Getränkematrizes und deren Einfluss auf qualitätsrelevante Merkmale. *Chemie Ingenieur Technik*, 2016. 88(12): p. 1911-1928.
2. Liguori, L., et al., Chapter 12 - Production of Low-Alcohol Beverages: Current Status and Perspectives, in *Food Processing for Increased Quality and Consumption*, A.M. Grumezescu and A.M. Holban, Editors. 2018, Academic Press. p. 347-382.
3. Brányik, T., et al., A review of methods of low alcohol and alcohol-free beer production. *Journal of Food Engineering*, 2012. 108(4): p. 493-506.
4. Mangindaan, D., K. Khoiruddin, and I.G. Wenten, Beverage dealcoholization processes: Past, present, and future. *Trends in Food Science & Technology*, 2018. 71: p. 36-45.
5. Priest, F.G. and G.G. Stewart, *Handbook of brewing*. 2006, CRC/Taylor & Francis: Boca Raton.
6. Hiralal, L.P., B.; Olaniran, A.O., Stability profile of flavour-active ester compounds in ale and lager beer during storage. *African Journal of Biotechnology* 2013. 12(5): p. 491-498.
7. Piornos, J.A., et al., Orthonasal and retronasal detection thresholds of 26 aroma compounds in a model alcohol-free beer: Effect of threshold calculation method. *Food Res Int*, 2019. 123: p. 317-326.
8. Meilgaard, M.C., *Flavor chemistry in beer: Part II: Flavor and flavor threshold of 239 aroma volatiles*. Master Brewers Association of the Americas, 1975. 12: p. 151-168.
9. Gernat, D.C., Brouwer, E., Ottens, E., Aldehydes as Wort Off-Flavours in Alcohol-Free Beers - Origin and Control. *Food and Bioprocess Technology*, in press.
10. Beal, A.D. and D.S. Mottram, Compounds contributing to the characteristic aroma of malted barley. *Journal of Agricultural and Food Chemistry*, 1994. 42(12): p. 2880-2884.
11. Perpète, P. and S. Collin, Contribution of 3-methylthiopropionaldehyde to the worty flavor of Alcohol-free beers. *Journal of Agricultural and Food Chemistry*, 1999. 47(6): p. 2374-2378.

12. Schonberg, A. and R. Moubacher, The Strecker Degradation of α -Amino Acids. *Chemical Reviews*, 1952. 50(2): p. 261-277.
13. Baert, J.J., et al., On the origin of free and bound staling aldehydes in beer. *J Agric Food Chem*, 2012. 60(46): p. 11449-72.
14. Andrés-Iglesias, C., et al., Comparison of carbonyl profiles from Czech and Spanish lagers: Traditional and modern technology. *LWT - Food Science and Technology*, 2016. 66: p. 390-397.
15. Saison, D., et al., Contribution of staling compounds to the aged flavour of lager beer by studying their flavour thresholds. *Food Chemistry*, 2009. 114(4): p. 1206-1215.
16. Evellin, F., P. Perpète, and S. Collin, Yeast ADHI disruption: A way to promote carbonyl compounds reduction in alcohol-free beer production. *Journal of the American Society of Brewing Chemists*, 1999. 57(3): p. 109-113.
17. Perpète, P. and S. Collin, Influence of beer ethanol content on the wort flavour perception. *Food Chemistry*, 2000. 71(3): p. 379-385.
18. Perpète, P. and S. Collin, Fate of the worty flavours in a cold contact fermentation. *Food Chemistry*, 1999. 66(3): p. 359-363.
19. Perpète, P. and S. Collin, How to improve the enzymatic worty flavour reduction in a cold contact fermentation. *Food Chemistry*, 2000. 70(4): p. 457-462.
20. Strejc, J., et al., Production of alcohol-free beer with elevated amounts of flavouring compounds using lager yeast mutants. *Journal of the Institute of Brewing*, 2013. 119(3): p. 149-155.
21. Van Iersel, M.F.M., et al., Influence of yeast immobilization on fermentation and aldehyde reduction during the production of alcohol-free beer. *Enzyme and Microbial Technology*, 2000. 26(8): p. 602-607.
22. Liguori, L., et al., Production and characterization of alcohol-free beer by membrane process. *Food and Bioproducts Processing*, 2015. 94: p. 158-168.
23. Loredana, L., et al., Impact of Osmotic Distillation on the Sensory Properties and Quality of Low Alcohol Beer. *Journal of Food Quality*, 2018. 2018: p. 11.
24. Flavourtech. Spinning Cone Column. 2018 [06.09.2019]; Available from: <https://flavourtech.com/products/spinning-cone-column/>.
25. Vesely, P., et al., Analysis of Aldehydes in Beer Using Solid-Phase Microextraction with On-Fiber Derivatization and Gas Chromatography/Mass Spectrometry. *Journal of Agricultural and Food Chemistry*, 2003. 51(24): p. 6941-6944.
26. Skoog, D.A., Leary, J.J., Nieman, T.A., *Principles of Instrumental Analysis*. 7th ed. 1998, Australia: Cengage Learning.

27. Analytica, EBC 9.39: Dimethyl Sulphide and other lower boiling point volatile compounds in beer by gas chromatography. 2000.
28. Ruehle, G., et al., Headspace gas chromatography/electron capture detector analysis of total vicinal diketones in beer. *Journal of the American Society of Brewing Chemists*, 2013. 71(4): p. 274-275.
29. Young, H.D., Statistical treatment of experimental data. McGraw-Hill paperbacks in physics. 1962, New York [etc.]: McGraw-Hill.
30. Tsukamoto, H., H. Yoneda, and K. Sagara, The Response of a Centrifugal Pump to Fluctuating Rotational Speed. *Journal of Fluids Engineering*, 1995. 117(3): p. 479-484.
31. Krogerus, K. and B.R. Gibson, 125th Anniversary Review: Diacetyl and its control during brewery fermentation. *Journal of the Institute of Brewing*, 2013. 119(3): p. 86-97.
32. Pripis-Nicolau, L., et al., Formation of Flavor Components by the Reaction of Amino Acid and Carbonyl Compounds in Mild Conditions. *Journal of Agricultural and Food Chemistry*, 2000. 48(9): p. 3761-3766.
33. Vanderhaegen, B., et al., The chemistry of beer aging – a critical review. *Food Chemistry*, 2006. 95(3): p. 357-381.
34. Smit, B.A., W.J.M. Engels, and G. Smit, Branched chain aldehydes: Production and breakdown pathways and relevance for flavour in foods. *Applied Microbiology and Biotechnology*, 2009. 81(6): p. 987-999.

3.7. Appendix

3.7.1. Sensory evaluation by trained panel

The samples were evaluated by a sensory descriptive panel, whose members are trained extensively on non-alcoholic beers and wort flavours. The attribute list is determined during a group discussion. The attribute intensities are quantified on a 100-point line scale during four individual sessions. Samples are offered one-by-one in randomized order. All samples were evaluated in duplicate measurements.

Panellists received 100ml of each product, presented in black-coated glasses, coded with three-digit codes. Samples were tasted at $\pm 7^{\circ}\text{C}$. Because two samples had to be mixed in advance of every taste session, all other samples were poured into a beaker as well and were treated in the same way. The sensory profile of AFB 1 and AFB 2 are compared in Figure 3.7.

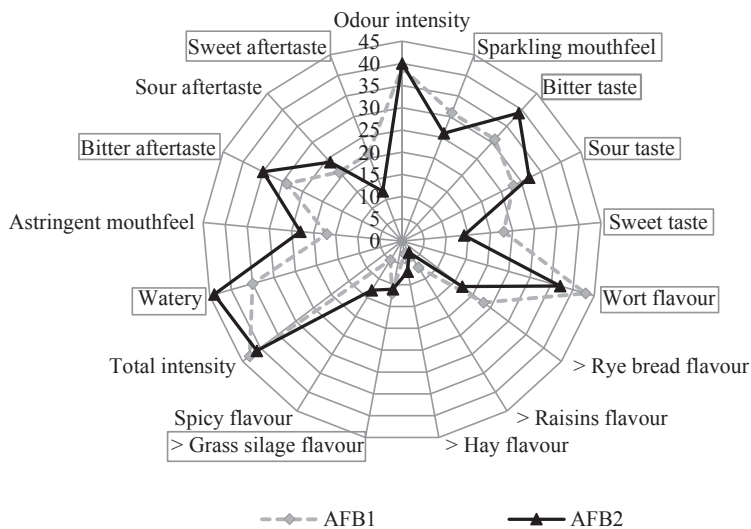
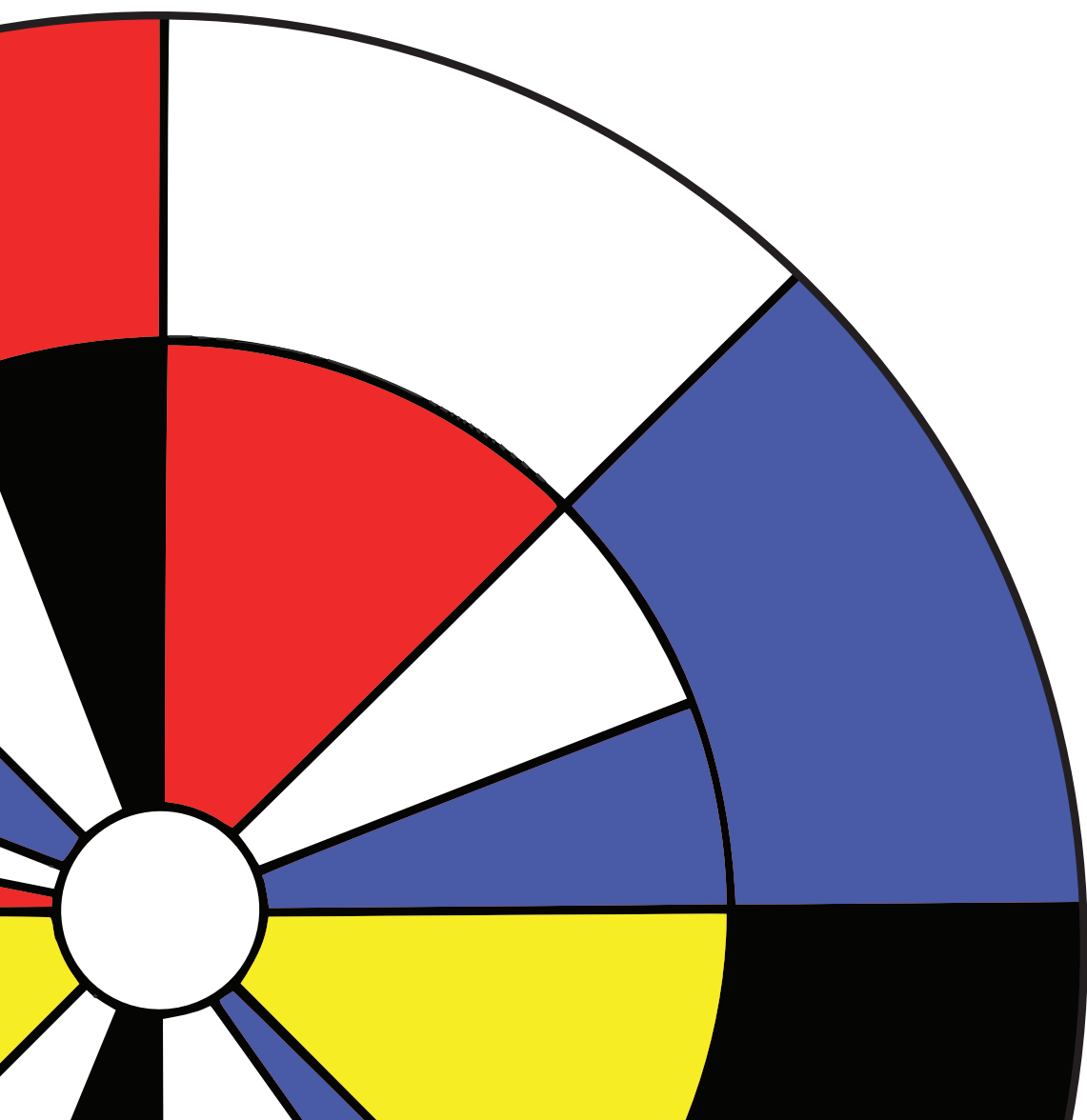


Figure 3.7: Sensory evaluation of AFB 1 and AFB t; Circled attributes have a significance level of <5%



Chapter 4

Selective off-flavour reduction by adsorption: A case study in alcohol-free beer

Abstract: A common sensory deficiency of alcohol-free beers (AFB) is caused by the presence of warty aldehydes. The aim of this study was to develop and proof the concept of a selective adsorption step, facilitating the removal of aldehydes from AFB. Therefore, the performance of 21 adsorbents (amine-functionalized polymers, hydrophobic resins and zeolites) was tested in wort. Among the studied adsorbents, hydrophobic ZSM-5 type zeolites (CBV28014, HiSiv3000 and ZSM-5 P-360) showed the best selectivity due to their 2-dimensional separation characteristics. Consequently, the obtained multicomponent isotherms in unhopped AFB revealed linear adsorption behaviour for all aldehydes, indicating non-competitive adsorption within the design space. The logarithms of the adsorption affinity constants were found to be linearly correlated to the compounds' hydrophobicity and solubility. The concept was proven at pilot scale of 150 L, resulting in a reduction of aldehydes between 43.7 – 70.2%, while conserving bitterness, pH and colour of the AFB. Future work will focus on the sensory evaluation of the flavour-improved product.

Published as: Gernat, D.C., Penning, M.M. , Swinkels, F.M., Brouwer, E.R., Ottens, M. Selective off-flavour reduction by adsorption: A case study in alcohol-free beer. J Food and Bioproducts Processing 121, 91-104 (2020)

4.1. Introduction

Current trends in the beverage industry show consumers' shift towards more health-conscious products [1, 2]. Therefore, there is an incentive to create alternative alcohol-free options, which preserve the high quality of the original beverage. A sensory imbalance often observed in alcohol-free beers (AFBs) is the over-perception of wort flavours [1-4]. These off-flavours are caused by so-called Strecker aldehydes, which are formed by a heat-induced reaction between a reducing sugar and an amino acid [5]. In particular, 2-methylbutanal (2-MB), 3-methylbutanal (3-MB) and methional (MT) [6, 7] have been found responsible for the wort flavour, but also 2-methylpropanal (2-MP) is relevant at the concentration range in AFBs [8]. Due to the changed composition of AFB, flavour detection thresholds are significantly lower than in regular beer [8-11]. For instance, the odour of 3-MB is detected at 56 µg/L in regular beer, while the threshold in AFB is with 0.44-0.61 µg/L more than 91 times lower [9, 10]. Their formation may also be caused by other reactive carbonyls, such as lipid derived carbonyls or quinones from polyphenol oxidation [12-15]. As a result of the complexity of involved reaction pathways, it is difficult to prevent Strecker aldehyde formation [10, 16]. Therefore, new process designs are required to engineer the desired flavour profile and fine-tune the aroma concentration to the respective product [11]. For this study, 2-MB, 3-MB, Met, 2-MP and furfural (FF) were taken into account, where FF was regarded as a general indicator for flavour instability in beer [17]. Their structures and flavour descriptors are outlined in Figure 4.1.

In brewing literature, studies have been performed on reducing Strecker aldehydes in alcohol-free beer by restricted or continuous fermentation (biological removal) [18-20] or by addition of certain beer constituents, such as amino acids, wort proteins or polyphenols that bind or mask aldehydes [20-22]. The drawbacks of these approaches are that the concentration of the target compounds is not sufficiently reduced and that ethanol is often a side product. Newer developments include membrane-based separation of flavours [23, 24] or adsorptive removal with activated carbon or resins [25, 26], but the selectivity for a targeted removal is still insufficient. Other approaches, as for instance extraction or reactive removal, have been restricted to an application in organic chemistry, food packaging or bulk chemical production [11, 27-30].

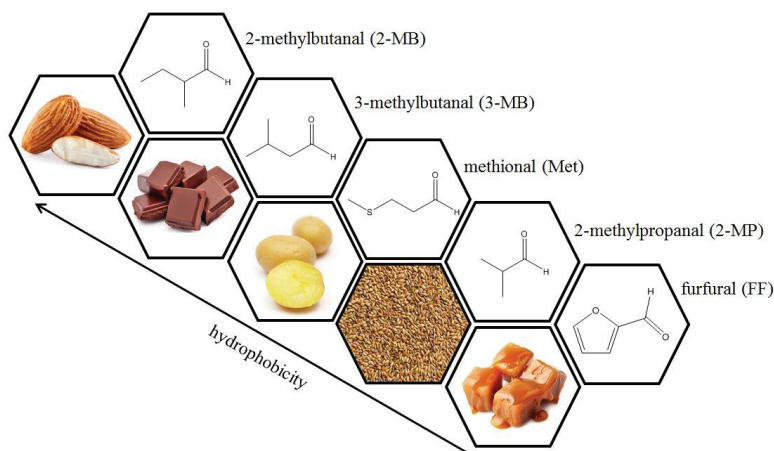


Figure 4.1: Molecular structure of selected wort flavour compounds and their associated flavour listed in order of hydrophobicity

Currently, there are no downstream unit operations available to selectively remove wort off-flavours without impacting the overall taste and nutritional quality of the product. The process requires a technology that combines a high selectivity at mild operation conditions with low capital investment and operational cost. A suitable choice for this challenging task is adsorption [31], which enables the separation of compounds present at low concentrations with a low heat impact on the product [32]. An application for the brewing industry was for instance demonstrated by Saffarionpour *et al.*, who captured flavours on polymeric resins [33, 34].

The goal of this article is to investigate the feasibility of a selective (off-)flavour removal step for the case of non-alcoholic beer by identifying an adsorbent material that can facilitate this specific separation under mild conditions. Therefore, batch uptake experiments with 21 adsorbents were performed in a hopped wort base to screen for the most promising separation medium. Three types of adsorbent were considered, i.e. hydrophobic resins (HR), amine-functionalized polymeric resins (AFP) and microporous silica-based materials (zeolites). The selection for further process development was then made based on a Pugh decision-matrix [35]. Subsequently, multicomponent isotherm data was determined by a mixture-amount design [36], and a suitable model to describe the thermodynamic data was applied. Furthermore, the impact of the product constituents on the model parameters was measured to identify potential process bottlenecks. Finally, the best performing adsorbent was applied at pilot scale and the effect on the chemical composition of the product quality was assessed to provide a proof of principle.

4.2. Materials and Methods

4.2.1. Chemicals

For the preparation of solutions, Milli-Q grade water (Merck Millipore, United States) or absolute ethanol (VWR International BV, The Netherlands) of analytic grade was used. The test kit 984345 for the enzymatic analysis of ethanol and free amino nitrogen (FAN) were purchased from Thermo Scientific (United States) and FoodLab (Italy), respectively. Iso- α -acids were acquired from Barth Haas Ltd (United Kingdom). All other chemicals were purchased in analytical grade from Sigma Aldrich.

4.2.2. Feedstocks

Wort and alcohol- and hop-free beer produced by restricted fermentation were obtained from a local brewery. Original extract, alcohol content and the concentration of iso- α -acids are specified in Table 4.1.

Table 4.1: Specification of original extract, alcohol and iso- α -acids content in wort and alcohol-free beer (AFB)

Parameter	Wort	AFB
Original extract [°P]	16.68 \pm 0.05	12.00 \pm 0.04
Ethanol [% v/v]	<0.06	<0.06
pH	5.0 \pm 0.02	4.40 \pm 0.02
Colour [EBC]	17.50 \pm 0.21	11.40 \pm 0.14
Total iso- α -acids [mg/L]	36.80 \pm 0.7	<0.04

4.2.3. Adsorbents

Polymeric resins, listed in Table 4.3, were investigated, differing in pore and particle size, surface area, and polymer type. Furthermore, amine-functionalized polymers and hydrophobic resins were purchased from Sigma Aldrich. The AFPs were chosen based on their functional group as depicted in Table 4.4. The presence of pores was not specified by the supplier and not visible by microscopic analysis (supplementary material). A total of nine silica-based materials were selected to study different zeolite types and a range of the molar SiO₂/Al₂O₃ ratios (15-360) of different suppliers as specified in Table 4.5. The specifications are as provided by the supplier, if not mentioned otherwise.

Table 4.3: Hydrophobic resins specifications

Name	Supplier	Pore Size [Å]	Pore Volume [ml/g]	Particle size [µm]	Surface area [m ² /g]	Polymer type
Amberlite XAD4	Sigma Aldrich	100	0.98	250-841	750	Styrene-divinylbenzene
Amberlite XAD16N	Sigma Aldrich	200	0.55	250-841	800	Styrene-divinylbenzene
Amberlite XAD7HP	Sigma Aldrich	300-400	0.5	250-841	380	Polyacrylics
Sepabeads SP20SS	Sigma Aldrich	260	1.01	50-100	~ 500	Styrene-divinylbenzene
Sepabeads SP850	Sigma Aldrich	38	~ 1.2	250-850	~ 1000	Styrene-divinylbenzene
Diaion HP-2MG	Sigma Aldrich	170	1.2	297-707	~ 500	Polymethacrylate

Table 4.4: Amine-functionalized polymers specifications

Name of functional group (polymer-bound)	Supplier	Particle size [µm]	Ligand density [mmol N/g]
Aminomethylpolystyrene	Sigma Aldrich	163-210	1.0-1.5
Diethylenetriamine	Sigma Aldrich	37-74	4.0-5.0
Sulfonyl amide	Sigma Aldrich	74-149	1.5-2.0
Tris(2-aminoethyl)amine	Sigma Aldrich	37-74	3.5-5.0
2-mercaptoethylamine	Sigma Aldrich	163-210	0.6-1.1
Ethylenediamine	Sigma Aldrich	74-149	4.0-5.7

Table 4.5: Silica-based materials specifications

Name	Supplier	Type	Nominal cation form	MR SiO ₂ /Al ₂ O ₃	Pore size [nm]	BET surface area [m ² /g]
CP811C-300	Zeolyst	beta	hydrogen	300	0.56-0.67 [37]	620
Beta-zeolite P-150	ACS material	beta	hydrogen	150	0.55-0.70	~500
ZSM-35	ACS material	ferrierite	hydrogen	15	0.5-0.6	~300
HiSiv1000	UOP	y-zeolite	n/a	n/a	0.8	>550
HiSiv3000	UOP	ZSM-5	n/a	>1000	0.6	>400
CBV28014	Zeolyst	ZSM-5	ammonium	280	0.53-0.59	400
ZSM-5 G-360	ACS material	ZSM-5	hydrogen	360	0.53-0.59	>340
ZSM-5 P-360*	ACS material	ZSM-5	hydrogen	360	0.53-0.59	>380
ZSM-5 P-25	ACS material	ZSM-5	hydrogen	25	0.53-0.59	>=340

Non-zeolites				MR SiO ₂ /TiO ₂		
Ti-Silicalite-1 (Type B)	ACS material	-	-	>25	~0.5	360-420

*ZSM-5 G-360 is the granular (binderless) form of ZSM-5 P-360

4.2.4. Experimental Design

The experimental strategy for the adsorbent selection pursued in this work is outlined in Figure 4.2. In the first step, the adsorptive aldehyde removal of 21 resins was investigated by batch uptake experiments in the hopped wort base. This base was chosen, as it is the most concentrated base during the brewing process (16.7°P) with the highest concentration of aldehydes, but also sugars and hop acids, hence effects of competing constituents are expected to be most pre-dominant in this base. The phase ratios used in this experiment are 50 g/g_{wet} and 100 g/g_{dry} for polymeric resins and molecular sieves, respectively. Since the wet/dry-resin ratios are between 0.32-0.64 g_{dry}/g_{wet}, these phase ratios are in a similar range. Preliminary experiments with varying phase ratios showed that the adsorption was linear in this range. In order to compare the capacity of all adsorbents with each other, the aldehyde loadings at 50 g/g_{wet} for all resins and 100 g/g_{dry} for silica-based materials were calculated. The obtained samples were additionally analysed for change in pH and fading in colour as well as the adsorbent's reusability. For selected batches, the uptake of iso- α -acids, originating from hops, was measured.

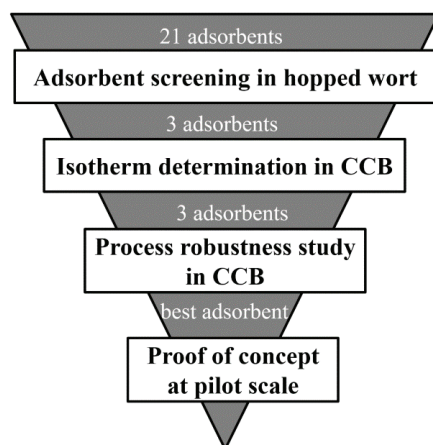


Figure 4.2: Sequential experimental design approach

In the second step, the three most promising adsorbents were selected, and batch uptake experiments based on a five-component mixture-amount design without centre points were

performed with a fixed phase ratio of 1000 gCCB/g_{dry} [36]. Here, the base chosen was an AFB produced by cold contact fermentation. Cold contact fermented beer (CCB) is made by contacting wort at low temperatures of 0-1°C with yeast, so that the metabolism of the microorganism is restricted and ethanol production is minimal [3]. The concentration of aldehydes is reduced by the yeast to a certain extent [21], while the concentration of other compounds, such as sugars, stays nearly the same, meaning that wort and CCB mainly differ in their aldehyde concentration. However, in order to be able to study the impact of different beer constituents, the base in this stage of the study was brewed hop-free. An overview of the concentration levels (amounts) of all components at the low (-), and high (+) sub-level are given in Table 11, where the ratio of the aldehydes to each other was fixed for each level. Thereby, chosen boundary conditions of the design are based on historic data for wort and CCB. The selected amounts of added aldehydes, $C_{\text{aldehydes, added}}$, are 0 (base), 850, 2700, and 3500 µg/kg, respectively. These amounts were spiked to the hop-free CCB, resulting in the total aldehyde concentration, $C_{\text{aldehydes, total}}$, of the spiked base beer. Due to the bias related to determining volatile multicomponent samples, there are deviations between the targeted and actually measured concentration.

Table 4.6: Overview on selected experiments for the mixture-amount design

Level	C ₂ -MP, added [µg/kg]	C ₂ -MB, added [µg/kg]	C ₃ -MB, added [µg/kg]	C _{MT} , added [µg/kg]	C _{FF} , added [µg/kg]	C _{aldehydes} , added [µg/kg]	C _{aldehydes} , total [µg/kg]
Base	0	0	0	0	0	0	464
1+	37.1	52.4	234.3	65.1	0	389	853
1-	22.1	7.5	35.5	41.2	316.6	423	887
2+	104.1	120.1	538.9	185.7	335.2	1284	1748
2-	72.3	24.7	116.4	135.1	1037	1386	1850
3+	167.9	184.3	828.3	300.3	653.6	2135	2599
3-	120.1	41.0	193.4	224.4	1722	2301	2765
4+	230.8	247.8	1114.1	413.5	968.1	2974	3438
4-	167.1	57.0	269.1	312.2	2397	3202	3666

In the third step, using the same CCB as above, a model robustness studies were performed by spiking possibly-interfering molecules to batch uptake tests. The aim was to determine the impact of matrix constituents, polyphenols (represented by addition of 15 mg/kg catechin), diketones (represented by addition of 50 µg/kg 2,3-pentanedion), and sulphur compounds (represented by spiking with 40 µg/kg of dimethyl sulphide (DMS)) on the adsorption efficiency at the upper end of the design space. Furthermore, the hop-originating molecules were assessed by spiking with 36.8 mg/kg iso- α -acids (level of wort from screening

experiment) and the influence of the pH variation (adjustment to wort pH 5.0 with 3 M NaOH). The conditions tested in triplicate are shown in Figure 4.3. Finally, the ZSM-5 G-360 was tested at pilot scale at a phase ratio of 0.15 L/g_{dry} to give a proof of concept and show the relevance of the results for the commercial scale.

4.2.5. Batch uptake experiments

Prior to each batch uptake experiment, adsorbents were washed in five consecutive steps with two volumes of 70 vol.% of ethanol and three volumes of Milli-Q water, allowing the adsorbent to equilibrate 30 min in the second and fourth washing step. Zeolites were dried at 220°C until they reached a stable weight to remove any residual liquid. The required amount of wet or dry resin was then added to a 40 mL screw-top vial (Supelco). Next, 35 g of wort or non-alcoholic beer were poured to the vial and spiked were applicable; the batch was stirred overnight with the screw top closed in a water bath at 15°C to reach equilibrium. Succeeding, the liquid was separated from the adsorbent by centrifugation and transferred into a fresh glass vial for analysis.

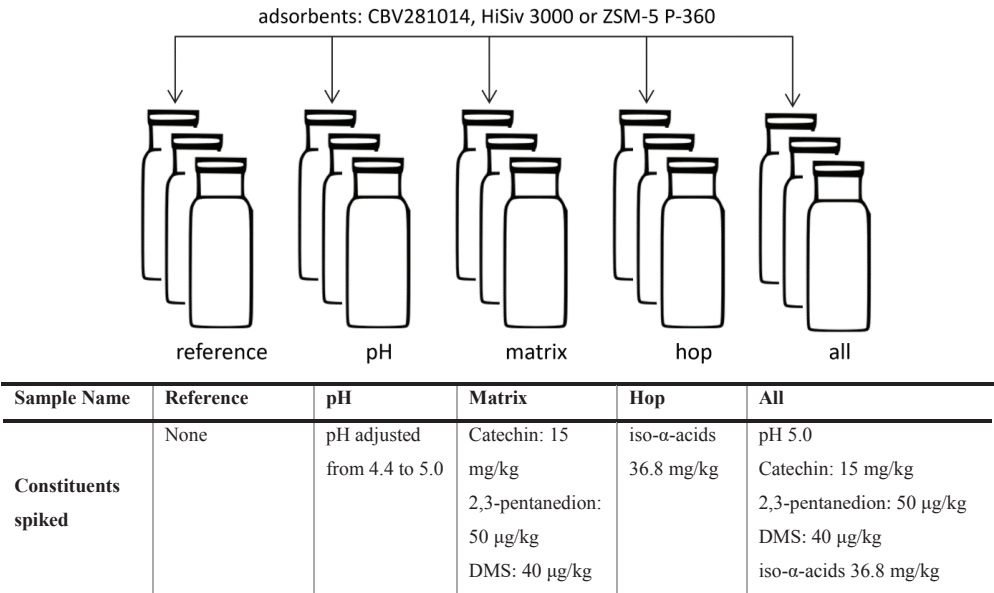


Figure 4.3: Overview on robustness study performed with CBV281014, HiSiv 3000 and ZSM-5 P-360. All aliquots were spiked with 300, 1300, 6000, 400 and 1000 µg/kg of 2-MP, 2-MB, 3-MB, Met and FF, respectively.

By forming the mass balance, the loading of the adsorbent q_i [µg/g_{ads}] was calculated according to equation 4.1, where $c_{ini,i}$ and $c_{e,i}$ [µg/L] are the initial and equilibrium concentration of the

aldehyde, respectively, m_{ads} [g] is the mass of added adsorbent, m_l [g] is the mass of added wort or beer and ρ_l is the density of the wort or the beer.

$$q_i = \frac{(c_{ini,i} - c_{e,i})}{m_{ads}} \frac{m_l}{\rho_l} \quad (4.1)$$

4.2.6. Pilot scale test

For the pilot scale, a batch of hopped wort was fermented at 2-4°C to produce a CBB meeting similar specifications as the base used during laboratory scale tests. The temperature was chosen slightly higher than the recommended 1°C in order to avoid local freezing of the wort. The batch was then split into two vessels of 1.5 hL, of which one was filled with 1.0 kg of zeolite granules (ZSM-5 G-360) and stirred overnight. Both batches were subsequently standardized to 5.2°P and filtered over Kieselguhr, pasteurized and bottled.

4.2.7. Adsorbent regeneration

In order to assess the reusability of the tested adsorbents, they were regenerated by the same procedure as described above and in the case of amine-functionalized resins, they were incubated overnight at room temperature in a 35 mL of a 0.03647 wt.% HCl solution. After neutralization with 2 M NaOH solution, the materials were rinsed with Milli-Q water, filtered and used for the batch uptake procedure described in previous section.

4.2.8. Analysis of volatile aldehydes

Strecker aldehydes were analysed by headspace solid-phase micro-extraction (HS-SPME) using a method adapted from Vesely *et al.* [38], in a GC-MS (Agilent 7890A and 5975C MSD) and a 30 m x 0.25 mm x 0.25 µm VF17MS column. The derivatization reaction was carried out with O-(2,3,4,5,6-pentafluorobenzyl)-hydroxylamine. Helium was used as the carrier gas at a flow rate of 1 mL/min. The calibration was performed for each medium, so that matrix effects on the measurement were accounted for [39].

4.2.9. Analysis of iso-α-acids

Iso-α-acids were analysed by reversed phase UPLC (Waters Acquity, Milford, United States) equipped with a PDA detector and a BEH C18 1.7 µm column (I.D. 2.1 x 150 mm) according to the EBC method 7.8 “Iso-alpha-, alpha- and beta-acids in Hop and Isomerized Hop Extracts by HPLC” [40].

4.2.10. Analysis of pH, colour and original extract

The determination of the specific gravity at 20°C/20°C and thus extract content of wort was obtained by digital density meters of the oscillation type (Xample 510, Anton Paar, Graz, Austria). For a quantitative measurement of changes in the beverage, the change in pH was measured with a pH-meter (Accumet Basics AB15, Fisher Scientific, Landsmeer, The Netherlands). The colour was determined according to the EBC method 9.6 [41] with a Spectrostar Nano spectrophotometer supplied by BMG Labtech (Ortenberg, Germany). The colour value was then calculated with the empiric equation 4.2, where A_{430nm} is the absorption at 430 nm and d the dilution factor.

$$colour [EBC] = A_{430nm} \cdot 25 \cdot d \quad (4.2)$$

4.2.11. Determination of leaching

A ligand leaching test for the amine-functionalized resins was performed using the LCK138 cuvette test kit for total N-content with a measuring range of 1-16 mg/L (Hach, Tiel, The Netherlands). The resins were washed as described and incubated in an HCl solution at pH 5.1. Hereafter, the resins were separated from the liquid, which was analysed for total N-content with a Hach DR3900 VIS spectrophotometer according to the method described by the manufacturer.

4.2.12. Analysis of ethanol

The ethanol concentration was measured with an enzymatic test kit available from Thermo Fisher Scientific (United States) as recommended in EBC method 9.3.1 [42]. The alcohol is enzymatically oxidized to acetaldehyde under alkaline conditions, which in turn is converted to acetate producing two moles of NADH per mole ethanol. The produced amount of NADH was determined spectrophotometrically by measuring the absorbance at 340 nm and 37°C with Thermo Fisher Scientific Gallary™ Plus Beermaster.

4.2.13. Analysis of DMS, esters and higher alcohols

The concentration of volatile compounds other than aldehydes was analysed by headspace gas chromatography (7820A, Agilent Technologies, The Netherlands) equipped with a flame ionization detector (7890B, Agilent Technologies, The Netherlands) as described in EBC method 9.39 [43]. The compounds were separated on a polar capillary narrow bore column (DBWaxETR, 60 m x 0.32 mm ID, 1µm fused silica). 4-heptanon and 1-butanol were used as internal standard to increase the accuracy.

4.2.14. Determination of foam stability, turbidity and FAN

The foam stability was measured according to EBC method 9.42.1 with a NIBEM-T meter (Pentair Haffmans, The Netherlands) at room temperature [44]. The turbidity was analysed according to MEBAK method 2.14.1.2 “Haze formation: Optical Method” [45]. FAN was determined with the CDR Beerlab FAN test kit with the procedure described by the manufacturer.

4.3. Calculations

4.3.1. Pugh evaluation matrix

In order to identify the most promising adsorbents, a Pugh evaluation matrix was employed as a tool to rank tested materials based on their capacity, selectivity, costs and simplicity to industrialization according to equation 4.3, weighted 30%, 40%, 10% and 20%, respectively. The score of each category was assigned based on Table 4.7.

$$Score = 0.3 \cdot Score_{capacity} + 0.4 \cdot Score_{selectivity} + 0.1 \cdot Score_{costs} + 0.2 \cdot Score_{industrialization} \quad (4.3)$$

Table 4.7: Score key for Pugh evaluation matrix

Score	-1	0	+1
Capacity*	$q_{2-MB} + q_{3-MB} + q_{Met} < 20$ $\mu\text{g/g}_{dry}$	$20 \mu\text{g/g}_{dry} < q_{2-MB} + q_{3-MB} + q_{Met} < 40$ $\mu\text{g/g}_{dry}$	$q_{2-MB} + q_{3-MB} + q_{Met} > 40$ $\mu\text{g/g}_{dry}$
Selectivity pH colour hop	Overall = average score (pH, colour, hop)		
	$\Delta\text{pH} > 0.6$	$0.3 < \Delta\text{pH} < 0.6$	$\Delta\text{pH} < 0.3$
	$\Delta\text{colour} > 3.0$ EBC	$1.5 \text{ EBC} < \Delta\text{colour} < 3.0$ EBC	$\Delta\text{colour} < 1.5$ EBC
	iso- α -acids adsorbed	n/a	iso- α -acids not adsorbed
Costs	Price > 1000 €/kg	n/a	Price < 1000 €/kg
Industrialization	Leaching of adsorbent components	Could be employed but material has to be certified	already employed in food industry

* wet weight was converted to dry weight with approximated conversion factor of $0.5\text{g}_{wet}/\text{g}_{dry}$

4.3.2. Isotherm model

Due to the low concentration of investigated components, a linear adsorption isotherm model was used to describe the thermodynamic equilibrium as depicted in equation 4.4, where k_i [L/g_{ads}] is the affinity constant characteristic for each component and adsorbent [46].

$$q_i = k_i c_{e,i} \quad (4.4)$$

4.3.3. Error Analysis and regression

The reported uncertainties were calculated, considering the statistical error resulting from random variation of measured values and the systematic error. The sample standard deviation and error propagation was calculated as described elsewhere [47]. For the systematic error only the uncertainty associated with the parameter regression of the calibration was taken into account, since other equipment errors were comparably negligible. To obtain the error of regressed isotherm parameters, the variance-covariance matrix M , calculated by multiplying the variance of the residuals of the best fit with the Jacobian J of the fitting function was used as described in equation 4.5.

$$M = \frac{(J^T J)^{-1} \sum_{i=1}^n res_i^2}{n - p} \quad (4.5)$$

where n is the number of data points and p the number of regressed parameters. The diagonal of the covariance matrix contains the variances of each parameter [48].

4.3.4. Determination of logD and solubility

The $\log D$ value was estimated with Advanced Chemistry Development, Inc. (ACD/Labs) [49]. The experimental solubility at 25°C was taken from EPISuites™ [50] when available or estimated from $\log P$ with the same program.

4.4. Results & Discussion

4.4.1. Adsorbent Screening

In order to choose the most suitable separation medium, three different adsorbent types, i.e. hydrophobic resins, amine-functionalized resins, and zeolites, making up to 21 adsorbents, were selected for a screening experiment. Their performance with respect to capacity and selectivity are depicted in Table 4.8 and Table 4.9. In order to estimate and compare the capacity of the tested adsorbents, the adsorbent loading was calculated for 2-MB, 3-MB and Met, respectively.

From the data presented, it is observed that the capacity of the hydrophobic resins is mainly related to the available surface area, rather than to the pore size or volume. Generally, the performance of poly(styrene-divinylbenzene) based resins is superior. From Table 4.8, it is conspicuous that amongst tested AFPs, only ethylenediamine (EthD)- and diethylenetriamine (DETA)-functionalized divinylpolystyrenes are comparable in capacity with the conventional hydrophobic resins. This might be due to the fact that the reaction of the primary amine group

with the aldehyde to form an imine is not favourable enough to ensure selectivity over organic acids, ketones and other reactive compounds contained in the wort. EthD and DETA are able to form imidazoline rings with aldehydes, which is a more specific reaction mechanism. The hypothesis is that this mechanism causes the observed higher reduction in aldehydes for EthD and DETA. Having a denser loading of functional groups, EthD thereby achieves a higher degree of aldehyde removal than DETA.

When considering product integrity and process variables such as throughput and capital investment costs, factors other than the capacity of reduction are highly important for selecting an optimal adsorbent. Therefore, the resulting wort-flavour reduced product was tested and evaluated for selected parameters, i.e. change in pH and colour, and adsorption of iso- α -acids (hop constituents), as well as reusability.

It is clear that the tested hydrophobic resins generally perform better with respect to the capacity, but more poorly in selectivity than most AFPs. This is because of the fact that all hydrophobic molecules in the feedstock interact with the solid surface, without any selectivity for functional groups or size. Nonetheless, these resins are tested in the food industry and FDA approved, enabling the fast scale-up and commercialization of this process.

The theoretical loading of the AFPs depends on the number of moles of nitrogen attached to the resin. It can be easily determined by a stoichiometric relation, neglecting impact factors such as steric hindrance. For most resins, the theoretical capacity is by a factor of 10^4 - 10^5 higher than the achieved loading in competitive batch uptake experiments, i.e. other beer constituents react with the scavenger groups or the equilibrium is not favourable. There are two other disadvantages, which make AFPs unattractive to optimize flavour in food products. First, the kinetics of the reaction are observed to be very slow and temperature-dependent (data provided in supplementary material), which may cause practical complications in food processing. Second, leaching of the functional group was measured (data not shown), which is an undesired effect and might lower the food safety and product quality.

When regarding the tested molecular sieves in comparison, both – high reduction and selectivity – is achieved. The drawbacks of the (functionalized) resins are overcome by their 2-dimensional separation mechanism, which selects on hydrophobicity as well as size. The choice of a small and defined pore-size ($<0.7\text{nm}$) and a high $\text{SiO}_2/\text{Al}_2\text{O}_3$ -ratio are of uttermost importance for the efficiency of the removal step. For instance, if the performance of ZSM-5 P-360 is compared to ZSM-5 P-25, the zeolite with the lower $\text{SiO}_2/\text{Al}_2\text{O}_3$ ratio depicts a lower capacity for the

flavour molecules, while a significant change in pH is observed. This indicates that ZSM-5 P-25 is also adsorbing small (organic) acids, despite the fact the pore size is the same. Similarly, a larger pore size of the beta- and Y-zeolites, lead to an increased uptake of larger molecules, such as iso- α -acids, potentially distorting the taste of the AFB. This in turn also reduces the affinity and hence the capacity of the adsorbent such as HiSiv1000. Interestingly, CP811C-300 and the β -zeolite from ACS Materials, show a different adsorption of iso- α -acids, despite the fact that their pore size and ring structure should be similar. Since CP811C-300 also exhibits a slightly higher surface area and the two-fold $\text{SiO}_2/\text{Al}_2\text{O}_3$ ratio, it is also unexpected that it adsorbs less hop acids.

Consequently, a Pugh evaluation matrix [35] was used as a decision tool to select the three most promising out of 21 materials as depicted in Table 4.10. Thereby, capacity, selectivity, costs and the ease of industrialization were taken into account, weighing the selectivity with 0.4 the most important category. Out of the tested adsorbents, molecular sieves generally show the highest score due to their superior selectivity and high capacity at acceptable material cost.

However, one drawback considered for molecular sieves, is the not-established food-grade. Another difficulty is that they are often only available in powder or larger pellet form, both of which are not advantageous for the scale-up to an adsorption column. The highest rated zeolites CBV28014, ZSM-5 P-360 and HiSiv3000 are selected for further study. Ti-Silicalite is ruled out, since it was observed that the sample turned hazy after the treatment, most likely due to the catalytic activity of Ti. The β -zeolite slightly adsorbs iso- α -acids, which in turn makes them a less attractive option. In the next step, the selected zeolites are studied in more detail, to obtain their isotherm data in the complex food matrix as well as the effects of other beer constituents on the regressed adsorption parameter.

Table 4.8: Affinity, selectivity (pH, colour, hop acid concentration), and economic factors of polymeric materials at PR 50 g/g_{wet}

Category	Parameter	7HP											
		XAD-16N	SP850	SP20SS	Diaion	XAD-7HP	XAD-4	EthD	AMP	DETA	SA	T2A	2ME
Capacity	q _{2-MB} [μg/g _{wet}]	4.7	4.7	4.3	2.5	3.2	4.7	4.6	0.5	2.7	0.8	1.0	2.3
	q _{3-MB} [μg/g _{wet}]	26.7	26.8	21.0	8.8	13.5	25.2	18.5	1.8	2.6	3.1	3.7	8.4
	q _{Met} [μg/g _{wet}]	10.5	10.7	6.4	3.7	3.5	10.9	9.3	0.9	1.2	1.5	3.3	2.1
Selectivity	Δ pH	0.1	0.1	0.1	0.1	0.1	0.1	1.0	0.0	0.3	0.1	0.2	0.1
	Δ colour [EBC]	-10.3	-7.6	-10.6	-5.8	-9.4	-6.0	-0.6	-5.4	-0.3	-0.1	-0.1	-0.4
	[(C ₁ -C ₂)/C] _{total iso-acids} [%]	n/a	99.1	n/a	n/a	n/a	80.1	47.5	n/a	7.3	n/a	n/a	n/a
Economics	Reusability	+	+	+	+	+	+	+	+	+	+	+	+
	Cost	+	+	-	+	+	+	-	-	-	-	-	-

Table 4.9: Affinity, selectivity (pH, colour, hop acid concentration), and economic factors of silica-based materials at PR 100 g/g_{dry}

Category	Parameter	CP-811C-300	β-zeolite P-150	ZSM-35-15	HSiv 1000	HSiv 3000	CBV 28014	ZSM-5 P-360	ZSM-5-25	Ti-Silicalite
Capacity	q _{2-MB} [µg/g _{dry}]	9.4	9.9	3.6	5.6	8.8	9.3	8.3	5.2	9.4
	q _{3-MB} [µg/g _{dry}]	39.4	10.6	1.7	8.8	16.7	39.8	15.9	5.6	10.0
	q _{MeI} [µg/g _{dry}]	20.1	5.2	3.5	9.7	23.6	23.2	22.7	2.8	5.4
Selectivity	Δ pH	0.1	-0.1	-0.3	0.2	0.3	0.1	0.0	-0.6	-0.1
	Δ colour [EBC]	3.6	1.1	1.0	2.8	0.8	1.1	-0.2	0.6	1.2**
	[(C ₁ -C ₂)/C ₁] _{total iso-acids} [%]	9.8	20.4	1.1	61.4	1.9	3.0	1.8	-2.7	7.2
Economics	Reusability	+	+	+	+	+	+	+	+	+
	Cost	+	+	-	+	+	+	+	+	-

** sample turned hazy

4.4.2. Isotherm determination

To determine the thermodynamic equilibrium data for the process design and to understand the multicomponent adsorption behaviour, batch uptake experiments were performed in unheated CCB. The adsorbent loading at the final equilibrium concentration was calculated, and the results are plotted in Figure 4.4. When considering the isotherm correlations in CCB, a clear linear relationship of the load and equilibrium concentration is found, indicating linear, non-competitive adsorption amongst aldehydes. Interestingly, the affinity constant k_i (see equation 4.4) of a compound is similar for all tested zeolites, with CBV28014 exhibiting slightly higher capacities for all aldehydes. This is due to the fact that these adsorbents all exhibit a high $\text{SiO}_2/\text{Al}_2\text{O}_3$ ratio (>280), a similar surface area ($\sim 380 - 400 \text{ m}^2/\text{g}$) and are of the same type (ZSM-5), ergo the micropore size is the same.

Table 4.10: Decision-matrix for Pugh concept selection

Adsorbents were evaluated based on their capacity at the given condition as well as selectivity with regard to change in pH, colour, iso- α -acid concentration and reusability and costs.

	Capacity (x 0.3)	Selectivity (x 0.4)	Costs (x 0.1)	Simplicity to Industrialization (x 0.2)	Score
CBV 28014	1	1.00	1	0	0.80
ZSM-5 P-360	1	1.00	1	0	0.80
HiSiv 3000	1	0.67	1	0	0.67
CP-811C-300	1	0.33	1	0	0.53
SP850	1	-0.33	1	1	0.47
XAD-16N	1	-0.33	1	1	0.47
XAD-4	1	-0.33	1	1	0.47
XAD-7HP	1	-0.33	1	1	0.47
SP20SS	1	-0.33	-1	1	0.27
β-zeolite	0	0.33	1	0	0.23
Ti-Silicalite	0	0.67	-1	0	0.17
Diaion	0	-0.33	1	1	0.17
2ME	0	1.00	-1	-1	0.10
HiSiv 1000	0	-0.33	1	0	-0.03
ZSM-5 MR 25	-1	0.33	1	0	-0.07
ZSM-35 MR 15	-1	0.67	-1	0	-0.13
EthD	1	-0.33	-1	-1	-0.13
SA	-1	1.00	-1	-1	-0.20
T2A	-1	1.00	-1	-1	-0.20
DETA	-1	0.67	-1	-1	-0.33
AMP	-1	0.00	-1	-1	-0.60

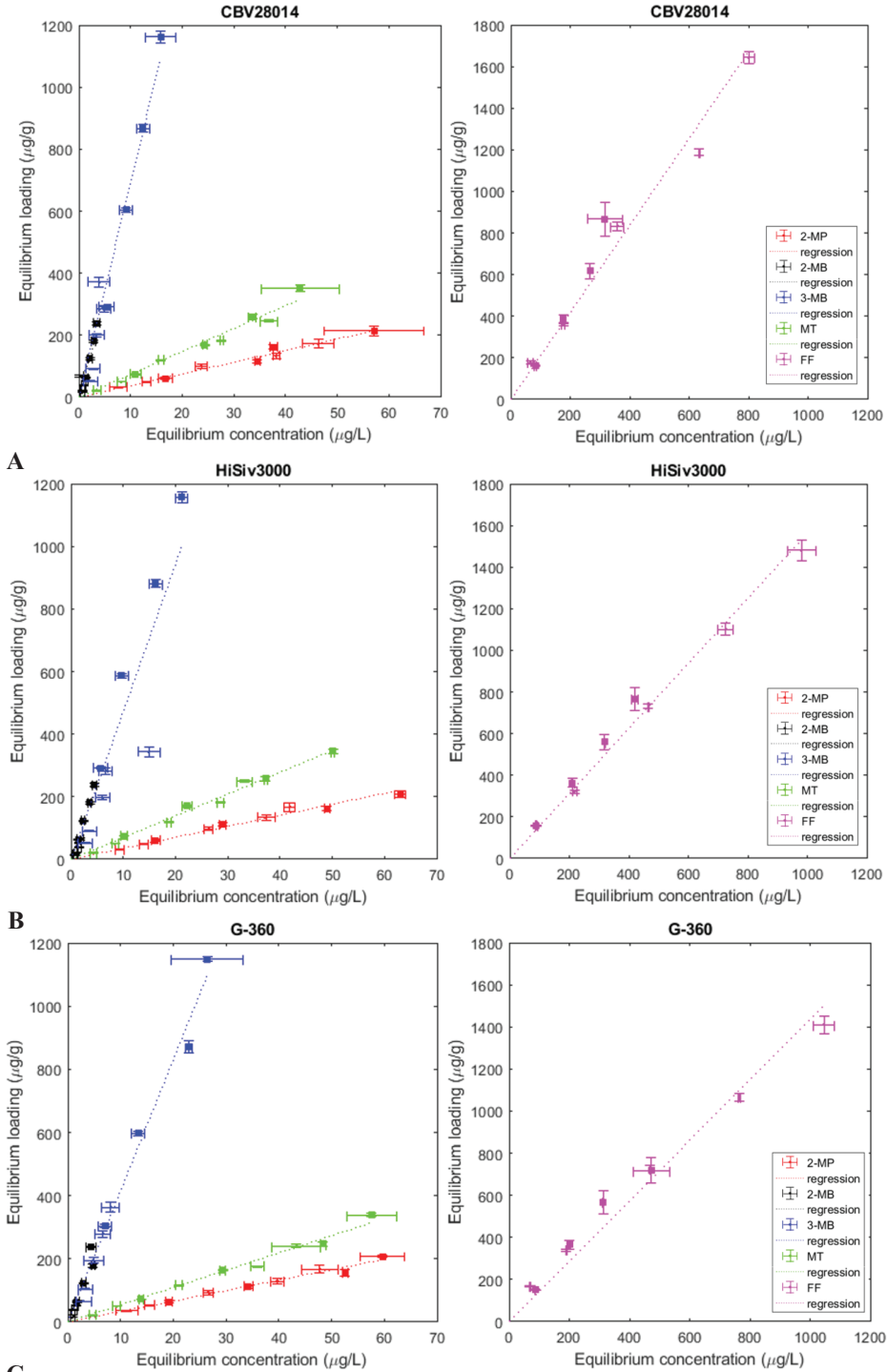


Figure 4.4: Experimental equilibrium data and regressed isotherms in unhopped CCB for A) CBV28014; B) HiSiv3000; C) ZSM-5 G-360 (crushed); full symbols represent sub-level (+) and dots sub-level (-) of the mixture-amount design

Another observation made is that the value of the affinity constant is correlated to the aldehyde's hydrophobicity. In the case of the studied aldehydes, the hydrophobic compounds 2- and 3-methylbutanal exhibit the highest affinity for the zeolites, while the affinity constants of methional, 2-methylpropanal and furfural are between factors of 6.2 – 33 smaller.

The relation of the compound's solubility and $\log D$ value to the regressed isotherm affinity constant is shown in Figure 4.5 and Figure 4.6, respectively. Here, the logarithmized isotherm affinity constant can be written as a linear function of the solubility in water or the $\log D$ value at pH 5.5, where the $\log D$ value is the octanol-water partition coefficient corrected for pH effects (ionization) [51]. It should be noted that the goodness of the fit strongly depends on the available experimental data and predictive model values for the solubility and the $\log D$ and as such are susceptible to the algorithm employed. Since beer is a very complex matrix, such a correlation is useful to estimate and predict the adsorption of other molecules to the adsorbent and hence assess, whether or not these could compete for vacant space on the adsorbent.

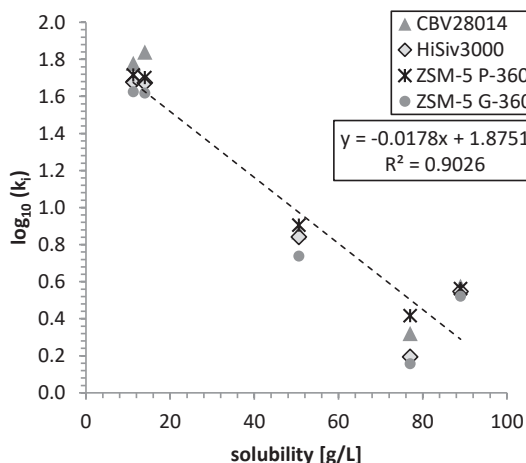


Figure 4.5: Logarithmized isotherm affinity constant $\log_{10}k_i$ in relation to solubility (from EPISuites [50]). Dashed line represents the regressed linear function taking the whole dataset into account.

However, because this correlation is only based on five molecules of the same chemical group, this should only be seen as an indication and not to precisely predict the impact of each molecule on the adsorption equilibrium. Thus, the approach followed in this work is not to define a universal model, taking into account every unique constituent of the beer, but rather to group beer constituents and assess their impact on the adsorption of aldehydes. This is to estimate,

whether or not a compound group could affect the measured adsorption parameters within defined variations in the process stream.

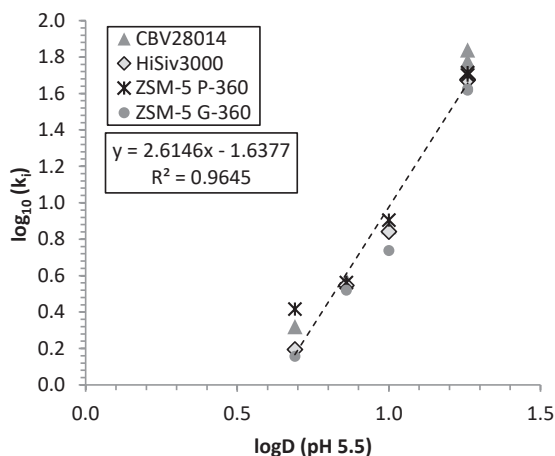


Figure 4.6: Logarithmized isotherm affinity constant $\log_{10}k_i$ versus to predicted $\log D$ value at pH 5.5 with ACD Labs model [49]. Dashed line represents the regressed linear function taking the whole dataset into account.

4.4.3. Identification of competing compounds

Table 4.11 lists important beer constituents their properties ($\log D$ value, solubility and geometry) and their relevance for the regarded process. To indicate the significance for the adsorption process, k_i is estimated based on the correlation in Figure 4.5 and Figure 4.6. It is obvious that many molecule groups can be excluded as competing molecules during the adsorption process. For instance, proteins are large molecules, which are not able to enter the small micropores of zeolites and hence are not directly impacting the adsorption equilibrium. Nonetheless, an indirect impact such as fouling or complexing with flavour compounds could be possible.

Several hydrophilic compounds are small enough to diffuse into the pores, however, are expected to have a very low affinity for the adsorbent due to their hydrophilicity. Even so, if present in high concentrations, hydrophilic compounds could have an effect on the thermodynamic equilibrium. For instance, sugars are present at g/L level, which according to literature causes a “salting out” effect [52]. This could lead to a higher affinity of hydrophobic molecules to the adsorbent. But since the sugar concentration is very well controllable during the brewing process, it is assumed to be a constant input parameter for the process and is not further studied.

Most likely, small volatile molecules that resemble the studied aldehydes in size and hydrophobicity will compete for vacant space on the adsorbent. Although they occur with a defined concentration range, small deviations could impact the process robustness.

For instance, components with a very high affinity to the adsorbent may take up more surface area and hence block vacant sites for aldehydes to attach. Furthermore, a change in the relative concentration ratios in the multicomponent system may influence the regressed affinity constants. Another aspect important for the process robustness are controlled changes in the input streams such as bitterness (related to hop acids) and pH. Esters and higher alcohols are expected to adsorb to the zeolite surface, however were not considered, since their concentration in alcohol-free beer is considerably low.

Consequently, the previously studied CCB is spiked with selected competing beer constituents to show the effect on the regressed affinity constants within a realistic deviation in the feed stream. Changes considered were an increase of the pH from 4.4 (beer) to 5.0 (wort), the addition of 36.8 mg/kg iso- α -acids (isohumulones) and a mix of other beer constituents. Based on Table 4.11, 2,3-pentanedione (50 $\mu\text{g/kg}$), DMS (40 $\mu\text{g/kg}$) and catechin (15 mg/kg) were selected to investigate the effect of matrix compounds on the regressed adsorption model parameters, since they all exhibited relevant estimations of k_i .

The resulting regressed affinity constants are depicted in Figure 4.7. When comparing the affinity constants of the different bases with each other, it is conspicuous that there is a relatively high spread around the reference value of the affinity constant. For 2-MB for instance, k_{2-MB} is around a third higher than the reference. Also, methional's affinity towards HiSiv3000 and P-360 seems to increase slightly, but significantly, when the base composition is changed. Some explanation could be hypothesized such as that at the lower pH, an ion exchange could take place, where the ammonium is replaced with a proton. This exchange could lead to a reduced pore size and hence to a decreased affinity. However, since the variation in the affinity constant is not observed for all aldehydes and there is no systematic phenomenon to be established, a more likely explanation is that the variation is based on the limited number of measurements. This is expected, since the affinity constants, regressed in Figure 4.7, are based on three measurements and not on a complete experimental design as shown in the previous section (isotherm determination). Nonetheless, there is no clear trend visible leading to the conclusion that k_i is not affected by the changes in the beer base and that the regressed affinity constants of the isotherm model are robust within the standard deviations for the studied case of CBV28014, HiSiv 3000 and ZSM-5 P-360 and could be used to design a pilot or industrial scale process.

For the pilot scale studies, the granular form of ZSM-5 P360 (G-360) was selected as it was readily available.

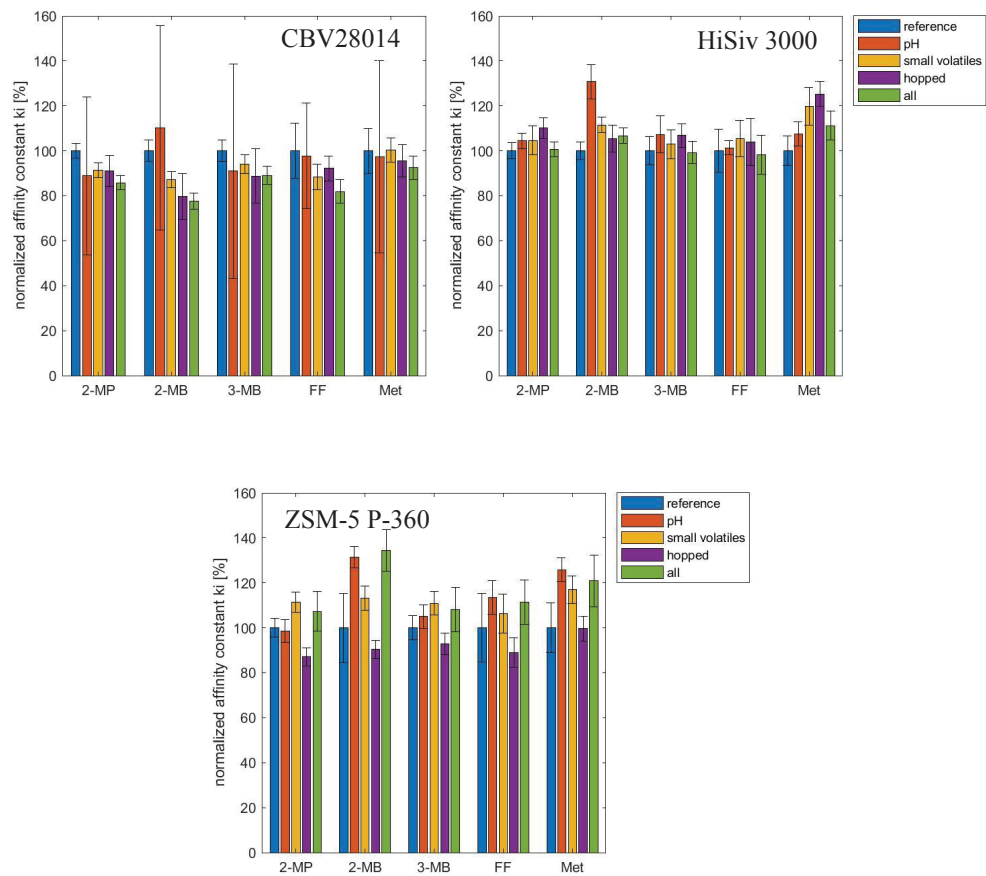


Figure 4.7: Impact of different base properties on regressed affinity constant k_i for CBV28014, HiSiv 3000 and ZSM-5 P-360 (blue: reference; red: pH increased; yellow: small volatiles added; purple: iso- α -acids spiked; green: pH increased, small volatiles and iso- α -acids added)

Table 4.11: Beer constituents and properties (logD at pH 5.5, solubility and minimal / maximal projection radius $r_{P,min}$ / $r_{P,max}$), and their relevance for the flavour adsorption process

Chemical group	Examples in beer	logD [49]	Solubility [g/L] [50]	$r_{P,min}$ - $r_{P,max}$ [Å] [53]	Relevance for flavour adsorption process
Aldehydes	3-MB	1.26	14.0	3.11-4.13	Target compounds, adsorb
	2-MB	1.26	11.23	3.47-4.03	
	2-MP	0.86	89	3.15-3.53	
	Furfural	0.69	77	3.08-4.12	
	Methional	1.00	50.55	2.91-4.97	
Solvent	Water	n/a	n/a	1.73-1.97	No adsorption
	Ethanol	-0.23	n/a	2.39 - 2.23	Could adsorb, but not relevant at low concentrations since $k_{est} = 0.005$ L/g _{dry} ² ; Modifier for matrix (AFB) hydrophobicity
Proteins					No access to micropores, thus no adsorption
	Protein Z	n/a	n/a	varying	Fouling
Lipids / fatty acids [54]	Linoleic acid	5.94	$3.77 \cdot 10^{-5}$	4.13-10.60	Could adsorb, but steric hindrance / slow kinetics likely
	Palmitic acid	6.23	0.00004	4.4 -11.87	
Sugars [55]	Glucose	-2.21	683	4.01-4.81	No adsorption;
	Maltose	-4.10	52.2	4.85-6.51	Possibly modifier for matrix (AFB) hydrophobicity
	Maltotriose	-4.49	n/a	5.28-7.18	
Minerals	Potassium	n/a	578		No adsorption
	Sodium	n/a	445.2		
Hop derived compounds	Isohumulones	1.14	0.01745	6.0 - 7.71	No adsorption due to size exclusion
	Cohumulone	4.31	0.04061	6.07-7.48	Blocking of pores or coking possible
	Adhumulone	2.41	$2.09 \cdot 10^{-3}$	6.65-7.53	Relative high, variable concentration (mg/L)
	Prehumulones	3.71	n/a	5.67-8.86	
Small volatiles	2,3-pentanedione	-0.28	66.7	3.17-3.89	Adsorbs; $k_{est} = 0.1 - 4.9$ L/g _{dry} ¹
	Diacetyl	-0.74	200	3.18-4.36	No adsorption
	DMS	1.32	22.0	2.58-3.54	Adsorbs, $k_{est} = 30.4-65.1$ L/g _{dry} ¹
	Ethyl acetate	0.87	80	2.85-4.46	Adsorbs, $k_{est} = 2.8 - 4.3$ L/g _{dry} ¹
	Isoamyl acetate	1.99	2	3.35-5.62	Adsorbs $k_{est} = 69.1 - 3676$ L/g _{dry} ¹
	Isoamyl alcohol	1.14	26.7	3.15-4.54	Adsorbs, $k_{est} = 22.0 - 25.1$ L/g _{ads} ¹
Vitamins	Riboflavin	-1.14	0.0847	6.33-7.48	No adsorption due to size exclusion
Polyphenols	Catechin	0.57	63.11	4.60-7.08	Might adsorb; $k_{est} = 0.7 - 5.6$ L/g _{ads} ¹
Free amino nitrogen (FAN)	Leucine	-1.86	21.5	3.41-5.12	Might adsorb; $k_{est} = 0 - 31.1$ L/g _{ads} ¹
	Methionine	-1.92	32.7-56.6	3.17-5.66	Might adsorb; $k_{est} = 0 - 19.6$ L/g _{ads} ¹
	Proline	-2.76	162.0	3.15-4.34	Might adsorption, $k_{est} = 0 - 0.4$ L/g _{ads} ¹
	Valine	-2.16	58.5 -74.4	3.32-4.18	Might adsorb; $k_{est} = 0 - 6.8$ L/g _{ads} ¹
	Tyrosine	-2.23	0.4-0.48	3.50-6.24	Might adsorb; $k_{est} = 0 - 73.8$ L/g _{ads} ¹

4.4.4. Proof of principle at pilot scale

To demonstrate the applicability of the principle at industrial scale, a test was performed at pilot scale of 1.5 hL using the same recipe as for the base beer as in previous section. Since it was

² Calculated by estimating k_i averaged for all adsorbents with correlation shown in Figure 4.5 and Figure 4.6

shown that hop compounds do not interfere with the adsorption process, the base was also hopped. Both, the reference and the treated CCB were analysed for their aldehyde concentration and general quality traits. The results are summarized in Figure 4.8 and Table 4.12, respectively.

The aldehyde concentrations measured in the final product are generally significantly lower than the reference sample. In the case of furfural, a decrease of 70.2% is measured, while compounds present in lower concentrations are reduced by 43.7 (MT) – 55.2 (2-MB)%. Since the concentration range is close, but well above the flavour detection threshold [9], it is expected that the reduction is also detectable by a sensory panel. However, based on the previously calculated affinity constants, the expected reduction was anticipated to be in the range of 90.5 – 99.6%. This difference could be explained by insufficient contact time and mixing during the tests: The granules exhibited a diameter of 2-3 mm, which is disadvantageous for the mass transfer in particular in the liquid systems, since the ratio of particle surface area to volume is significantly lower and the diffusion path much longer than for the powdered material. Hence, in order to utilize the whole intracrystalline surface area for adsorption and thus capacity of the adsorbent, the molecules have to diffuse through the stagnant layer of the particles as well as the macro- and micropores. At less optimal mixing conditions, film mass transfer is affected causing a significant increase in equilibrium time. Due to their weight, a portion of the granules was not suspended in the beer during the test. Another explanation is that part of the granules might not at all be accessible for the liquid, since the zeolite crystals are shaped into a densely pressed material. Thus, only a fraction of the theoretical capacity is utilized. Overall, this could have led to the point that the measured system was not yet in its equilibrium state and the observed non-optimal performance.

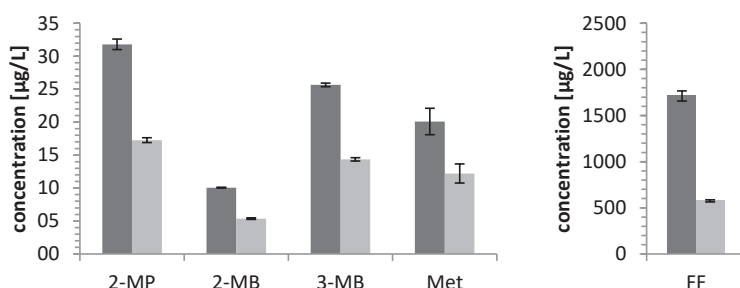


Figure 4.8: Concentration of aldehydes in reference AFB (dark grey) and AFB treated with ZSM-5 G-360 (light grey)

When comparing other quality parameters of the reference beer with the treated one, similar results were obtained for the colour, ethanol and FAN concentration, original extract, pH and

turbidity as depicted in Table 4.12. Small differences are found in the concentration of iso- α -acids, which is slightly increased and a decrease in foam stability of 7.8%. The latter might be due to the uptake of foam stabilizing components in the beer, while former is more difficult to explain. The concentration of alpha-acids was unchanged, indicating that no isomerization during the adsorption process could have occurred. Besides aldehydes, amyl alcohols, originally contained at 11.7 mg/L, were also removed from the product, so that their final concentration is below the detection limit (<1.1 mg/L). On the contrary, the amount of acetaldehyde was only slightly affected (decrease of 10%, from 1.9 to 1.7 mg/L). The concentrations of DMS and esters were below the detection limit and hence adsorption could not be observed. These findings correlate well with the results from the screening test and it is hence concluded that with some optimization of the mixing tank and zeolite granules, the process is scalable to industrial capacity.

Table 4.12: Quality parameters of AFBs produced at pilot scale after dilution from 12°P to 5.2°P

Quality trait	Reference beer	AFB treated with ZSM-5 G-360
Colour [EBC]	4.5 ± 0.1	4.6 ± 0.1
Ethanol [% v/v]	0.007 ± 0.0015	0.010 ± 0.0015
FAN [mg/L]	103 ± 2	103 ± 2
Foam stability [s]	309 ± 6	285 ± 5
Original extract [% m/m]	5.12 ± 0.02	5.28 ± 0.02
pH	4.55 ± 0.02	4.51 ± 0.02
Total iso- α -acids [mg/L]	24.8 ± 0.5	26.5 ± 0.5
Turbidity [[EBC]	0.5 ± 0.1	0.5 ± 0.1

4.5. Conclusion

This study successfully identified an adsorbent that can selectively remove wort flavour from complex food streams, such as alcohol-free beers. Out of the tested adsorbent, i.e. amine-functionalized polymers, hydrophobic resins and zeolites, the latter scored highest in their potential for selective wort flavour removal. Although zeolites have been used before to remove undesirable molecules from foodstuffs, the technology was applied to wort flavour removal from alcohol-free beers and a more fundamental approach was taken to systematically analyse the constituents of the complex mixture and to gain insight into their impact on the thermodynamic equilibrium of the involved adsorption mechanism. The experimental effort was reduced by combining a comprehensive screening experiment with a mixture-amount experimental design. In doing so, we showed that the suitability of the adsorbent is related to the matrix composition and that a careful selection of pore diameter and $\text{SiO}_2/\text{Al}_2\text{O}_3$ -ratio is

required to achieve the desirable selectivity. Hydrophobic ZSM-5 type zeolites achieved the best performance. Their adsorption equilibrium could be described with a linear isotherm in the AFB matrix, indicating a non-competitive adsorption step in this given matrix. The regressed affinity constants were directly related to the hydrophobicity of the flavour compounds. Consequently, it was shown that small changes in the matrix do not affect the regressed affinity constants. It is hence possible to design a new processing operation based on this data that facilitates a controlled off-flavour capture. Furthermore, a pilot scale test showed promising results with regard to the reduction in wort flavour. In the next step, it is aimed to prove the impact on the sensory perception with a trained panel.

Moreover, this technology is transferrable to other food systems and not restricted to a capturing step only. By extending the isotherm database to more flavours, a chromatographic separation and fractionation step could be introduced to fine-tune or control the aroma profile of foodstuffs. Future work should consequently also focus on the correlation of the measured flavour profile and the actual aroma and taste as evaluated by a sensory panel.

4.6. Acknowledgement

The authors would like to thank Heineken Supply Chain B.V. for funding this project and providing the raw materials and carrying out the pilot scale tests at their facilities. In particular, we would like to acknowledge Fred Olierook for his support with and technical knowledge on the analytical equipment.

4.7. References

1. Liguori, L., et al., Chapter 12 - Production of Low-Alcohol Beverages: Current Status and Perspectives, in Food Processing for Increased Quality and Consumption, A.M. Grumezescu and A.M. Holban, Editors. 2018, Academic Press. p. 347-382.
2. Blanco, C.A., C. Andres-Iglesias, and O. Montero, Low-alcohol Beers: Flavor Compounds, Defects, and Improvement Strategies. *Crit Rev Food Sci Nutr*, 2016. 56(8): p. 1379-88.
3. Brányik, T., et al., A review of methods of low alcohol and alcohol-free beer production. *Journal of Food Engineering*, 2012. 108(4): p. 493-506.
4. Mangindaan, D., K. Khoiruddin, and I.G. Wenten, Beverage dealcoholization processes: Past, present, and future. *Trends in Food Science & Technology*, 2018. 71: p. 36-45.
5. Schonberg, A. and R. Moubacher, The Strecker Degradation of α -Amino Acids. *Chemical Reviews*, 1952. 50(2): p. 261-277.

6. Beal, A.D. and D.S. Mottram, Compounds contributing to the characteristic aroma of malted barley. *Journal of Agricultural and Food Chemistry*, 1994. 42(12): p. 2880-2884.
7. Perpète, P. and S. Collin, Contribution of 3-methylthiopropionaldehyde to the worty flavor of Alcohol-free beers. *Journal of Agricultural and Food Chemistry*, 1999. 47(6): p. 2374-2378.
8. Meilgaard, M.C., Flavor chemistry in beer: Part II: Flavor and flavor threshold of 239 aroma volatiles. *Master Brewers Association of the Americas*, 1975. 12: p. 151-168.
9. Piornos, J.A., et al., Orthonasal and retronasal detection thresholds of 26 aroma compounds in a model alcohol-free beer: Effect of threshold calculation method. *Food Res Int*, 2019. 123: p. 317-326.
10. Saison, D., et al., Contribution of staling compounds to the aged flavour of lager beer by studying their flavour thresholds. *Food Chemistry*, 2009. 114(4): p. 1206-1215.
11. Gernat, D.C., Brouwer, E., Ottens, M., Aldehydes as Wort Off-Flavours in Alcohol-Free Beers - Origin and Control. *Food and Bioprocess Technology*, 2020. 13: p. 195-216.
12. Rizzi, G.P., The Strecker Degradation of Amino Acids: Newer Avenues for Flavor Formation. *Food Reviews International*, 2008. 24(4): p. 416-435.
13. Hidalgo, F.J., R.M. Delgado, and R. Zamora, Intermediate role of α -keto acids in the formation of Strecker aldehydes. *Food Chemistry*, 2013. 141(2): p. 1140-1146.
14. Hidalgo, F.J. and R. Zamora, Strecker-type Degradation Produced by the Lipid Oxidation Products 4,5-Epoxy-2-Alkenals. *Journal of Agricultural and Food Chemistry*, 2004. 52(23): p. 7126-7131.
15. Delgado, R.M., R. Zamora, and F.J. Hidalgo, Contribution of Phenolic Compounds to Food Flavors: Strecker-Type Degradation of Amines and Amino Acids Produced by o- and p-Diphenols. *Journal of Agricultural and Food Chemistry*, 2015. 63(1): p. 312-318.
16. Baert, J.J., et al., On the origin of free and bound staling aldehydes in beer. *J Agric Food Chem*, 2012. 60(46): p. 11449-72.
17. Andrés-Iglesias, C., et al., Comparison of carbonyl profiles from Czech and Spanish lagers: Traditional and modern technology. *LWT - Food Science and Technology*, 2016. 66: p. 390-397.
18. Van Iersel, M.F.M., et al., Influence of yeast immobilization on fermentation and aldehyde reduction during the production of alcohol-free beer. *Enzyme and Microbial Technology*, 2000. 26(8): p. 602-607.
19. Lehnert, R., et al., Effect of oxygen supply on flavor formation during continuous alcohol-free beer production: A model study. *Journal of the American Society of Brewing Chemists*, 2008. 66(4): p. 233-238.

20. Perpète, P. and S. Collin, Fate of the worty flavours in a cold contact fermentation. *Food Chemistry*, 1999. 66(3): p. 359-363.
21. Perpète, P. and S. Collin, How to improve the enzymatic worty flavour reduction in a cold contact fermentation. *Food Chemistry*, 2000. 70(4): p. 457-462.
22. Loredana, L., et al., Impact of Osmotic Distillation on the Sensory Properties and Quality of Low Alcohol Beer. *Journal of Food Quality*, 2018. 2018: p. 11.
23. Catarino, M., A. Ferreira, and A. Mendes, Study and optimization of aroma recovery from beer by pervaporation. *Journal of Membrane Science*, 2009. 341(1-2): p. 51-59.
24. Catarino, M. and A. Mendes, Non-alcoholic beer - A new industrial process. *Separation and Purification Technology*, 2011. 79(3): p. 342-351.
25. Shimizu, C.T., M., Process for producing malt alcoholic drink, in *Patentscope*, S.B. Limited, Editor. 2003.
26. Itakura, T., Ota, T., Owa, Y., Unfermented beer-flavored malt beverage having reduced unpleasant wort flavor and method for producing the same, in *FreePatentsOnline*, K. Beer, Editor. 2012.
27. Drese, J.H., A.D. Talley, and C.W. Jones, Aminosilica Materials as Adsorbents for the Selective Removal of Aldehydes and Ketones from Simulated Bio-Oil. *ChemSusChem*, 2011. 4(3): p. 379-385.
28. Jeřábek, K., L. Hanková, and Z. Prokop, Post-crosslinked polymer adsorbents and their properties for separation of furfural from aqueous solutions. *Reactive Polymers*, 1994. 23(2): p. 107-112.
29. Suloff, E.C., Sorption behaviour of an aliphatic series of aldehydes in the presence of poly(ethylene terephthalate) blends containing aldehyde scavenging agents. 2002, Virginia Polytech Institute and State University: Blacksburg, Virginia.
30. DelNobile, M.A., et al., Modeling of Hexanal Sorption Kinetic in an Aldehydes Scavenger Film Intended for Food Packaging Applications. *Journal of Food Science*, 2002. 67(7): p. 2687-2691.
31. Knaebel, K., Adsorption, in *Albright's Chemical Engineering Handbook*. 2008, Boca Raton: CRC Press.
32. Brauer, H., Adsorption Technology - An Area with Potential. *Chemie-Ingenieur-Technik*, 1985. 57(8): p. 650-663.
33. Saffarionpour, S., et al., Selective adsorption of flavor-active components on hydrophobic resins. *Journal of Chromatography A*, 2016. 1476: p. 25-34.
34. Ottens, M., S. Saffarionpour, and T.R. Noordman, Method of producing beer having a tailored flavour profile (EP14183788.0), in *Patentscope*. 2016, Heineken Supply Chain B.V.

35. Pugh, S., Total Design: Integrated Methods for Successful Product Engineering. 1 ed. 1991: Addison-Wesley.
36. Cornell, J.A., Experiments with Mixtures: Designs, Models, and the Analysis of Mixture Data. 3rd ed. 2002: John Wiley & Sons, Inc. New York.
37. Baerlocher, C., L.B. McCusker, and D.H. Olson, BEA - P4122, in Atlas of Zeolite Framework Types (Sixth Edition). 2007, Elsevier Science B.V.: Amsterdam. p. 72-73.
38. Vesely, P., et al., Analysis of Aldehydes in Beer Using Solid-Phase Microextraction with On-Fiber Derivatization and Gas Chromatography/Mass Spectrometry. Journal of Agricultural and Food Chemistry, 2003. 51(24): p. 6941-6944.
39. Skoog, D.A., Leary, J.J., Nieman, T.A., Principles of Instrumental Analysis. 7th ed. 1998, Australia: Cengage Learning.
40. Analytica, EBC of the European Brewery Convention, Fifth edition, 1998, fifth supplement, Method 7.8 (Iso-alpha-, alpha- and beta-acids in Hop and Isomerised Hop Extracts by HPLC). 2005.
41. White, F.H., Spectrophotometric determination of malt colour. J. Inst. Brew., 1995. 101: p. 431-433.
42. Analytica, EBC 9.3.1: Ethanol in alcohol-free and low alcohol beers: Enzymatic Method (IM). 2013.
43. Analytica, EBC 9.39: Dimethyl Sulphide and other lower boiling point volatile compounds in beer by gas chromatography. 2000.
44. Analytica, EBC 9.42.1: The determination of the foam stability of beer using the NIBEM-T meter. 2004.
45. MEBAK-E.V., 2.14.1.2. Haze Formation Optical Method. 2013: Freising, Germany.
46. Guiochon, G., Fundamentals of preparative and nonlinear chromatography. 2nd ed. ed. 2006, Boston: Elsevier.
47. Young, H.D., Statistical treatment of experimental data. McGraw-Hill paperbacks in physics. 1962, New York [etc.]: McGraw-Hill.
48. Tellinghuisen, J., Statistical Error Propagation. The Journal of Physical Chemistry A, 2001. 105(15): p. 3917-3921.
49. Advanced Chemistry Development, I.A.L. ACD/Percepta Platform. 2019 28.08.2019]; 2018.1:[Available from: www.acdlabs.com.
50. Agency, U.E.P., Estimation Programs Interface Suite™ for Microsoft® Windows. 2019, United States Environmental Protection Agency: Washington, DC, USA.

51. Xing, L. and R.C. Glen, Novel Methods for the Prediction of logP, pKa, and logD. *Journal of Chemical Information and Computer Sciences*, 2002. 42(4): p. 796-805.
52. Perpète, P. and S. Collin, Influence of beer ethanol content on the wort flavour perception. *Food Chemistry*, 2000. 71(3): p. 379-385.
53. Chemicalize. Geometrical Descriptors Plugin. 2019 [cited 2019; Available from: <https://chemicalize.com>.
54. Bravi, E., et al., Determination of free fatty acids in beer wort. *Food Chemistry*, 2014. 151: p. 374-378.
55. He, Y., et al., Wort composition and its impact on the flavour-active higher alcohol and ester formation of beer - A review. *Journal of the Institute of Brewing*, 2014. 120(3): p. 157-163.

4.8. Supplementary Material

4.8.1. Microscopic analysis

The microscopic analysis of Ethylenediamine-functionalized resins was performed with a scanning electron microscope (SEM) of type JSM6300 (JEOL, Tokyo, Japan). Therefore, the sample coated with gold, placed on a holder and fixed with carbon tape. The measurement was performed at a pressure of $<5 \cdot 10^{-5}$ Pa. The obtained pictures are presented in Figure 4.9.

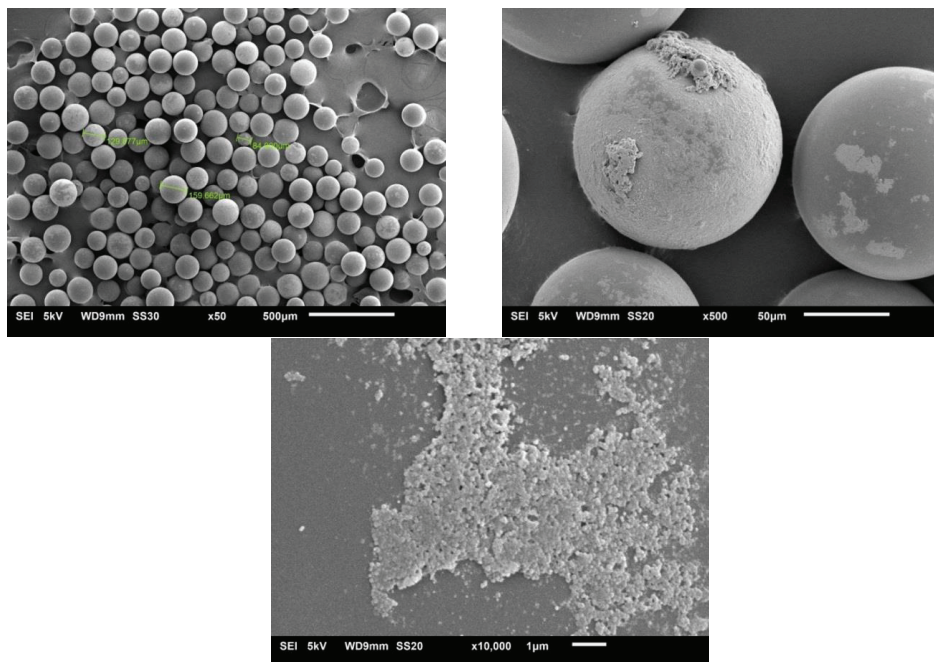


Figure 4.9: SEM pictures polymer bound Ethylenediamine 50x (left), 500x (right) and 10 000 x (bottom magnified. Scale bar 500 μm. Diameter of several particles are indicated in green and measured in μm.

4.8.2. Supplementary data

To establish the dependency of the chemisorption process on temperature, the adsorption capacity of polymer-bound ethylenediamine was studied at 5, 15, room temperature (RT) and 30 °C. The results are shown in Figure 4.10. Furthermore, regressed isotherm parameters for all studied adsorbents are summarized in Table 4.13.

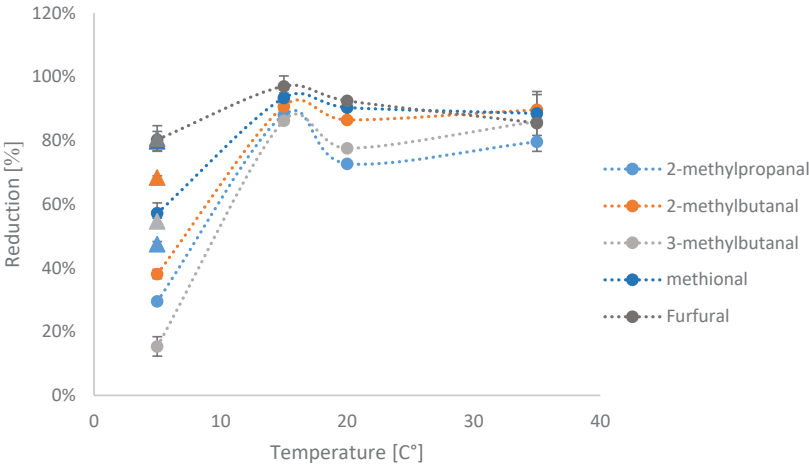
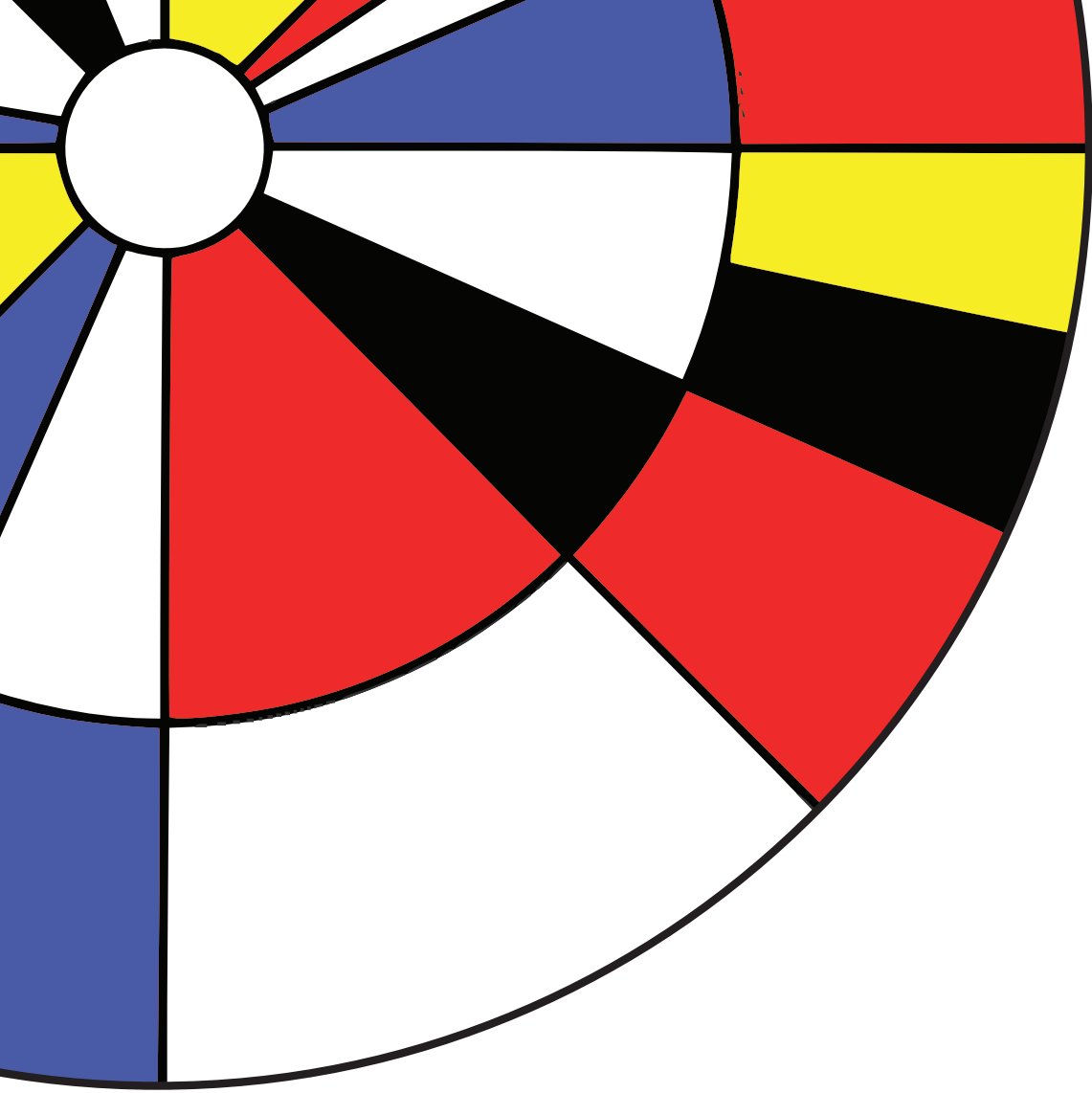


Figure 4.10: Temperature influence on adsorption with polymer-bound ethylenediamine (50 g/g) at 5, 15, RT and 30 degrees incubated for four hours and at 20 hours (separate triangles). The concentration difference after adsorption is shown in percentage reduction.

Table 4.13: Regressed isotherm parameters for CBV28014, HiSiv 3000, P-360 and G-360

Aldehyde	CBV 28014 k_i [L/g]	HiSiv 3000 k_i [L/g]	P-360 k_i [L/g]	G-360 (crushed) k_i [L/g]
2-MP	3.8 ± 0.7	3.52 ± 0.06	3.65 ± 0.17	3.32 ± 0.05
2-MB	60 ± 4	48 ± 2	52 ± 4	42 ± 2
3-MB	69 ± 2	47 ± 3	50 ± 2	41.5 ± 0.8
Met	7.38 ± 0.17	6.94 ± 0.10	8.0 ± 0.3	5.47 ± 0.09
FF	2.09 ± 0.06	1.56 ± 0.03	2.60 ± 0.14	1.43 ± 0.03



Chapter 5

Flavour-improved alcohol-free beer – quality traits, ageing and sensory perception

Abstract: The increasing popularity of alcohol-free beers (AFBs) fosters the industry interest in delivering the best possible product. Yet, a remaining sensory defect of AFBs is the over-perception of wort flavour, caused by elevated concentrations of small volatile flavour compounds (i.e. aldehydes). Previously, molecular sieves (hydrophobic ZSM-5 type zeolites) were found most suitable to remove these flavours by adsorption with high selectivity from the AFBs. In this work, a flavour-improved beer is produced at pilot-scale using this novel technology, and its chemical composition, sensory profile and stability are evaluated against a reference. Aldehyde concentrations in the flavour-improved product were found 79-93% lower than in the reference. The distinct difference was confirmed with a trained sensory panel and could be conserved even after three months ageing at 30°C. Future work will focus on the process design to scale up this technology.

Published as: Gernat, D.C., Brouwer, E.R., Faber-Zirkzee, R.C., Ottens, M., Flavour-improved alcohol-free beer – quality traits, ageing and sensory perception (2020). Food and Bioproducts Processing, 123, pp. 450-458.

5.1. Introduction

Due to increasing awareness, the importance of responsible drinking as well as other motivators such as religion or fitness, one of the fastest growing categories in the beverage industry are currently low- and alcohol-free drinks [1, 2]. Nonetheless, alcohol-free beers still lack behind their regular counterparts, due to several sensory defects that can occur as a consequence of their altered production process [2-4]. Therefore, a new process to produce a flavour-improved alcohol-free beer (AFB) has been developed recently [5]: Zeolites, a type of molecular sieve, are used to adsorptively remove wort off-flavours from biologically produced alcohol-free beers, resulting in a product with a significantly reduced amount of Strecker aldehydes, which are commonly known to cause the undesired wort off-flavour in AFBs. To be specific, 2- and 3- methylbutanal (2-MB and 3-MB) as well as methional (Met) have most often been related to the wort flavour perception, but recent studies found more compounds such as 2-methylpropanal (2-MP) to be involved [6-8].

Strecker aldehydes are formed through a heat-induced reaction between an amino acid and a reducing sugar [9], but also alternative pathways through numerous reactive carbonyls are possible [10-13]. It is therefore difficult to prevent their formation. Previous researchers in brewing have addressed this matter in different ways, for instance by addition of masking compounds, removal through fermentation or co-separation with ethanol during dealcoholisation by thermal or membrane technologies. So far, either the degree in wort flavour decrease or the selectivity has been limiting [14]. The advantage of using an adsorbent and in particular zeolites for the separation task is their 2-fold selectivity based on molecular size and hydrophobicity. In this way, only small (volatile), hydrophobic compounds are removed from the product.

In this work, we present the quality traits of this novel product, as well as its sensory characteristics. Furthermore, the ageing process of the AFB is studied for selected compounds. The chemical and physical analysis presented in this work includes a comprehensive representation of chemical groups and quality indicators. Particular focus lies, however, on four common Strecker aldehydes, whose flavour descriptors and orthonasal (forward or sniffing-smell) and retronasal (backwards or mouth-smell) thresholds in AFB are given in Table 5.1. Furthermore, furfural (FF) as a representative for compounds formed by heat-induced reactions and trans-2-nonenal (t2N), a common indicator for ageing were studied in more detail [15].

Table 5.1: Flavour detection thresholds in alcohol-free beer determined by logistic regression and adjusted for false positives [8, 15]

Compound	Flavour/Odour	Detection threshold [$\mu\text{g/L}$] in AFB	
		Orthonasal	Retronasal
2-MP	Fruity, grainy, nutty, chocolate	4.32	0.86
2-MB	Fruity, sweet, almond, malt	23.4	8.99
3-MB	Malty, nutty, chocolate	0.61	0.44
Met	Boiled potato, metallic, wort	0.47	0.73

5.2. Materials & Methods

5.2.1. Chemicals

The adsorbent ZSM-5 G-360 was purchased from ACS Materials (United States). To prepare solutions in the laboratory, either Milli-Q grade water (Merck, Millipore, United States) or analytical grade, absolute ethanol (VWR International BV, The Netherlands) was utilized. The pre-isomerized iso- α -acid solution was obtained from Joh. Barth & Son (Germany). If not mentioned otherwise, other chemicals were purchased from Sigma Aldrich (United States).

5.2.2. Preparation of wort-flavour reduced beer

The adsorbent was prepared by soaking it in 70% ethanol for one hour and applying three consequent washing steps with water, to remove less volatile hydrophobic compounds that might have adsorbed during storage. It was then dried at 220°C until a stable weight was reached. After cooling, 4 kg of dry adsorbent were filled into a column with a diameter of 20 cm and adjustable height (Evolve 200, Astrea Bioseparations Ltd, United Kingdom) and purged with sterile filtered nitrogen gas for 3 hours to remove as much oxygen as possible. Finally, it was wetted by flushing the column with oxygen-free process water. As a substrate, an AFB was produced by fermenting hop-free wort at 2-4°C, with the composition outlined in Table 5.2. Due to the low fermentation temperature, the formation of ethanol was inhibited. The resulting unhopped, alcohol-free product was stabilized (Polyvinylpyrrolidone and silica) and filtered through a Beer Membrane Filtration System (Pentair, The Netherlands). The batch was then split into two vessels with a liquid volume of 200 L, respectively, adding a slight over-pressure to avoid foaming. One of the vessels was then connected to the zeolite-filled column, avoiding the introduction of air as much as possible. The AFB contained in this vessel was then circulated over the column and samples were taken frequently. After 42 hours, the tank was disconnected and both AFBs (flavour-improved and reference) were again filtered,

standardized to 5.3°P (1°P equals 10 g sugar per kilogram wort), pasteurized with 50 PU (1 PU equals pasteurization for 1 min at 60°C) and bottled into 0.3 L bottles made from brown glass.

Table 5.2: Specification of original extract, alcohol content, pH and colour in feed

Parameter	Feed
Original extract [°P]	12.12
Ethanol [% v/v]	0.015
pH	4.2
Colour [EBC]	8.54
Total iso- α -acids [mg/L]	<0.4

5.2.3. Ageing of samples

The bottled products were stored at 30°C in a dry, dark room for a maximum of 4 months. Each month, two bottles were sampled to analyse for ageing indicators. After 3 months samples were tested by a sensory panel as described in section 5.2.9.

5.2.4. Determination of original extract, oxygen content, pH and colour

The original extract and pH of a product were determined by a digital density meter of the oscillation type (Xample 510, Anton Paar, Austria) and a pH meter (Accumet Basics AB15, Fisher Scientific, The Netherlands), respectively. The oxygen content was analysed with the Haffmans CO₂/O₂ Gehaltemeter, type c-DGM (Pentair, The Netherlands) according to the supplier instructions. To measure the product colour, the EBC method 9.6 was employed, i.e. spectrophotometrically (Spectrostar Nano, BMG Labtech, Germany) and converted to the EBC unit by equation 5.1, where A_{430nm} is the absorption at 430 nm and d the dilution factor.

$$\text{Colour [EBC]} = A_{430nm} \cdot 25 \cdot d \quad (5.1)$$

5.2.5. Analysis of volatile aldehydes

Aldehydes, other than acetaldehyde, were analysed with an adapted method of Vesely et al. [16] where the sample was concentrated by headspace solid-phase micro-extraction on a PDMS/DVB fibre (57327-U, Supelco, United States) and then injected to a gas chromatograph (Agilent 7890A) equipped with a 30m×0.25mm×0.25 μ m VF17MS column and a mass spectrometer as the detector in negative ionisation mode (Agilent 5975C MSD). To improve the selectivity O-(2,3,4,5,6- pentafluorobenzyl)-hydroxylamine was used as derivatisation agent.

5.2.6. Analysis of other volatiles

The concentration of ethanol was determined with an enzymatic method with the test kit obtained from Thermo Fisher Scientific (The Netherlands) according to the recommended EBC method 9.3.1 [17]. Diacetyl and 2,3-pentanedione are quantified with an adapted method of Ruehle et al. [18] by headspace gas chromatography (7820A, Agilent Technologies, The Netherlands) equipped with a fused silica WCOT CP Sil CB wide bore column (50 m x 0.53 mm x 1 µm) and detected with an electron capture detector. To increase accuracy, 2,3-hexanedione was used as internal standard.

Acetaldehyde, ethyl acetate, isoamyl acetate and isoamyl alcohols were analysed by headspace gas chromatography (7820A, Agilent Technologies, The Netherlands) equipped with a flame ionization detector (7890B, Agilent Technologies, The Netherlands) according to EBC method 9.39 [19]. The compounds were separated over a polar capillary narrow bore column (DBWaxETR, 60 m * 0.32 mm ID, 1 µm fused silica) and 4-heptanone and 1-butanol were added to each sample as internal standard.

5.2.7. Analysis of non-volatile compounds

The total of fermentable sugars was calculated from the summation of glucose, fructose, sucrose, maltose and maltotriose. These sugars were quantified by UPLC (Water Acquity, Milford, United States) equipped with a RI detector and a BEH Amide column 1.7 µm (2.1 x 150 mm) as described in EBC method 9.27 [20]. To determine the free-amino nitrogen (FAN), a CDR Beerlab test kit from FoodLab (Italy) was used according to the procedure described by the manufacturer.

5.2.8. Analysis of foam stability and turbidity

The foam stability was determined at room temperature in a NIBEM-T meter from Pentair (The Netherlands) [21]. Following MEBAK method 2.141.2, the sample's turbidity was analysed [22].

5.2.9. Sensory evaluation

To evaluate the improvement in the flavour of the AFB that has been contacted with the selective adsorbent, three different sensory evaluation sessions were held. In the first session, the unhopped base products, i.e. the flavour-improved (I A) and the reference (I B) were tasted. To understand the impact of the adsorptive removal step on the final product, the base AFBs

(both flavour-improved A and reference B) were spiked with a fruity/estery flavour mix (sample III) as well as the fruity flavour mix and iso- α -acid solution (sample IV) and compared to the base AFB (sample II) in the second session. Furthermore, the base AFBs were again tasted after 3 months ageing at 30°C in a third session. The overview of all tastings is given in Table 5.3. The sensory evaluation of produced AFBs was performed with a trained sensory descriptive panel consisting of a total of 16 trained assessors with a modified Quantitative Descriptive Analysis (QDA) [23]. First, an attribute list was determined during a group discussion. Attribute intensities were quantified in duplicate on a 100-point line scale during two individual sessions. Panellists were aligned in their line scale usage and the samples were offered one-by-one in randomized order. In a subsequent session, panellists were seated in individual sensory booths and received 100 mL of each sample, presented in black-coated glasses that are coded with three-digit codes. They were given approximately 10 minutes to evaluate each sample, allowing to neutralise their palate in between. Per session, the panel evaluated a maximum of six samples.

Table 5.3: Overview on tastings of flavour-improved (A) and reference (B) AFBs performed with the descriptive panel

Session	Products included	Storage	# of panellists
1	I) Base AFBs (A and B)	Fresh	13
2	II) Base AFBs (A and B) III) Base AFBs spiked with fruity flavour mix (A and B) IV) Base AFBs spiked with fruity flavour mix and iso- α -acids to adjust to 15 BU*(A and B)	Fresh	13
3	V) Base AFBs (A and B)	Aged	11

*BU (bitterness unit) = $50 \cdot A_{275\text{nm}}$, where $A_{275\text{nm}}$ is the absorbance at 275 nm of a beer isooctane extract

5.2.10. Statistical analysis

The standard deviation of the sample σ and the standard error σ_m of each measurement were determined according to equation 5.2 and 5.3, respectively. The propagated error σ_{mQ} was determined as described elsewhere [24]. Thereby, the statistical error of the sample, as well as the systematic error of the regressed calibration parameter, were taken into account. All errors in the result section represent the standard propagated error, if not mentioned otherwise.

$$\sigma = \sqrt{\frac{1}{(n-1)} \sum_{i=1}^n (x_i - \bar{x})^2} \quad (5.2)$$

$$\sigma_m = \frac{\sigma}{\sqrt{n}} \quad (5.3)$$

The data collection for the sensory evaluation is done in EyeQuestion 4.11.32. EyeOpenR (part of EyeQuestion) is used for statistical analysis. EyeOpenR is based on the statistical language R. The analysis is verified and documented by Qi Statistics Ltd.

5.3. Results & Discussion

5.3.1. Flavour-improved product

During the adsorptive removal through recirculation of the alcohol-free beer over the zeolite-filled column, samples were taken frequently to monitor the reduction in wort flavour over time. The normalized results are depicted in Figure 5.1. The concentration decreases exponentially over time, equilibrating at a plateau of 6-10% of their initial concentration, thus distinctly decreasing the wort flavour in the product. According to previously reported data [5], however, the theoretical capacity of the adsorbent should allow for a decrease of free aldehydes to near zero.

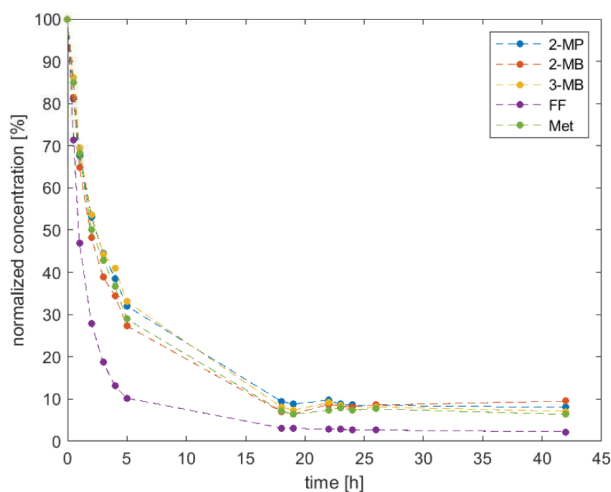


Figure 5.1: Evolution of aldehyde concentrations during the adsorptive removal step

There could be several reasons for this observation, but, when considering the absolute concentration range (<15 µg/L) and the fact that the oxygen level was significantly increased during the trial (~210-1000 µg/L) one could suspect that oxygen caused the formation of new Strecker aldehydes for instance through the formation of reactive dicarbonyls. Furfural's concentration shows a different behaviour, decreasing to 2% of its original amount, while still further reducing in concentration after 42 hours. Contrary to the Strecker aldehydes, 2-MP, 2-

MB, 3-MB and Met, whose formation are closely related to oxygen [25], furfural originates from the reaction of a pentose with an amine or amino group to an imine called Schiff base, which at $\text{pH} < 5$ further reacts to 3-deoxyosone. During a condensation reaction, ring formation occurs and furfural is the product [26]. Thus, since oxygen is hence not involved in the formation mechanism of furfural, the observed difference to Strecker aldehyde gives evidence to support the theory of oxygen being the cause for the lower limit of Strecker aldehyde removal.

Overall, however, the concentration in wort flavours is significantly decreased. Figure 5.2 shows the absolute concentration of the selected aldehydes in the end-product of the treated product and the reference. The achieved reduction amounts to 79-93%. This reduction is less pronounced than what was measured during the test, due to the intermediate pasteurization step, where the aldehyde concentration is slightly increased again (data not shown).

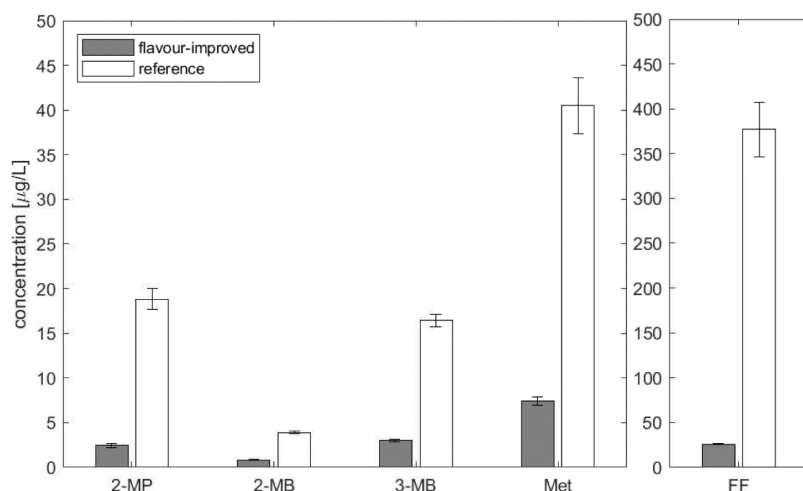


Figure 5.2: Concentration of 2-methylpropanal, 2- and 3-methylbutanal, methional and furfural in alcohol-free beer directly after pasteurization

To gain a full understanding of the effect of the adsorbent on the product quality, a thorough analysis of numerous quality indicators was performed. The most informative data is summarized in Table 5.4. Both products were adjusted to a similar original extract to make the analysis comparable. Due to the process-related handling, the oxygen concentration in the flavour-improved product was increased significantly. However, when scaling up, it is expected that with a more sophisticated set-up, the introduction of oxygen can be avoided.

Table 5.4: Specifications and their standard error of bottled products (reference and flavour-improved)

		Flavour-improved	Reference
adjusted	Original extract [°P]	5.23 ± 0.02	5.30 ± 0.02
Process related	Oxygen [µg/L]	61.1 ± 3.2	16.3 ± 1.3
	Colour [EBC]	3.4 ± 0.0	3.3 ± 0.0
	Ethanol [% V/V]	0.01 ± 0.00	0.01 ± 0.00
	FAN [mg/L]	88 ± 2	90 ± 2
	pH	4.76 ± 0.02	4.74 ± 0.02
unchanged	Total fermentable sugars [g/L]	34.0 ± 1.5	33.9 ± 1.5
	Turbidity [EBC]	0.2 ± 0.0	0.1 ± 0.0
	Turbidity after 7 days at 57°C	0.1 ± 0.0	0.2 ± 0.0
increased	Foam Stability [s]	256 ± 5	217 ± 4
	Acetaldehyde [mg/L]	1.4 ± 0.1	2.3 ± 0.1
decreased	Diacetyl [µg/L]	3.9 ± 0.3	15.9 ± 1.1
	Ethylacetate [mg/L]	<0.2 ± n/a	0.3 ± 0.0

The measurements confirm that the optical appearance of the aroma-improved AFB is unchanged. It exhibits the same colour and turbidity as the reference and even has a slightly improved foam stability. Relatively polar compounds such as sugars and ethanol are not removed and also the FAN content is similar to the reference. According to expectation, the adsorbent removes small volatile compounds such as acetaldehyde, diacetyl or ethylacetate. Isoamylacetate (<0.05 mg/L), amyl alcohols (<1.1mg/L) and 2,3-pentanedione (<2 µg/L) were found below their respective detection limits for both samples and could hence not be included in the analysis.

To confirm that the analytical results are also perceivable during consumption and to establish whether the reduction in wort flavour is significantly lower as intended, a QDA was performed with a trained descriptive panel. In the first set of tasting, only the hop-free base products (I A and I B) were tasted by the panellists. The outcome is represented in the diagram of Figure 5.3. The panellist found a clear difference in the perceived wort flavour (-8 points) between the two samples. Particularly, raisins and rye bread flavour diminished, which is desired for AFBs. Furthermore, the bitter and sour (after) taste was reduced. As a consequence, the treated sample was found more watery and exhibited a lower odour and total intensity (-6 / -5 points).

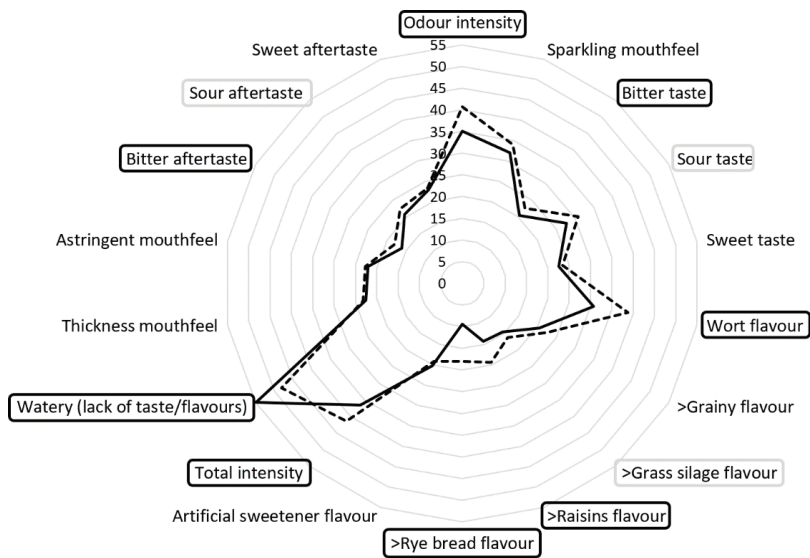


Figure 5.3: Sensory profile of base AFB, flavour-improved (solid line) and reference (dashed line). Attributes who differ with a significance level of 95% are circled in black and with a significance level of 90% in grey

To assess which impact the flavour improvement has on the final product, i.e. a product exhibiting fruity beer flavour (not containing wort flavour) and bitterness, the second set of tastings was executed. For this purpose, the base AFBs (II A and II B), a flavoured AFB (III A and III B) and a flavoured AFB adjusted to 15 BU in bitterness (IV A and IV B) were tasted. The results for the QDA are listed in Table 5.5. At first glance, it is prominent that the difference in wort flavour between matching samples persists, although it is perceived less pronounced. For instance, if sample II A and II B are compared, they differ in 3 points in wort flavour contrary to the 8 points when the same samples (IA and I B) were tasted in a separate session. It should be noted that samples I and II are the same sample, but tasted in different sessions. The relative different perception of wortiness reduction is not related to the uncertainty of the sensory evaluation. It rather means that the presence of fruity flavours and bitterness in one or more samples tasted in the same session influences the panellist's focus on the wort character. Nonetheless, a significant difference in particular in rye bread flavour is detected. In between samples II, III and IV one can clearly observe the masking effect of adding a fruity flavouring and bitterness with respect to the wort character of the products. Interestingly, the panellists perceived flavoured samples of the improved base higher in tropical fruit flavour than the reference. As a consequence, flavour dosing could be reduced in the final product to achieve the same sensory profile.

Table 5.5: Sensory attributes quantified by the descriptive panel

	II A	II B	III A	III B	IV A	IV B	<i>p-value</i>
Odour intensity	37	40	39	40	38	38	0.14
Sparkling mouthfeel	31	31	32	32	31	29	0.19
Bitter taste	24	24	24	24	35	35	0.00
Sour taste	29	29	28	29	30	29	0.72
Sweet taste	22	23	22	22	21	22	0.19
Wort flavour	34	37	28	32	29	31	0.00
Grainy flavour	24	25	18	22	18	21	0.00
Grass silage flavour	16	19	14	17	18	16	0.45
Raisins flavour	12	17	9	12	9	9	0.04
Rye bread flavour	14	17	5	12	5	11	0.00
Fruity/estery flavour	26	25	39	34	37	35	0.00
Peardrop flavour	23	22	34	31	34	32	0.00
Tropical fruit flavour	8	7	20	12	18	15	0.00
Artificial sweetener flavour	16	14	14	15	12	12	0.23
Total intensity	41	41	43	40	43	43	0.02
Watery (lack of taste/flavours)	41	41	41	42	39	39	0.35
Thickness mouthfeel	22	22	21	22	21	22	0.48
Astringent mouthfeel	22	22	22	19	24	23	0.02
Bitter aftertaste	20	20	20	21	34	33	0.00
Sour aftertaste	24	24	23	23	25	22	0.04
Sweet aftertaste	22	21	22	20	19	19	0.01

5.3.2. Ageing

Aldehydes are not only known wort off-flavours in AFBs, but also related to ageing during storage. There is a vast variety of literature available, investigating flavours and their chemical pathways involved in ageing of beers [26, 27]. In this study, we focus on a selected set of aldehydes. The most recent studies in regular beer indicate that *de novo* formation of aldehydes during the ageing process is limited and that the most dominant mechanism causing the increase in aldehyde concentration over time is the release from cysteine and bisulphite adducts [28, 29]. To our knowledge, this is the first study to measure ageing in AFB. Figure 5.4 and Table 5.6 depict the time-wise concentration profile of the flavour-improved and reference beer for all studied aldehydes during four months and their regressed formation rates, respectively. The first remarkable observation is that the formation rate, i.e. the slope, of the flavour-improved and the reference AFB are relatively similar in the case of 2-MP, 2-MB and FF, although the formation rate of the treated AFB is generally lower. This means that the difference in concentration between the improved and reference AFB will remain similar or even increase

over the storage time. This is also the case for t2N, but here the treated product slightly decreases in the ageing compound. This is different for 3-MB: here the formation rate in the improved product is higher and hence the difference is lessening during storage. Methional's concentration is inclining in the improved product, however, barely seems to change in the reference. The reason behind this different behaviour can only be speculated and are hence ground for further research. Considering that the starting concentration of methional in the reference is the highest of all measured Strecker aldehydes, one could postulate that it already is in equilibrium with its educts. Another possible explanation is that it is simultaneously formed and converted to degradation products such as methanethiol and acrolein as previously reported in literature [30-32].

Table 5.6: Formation rate of aldehydes in flavour-improved and reference base beer during storage at 30 °C and comparison with literature range

Compounds	Formation rate [µg/month]		Approximated formation rate ³ range from [33, 34] [µg/month]
	improved	reference	
2-MP	1.2 ± 0.1	1.8 ± 0.2	4.7-28.8
2-MB	0.7 ± 0.0	0.8 ± 0.1	0.6-1.9
3-MB	2.2 ± 0.3	1.3 ± 0.4	1.4-3.2
FF	53 ± 9	69 ± 15	63 - 99
Met	1.3 ± 0.3	-0.1 ± 0.7	0.9-2.1
t2N	-0.006 ± 0.004	0.016 ± 0.026	0.003-0.033

Since the beer is fermented at low temperatures resulting in minimal yeast activity, the studied beer has several properties, which makes this case interesting to study and compare with data reported in literature:

1. The starting concentration in the fresh beer is higher than in regular beer, particularly in the reference product.
2. The ethanol content is <0.01 vol.% in ethanol
3. No sulphite is produced by yeast.
4. The fermentable sugar concentration is higher than in regular beer since they are not consumed during fermentation.

Furthermore, no compounds originating from hops are contained in the AFB. Jaskula-Goiris et al. (2011) studied the beer stability of pale lager beers from different breweries [33].

³ visual estimation from plotted data

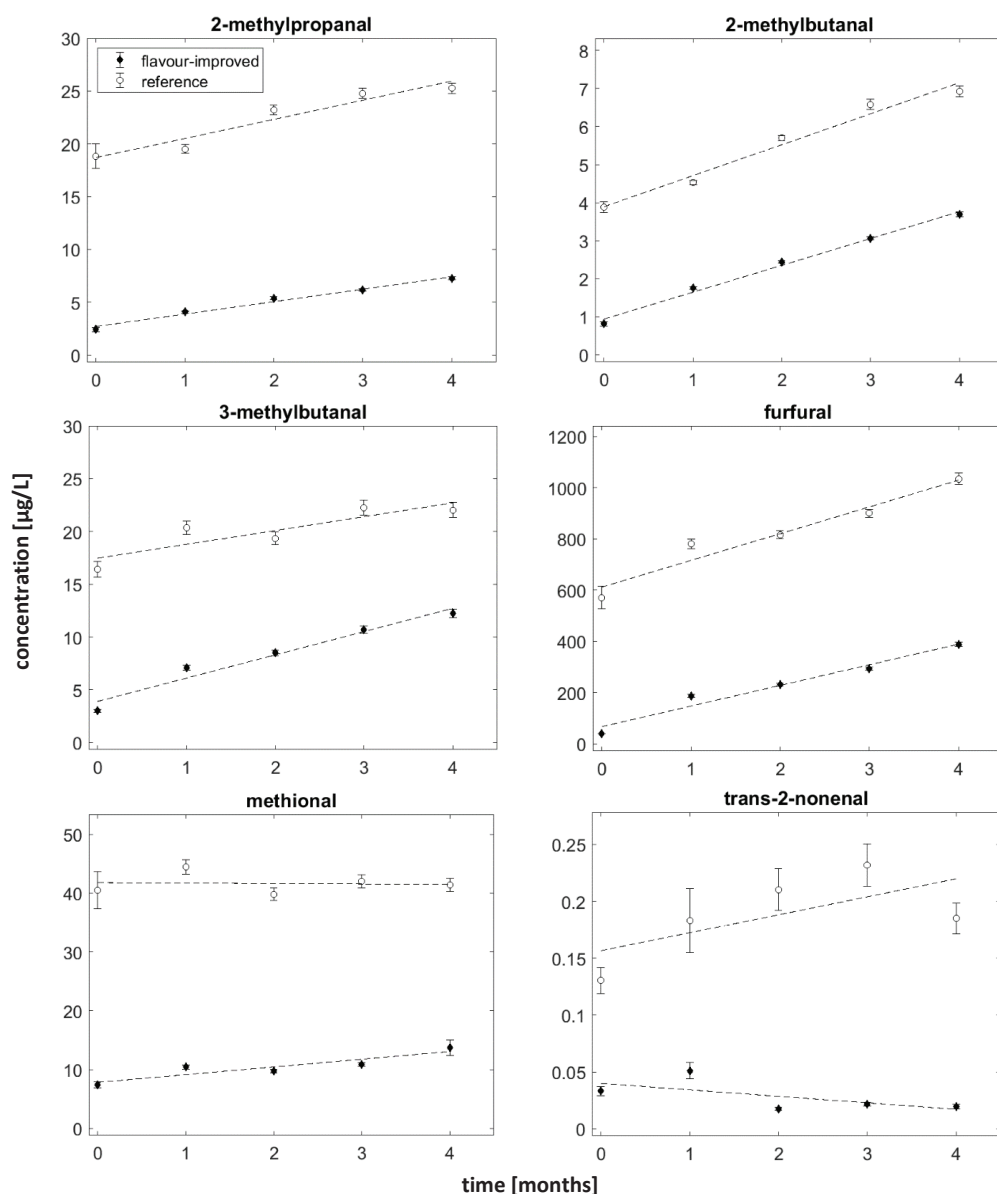


Figure 5.4: Concentration of selected compounds over a course for 4 months for treated (dark) and reference product (white)

Surprisingly, despite the numerous differences in the beer composition, the formation rate in aldehydes is quite comparable (see Table 5.6). They found that staling was positively correlated with the residual FAN content, and thus the concentration of amino acids in beer. In their study,

fresh beers contained between 49.1-141.2 mg/L FAN, where in our products comparable levels of 88-90 mg/L were determined. This observation supports the hypothesis that aldehyde formation is strongly linked to the presence of amino acids in beer. Other authors report that unhopped beer barely produces any aged flavour [35], contrary to what is observed in this analysis.

When comparing the sensory profile of the aged products with each other, as shown in Figure 5.5, the difference between the flavour-improved and the reference product generally become less distinct, i.e. in odour/total intensity and wort flavour is still found to be significant between the two samples, however, this difference is less pronounced. The panellists also cannot perceive clear differences in raisins and rye bread flavour anymore. Attributes that were found slightly divergent in the fresh product such as the bitter taste and aftertaste are now perceived similar. At a closer look, it is observed that the identified attributes slightly differ from the tasting of the fresh product. While the artificial sweetener flavour is not recognized anymore, the sweet aftertaste of the sample is becoming more pronounced in the reference beer and a syrup flavour is noted by the panellists.

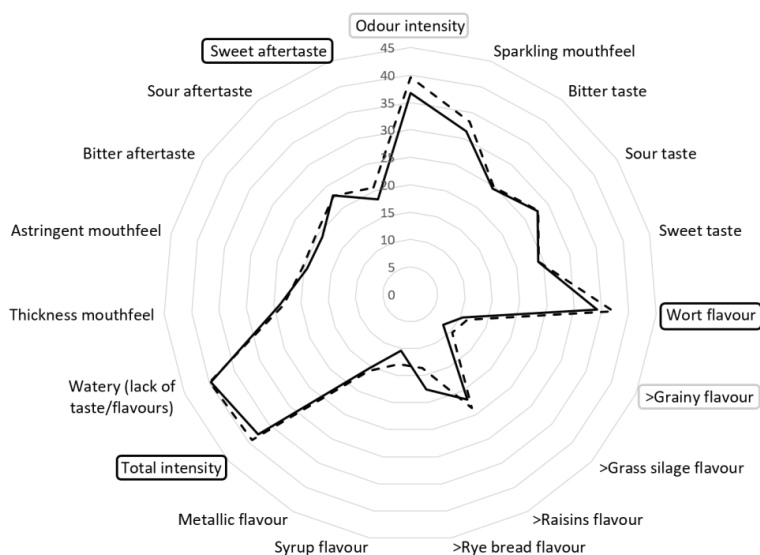


Figure 5.5: Sensory profile of base AFB, flavour-improved (VA, solid line) and reference (VB, dashed line) aged for 3 months at 30 °C. Attributes differing with a significance level of 95% are circled in black and with a significance level of 90% in grey

In literature, it is reported that over the whole course of ageing, sweetness and toffee-like or caramel aroma increases and bitterness decreases [36, 37]. Ribes and cardboard flavour may

appear during the ageing process, but after reaching a peak at about 4 weeks disappear again [27, 38]. Thus, the above findings resonate well with the expectations from literature. Although the difference in the actual concentration in wort flavour between the flavour-improved and the reference product is still very similar as in the fresh product, the same degree of wort flavour reduction is not reflected in the sensory evaluation. One reason for this might be that the curve of concentration and response in flavour intensity follows a sigmoidal shape, hence is nearly linear in the range close to the flavour threshold, but, at higher concentrations this response declines and might even saturate [39]. The same absolute difference in concentration in two samples is hence less obvious at higher concentrations. Additionally, synergetic effects can enhance this phenomenon [40].

5.4. Conclusion

In this work, a flavour-improved AFB was produced with a significantly decreased concentration in characteristic wort flavours, resulting in a clean-tasting base beer. This difference was confirmed during sensory evaluation with a trained panel. Due to the high selectivity of the adsorbent, only small volatile compounds were removed, while other parameters such as colour, foam stability or sugar content were similar. Addition of fruity flavours and bitterness decreased the relative perceived difference in wort flavour between the improved AFB and the reference, but a significantly lower wortiness remained. Even after three months of forced ageing, quality differences were still detectable. Future work will focus on designing a scalable and economically feasible process unit operation and investigate the regenerability of the absorbent. Furthermore, more detailed investigations of the ageing behaviour for instance with hopped AFB are necessary to improve the understanding of the involved mechanisms.

5.5. Acknowledgements

The authors acknowledge Heineken Supply Chain B.V. for the funding provided for this project and the opportunity to carry out the pilot scale tests at their facilities.

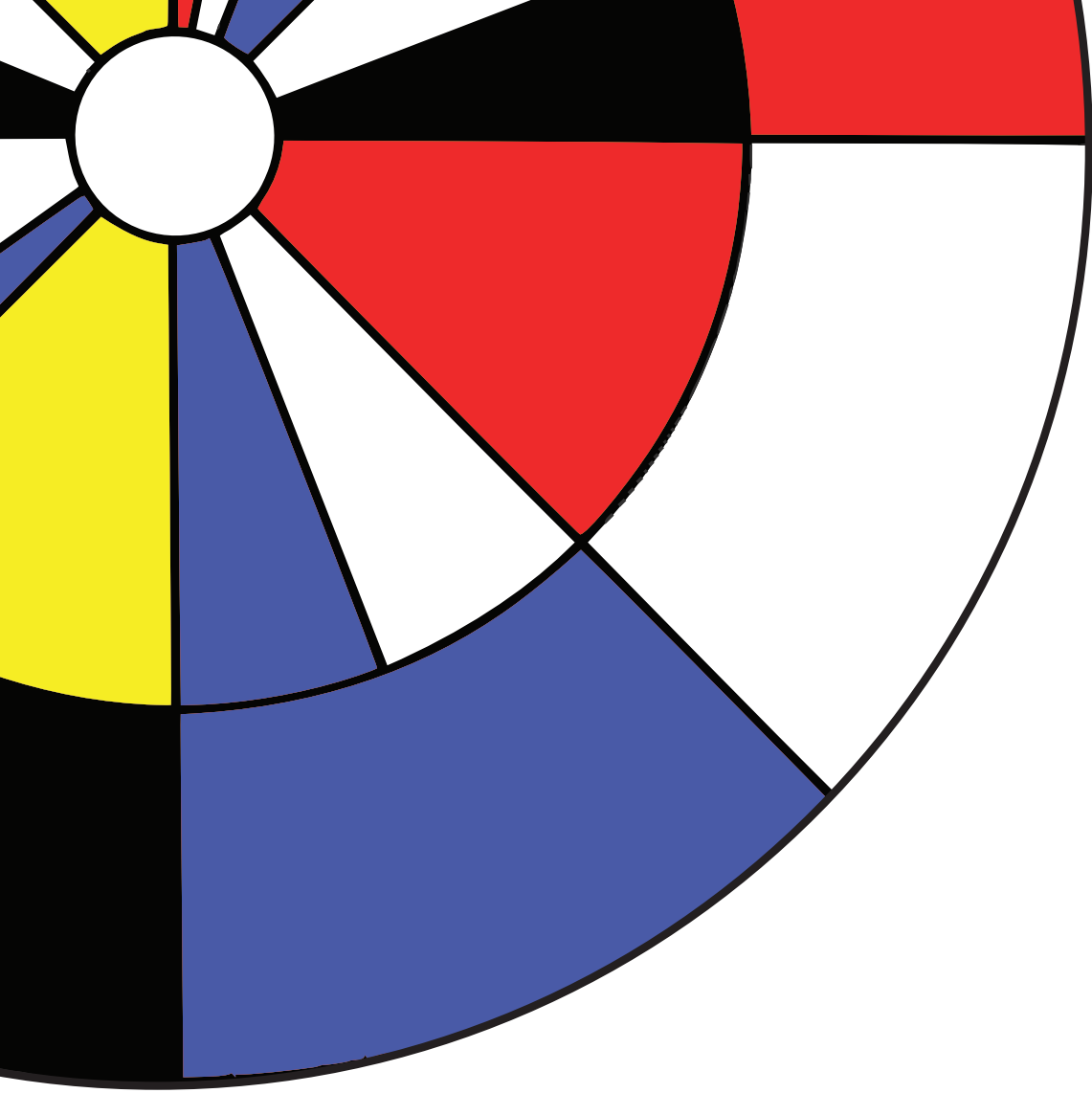
5.6. References

1. Liguori, L., et al., Chapter 12 - Production of Low-Alcohol Beverages: Current Status and Perspectives, in Food Processing for Increased Quality and Consumption, A.M. Grumezescu and A.M. Holban, Editors. 2018, Academic Press. p. 347-382.

2. Blanco, C.A., C. Andres-Iglesias, and O. Montero, Low-alcohol Beers: Flavor Compounds, Defects, and Improvement Strategies. *Crit Rev Food Sci Nutr*, 2016. 56(8): p. 1379-88.
3. Brányik, T., et al., A review of methods of low alcohol and alcohol-free beer production. *Journal of Food Engineering*, 2012. 108(4): p. 493-506.
4. Mangindaan, D., K. Khoiruddin, and I.G. Wenten, Beverage dealcoholization processes: Past, present, and future. *Trends in Food Science & Technology*, 2018. 71: p. 36-45.
5. Gernat, D.C., et al., Selective off-flavor reduction by adsorption: A case study in alcohol-free beer. *Food and Bioproducts Processing*, 2020. 121: p. 91-104.
6. Beal, A.D. and D.S. Mottram, Compounds contributing to the characteristic aroma of malted barley. *Journal of Agricultural and Food Chemistry*, 1994. 42(12): p. 2880-2884.
7. Perpète, P. and S. Collin, Contribution of 3-methylthiopropionaldehyde to the worty flavor of Alcohol-free beers. *Journal of Agricultural and Food Chemistry*, 1999. 47(6): p. 2374-2378.
8. Piornos, J.A., et al., Orthonasal and retronasal detection thresholds of 26 aroma compounds in a model alcohol-free beer: Effect of threshold calculation method. *Food Res Int*, 2019. 123: p. 317-326.
9. Schonberg, A. and R. Moubacher, The Strecker Degradation of α -Amino Acids. *Chemical Reviews*, 1952. 50(2): p. 261-277.
10. Rizzi, G.P., The Strecker Degradation of Amino Acids: Newer Avenues for Flavor Formation. *Food Reviews International*, 2008. 24(4): p. 416-435.
11. Hidalgo, F.J., R.M. Delgado, and R. Zamora, Intermediate role of α -keto acids in the formation of Strecker aldehydes. *Food Chemistry*, 2013. 141(2): p. 1140-1146.
12. Hidalgo, F.J. and R. Zamora, Strecker-type Degradation Produced by the Lipid Oxidation Products 4,5-Epoxy-2-Alkenals. *Journal of Agricultural and Food Chemistry*, 2004. 52(23): p. 7126-7131.
13. Delgado, R.M., R. Zamora, and F.J. Hidalgo, Contribution of Phenolic Compounds to Food Flavors: Strecker-Type Degradation of Amines and Amino Acids Produced by o- and p-Diphenols. *Journal of Agricultural and Food Chemistry*, 2015. 63(1): p. 312-318.
14. Gernat, D.C., Brouwer, E., Ottens, E., Aldehydes as Wort Off-Flavours in Alcohol-Free Beers - Origin and Control. *Food and Bioprocess Technology*, 2020. 13(2): p. 195-216.
15. Saison, D., et al., Contribution of staling compounds to the aged flavour of lager beer by studying their flavour thresholds. *Food Chemistry*, 2009. 114(4): p. 1206-1215.

16. Vesely, P., et al., Analysis of Aldehydes in Beer Using Solid-Phase Microextraction with On-Fiber Derivatization and Gas Chromatography/Mass Spectrometry. *Journal of Agricultural and Food Chemistry*, 2003. 51(24): p. 6941-6944.
17. Analytica, EBC 9.3.1: Ethanol in alcohol-free and low alcohol beers: Enzymatic Method (IM). 2013.
18. Ruehle, G., et al., Headspace gas chromatography/electron capture detector analysis of total vicinal diketones in beer. *Journal of the American Society of Brewing Chemists*, 2013. 71(4): p. 274-275.
19. Analytica, EBC 9.39: Dimethyl Sulphide and other lower boiling point volatile compounds in beer by gas chromatography. 2000.
20. Analytica, EBC 9.27: Fermentable carbohydrates in beer by HPLC (IM). 1997.
21. Analytica, EBC 9.42.1: The determination of the foam stability of beer using the NIBEM-T meter. 2004.
22. MEBAK-E.V., 2.14.1.2. Haze Formation Optical Method. 2013: Freising, Germany.
23. Stone, H., et al., “Sensory Evaluation By Quantitative Descriptive Analysis”, in *Descriptive Sensory Analysis in Practice*. 2004.
24. Young, H.D., *Statistical Treatment of Experimental Data*, ed. M.-H.B.C. Inc. 1962, United States of America.
25. Wietstock, P.C., T. Kunz, and F.-J. Methner, Relevance of Oxygen for the Formation of Strecker Aldehydes during Beer Production and Storage. *Journal of Agricultural and Food Chemistry*, 2016. 64(42): p. 8035-8044.
26. Vanderhaegen, B., et al., The chemistry of beer aging – a critical review. *Food Chemistry*, 2006. 95(3): p. 357-381.
27. Baert, J.J., et al., On the origin of free and bound staling aldehydes in beer. *J Agric Food Chem*, 2012. 60(46): p. 11449-72.
28. Baert, J.J., et al., Exploring Aldehyde Release in Beer by 4-Vinylpyridine and the Effect of Cysteine Addition on the Beer’s Pool of Bound Aldehydes. *Journal of the American Society of Brewing Chemists*, 2018. 76(4): p. 257-271.
29. Baert, J.J., et al., Further elucidation of beer flavor instability: The potential role of cysteine-bound aldehydes. *Journal of the American Society of Brewing Chemists*, 2015. 73(3): p. 243-252.
30. Gijs, L., et al., 3-Methylthiopropionaldehyde as Precursor of Dimethyl Trisulfide in Aged Beers. *Journal of Agricultural and Food Chemistry*, 2000. 48(12): p. 6196-6199.

31. Wainwright, T., J.F. McMahon, and J. McDowell, Formation of methional and methanethiol from methionine. *Journal of the Science of Food and Agriculture*, 1972. 23(7): p. 911-914.
32. Ballance, P.E., Production of volatile compounds related to the flavour of foods from the Strecker degradation of DL-methionine. *Journal of the Science of Food and Agriculture*, 1961. 12(7): p. 532-536.
33. Jaskula-Goiris, B., et al., Detailed multivariate modeling of beer staling in commercial pale lagers. *BrewingScience*, 2011. 64(11-12): p. 119-139.
34. Baert, J.J., Unravelling the Role of Free and Bound-state Aldehydes in Beer Flavor Instability, in *Faculty of Bioscience Engineering*. 2015, KU Leuven: Leuven.
35. Hashimoto, N. and T. Eshima, Oxidative degradation of isohumulones in relation to flavour stability of beer. *Journal of the Institute of Brewing*, 1979. 85(3): p. 136-140.
36. Vanderhaegen, B., et al., The chemistry of beer aging - A critical review. *Food Chemistry*, 2006. 95(3): p. 357-381.
37. Dalglish, C.E., Flavour stability. *Proceedings of the European Brewery Convention Congress*, 1977: p. 623-659.
38. Zufall, C.R., G.; Gasparri, M.; Franzquiz, J. Flavour stability and ageing characteristics of light-stable beers. in *30th European Brewery Convention*. 2005. Fachverlag Hans Carl, Nürnberg, Germany.
39. Breslin, P.A.S., Interactions among salty, sour and bitter compounds. *Trends in Food Science and Technology*, 1996. 7(12): p. 390-399.
40. Singh, V., et al., Competitive binding predicts nonlinear responses of olfactory receptors to complex mixtures. *Proceedings of the National Academy of Sciences of the United States of America*, 2019. 116(19): p. 9598-9603.



Chapter 6

Mass transfer limitations in binderless ZSM-5 zeolite granules during adsorption of flavour compounds from aqueous streams

Abstract: Recently, a new process concept has been proposed to selectively adsorb wort off-flavours, i.e. aldehydes, from alcohol-free beers with hydrophobic zeolites. In this work, we investigated the uptake of a mixture of wort flavour compounds (2-methylpropanal, 2-methylbutanal, 3-methylbutanal, furfural and methional), from a model solution onto binderless, hydrophobic ZSM-5 zeolite granules to quantify mass transfer parameters and identify bottlenecks. Subsequently, the homogenous solid diffusion model was employed to regress the effective diffusion coefficients for each molecule and experimental condition, which ranged between 10^{-15} and 10^{-13} m²/s, indicating strong intraparticle mass transfer limitation. Furthermore, it was found that the effective diffusion coefficient is inversely correlated to the molecules' hydrophobicity, expressed as the logD value and its isotherm affinity constant. These results give valuable insight to design and improve the adsorbent material and an off-flavour removal unit at industrial scale.

Published as: Gernat, D.C. Rozenbroek, R., Brouwer, E.R., van der Wielen, L.A.M., Ottens, M. Mass transfer limitations in binderless ZSM-5 zeolite granules during adsorption of flavour compounds from aqueous streams. (2020) J Chem Technol Biotechnol., 95 (12), pp.3134-3148.

6.1. Introduction

Mass transfer during gas adsorption in microporous materials has been widely studied [1-4]. Less studies are available investigating mass transfer in shaped microporous materials in liquids, and more specifically, aggregated pellets or granules in dilute aqueous environments. Even so, new applications of zeolites in aqueous systems are emerging. For instance, wastewater treatment [5-7] or the separation and conversion of sugars has been investigated in the past [8-12]. In the production of biofuels, zeolites have also been employed to optimize production [13, 14]. In a recent study, a new technology has been developed to selectively remove off-flavours from complex aqueous food streams, in particular, wort flavour from alcohol-free beer with ZSM-5 type zeolites [15]. Wort flavour compounds, namely (Strecker) aldehydes are often present in elevated concentrations, which distorts the sensory perception of the product. The most dominant contributors to the wort flavour are 2-methylbutanal (2-MB), 3-methylbutanal (3-MB) and methional (Met) [16, 17] as well as 2-methylpropanal (2-MP) [18]. Furthermore, furfural (FF), as a general indicator for flavour instability [19] is of interest in this study. The authors reported that the separation based on hydrophobicity and size exclusion ensured a high selectivity and capacity. Hydrophobic ZSM-5 type zeolites ($\text{SiO}_2/\text{Al}_2\text{O}_3$ molar ratio 360) proved to be particularly promising to target unwanted aldehydes while retaining major contributors to the taste and flavour of the beer such as hop and small organic acids in the product [15]. In order to show the technical and ultimately economic feasibility of such a technology, the mass transfer in such a multicomponent system needs to be studied and characterized thoroughly.

Previous work has mainly focused on studying the mass transfer in single-component systems, e.g. sugar molecules in aqueous solutions [20-26], simple alcohols, ketones and aromatics [27, 28] or amino acids [29]. Relevant data is summarized in Table 6.1. The reported diffusivities range vastly, from $8.0 \cdot 10^{-17}$ to $2.4 \cdot 10^{-11} \text{ m}^2\text{s}^{-1}$. Most commonly, a simplified equation of the homogenous solid diffusion model (HSDM) is employed to regress the diffusivity, but the table also illustrates that simplifications and assumptions of different mass transfer models are applied, potentially leading to different results. This makes a comparison, even in the order of magnitude, rather difficult.

The objective of this work is to quantify mass transfer parameters and identify possible bottlenecks for mass transportation in the zeolite. In addition, a better understanding of the main impact factors on transport is gained.

Table 6.1: Relevant diffusion coefficients for small molecules in aqueous solutions into zeolites as reported in literature

Adsorbent	Adsorbate	Adsorbent shape	Diameter	T [°C]	Mass transfer model	D [m ² s ⁻¹]	Ref
Silicalite	Methanol	Powder	d _c = 1.2 μm	30	Direct time domain fitting of the liquid chromatography response peaks	D _{c, MeOH} = 3.40·10 ⁻¹⁴	[27]
	Ethanol					D _{c, EtOH} = 2.24·10 ⁻¹⁴	
	Acetone					D _{c, AcO} = 2.04·10 ⁻¹⁵	
Hydrophobically modified NaY-zeolite	Benzene	Powder	n/a	28	HSDM	D _{c, Benz} = 1.39·10 ⁻¹³	[28]
	Toluene					D _{c, Tol} = 1.11·10 ⁻¹⁴	
	Ethylbenzene					D _{c, EtB} = 1.11·10 ⁻¹⁴	
	m,p-Xylene					D _{c, mp} = 5.56·10 ⁻¹⁴	
	o-Xylene					D _{c, Xy} = 9.72·10 ⁻¹⁴	
FAU (Si/Al 150)	Isomaltotriose	Powder	d _c = 6 μm	5	Not specified	D = 4·10 ⁻¹³	[24]
BEA50	Isomaltose	Powder	d _c = 30 μm	30	Simplified HSDM regressing initial	D _c = 1.9·10 ⁻¹²	[20]
BEA150 (extrudate of BEA50)	Isomaltose	Extrudate	d _{extr} = 0.5 mm	30	slope of uptake curve §[52]	D _{ext} = 2.4·10 ⁻¹¹	
BEA50	Laminaribiose	Powder	d _c = 30 μm	40	Infinite bath solution of HSDM for cylindrical particles**	D _c = 1.47·10 ⁻¹⁴	[25]
BEA150	Laminaribiose	Extrudate	d _{extr} = 0.5 mm			D _{ext} = 4.39·10 ⁻¹¹	
Hydrophobic Y-zeolite	Difructose dianhydrides	Powder	d _c = 6.6 μm	20-25	Long-term solution of HSDM [31]††	D _c = 8·10 ⁻¹⁷	[21]
Y-zeolite	Sucrose	Powder	d _p = 6 μm	5	Micropore diffusion control [31]	D _c = 1·10 ⁻¹⁴	[22]
Hydrophilic KX-zeolite	Glucose	Powder	d _p = 50 μm	25	Extended van Deemter equation‡‡	D _c = 1.1·10 ⁻¹³	[26]
	Fructose					D _c = 1.3·10 ⁻¹³	
	Glycine					D _{c, gly} = 1.9·10 ⁻¹²	[29]
	Alanine					D _{c, ala} = 7.2·10 ⁻¹³	
	Lysine					D _{c, lys} = 1.8·10 ⁻¹³	
Dealuminated, hydrophobic Y-zeolite	Glucose	crushed granulated pellets	d _p = 0.28 - 0.56 mm	20-25	Extended van Deemter equation §§	D _{c, glucose} = 2.1·10 ⁻¹³	[23]
	Sucrose					D _{macro, glucose} = 1.4·10 ⁻¹⁰ D _{c, sucrose} = 1.0·10 ⁻¹⁴ D _{macro, sucrose} = 3.1·10 ⁻¹⁰	

§ $\frac{q_t - q_0}{q_{\infty} - q_0} = \frac{2A}{V} \sqrt{\frac{D \cdot t}{\pi}}$
 ** $\frac{q_t}{q_{\max}} = 1 - 4 \sum_{n=1}^{\infty} \frac{1}{n^2} \exp\left(-\frac{\xi_n^2 D t}{r^2}\right)$
 †† $q = 1 - \frac{6}{\pi^2} e^{-\left(\frac{\pi^2 D t}{r^2}\right)}$
 ‡‡ HETP $\approx \frac{2D_p}{v} + \frac{2\epsilon v}{(1-\epsilon)k_{eff}K} \left(1 + \frac{\epsilon}{(1-\epsilon)K}\right)^{-2}$ with $\frac{1}{k_{eff}K} = \left(\frac{r^2}{15DK_c}\right)$
 §§ with k_{eff} defined as $\frac{1}{k_{eff}K} = \frac{1}{R_p^2} + \frac{R_p^2}{15\epsilon D_p} + \frac{R_p^2}{15KD_c}$ with $D_p = \frac{D}{\tau^2}$

This may lead to more insight for designing an adsorbent material with improved mass transfer properties. Furthermore, the data can be implemented in process simulations for a conceptual design of an adsorptive off-flavour removal unit. To do so, the structural properties of the solid adsorbent were studied first, to obtain insight into the macro- and microstructure of the material. Then, the adsorption process dynamics were determined during hydrodynamically defined batch uptake experiments, varying the particle size of the ZSM-5 G-360 granules as well as the solute starting concentrations. Subsequently, the HSDM was employed to regress effective diffusion coefficients, which were then correlated to the respective molecular properties.

6.2. Theory

6.2.1. Isotherm model

The equilibrium isotherms of the tested solutes were regressed from experimental adsorption data with the Freundlich isotherm model, according to equation 6.1 [30]. If n converges towards 1, the equation equals the linear adsorption model isotherm and the assumptions of a non-competitive adsorption process can be considered within the defined experimental design space, making a multicomponent isotherm model obsolete.

$$q_{e,i} = K_F \cdot c_{e,i}^{1/n} \quad (6.1)$$

6.2.2. Adsorption model

In principle, there are two types of microporous adsorbents; homogenous particles, which exhibit a wide pore size distribution, and composite pellets, which are consisting of microparticles (crystals) shaped into the desired form, that often show a well-defined bimodal pore size distribution [31]. In the latter case, micropores and meso/macropores can be clearly distinguished. Both pore type diffusivities can be limiting – depending on the conditions and the system. Hence, mass transfer is classified into i) liquid film diffusion and ii) intraparticle diffusion, consisting of diffusion through the macro- and micropores see Figure 6.1-A. While within the macropore, two transport mechanisms are possible, i.e. pore diffusion through the liquid and surface diffusion along the solid adsorbent surface, the transport in the micropores of the crystals is limited to intracrystalline diffusion, which resembles surface diffusion in the mechanism [32]. Additionally to the above explained transport mechanisms, surface barriers e.g. at the particle shell or the crystal surface may occur and affect the sorption dynamics [31, 33-35]. Since mass action is a very rapid process in physisorption, it is neglected and hence, either film or intraparticle diffusion always is the rate-limiting step [31].

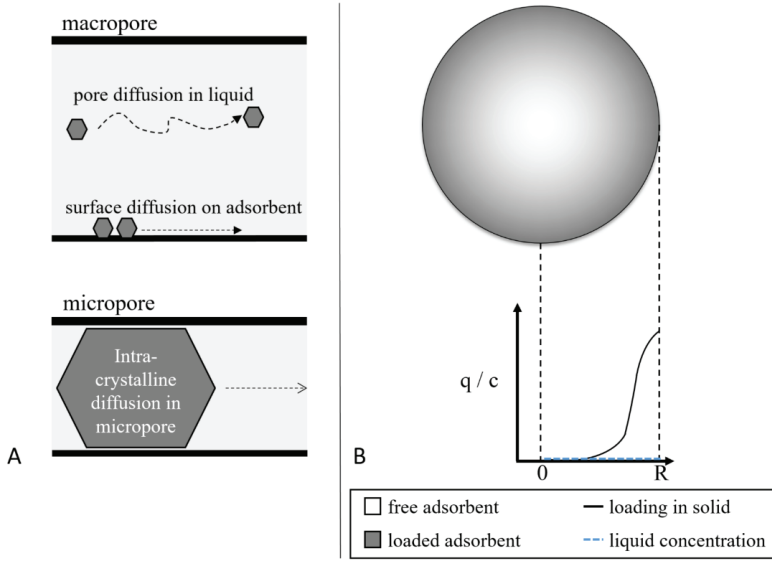


Figure 6.1: (A) Mechanisms of diffusion in macro- and micropores (B) schematic representation of the HSDM.

For this work, we created experimental conditions to eliminate external mass transfer conditions as much as possible to measure the intraparticle diffusivity. The film mass transfer coefficient, k_f , was calculated according to the widely accepted correlation given in equations 6.2 – 6.3 [30, 36, 37].

$$k_f = \sqrt{\frac{4D_m u}{\pi d_p}} \quad (6.2)$$

$$D_m = \frac{T}{\eta} 7.4 \cdot 10^{-8} \frac{(\psi M)^{1/2}}{V_m^{0.6}} \quad (6.3)$$

In our case, granular particles of different diameters composed of small crystals are used. Such aggregated materials can be controlled by micropore or macropore diffusion or even by a mixed mechanism, where the adsorbate is transported through the relatively large macro- or mesopores by (fast) pore diffusion and then diffuses into the solid microporous crystals through slower intracrystalline diffusion. Although the studied material has a heterogeneous structure, the above explanation shows that the underlying mass transfer mechanisms can be complex and simplifications to model the adsorption process are required. Such a model, commonly employed for representing intraparticle mass transfer in zeolites, is the homogenous solid diffusion model (HSDM) [38, 39], which is described through equation 6.4-6.6. The HSDM does not attempt to describe the adsorption process based on structural characteristics of the

material such as surface area or pore size (distribution), but rather as a simplified process, where the target compound adsorbs at the surface of the particle and then diffuses through it solely by means of solid diffusion. Thereby, the solid concentration profile is gradually decreasing and the intraparticle sorbate concentration in the liquid phase equals zero as shown in Figure 6.1-B. This means, that the regressed diffusion coefficient is an effective one, rather than the specific diffusivity of the solute in the material [40].

$$V_b \frac{\partial c_i}{\partial t} = -J_i A_s \quad (6.4)$$

$$J_i = k_f (c_i - c_{i,s}) \quad (6.5)$$

$$\frac{\partial q_i}{\partial t} = D_{eff} \left(\frac{\partial^2 q_i(r, t)}{\partial r^2} + \frac{2}{r} \frac{\partial q_i}{\partial r} \right) \quad (6.6)$$

Following assumptions are taken to simplify the system:

- Adsorbates do not interact with each other, only with the adsorbent.
- A non-competitive adsorption model (Freundlich) can describe the multicomponent equilibrium between the liquid and the solid according to equation 6.1.
- The HSDM assumes storage and transport of the sorbate only in the solid phase, making surface diffusion the predominant transport mechanism.
- The effective diffusivity is independent of the concentration.
- The experimental conditions are as such that there is no concentration gradient over the column bed of adsorbent particles so that the system can be modelled as an ideally mixed, finite bath.
- The average particle diameter of the granule is representative of the sample.

Equation 6.6 is solved with the boundary conditions defined in equation 6.7 - 6.9 meaning that there is no flux across the centre of the particle, as well as that the concentration of the bulk is c_0 at $t=0$ and initial loading of the solid is equal to zero.

$$\frac{\partial q_i(r = 0, t)}{\partial r} = 0 \quad (6.7)$$

$$c_b(t = 0) = c_0 \quad (6.8)$$

$$q_i(r, t = 0) = 0 \quad (6.9)$$

6.2.3. Statistical analysis

The standard deviation of the sample σ , was determined for the statistical deviations of the batch uptake experiment and the analytical measurement (see equation 6.10). Furthermore, the

systematic error of the calibration was taken into account. The propagated overall error of a quantity Q was then calculated from the standard error, σ_m , according to equation 6.11 – 6.12 [41].

$$\sigma = \sqrt{\frac{1}{(n-1)} \sum_{i=1}^n (x_i - \bar{x})^2} \quad (6.10)$$

$$\sigma_m = \frac{\sigma}{\sqrt{n}} \quad (6.11)$$

$$\sigma_{mQ} = \sqrt{\sum_i \left(\frac{\partial Q}{\partial i}\right)^2 \sigma_{mi}^2} \quad (6.12)$$

The error of regressed parameters was determined from the variance-covariance matrix, calculated from the Jacobian of the fitting function.

6.3. Materials and methods

6.3.1. Materials

Solutions were prepared with milli-Q grade water (Merck Millipore, United States) or absolute ethanol (VWR International BV, The Netherlands). Maltodextrin type C*Dry MD 01958 was obtained from Cargill (Belgium) and phosphoric acid from J.T. Baker (The Netherlands). The binderless zeolite granules ZSM-5 G-360 were purchased from ACS Materials (United States). All other chemicals were purchased from Sigma Aldrich (The Netherlands).

6.3.2. Model solution

The physical properties and chemical composition of the model solution were chosen to resemble an alcohol-free beer. The viscosity was set to 2.8 mPa·s by adding 65 g/L maltodextrin. Maltodextrin was also chosen to represent sugars contained in alcohol-free beers produced by arrested/restricted fermentation. The pH was adjusted to 4.2 by adding phosphoric acid. Depending on the experiment, either 0.5, 0.25 or 0.125 mg/L of each flavour compound (2-MP, 2-MB, 3-MB, FF and Met) dissolved in pure ethanol was added to the solution. The resulting ethanol content was 0.1 vol. %.

6.3.3. Adsorbent preparation

Zeolite granules were sieved into three different particle sizes (small 2.35 ± 0.11 mm; medium 2.66 ± 0.10 mm; big 3.12 ± 0.20 mm) or crushed with a mortar and pestle with the addition of

a small amount of water to avoid dust formation. Before the experiment, granules were incubated overnight in 70 % ethanol. Then the ethanol was removed via vacuum filtration and the particles were additionally washed with milli-Q grade water over the filter. After washing, the particles were dried overnight at 220 °C to remove all liquid and reach a stable dry weight.

6.3.4. Determination of material characteristics

Gravimetric method to determine porosity

To understand the accessibility of the particles to liquid, the volumetric uptake of water and ethanol-water mixtures was studied. First, the solid density was determined in a pycnometer. To do so, it was filled with dried adsorbent particles and the mass was measured. Thereafter, it was filled with 20 v/v % ethanol and left to equilibrate. After topping the pycnometer with liquid, the weight was determined again. Knowing the density of the liquid, this allowed to calculate the solid density according to equation 6.13. To calculate the porosity, the difference in adsorbent liquid and dry weight was determined with 70 v/v % ethanol and milli-Q grade water, respectively, and determined according to equation 6.14 and 6.15.

$$\rho_s = \frac{m_{ads,dry}}{V_{total} - V_{ethanol}} \quad (6.13)$$

$$V_{pore} = \frac{m_{ads,wet} - m_{ads,dry}}{\rho_l m_{ads,dry}} \quad (6.14)$$

$$\varepsilon_p = \frac{V_{pore}}{V_{pore} + V_{solid}} = \frac{V_{pore}}{V_{pore} + m_{ads}/\rho_{solid}} \quad (6.15)$$

Determination of pore size distribution by volumetric adsorption measurement with nitrogen

A defined amount of sample was degassed at 105 °C under vacuum prior to the measurement, yielding in an approximate mass of 1.8 g of material for analysis. The sorption measurement of oxygen-free nitrogen gas (B.O.C., United Kingdom) on ZSM-5 G-360 was carried out at -196 °C with a surface area and porosimetry analyser (ASAP 2420, Micrometrics, United States) using 40 adsorption and 30 desorption pressure points, respectively. Prior the analysis the sample was outgassed under a vacuum of 10 µmHg at 50 °C, and subsequently 110 °C, for 2 hours. The corresponding isotherm was consequently analysed with the B.E.T. model [42], assuming unrestricted multilayer formation according to equation 6.16. The measurement was carried out in duplicate. The calculation of the overall and the micropore volume was done with analysis software VersaWin (version 2.0) of Quantachrome Instruments.

$$\frac{p}{q_p(p^o - p)} = \frac{1}{q_{mono}C} + \frac{(C - 1)p}{q_{mono}C p^o} \quad (6.16)$$

Determination of pore size distribution by volumetric adsorption measurement with mercury

A defined amount of sample was conditioned for 6 hours at 300°C and analysed in a mercury porosimeter (Pascal 140 and 440, Porotech, Germany). The analysis was evaluated according to ISO 15901-1 [43].

6.3.5. Microscopic analysis

Microscopic pictures were taken with a light microscope from Leica type M202 FA (Germany) equipped with a digital camera (Leica DFC240) and a scanning electron microscope (SEM) EVO LS 25 (Zeiss, Germany). Additionally, samples were analysed with energy dispersive X-ray (EDX) of detector XFlash 5030 (BRUKER, United States).

6.3.6. Determination of multicomponent isotherm

To obtain multicomponent isotherms, simple batch uptake experiments were carried out with crushed zeolite particles. The pre-determined amount of adsorbent was weighed into a glass vial and the model solution was consequently added by carefully pouring it into the vial. The vials were stirred overnight with a closed cap at 5 °C. An overview of the experiments performed to determine the isotherm is given in Table 6.4 in the appendix. All experiments were done in duplicate.

6.3.7. Hydrodynamically defined batch uptake experiments

Prior to the experiment, 1.5 g of washed and dried particles were incubated overnight in milli-Q grade water to ensure equilibration with the solvent. They were then packed into a glass column with a diameter of 1 cm and adjustable length (Omnifit, USA), which was connected to a double-walled stirred reactor of 2 L capacity (Applikon, The Netherlands). The scheme of the set-up is shown in Figure 6.2. During the duration of the experiment the temperature was controlled with a water bath at 5 °C and the system was kept closed to avoid losses due to evaporation. To start the experiment, the reactor was filled with 1.5 L model solution and stirred at 600 rpm. A blank sample was taken from the sample port and after, the model solution was circulated at a flow rate of 60 mL/min, resulting in a superficial velocity of 76.4 cm/min. The flow rate was chosen as such that the concentration gradient over the column as well as external mass transfer limitations were minimal to negligible (data is shown in appendix material, Figure 6.12). Samples were taken frequently during a period of 22.5 hours to follow the uptake of

aldehydes and each experiment was carried out in duplicate to estimate the experimental error. Three different particle sizes were tested. In order to ensure that equilibrium can be reached, a prolonged batch of 54 hours was carried out in duplicate with particles of a diameter of 2.35 mm. The initial concentration of all five compounds of interest was set to $c_0 = 0.5$ mg/L.

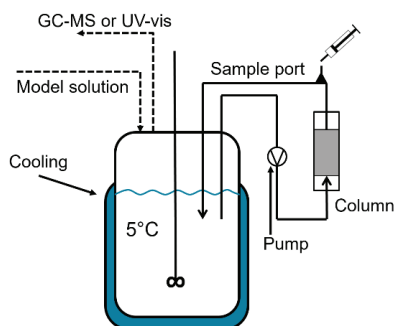


Figure 6.2: Schematic set-up for hydrodynamically defined batch uptake experiments

6.3.8. Analysis of aldehydes

To analyse the concentration of aldehydes, samples were diluted with 65 g/L maltodextrin solution to the calibration range (<100 $\mu\text{g/kg}$) and consequently analysed by headspace solid-phase micro-extraction (HS-SPME) in a GC-MS (Agilent 7890A and 5975C MSD) and a 30 m x 0.25 mm x 0.25 μm 142 VF17MS column with an adapted protocol of Vesley *et al.* (2003) [44]. The carrier gas (helium) was used at a flow rate of 1 mL/min. The calibration was performed by internal standard addition to increase the accuracy.

6.3.9. Mathematical modelling

The model of the intraparticle mass transfer was built in COMSOL Multiphysics (version 5.3a) and the regression was performed by coupling the model to Matlab R2018b, to identify the optimal solution with *lsqcurvefit*, a nonlinear least-squares solver. Advanced Chemistry Development Inc. (ACD/Labs) software [45] was used to estimate the logD values and the molar volume.

6.4. Results & Discussion

6.4.1. Adsorbent characterization

The general structure of ZSM-5 G-360 granules is depicted in the light microscope images in Figure 6.3-A and B. The granules consist of small zeolite crystals pressed into a spherical shape

in a kind of ring formation. The edge where breakage occurs is, hence, spherical as well. A closer look with SEM images in Figure 34C and D reveal a denser layer at the outer side of the particle, forming a shell around the granule for stability purposes. In order to understand the hierarchical structure of the material, further characterisation techniques were applied.

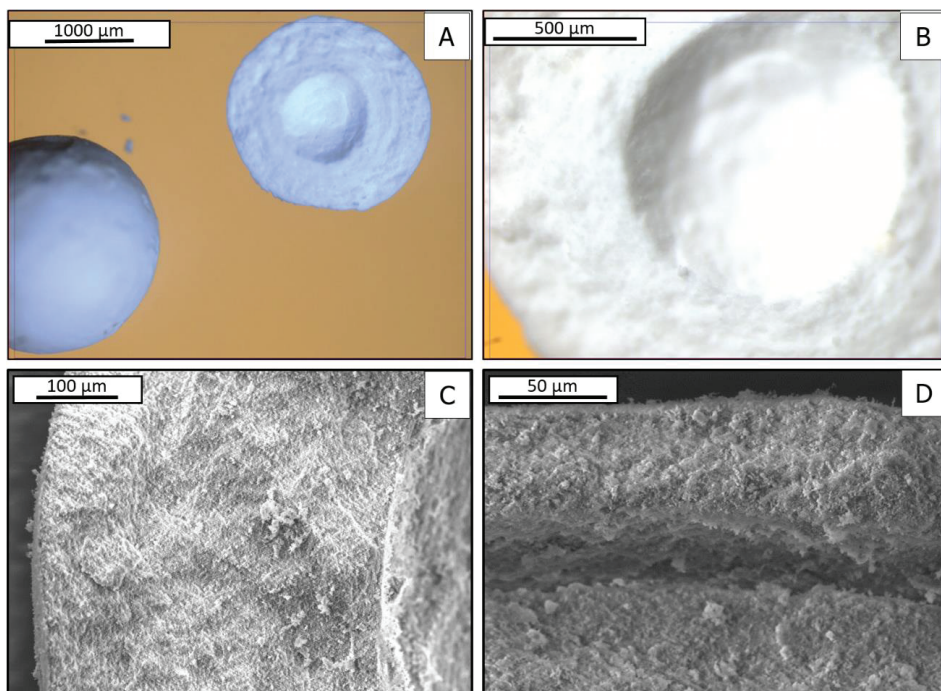


Figure 6.3: Light microscope images (top) and scanning electron microscopy picture of zeolite G-360 (C) core and (D) shell

The analysis of the material by nitrogen adsorption (data in appendix) led to following findings: As expected, the material exhibits a high micropore volume, caused by the for ZSM-5 characteristic micropores of 5.4-5.6 Å. Small mesopores were found in the range of 2.0-3.0 nm, while pores > 5 nm were absent. Since the hysteresis observed in the N₂ isotherm is relatively narrow, we can conclude that also the pore size distribution is well defined. Furthermore, the plateau of the isotherm indicates that there is only a small volume of mesopores present. This was confirmed by analyzing the respective pore volumes: After applying the Rouquerol correction, the micropore volume was determined with the t-plot method to 0.175 cm³/g. The combined meso- and micropore volume was calculated to 0.195 cm³/g, meaning that the resulting mesopores volume is approximately 0.020 cm³/g.

Additionally, the porosity of larger pores in the range of $\sim 10\text{ nm} - 100\text{ }\mu\text{m}$ was studied by mercury porosimetry. A distinct peak was found around $\sim 180\text{ nm}$. This suggests that the granule originally contained a binder that was removed during calcination, forming homogeneous macropores for transport of the adsorbate to the crystals, rather than being synthesized and grown from the seed. The macropore volume from the measurement amounted to $0.28\text{ cm}^3/\text{g}$ and the mesopore volume ($10 - 50\text{ nm}$) to $0.015\text{ cm}^3/\text{g}$. The mesopores volume is comparable to that found during N_2 sorption, however, in a higher pore size range. The mesopores pore volume of pores $< 10\text{ nm}$ is not evaluated, since the applied high pressure could potentially destroy the material structure.

To determine the accessible volume for liquids, the porosity also was determined with a gravimetric method using ethanol as a sorbate. The solid density and porosity were averaged over all particle sizes, resulting in $2.23 \pm 0.3\text{ kg/L}$ and 0.54 ± 0.2 , respectively. The apparent particle density hence is $1.05 \pm 0.04\text{ kg/L}$. The same experiment carried out with water led to a 20 % lower porosity, indicating that the granule is not fully accessible to the polar liquid. This observation was previously made by Wach et al. (2018) as well, who found that the total porosity experimentally determined by the retention of D_2O was about 10 % lower than the total porosity determined through N_2 and Hg porosimetry [23]. Assuming the same solid density, the porosity determined with the gravimetric method is compared to the porosity from N_2 and Hg adsorption. Here, a value of 0.51 is calculated, which is in good agreement with the gravimetric value. The slightly higher value could be explained by the fact that microporosity is often underestimated by the t-plot method in hierarchical materials [46], but also experimental errors play a role. Because we are investigating the behaviour of organic compounds in a liquid system, we consider the accessibility of the target molecules to the pores resemble most likely those of ethanol. We hence chose to base our proceeding analysis based on the results of the gravimetric method with water and ethanol.

6.4.2. Adsorption equilibrium

To be able to investigate the dynamics of the studied system, the equilibrium conditions, i.e. the adsorption isotherms must be determined. Therefore, batch uptake experiments were performed at different compositions of the model solution. The results are plotted in Figure 6.4. Generally, the equilibrium uptake can be characterized by the Freundlich isotherm with a slight decline in isotherm slope with increasing concentration. The parity plot confirms that the distribution is equally spread and the model is a good representation of the experimental data.

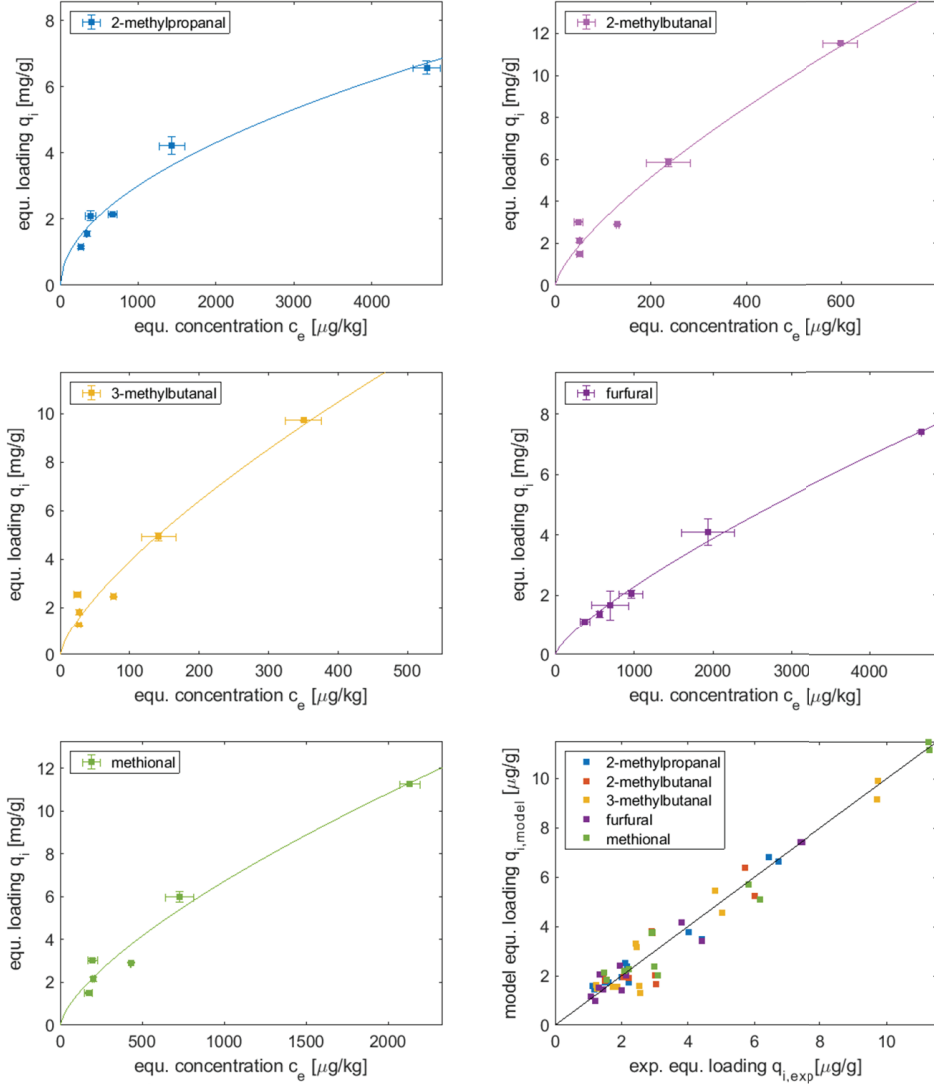


Figure 6.4: Freundlich isotherms and parity plot for all compounds of the model solution at pH 4.2

When regarding the affinities of the compounds to the adsorbent, one can find a relation between the hydrophobicity of the compound with the affinity to the adsorbent. This was also reported in previous research on alcohol-free beer [15]. 2- and 3-MB adsorb the strongest, followed by Met, while 2-MP and FF show the lowest adsorption loading under given conditions. Although there are multiple compounds in the system, we assume that the diffusivity can be regressed for a single compound. This is based on the following reasoning: 1. The system is very dilute ($c < 0.5$ mg/L) and 2. The isotherms show a near linear behaviour

in the observed range (<0.5 mg/L), hence, allowing the assumption of non-competitive adsorption process.

6.4.3. Investigating mass transfer in model solution

In this section, the experimental data of uptake experiments is presented and the effective diffusivity is regressed with the HSDM. Representative for all settings, Figure 6.5 shows the uptake of 2-MP, 2-MB, 3-MB, FF and Met from the model solution starting at 0.5 mg/L and $d_p = 2.35$ mm. From Figure 6.5 we can observe that the uptake follows an asymptotic behaviour and is relatively similar in shape for 2-MB, 3-MB, Met and FF, converging towards the equilibrium loading. Nonetheless, even after an experimental time of 54 hours, the equilibrium state is not reached.

While overall, the model describes the experimental data sufficiently well, a general trend of overestimating the initial diffusivity and underestimating it in the later stage is observed. This effect is emphasized in the parity plot of Figure 6.5, showing a deviation from the predicted values in the lower range of concentrations. On the contrary to other studied compounds, the uptake of 2-MP is very well described by the model ($R^2 = 0.99$). Remarkably, 2-MP follows a less pronounced decline, only reducing to 40 % of its initial concentration in the bulk after 54 hours, despite being the smallest molecule studied. This goes against the expectation that mass transfer is related to the molecular size.

The regressed effective diffusion coefficients, their average relative error (ARE) and associated coefficient of determination (R^2) of all performed tests are listed in Table 6.2. At first glance, we can observe that the effective diffusivities are very small and range vastly from $1.6 \cdot 10^{-15}$ (3-MB) to $4.1 \cdot 10^{-13}$ (FF) m^2/s , which is nearly a factor 100 difference. This range is comparable to literature values presented in Table 6.1. The coefficients of determination are > 0.9 , except for the medium-sized granules. Here, the initial slope in the bulk concentration is even flatter, resulting in a less good fit with the model. Although the experiment was carried out in duplicate, this might be related to non-optimal flow conditions resulting in additional resistance to the mass transfer. The ARE is within a range of 2-15% reasonable and the model is, hence, able to predict the mass transfer phenomena. Only methional's diffusivity in the small granules shows a larger ARE, which is due to the higher deviation of the predicted and experimental concentrations as described above at $c_i \ll c_0$.

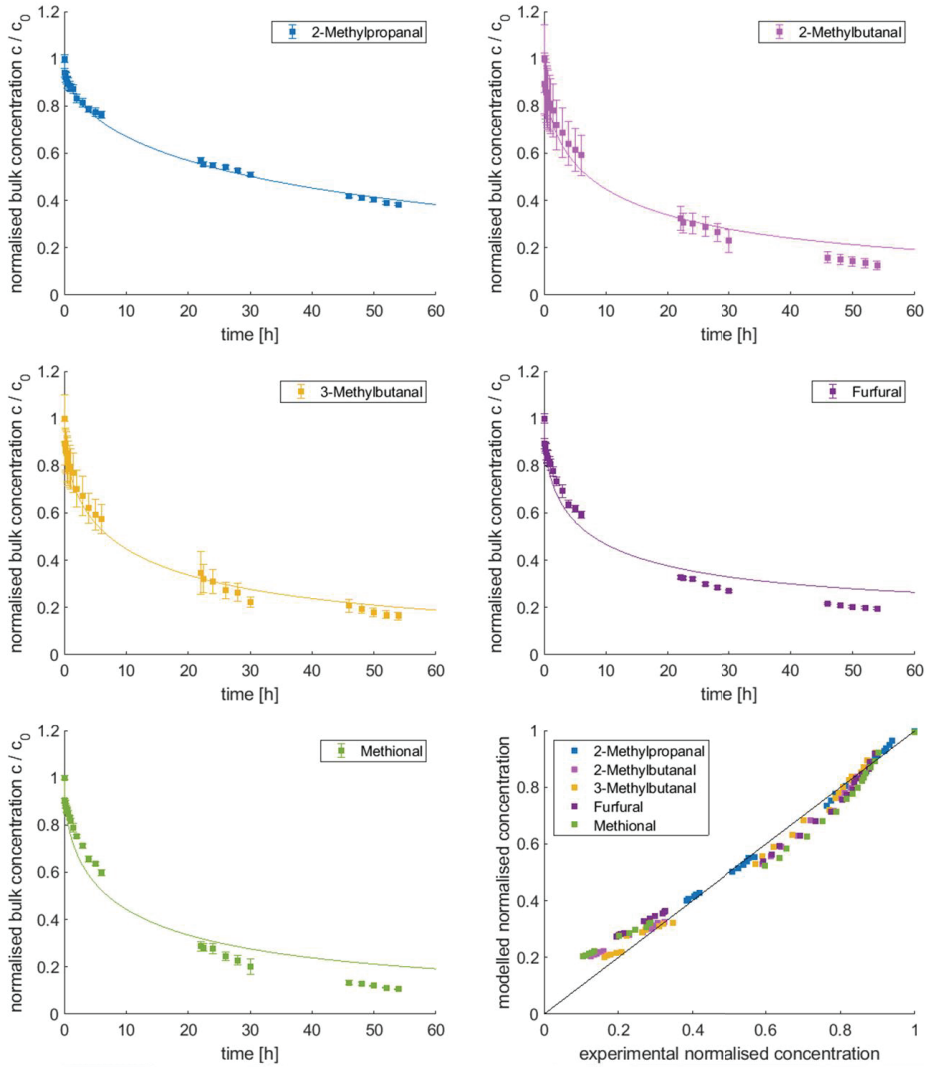


Figure 6.5: Experimental and model-based decrease of bulk concentration in model solution for 2-MP, 2-MB, 3-MB, FF, and Met for particles with a radius of 1.175 mm (small)

Table 6.2: Regressed effective diffusion coefficients, coefficient of determination and associated error

d_p [mm]	C_0 [mg/L]	2-MP				2-MB			
		D_{eff} [m ² /s]	σ_{Deff} [m ² /s]	ARE [%]	R ²	D_{eff} [m ² /s]	σ_{Deff} [m ² /s]	ARE [%]	R ²
2.35	0.5	$3.0 \cdot 10^{-14}$	$2.2 \cdot 10^{-15}$	2.0	0.99	$6.5 \cdot 10^{-15}$	$1.5 \cdot 10^{-15}$	13.4	0.98
2.656	0.5	$2.5 \cdot 10^{-14}$	$9.5 \cdot 10^{-15}$	5.4	0.87	$2.8 \cdot 10^{-15}$	$2.3 \cdot 10^{-15}$	15.4	0.75
3.118	0.5	$2.9 \cdot 10^{-14}$	$4.0 \cdot 10^{-15}$	1.7	0.98	$3.9 \cdot 10^{-15}$	$1.7 \cdot 10^{-15}$	11.2	0.91
2.35	0.25	$2.2 \cdot 10^{-14}$	$5.8 \cdot 10^{-15}$	3.2	0.95	$4.5 \cdot 10^{-15}$	$2.2 \cdot 10^{-15}$	9.4	0.93
2.35	0.125	$1.5 \cdot 10^{-14}$	$2.8 \cdot 10^{-15}$	1.6	0.97	$3.7 \cdot 10^{-15}$	$1.5 \cdot 10^{-15}$	8.7	0.95

d_p [mm]	C_0 [mg/L]	3-MB				FF			
		D_{eff} [m ² /s]	σ_{Deff} [m ² /s]	ARE [%]	R ²	D_{eff} [m ² /s]	σ_{Deff} [m ² /s]	ARE [%]	R ²
2.35	0.5	$4.2 \cdot 10^{-15}$	$7.4 \cdot 10^{-16}$	6.5	0.98	$4.1 \cdot 10^{-13}$	$1.2 \cdot 10^{-13}$	13.0	0.97
2.656	0.5	$2.0 \cdot 10^{-15}$	$1.4 \cdot 10^{-15}$	14.5	0.80	$2.9 \cdot 10^{-13}$	$9.5 \cdot 10^{-14}$	4.1	0.95
3.118	0.5	$2.5 \cdot 10^{-15}$	$8.8 \cdot 10^{-16}$	11.2	0.93	$2.4 \cdot 10^{-13}$	$7.6 \cdot 10^{-14}$	2.4	0.95
2.35	0.25	$3.3 \cdot 10^{-15}$	$1.6 \cdot 10^{-15}$	8.2	0.93	$1.7 \cdot 10^{-13}$	$4.8 \cdot 10^{-14}$	3.0	0.96
2.35	0.125	$2.3 \cdot 10^{-15}$	$9.0 \cdot 10^{-16}$	7.2	0.95	$7.9 \cdot 10^{-14}$	$2.5 \cdot 10^{-14}$	5.3	0.95

d_p [mm]	C_0 [mg/L]	Met			
		D_{eff} [m ² /s]	σ_{Deff} [m ² /s]	ARE [%]	R ²
2.35	0.5	$3.8 \cdot 10^{-14}$	$1.2 \cdot 10^{-14}$	22.4	0.96
2.656	0.5	$2.3 \cdot 10^{-14}$	$1.1 \cdot 10^{-14}$	14.3	0.90
3.118	0.5	$2.5 \cdot 10^{-14}$	$9.6 \cdot 10^{-15}$	7.2	0.93
2.35	0.25	$1.8 \cdot 10^{-14}$	$9.0 \cdot 10^{-15}$	6.9	0.92
2.35	0.125	$1.4 \cdot 10^{-14}$	$4.7 \cdot 10^{-15}$	8.2	0.96

6.4.4. Implication of results

In addition to the quantitative analysis of the mass transfer to regress diffusivities, the results were analysed qualitatively to understand what the most dominant transport mechanism is and where the highest resistance lies. Considering the order of magnitude of the regressed effective diffusivities, the relatively large granule size and the high interstitial velocity, intraparticle mass transport is supposedly the controlling step during the adsorption process. This is confirmed, when calculating the respective Biot numbers (equation 6.17), which are presented in Table 6.3. A Biot number $\gg 10$ indicates mass transfer controlled through intraparticle diffusion, while $1 < Bi < 10$ mark a transitional regime, where both, external and intraparticle mass transfer determine the adsorption process. In our case, intraparticle transport is indeed limiting ($Bi \gg 10$). In the case of furfural at $c_0 = 0.5$ mg/L and $d_p = 2.35$ and 2.66 mm, the Biot number

is found between 10 and 100, meaning that at lower flow rates, film diffusion may become dominant eventually.

$$Bi = \frac{k_f r_p c_0}{D_{eff} \rho_p q_{eq}(c_0)} \quad (6.17)$$

When regarding the intraparticle mass transfer, particularly in composite pellets and granules, macro-/meso-pore and micro-pore (i.e. intracrystalline) diffusivities can be differentiated. Both of these resistances can be limiting to mass transport, depending on the relation of the diffusional time constants $(D_{micro}/r_c^2)/(D_{macro}/r_p^2)$. Varying the particle size during experimental uptake tests is hence a way of understanding the bottleneck of the transport path [31]. Figure 6.6 shows the relation of the regressed effective diffusivities of all studied compounds to the initial concentration and the particle size, respectively.

Table 6.3: Calculated Biot numbers for all conditions

d_p [mm]	C_0 [mg/L]	Biot number []				
		2-MP	2-MB	3-MB	FF	Met
2.35	0.5	435	420	529	55	182
2.656	0.5	555	1037	1180	82	320
3.118	0.5	519	806	1023	108	319
2.35	0.25	425	501	551	112	310
2.35	0.125	447	504	648	205	321

From the figure, it appears that increasing the initial concentration slightly increases the diffusion coefficient and that the diffusivity slightly decreases with increasing particle diameter. However, due to the error associated with the regression, no significant statement can be made. From the regressed experimental data, it is hence not clear, whether the diffusivity in the transport macropores or the micropores of the zeolite crystals is limiting. A thorough study of recent literature also reveals that beside macro- or micropore limitations also other effects, such as surface barriers at the crystal surface [34, 35, 47] can be involved, making a straight-forward analysis of the time-constants difficult. Other factors such as distribution in crystal size or agglomeration of these may also influence the results [34]. The effect of the concentration, depicted in Figure 6.6 is also important with regard to the assumption of a non-competitive adsorption process. If vacant adsorption sites would be limiting, the diffusivity should be lower at the higher initial concentration. Hence, we conclude that the separate analysis of compounds holds.

As mentioned above, neither a correlation between the molecular weight and the diffusivity nor a correlation between the molecular radius and the diffusion coefficients could be made. A

tentative relation between increasing molecular volume and decreasing effective diffusivity can be suggested as shown in Figure 6.7. However, there is a remarkable correlation between the hydrophobicity (represented by the logD value) and hence the adsorbent affinity constant with the diffusivity. That is, the more hydrophobic a compound and the higher the affinity to the adsorbent, the slower the transport through the particle.

When considering equation 6.18 [23], the effect of the adsorption affinity constant on the overall intraparticle mass transfer coefficient can be understood. Thus, this observation could be interpreted as a manifestation of (macro)pore diffusion being the controlling mechanism as the characteristic time of the macropore mass transfer is proportional to the affinity constant $K(c)$.

$$\frac{1}{k_{intra,eff}} = \frac{K(c)r_p^2}{15\epsilon D_p} + \frac{r_c^2}{15D_c} \quad (6.18)$$

Alternatively, the dependency on the affinity constant could be related to intracrystalline diffusion controlling the mass transfer. A similar relation on the adsorbent affinity constant was reported by Wach et al (2018) for sugar molecules on hydrophobic Y-zeolite [23]. The authors of the study concluded that a higher adsorbent affinity results in a slowed diffusion through the micropores i.e. decreased intracrystalline diffusivity. Another systematic study of non-volatile phenolic compounds' diffusion in zeolite beta and silicalite crystals was performed by Linh et al. (2016). Also in their case, the adsorption affinity rather than the critical diameter of the adsorbate was correlated to the intracrystalline diffusivity [48]. This mechanism resembles that of surface diffusion, which is limited by the adsorption energy of the sample. The migration of strongly adsorbing compounds is hence restricted by the adsorbate-adsorbent-interaction [49, 50].

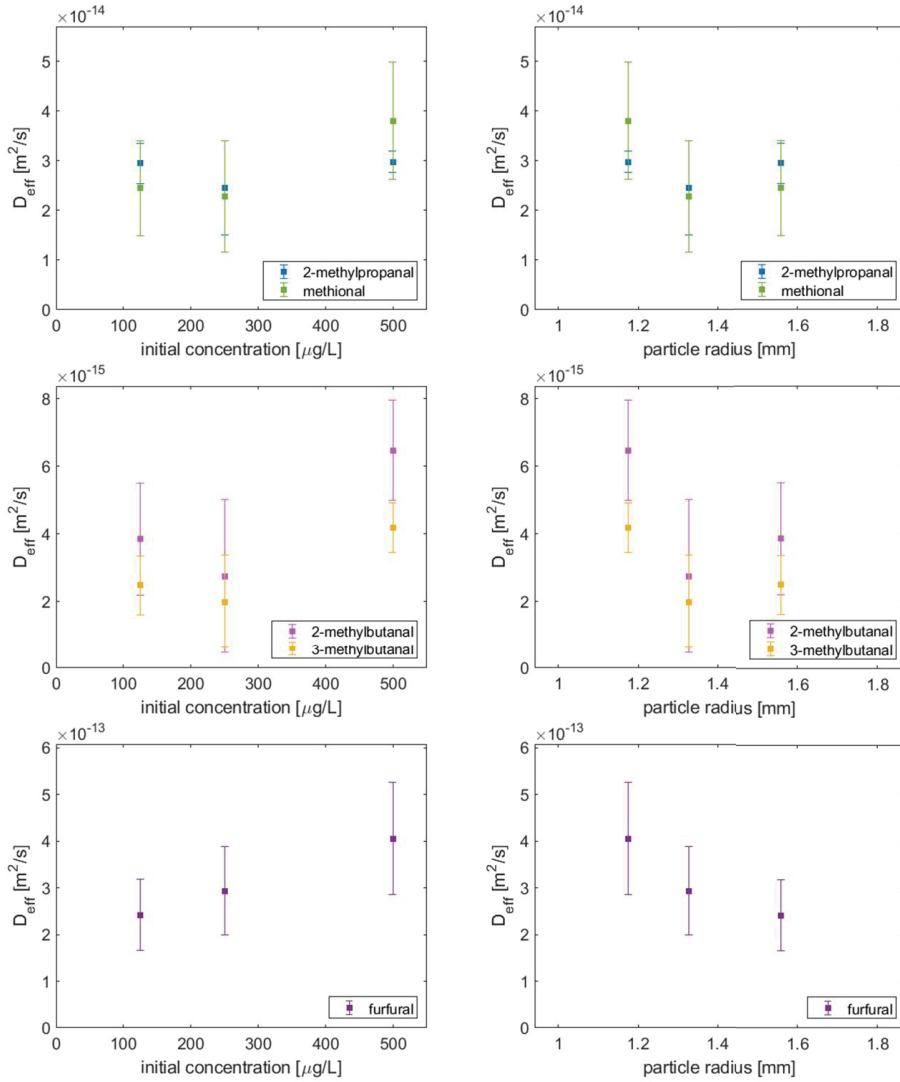


Figure 6.6: Regressed effective diffusion coefficient versus initial bulk concentration (left) and particle radius (right)

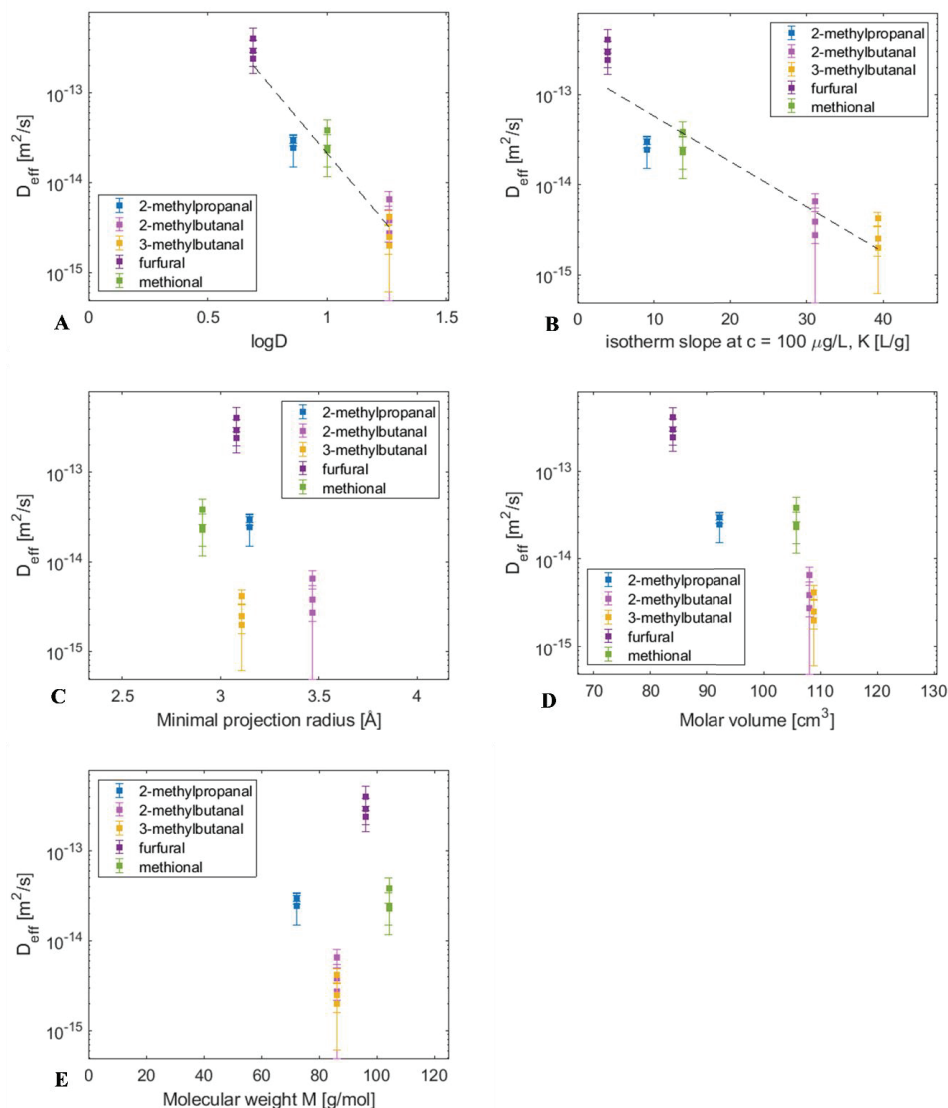


Figure 6.7: Correlation of regressed effective diffusion coefficient to (A) the molecular hydrophobicity (expressed as $\log D$) and (B) the isotherm affinity constant as well as (C) the minimal projection radius, (D) the molecular volume, and (E) the molar weight

Since the resistances in macro- and micropores are additive, it is probable that both, macropore diffusion and intracrystalline diffusion, play a major role in our case. Moreover, in Figure 6.5, it was observed that the model fit resulted in an overestimation of the diffusivity in the initial stage of the uptake and an underestimation at higher adsorbent loading when the equilibrium state was nearly reached. Overall, a logical explanation for the observed behaviour could be

similar to the following: Initially, the adsorbate has to overcome the surface barrier posed by the outer shell of the granule. It then diffuses along the macropore system, while at the same time, the adsorbate begins to penetrate the surface and micropores of the (agglomerated) crystals, which poses an additional transport resistance. After the adsorbate has fully penetrated the macropores of the granule, the uptake rate solely depends on the micropore diffusivity. Since the full volume of the granule is filled with adsorbate now, the uptake appears faster than in the beginning. The effect of varying particle size could, therefore, become much less sharp. Surely, other effects, such as agglomeration of crystals and the resulting variation of the micropore resistance may play a role as well.

Even though the actual mass transfer mechanism remains hypothetical, some conclusions for improving the material can be drawn. Decreasing the particle size of the granule itself, but also the crystals (i.e. reduce crystal agglomerated sizes) would be an effective measure to accelerate the mass transfer. However, also increasing the overall proportion of the transport pores would be beneficial to accelerate the mass transfer through the particle. This could, for instance, also mean introducing hierarchical structures into the zeolite crystals themselves in the form of mesopores [51].

Knowing these limitations, a sophisticated process unit design will help to increase productivity despite the mass transfer limitations. Both, the choice of a superior material (shape) as well as the process conduct, must be optimized to make the selective wort flavour removal feasible. Thereby, it is important to find a trade-off between fast mass transfer, which would be best in a powder shaped adsorbent, and regenerability and practical handling, where shaped zeolites are of advantage. A conceptual process design will give further insight into the optimal solution for this case.

6.5. Conclusion

In this study, the mass transfer of five flavour compounds in binder-free, hydrophobic ZSM-5 granules was investigated. The characterization of the material indicated that the granule consists of small crystals, connected by macropores of 180 nm and shaped into the bigger granule that is surrounded by a denser outer layer or shell for mechanical stability. We found the porosity calculated from gravimetrical experiments with ethanol were most representative for the accessible pore volume for small organic molecules, including the void in intracrystalline micropores. Following, the equilibrium of the multicomponent model solution was studied, to obtain the adsorption isotherms described by the Freundlich model. Due to the

near linear shape of the isotherms, it was concluded that the adsorption process is non-competitive and hence, the behaviour of the single compounds can be studied independently in the multicomponent solution.

Subsequently, during hydrodynamically well-defined batch uptake experiments, the dynamics of the adsorption process were measured and the effective diffusivities were obtained by applying the HSDM. The diffusivities ranged in the order of magnitude of 10^{-13} - 15^{-15} m²/s. The HSDM was suitable to regress the effective diffusion coefficient but showed some deviation at the asymptotic area of the uptake curve. Because of the relative high associated error of the diffusivities, there was no clear impact of a varying particle diameter or a concentration effect visible. Furthermore, there was no obvious correlation between the diffusivity with the molecular size or weight. Yet, a strong correlation between the intraparticle diffusion and the hydrophobicity and hence the affinity of the compound to the adsorbent material was found. While this data is very useful to model and design a unit operation to remove such flavour from liquid food streams, the exact mass transfer mechanism remains hypothetical. Most likely, the transport through the pores in combination with high resistance in the intracrystalline micropores form the bottleneck in the mass transfer process.

Concluding, we recommend to develop materials that have a more optimal particle and crystal size distribution of for liquid adsorption and/or a higher proportion of transport meso- and macropores to ensure fast uptake of the target compounds and transport to the micropores. Possibly, high-end analytical techniques such as micro-imaging [47] or NMR studies [31] could help to elucidate the actual mechanism inside the granule. Many of these, however, do not apply to liquids at such low concentrations and small crystal sizes. For future work, it would be interesting to verify, if the correlation of diffusivity and hydrophobicity also holds for other materials (shapes) and molecule groups. Furthermore, a conceptual process design study will reveal the feasibility of the process at commercial scale.

6.6.Acknowledgements

We gratefully acknowledge Heineken Supply Chain B.V. for funding this project. Furthermore, we would like to thank Dr. C. Bläker (Universität Duisburg-Essen) and Dr. A. Fletcher (University Strathclyde) for carrying out the sorption experiments for the material characterization as well as Dr. D. Hartig (Technische Universität Braunschweig) for taking the SEM pictures. We also would like to thank and Dr. P. van den Broeke for his feedback and Dr. C. Picioreanu (Delft University of Technology) for his contribution to the computational work.

6.7.Nomenclature

Symbol	Explanation/ SI units
A_s	External surface area of adsorbent granules [m^2]
Bi	Biot number []
c	Concentration in the bulk liquid [mol/m^3] or [kg/kg]
c_s	Concentration at the surface [mol/m^3]
C	Brunauer–Emmett–Teller (BET) constant []
D_c	Intracrystalline diffusivity [m^2/s]
d_c / d_p	Crystal/particle diameter [m]
D_{eff}	Effective diffusivity [m^2/s]
d_{extr}	Diameter extrudate [m]
D_L	Axial dispersion [m^2/s]
D_m	Molecular diffusivity in water [m^2/s]
D_{macro}	Macropore diffusivity [m^2/s]
J	Flux [$mol/s/m^2$]
K	Adsorption equilibrium constant []
k_{eff}	Overall mass transfer coefficient [$1/s$]
k_f	Film mass transfer coefficient [m/s]
K_F	Adsorption equilibrium constant Freundlich model (unit variable)
M	Molecular weight [kg/mol]
m	Mass [kg]
n	Adsorption equilibrium constant Freundlich model (unit variable)
p / p^o	Pressure / saturation vapour pressure [$kg \cdot m/s^2$]
Q	Quantity (unit variable)
q_e	Loading of adsorbent at equilibrium [mol/kg] or [kg/kg]
q_t	Loading of adsorbent at time t [kg/kg]
q_p	Loading at pressure p [mol/kg]
q_{mono}	Loading at monolayer coverage [mol/kg]
r_p / r_c	Radius of particle / crystal [m]
t	Time [s]
T	Temperature [K]
u	Interstitial velocity [m/s]
V_b	Liquid bulk volume [m^3]
V_m	Molecular volume [m^3]

Symbol	Explanation
ε	Particle porosity []
η	Viscosity [$\text{kg}/(\text{m} \cdot \text{s}^2)$]
ρ	Density [kg/m^3]
ξ	Eigenvalue of Bessel function []
σ	Standard deviation (unit variable)
σ_m	Standard error (unit variable)
τ	Tortuosity []
ψ	Constant solute-solvent interaction []

Abbreviations	
ARE	Average relative error
BEA	Zeolite framework type (beta)
EDX	Energy dispersive X-ray
FAU	Zeolite framework type (faujasite)
FF	Furfural
HSDM	Homogeneous surface diffusion model
2-MB	2-Methylbutanal
3-MB	3-Methylbutanal
2-MP	2-Methylpropanal
Met	Methional
R^2	Coefficient of determination
SEM	Scanning electron microscope
ZSM-5	Zeolite Socony Mobil-5

6.8. References

1. Chmelik, C. and J. Kärger, *In situ study on molecular diffusion phenomena in nanoporous catalytic solids*. Chemical Society Reviews, 2010. 39(12): p. 4864-4884.
2. Hwang, S. and J. Kärger, *NMR diffusometry with guest molecules in nanoporous materials*. Magnetic Resonance Imaging, 2019. 56: p. 3-13.
3. Kärger, J. and D.M. Ruthven, *Diffusion in nanoporous materials: Fundamental principles, insights and challenges*. New Journal of Chemistry, 2016. 40(5): p. 4027-4048.
4. Krishna, R., *The Maxwell-Stefan description of mixture diffusion in nanoporous crystalline materials*. Micropor Mesopor Mat, 2014. 185: p. 30-50.
5. Babel, S. and T.A. Kurniawan, *Low-cost adsorbents for heavy metals uptake from contaminated water: A review*. Journal of Hazardous Materials, 2003. 97(1-3): p. 219-243.
6. Erdem, E., N. Karapinar, and R. Donat, *The removal of heavy metal cations by natural zeolites*. Journal of Colloid and Interface Science, 2004. 280(2): p. 309-314.

7. Wang, S. and Y. Peng, *Natural zeolites as effective adsorbents in water and wastewater treatment*. Chemical Engineering Journal, 2010. 156(1): p. 11-24.
8. Moliner, M., Y. Román-Leshkov, and M.E. Davis, *Tin-containing zeolites are highly active catalysts for the isomerization of glucose in water*. Proceedings of the National Academy of Sciences of the United States of America, 2010. 107(14): p. 6164-6168.
9. Holm, M.S., S. Saravanamurugan, and E. Taarning, *Conversion of Sugars to Lactic Acid Derivatives Using Heterogeneous Zeotype Catalysts*. Science, 2010. 328(5978): p. 602-605.
10. Berensmeier, S. and K. Buchholz, *Separation of isomaltose from high sugar concentrated enzyme reaction mixture by dealuminated β -zeolite*. Separation and Purification Technology, 2004. 38(2): p. 129-138.
11. Wach, W., et al., *Chromatographic separation of saccharide mixtures on zeolites*. Food and Bioproducts Processing, 2019. 114: p. 286-297.
12. Ching, C.B., et al., *Experimental study of a simulated counter-current adsorption system-V. Comparison of resin and zeolite absorbents for fructose-glucose separation at high concentration*. Chemical Engineering Science, 1987. 42(11): p. 2547-2555.
13. Sánchez, Ó.J. and C.A. Cardona, *Trends in biotechnological production of fuel ethanol from different feedstocks*. Bioresource Technology, 2008. 99(13): p. 5270-5295.
14. Taarning, E., et al., *Zeolite-catalyzed biomass conversion to fuels and chemicals*. Energy and Environmental Science, 2011. 4(3): p. 793-804.
15. Gernat, D.C., et al., *Selective off-flavor reduction by adsorption: A case study in alcohol-free beer*. Food and Bioproducts Processing, 2020. 121: p. 91-104.
16. Beal, A.D. and D.S. Mottram, *Compounds contributing to the characteristic aroma of malted barley*. Journal of Agricultural and Food Chemistry, 1994. 42(12): p. 2880-2884.
17. Perpète, P. and S. Collin, *Contribution of 3-methylthiopropionaldehyde to the worty flavor of Alcohol-free beers*. Journal of Agricultural and Food Chemistry, 1999. 47(6): p. 2374-2378.
18. Meilgaard, M.C., *Flavor chemistry in beer: Part II: Flavor and flavor threshold of 239 aroma volatiles*. Master Brewers Association of the Americas, 1975. 12: p. 151-168.
19. Andrés-Iglesias, C., et al., *Comparison of carbonyl profiles from Czech and Spanish lagers: Traditional and modern technology*. LWT - Food Science and Technology, 2016. 66: p. 390-397.
20. Holtkamp, M. and S. Scholl, *Adsorption properties of BEA zeolites and their aluminum phosphate extrudates for purification of isomaltose*. Adsorption, 2011. 17(5): p. 801-811.
21. García, M.G., J.M. García Fernández, and C. Buttersack, *Adsorption of difructose dianhydrides on hydrophobic Y-zeolites*. Microporous and Mesoporous Materials, 2020. 292.

22. Fornefett, I., et al., *Correction: Adsorption of sucrose on zeolites (Green Chemistry (2016) 18 (3378-3388) DOI: 10.1039/C5GC02832A)*. Green Chemistry, 2018. 20(15): p. 3643.
23. Wach, W., C. Buttersack, and K. Buchholz, *Chromatography of mono- and disaccharides on granulated pellets of hydrophobic zeolites*. Journal of Chromatography A, 2018. 1576: p. 101-112.
24. Buttersack, C., et al., *High specific interaction of polymers with the pores of hydrophobic zeolites*. Langmuir, 1996. 12(13): p. 3101-3106.
25. Waluga, T. and S. Scholl, *Process Design Aspects for Reaction-Integrated Adsorption in Multi-Enzymatic Catalysis*. Chemical Engineering and Technology, 2015. 38(10): p. 1817-1826.
26. Ching, C.B. and D.M. Ruthven, *A liquid phase chromatographic study of sorption and diffusion of glucose and fructose in NaX and KX zeolite crystals*. Zeolites, 1988. 8(1): p. 68-73.
27. Ma, Y.H. and Y.S. Lin, *Adsorption and diffusion of liquids in silicalite using HPLC*. in *AIChE Symposium Series*. 1987.
28. Vidal, C.B., et al., *Experimental and theoretical approach to multicomponent adsorption of selected aromatics on hydrophobically modified zeolite*. Journal of Chemical and Engineering Data, 2014. 59(2): p. 282-288.
29. Ching, C.B. and D.M. Ruthven, *Sorption and diffusion of some amino acids in KX zeolite crystals*. The Chemical Engineering Journal, 1989. 40(1): p. B1-B5.
30. Guiochon, G., *Fundamentals of preparative and nonlinear chromatography*. 2nd ed. ed. 2006, Boston: Elsevier.
31. J Kärger, D.M.R., *Diffusion in Zeolites and Other Microporous Solids*. 1992, New York: Wiley & Sons INC. 605.
32. Choi, J.G., D.D. Do, and H.D. Do, *Surface diffusion of adsorbed molecules in porous media: Monolayer, multilayer, and capillary condensation regimes*. Industrial and Engineering Chemistry Research, 2001. 40(19): p. 4005-4031.
33. Kärger, J., et al., *NMR study of mass transfer in granulated molecular sieves*. AIChE Journal, 1988. 34(7): p. 1185-1189.
34. Rao, S.M., et al., *Surface barriers as dominant mechanism to transport limitations in hierarchically structured catalysts – Application to the zeolite-catalyzed alkylation of benzene with ethylene*. Chemical Engineering Journal, 2017. 329: p. 45-55.
35. Teixeira, A.R., et al., *Dominance of Surface Barriers in Molecular Transport through Silicalite-1*. The Journal of Physical Chemistry C, 2013. 117(48): p. 25545-25555.
36. Wilke, C.R. and P. Chang, *Correlation of diffusion coefficients in dilute solutions*. AIChE Journal, 1955. 1(2): p. 264-270.

37. Bird, R.B., W.E. Stewart, and E.N. Lightfoot, *Transport phenomena*. 2nd, Wiley international ed. ed. 2002, New York: J. Wiley.
38. Weber, T.W. and R.K. Chakravorti, *Pore and solid diffusion models for fixed-bed adsorbers*. *AIChE Journal*, 1974. 20(2): p. 228-238.
39. Rosen, J.B., *Kinetics of a fixed bed system for solid diffusion into spherical particles*. *The Journal of Chemical Physics*, 1952. 20(3): p. 387-394.
40. Ijzer, A.C., et al., *Adsorption kinetics of Dowex™ Optipore™ L493 for the removal of the furan 5-hydroxymethylfurfural from sugar*. *Journal of Chemical Technology and Biotechnology*, 2016. 91(1): p. 96-104.
41. Skoog, D.A., F.J. Holler, and S.R. Crouch, *Principles of instrumental analysis*. 6th ed. ed. 2007, Belmont, CA: Thomson-Brooks/Cole.
42. Brunauer, S., P.H. Emmett, and E. Teller, *Adsorption of Gases in Multimolecular Layers*. *Journal of the American Chemical Society*, 1938. 60(2): p. 309-319.
43. *International Organization for Standardization, ISO 15901-1:2016 - Evaluation of pore size distribution and porosity of solid materials by mercury porosimetry and gas adsorption — Part 1: Mercury porosimetry*. 2016. p. 19.
44. Vesely, P., et al., *Analysis of Aldehydes in Beer Using Solid-Phase Microextraction with On-Fiber Derivatization and Gas Chromatography/Mass Spectrometry*. *Journal of Agricultural and Food Chemistry*, 2003. 51(24): p. 6941-6944.
45. Advanced Chemistry Development, I.A.L. *ACD/Percepta Platform*. 2019 28.08.2019]; 2018.1:[Available from: www.acdlabs.com.
46. Galarneau, A., et al., *Validity of the t-plot method to assess microporosity in hierarchical micro/mesoporous materials*. *Langmuir*, 2014. 30(44): p. 13266-13274.
47. Remi, J.C.S., et al., *The role of crystal diversity in understanding mass transfer in nanoporous materials*. *Nature Materials*, 2016. 15(4): p. 401-406.
48. Linh, T.N., H. Fujita, and A. Sakoda, *Diffusion of non-volatile phenolic compounds in zeolite beta and silicalite in liquid phase*. *Adsorption*, 2016. 22(7): p. 1001-1011.
49. Miyabe, K. and G. Guiochon, *Surface diffusion in reversed-phase liquid chromatography*. *Journal of Chromatography A*, 2010. 1217(11): p. 1713-1734.
50. Miyabe, K. and G. Guiochon, *Correlation between surface diffusion and molecular diffusion in reversed-phase liquid chromatography*. *Journal of Physical Chemistry B*, 2001. 105(38): p. 9202-9209.
51. Groen, J.C., et al., *Direct demonstration of enhanced diffusion in mesoporous ZSM-5 zeolite obtained via controlled desilication*. *Journal of the American Chemical Society*, 2007. 129(2): p. 355-360.

52. Breck, D.W., *Zeolite Molecular Sieves: Structure, Chemistry and Use*, ed. J.W.S. Inc. 1974, New York.

6.9. Appendices

6.9.1. Measurement of pore size distribution

Figure 6.8 to Figure 6.10 depict the adsorption and desorption isotherm of nitrogen and mercury as well as the resulting pore size distribution, respectively.

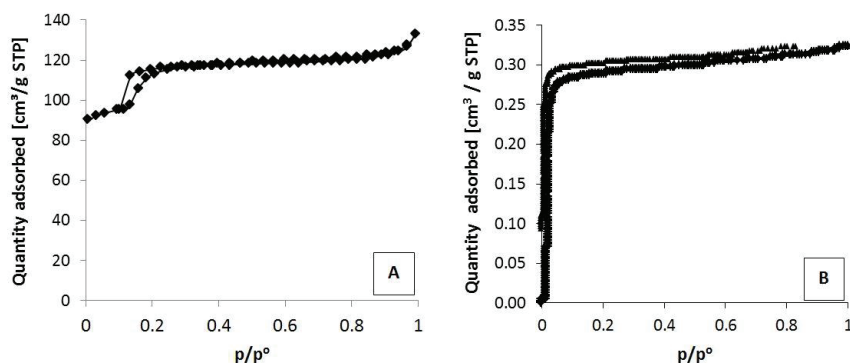


Figure 6.8: Adsorption / desorption isotherm of ZSM-5 G-360 of (A) nitrogen and (B) mercury

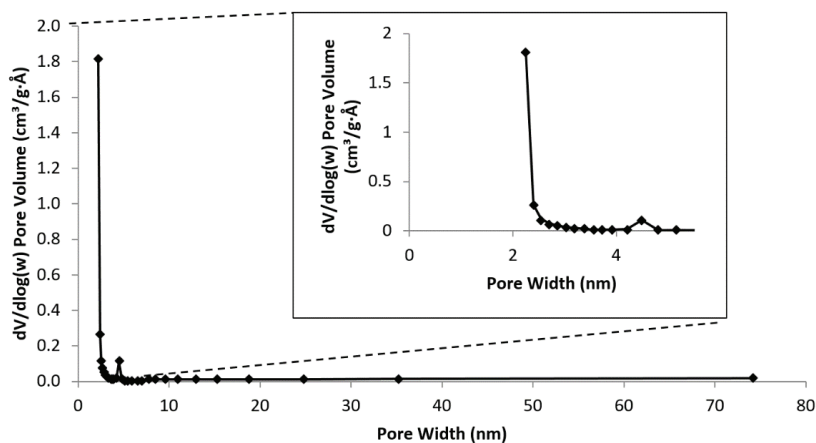


Figure 6.9: Pore size distribution of ZSM-5 G-360 resulting from BET measurement with nitrogen

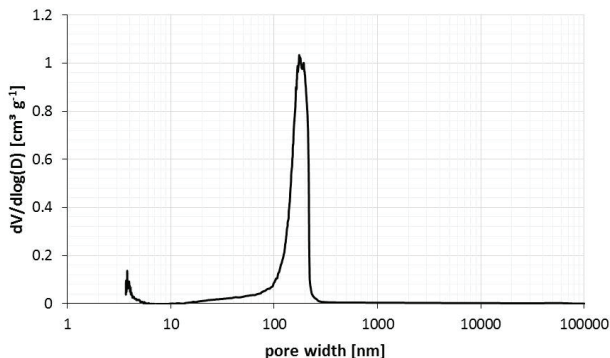


Figure 6.10: Pore size distribution of ZSM-5 G-360 resulting from sorption measurement with mercury

6.9.2. Equilibrium batch uptake experiments

Table 6.4 summarized all tested conditions to obtain the adsorption equilibrium.

Table 6.4: Overview on selected batch uptake experiments to determine the multicomponent isotherm

#	Phase [kg _{liq} /g _{ads}]	ratio	c _i [mg/kg _{liq}]
1	2.0		c _{2-MP} = 1.425
2	1.5		c _{2-MB} = 1.540
			c _{3-MB} = 1.280
3	1.0		c _{FF} = 1.521
			c _{Met} = 1.700
			c _{2-MP} = 2.849
			c _{2-MB} = 3.081
4	1.0		c _{3-MB} = 2.560
			c _{FF} = 3.042
			c _{Met} = 3.397
			c _{2-MP} = 5.698
			c _{2-MB} = 6.161
5	1.0		c _{3-MB} = 5.120
			c _{FF} = 6.084
			c _{Met} = 6.793
			c _{2-MP} = 11.396
			c _{2-MB} = 12.322
6	1.0		c _{3-MB} = 10.240
			c _{FF} = 12.168
			c _{Met} = 13.586

6.9.3. Determination of viscosity and choice of model solution composition

The viscosity at various shear rates was measured with a rolling-ball viscometer (LOVIS 2000 ME, Anton Paar, Austria) according to the procedures recommended by the manufacturer. Figure 6.11 shows the viscosity of various maltodextrin solutions in dependency of the shear rate. Furthermore, the viscoelastic behaviour of alcohol-free beer (AFB) was analysed. Hence, it was found that a maltodextrin solution of 65 g/L mimics the viscosity of AFB best.

6.9.4. Investigation of hydrodynamic conditions during uptake experiments

In Figure 6.12, a preliminary experiment was performed with the model solution containing only furfural ($c_0 = 9 \text{ mg/L}$) to ensure that the flow rate does not effect the uptake dynamics during the ZGC measurement. Despite some variance in the measurements, there is no statistically significant difference between the uptake experiments at different flow rates and also no trend can be observed. It is hence concluded, that at the chosen conditions (flow rate 60 mL/min), the affect of the intraparticle transport is isolated and can be observed independently from the effect of film mass transfer or external diffusion limitations, i.e. the bulk is ideally mixed.

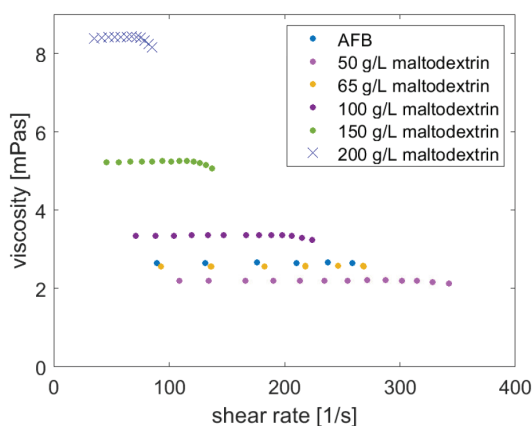


Figure 6.11: Viscosity of various maltodextrin solutions at pH 4.2 and alcohol-free beer in dependency of the shear rate

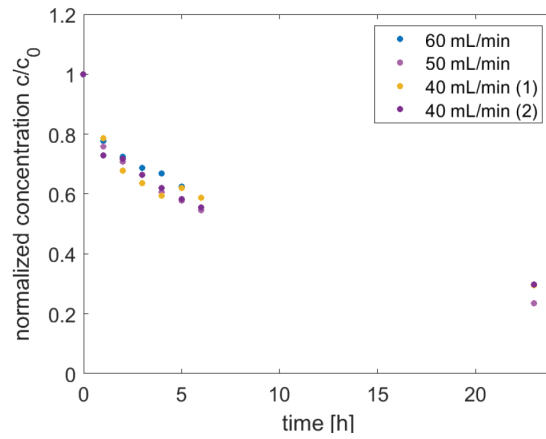
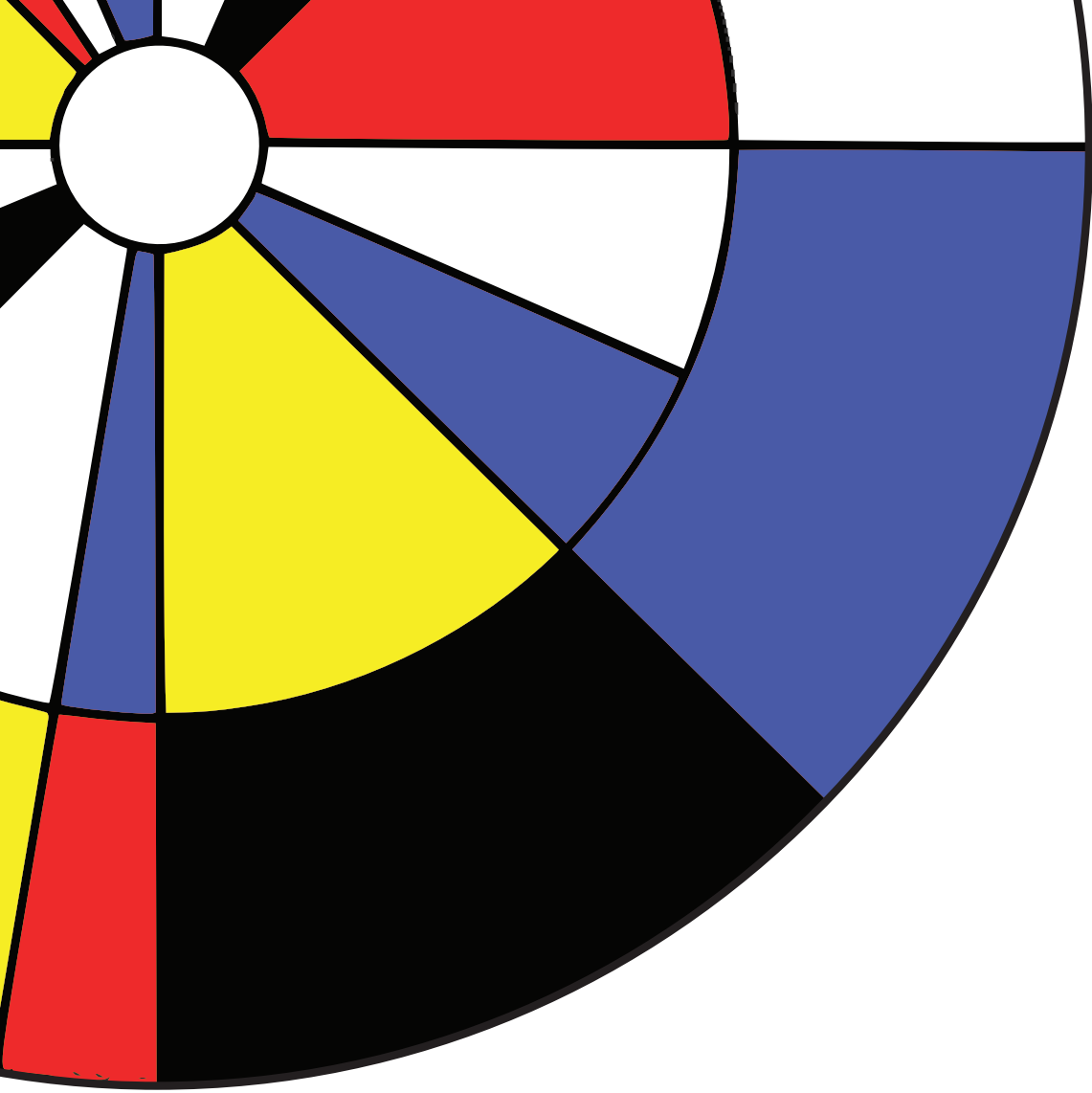


Figure 6.12: Uptake of furfural at different flow rates over the hydrodynamically-defined batch uptake experiment



Chapter 7

Prospect and Challenges for the Production of Flavour-Improved Alcohol-Free Beer

Abstract: The recent increase in the popularity of alcohol-free beverages has motivated the development of new technologies to produce alcohol-free beers with better taste at lower production costs. In this context, the adsorptive removal of wort off-flavours with zeolites has been demonstrated successfully. The process represents a great alternative to the commercial dealcoholisation process since the typical wort flavour of the beverage is reduced and thermal treatment is not necessary. This work addresses the design of the unit operation based on an exemplary case study and the assessment of its technical and economic feasibility. Overall, with current assumptions taken, the new process results in 40% lower production costs than thermal dealcoholisation. Resulting from the analysis the adsorbent regenerability proves to be the most critical parameter, which should be verified in follow-up research. Moreover, hurdles of material stability and food safety need to be overcome.

7.1. Introduction

Contributing to the increasing awareness of misuse of alcohol and a general trend to a healthier lifestyle, the brewing industry has strongly focused their efforts in the development of great-tasting, alcohol-free beers (AFBs) in recent years. Furthermore, the expansion of their product portfolio opens the market for new consumer groups. Nevertheless, currently available products still exhibit an over-pronounced and hence undesired wort-flavour, which is caused by small volatile aldehydes formed through Strecker degradation [1-3]. Literature indicates that wort flavour is related to Strecker aldehydes and in particular, 2-methylpropanal (2-MP) [4, 5], 2- and 3-methylbutanal (2-MB, 3-MB) and methional (Met) [5, 6], which all exhibit a very low flavour threshold in the range of 0.5-23.4 $\mu\text{g/L}$ in AFBs. Furfural (FF) is a common indicator for heat-induced (Maillard) reactions [7] and is considered as a representative for unidentified wort flavour with a more hydrophilic behaviour.

Recently, a new technology has been developed to specifically remove these off-flavours from AFBs through adsorption onto zeolites. Zeolites are a type of molecular sieve, which exhibit a highly defined pore size and can, therefore, enable separations with high specificity. In particular, hydrophobic ZSM-5 type zeolites are suited, since they can exclude larger hop constituents or more hydrophilic organic acids from being taken up in the adsorbent pores [8]. A flavour-improved beer produced with this technology was shown to significantly reduce the wort flavour and improve the taste of the aged product as well [9]. However, the adsorption process is highly limited by intraparticle mass transfer [10]. This limitation may be overcome by a suitable choice of the shape of the material as well as the most suitable design of the unit operation.

In this chapter, we will compile the collected data of previous work and synthesize different unit operation designs to produce a flavour-improved AFB. Exemplarily, an adsorption unit for the production of 231000 hL AFB annually is designed. The aim is to show the feasibility of the process, both technically and economically. Furthermore, direction to future research is given by elucidating which process mode and configuration is most promising and which parameters are critical to making the process feasible and more efficient.

7.2. Process assumptions

7.2.1. Process definition, Plant location, capacity and battery limits

The suggested process is an alternative production process of AFBs and is hence compared to commercialized dealcoholisation processes and biologically produced AFBs. The continuous throughput of a commercial vacuum rectification plant commonly is 100 hL/h, running approximately 8 h a day. The annual capacity at a plant utilization of 2100 h/a (= 87.5 d/a) is hence 70000 hL/a (high-gravity product), which is equal to 231000 hL product at final specifications. This is approximately one-third of the Dutch AFB market [11], and if surrounding bigger markets, such as Germany are considered, the plant capacity is suitable for the current market. The flavour removal unit should consequently be able to process 800 hL (high-gravity product) within 24 hours. As the production site, the Netherlands are selected. As aforementioned, only the design of the adsorptive off-flavour capture unit is considered as outline in Figure 7.1.

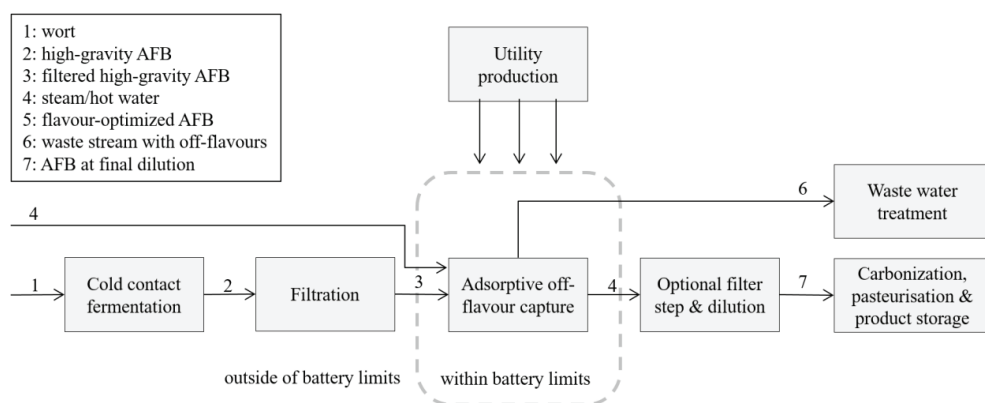


Figure 7.1: Overview of the production process of flavour-improved beer and battery limits for the unit operation design

7.2.2. Feed composition and product specifications

To achieve a significant reduction in wort flavour, the maximal allowable concentration of the regarded wort flavours in the final product is 10 % of its feed stream concentration, as it was proven that this results in a significantly reduced wort flavour [9]. Table 7.1 lists feed and outlet concentrations of targeted wort flavours as well as the allowed concentration in the final product. The matrix is modelled as an aqueous stream containing the studied wort off-flavours. The impact of other beer constituents such as ethanol, small volatiles, sugars, proteins and polyphenols is neglected since it has been shown previously that the model parameters are

regressed isotherm constants which are not systematically affected by potentially competing adsorbates within the design space. Furthermore, the feed does not contain CO₂. The viscosity of the stream has been previously determined to a value of 2.8 mPas [10] and the pH is set to 4.2-4.4, the conditions at which the isotherm parameters were determined.

Table 7.1: Specifications for feed and maximal outlet concentrations of wort flavour compounds

Compound	c _{feed} [µg/L]	C _{outlet, max} [µg/L]	C _{final, max} [µg/L]
2-MP	50	5	1.5
2-MB	10	1	0.3
3-MB	40	4	1.2
FF	1000	100	30.3
Met	100	10	3.0

7.3. Material & Methods

7.3.1. Chromatographic model

Assuming radial homogeneity, incompressibility of the mobile phase and a constant bulk liquid density, the equilibrium-transport-dispersive model described in equation 7.1 [12] is employed in combination with linear driving force approximation as a function of the solid loading depicted in equation 7.2 to model the chromatographic process. This approximation lumps the mass transfer resistances of the film and the particle into one coefficient [13].

$$\frac{\partial c_i}{\partial t} + F \frac{\partial q_i}{\partial t} + v \frac{\partial c_i}{\partial z} = D_L \frac{\partial^2 c_i}{\partial z^2} \quad (7.1)$$

$$\frac{\partial q_i}{\partial t} = k_{ov,i} (q_{eq,i}^* - q_i) \quad (7.2)$$

The initial and boundary conditions for the inlet conditions required to solve the partial differential equations are considered as in equation 7.3 and 7.4.

$$c_i(t = 0, x) = c_i^{ini} \quad (7.3)$$

$$c_i(t, x = 0) = c_i^{feed} \quad (7.4)$$

Since equation 7.1 contains two functions, c_i and q_i , another equation defining their relation is required. For this purpose, the equilibrium isotherm is introduced (equation 7.5), which has previously been shown to be a linear function of the liquid concentration in equilibrium [8].

The mobile phase is aqueous and the adsorbent is hydrophobic, therefore it is furthermore assumed that the mobile phase is not adsorbed.

$$q_i = K \cdot c_{eq,i} \quad (7.5)$$

The pressure drop in the column is estimated locally, that is, for every node according to the equation of Carman-Kozeny see equation 7.6 [14]. To solve the partial differential equation, the column is discretized with the upwind differencing scheme with 20 nodes as explained in section 7.3.3. This equation is valid for the laminar flow regime in packed beds.

$$\frac{\partial p}{\partial x} = \frac{-150\eta(1 - \varepsilon_b)^2}{(d_p \Phi)^2 \varepsilon_b^3} v \quad (7.6)$$

7.3.2. Model parameters

The parameters required for the equilibrium-transport-dispersive model are either available from experimental studies described in previous publications [8, 10, 15] or estimated based on commonly accepted correlations from literature. First, the axial dispersion coefficient, D_L , is calculated along the column using the relation of equation 7.7 and 7.8 [16].

$$D_L = \frac{v \cdot d_p}{0.2 + 0.011 \cdot Re^{0.48}} \text{ for } 10^{-3} \leq Re \leq 10^3 \quad (7.7)$$

$$Re = \frac{d_p v \rho_l}{\varepsilon_b \eta_l} \quad (7.8)$$

The lumped mass transfer coefficient k_{ov} defined in equation 7.9 consists of the resistance through the film, with the coefficient given in equation 7.10, as well as the intraparticle resistance, which is calculated from the effective intraparticle diffusivity D_{eff} [17, 18]. For the adsorption process, the values for the effective diffusivity are regressed from experimental batch uptake data in AFB or model solution according to the method described previously [10] and listed in Table 7.2. Two material shapes are differentiated for the mass transfer coefficients, i.e. a granular and a powder-like form, to receive accurate predictions from the process simulations. The powder-like form consists of crushed granular material, which has been sieved and microscopically analysed to determine the particle size distribution (data not shown).

$$k_{ov,i} = \left[\frac{r_p}{3k_{f,i}} + \frac{r_p^2}{15D_{eff,i}} \right]^{-1} \quad (7.9)$$

$$k_f = \sqrt{\frac{4D_m u}{\pi d_p}} \quad (7.10)$$

Furthermore, the linear isotherm constants of each component determined in AFB of pH 4.4 as well as column specific and physical properties of the material are presented in Table 7.2. Since the bed porosity is unknown, it was estimated from equation 7.11 according to Pushnov (2006) [19].

$$\varepsilon_b = \frac{A}{(D/d_p)^n} + B \quad (7.11)$$

Where A , B and n are constant equal to 1.0, 0.375 and 2.0 for spheres, respectively.

Table 7.2: Model parameters used for process simulations

Model parameter	Value
Isotherm affinity constant (linear) [L/g]	$K_{2MP} = 3.32 \pm 0.05$
	$K_{2MB} = 42.0 \pm 2.0$
	$K_{3MB} = 41.5 \pm 0.8$
	$K_{FF} = 1.43 \pm 0.03$
	$K_{Met} = 5.47 \pm 0.09$
Effective diffusivities [$m^2 \cdot s^{-1} \cdot 10^{-14}$] granular form	$D_{eff,2-MP} = 1.5 \pm 0.3$ ($R^2 = 0.97$)
	$D_{eff,2-MB} = 0.37 \pm 0.15$ ($R^2 = 0.95$)
	$D_{eff,3-MB} = 0.23 \pm 0.09$ ($R^2 = 0.95$)
	$D_{eff,FF} = 41 \pm 12$ ($R^2 = 0.97$)
	$D_{eff,Met} = 1.4 \pm 0.5$ ($R^2 = 0.96$)
Effective diffusivities [$m^2 \cdot s^{-1} \cdot 10^{-14}$] powder-like form	$D_{eff,2-MP} = 1.4 \pm 1.2$ ($R^2 = 0.96$)
	$D_{eff,2-MB} = 0.034 \pm 0.061$ ($R^2 = 0.92$)
	$D_{eff,3-MB} = 0.029 \pm 0.047$ ($R^2 = 0.93$)
	$D_{eff,FF} = 19.0 \pm 25.1$ ($R^2 = 0.96$)
	$D_{eff,Met} = 0.85 \pm 0.75$ ($R^2 = 0.96$)
Column specific & physical material parameters	
Average particle diameter powder-like	262 μm
Average particle diameter granules	2350 μm
Intraparticle porosity []	0.54
Bed porosity []	0.375 for granules
	0.35 for lumps of irregular shape
Overall porosity	0.71 for granules
	0.70 for lumps of irregular shape
Adsorbent solid density [kg/L]	2.23

Desorption equilibrium and dynamics were not studied experimentally, hence, respective parameters are estimated. In this case study, wort off-flavours are desorbed through heat in the form of hot water. Alternatively, steam could be used. To quantify the impact of temperature

on the affinity constant of target molecules to the adsorbent, the van 't Hoff equation (see equation 7.12 and 7.13) [20] was employed to calculate the respective parameters at $T = 145^{\circ}\text{C}$. Since the adsorption enthalpy is unknown and strongly dependant on the adsorbent and adsorbate interaction, data from literature was not available for the studied system. Knowing the isotherm constants at 288.15 K and assuming a value for the entropy, the adsorption enthalpy was calculated from the van 't Hoff equation. The entropy values for branched alkanes on silicalite-1 were found in a range of $(-65) - (-172) \text{ J/mol/K}$ [21], so ΔS was assumed as -110 J/mol/K .

$$K_i^{ads} = e^{\frac{\Delta S_i^{ads}}{R}} - 1 e^{\frac{-\Delta H_i^{ads}}{RT}} \quad (7.12)$$

$$\ln \frac{k_2}{k_1} = \frac{-\Delta H_{ads}}{R} \left(\frac{1}{T_2} - \frac{1}{T_1} \right) \quad (7.13)$$

Because in previous work it was shown that the effective intraparticle diffusion coefficient is inversely correlated to the isotherm affinity constant, intraparticle mass transfer during desorption [10] is expected to be significantly faster than during adsorption. Using the relation of D_{eff} versus K to extrapolate the diffusion coefficient during desorption results in values in the order of magnitude of the calculated molecular diffusivity. Thus, since the interaction of adsorbent-adsorbate is much smaller than during adsorption, the intraparticle diffusivity was calculated based on the generally accepted correlation depicted in equation 7.14-7.16 [12].

$$D_p = \frac{\varepsilon D_m}{\tau} \quad (7.14)$$

$$\tau = \frac{(2 - \varepsilon_p)^2}{\varepsilon_p} \quad (7.15)$$

$$D_m = \frac{T}{\eta} 7.4 \cdot 10^{-8} \frac{(\Phi M)^{0.5}}{V_m^{0.6}} \quad (7.16)$$

7.3.3. Simulation of the adsorptive capture step

The chromatographic model described in section 7.3.1 was implemented in the simulation environment Aspen Chromatography V8.8. The upwind differencing scheme (1) with 20 nodes was used as partial differential equation discretization method.

7.3.4. Estimation of costs

To provide a rough estimate of capital costs, Lang's preliminary factorial estimates were used, which estimates the capital costs by multiplying the bare equipment costs with the *Lang factor* characteristic for the process. Since the process handling is predominantly fluids, a factor of 6.00 was chosen according to an updated analysis of Sinnott & Towler (2012) [22]. The operation costs were calculated based on the material, utility costs as well as costs for maintenance and additional operating supplies resulting in the minimal direct operational costs. The costs for maintenance and operating supplies were estimated at 5% and 1% of the capital costs, respectively. The cost price of the studied adsorbent for the laboratory scale is 300 USD/kg (ca. 266 €/kg) [23], however, at industrial scale, a reduction in pricing can be expected. Hence, for the feasibility study, a cost price of at 200 €/kg (25 % discount) is used. Another considerable aspect that contributes substantially to the economics is the regenerability of the adsorbent. For powdered or powder-like materials, handling is generally more difficult and regenerability lower than for pelleted or granular materials [24]. For such a powder-like material, Holtkamp (2010) found that it could be regenerated for at least 5 cycles with some loss in capacity [25]. For pellets, after optimizing the regeneration procedure, 10 cycles were concluded without loss in capacity, indicating that more cycles of reuse are possible. For this study, we assume a scenario where the granules can be regenerated 10 times, and include this factor in the sensitivity analysis to understand the impact of this assumption on the overall feasibility. Prices for utilities and equipment were taken from the DACE price booklet edition 33 [26]. Overall production costs per volume unit were calculated according to equation 7.17, where a project life-time of 10 years was used.

$$production\ costs = \frac{\left(\frac{capital\ costs}{project\ life\ time} + operation\ costs \right)}{annual\ capacity} \quad (7.17)$$

7.4. Results & Discussion

7.4.1. Options synthesis & selection

To design a feasible unit operation, several options are synthesized considering batch or (semi-) continuous operation as well as different particle shapes and regenerability of the adsorbent, resulting in 10 options as depicted in Figure 7.2. Three different degrees of regenerability are assumed: 1. Slurries of zeolite crystals that are cumbersome to filter off and recycle and are therefore only considered for single-use, 2. Powder-like materials consisting of fine particles

with limited regenerability of 5 cycles and 3. Good regenerability of 10 cycles, achieved with granular material. Furthermore, to be competitive with commercial thermal dealcoholisation units, the maximum allowable material cost price is fixed to 1.50 €/hL, based on industrial experience. In the following, all options are systematically compared to converge to the most feasible solution.

In the first step, the required adsorbent mass under equilibrium conditions is calculated from known isotherm parameters to achieve the desired reduction of >90% in wort flavours for each option.

	No regeneration N = 1 (slurry / crystals)	Limited regeneration N = 5 (powder-like/fine particles)	Good regeneration N=10 cycles (granules)
Batch	1. STR with slurry 2. Single-use disc-column	5. Packed bed with recirculation 6. Cyclic packed bed	8. Packed bed with recirculation 9. Cyclic packed bed
(Semi-) continuous	3. CSTR with slurry 4. PFR with slurry	7. Capture SMB	10. Capture SMB

Figure 7.2: Overview of options for different unit operation configurations

Since furfural has the lowest affinity for the adsorbent, it is the capacity determining adsorbate. Taking into account the dilution factor of 3.3 to obtain the final product and the material cost price of 200 €/kg, the minimal material cost price per volume unit final product can be calculated. The results are shown in Table 7.3, from which becomes clear that several options are unfeasible as they exceed the allowed material cost price of 1.50 €/hL.

Table 7.3: Benchmark data for synthesized design options

Option #	1	2	3	4	5	6	7	8	9	10
$m_{ads,min,FF}$ [g/hL]	629	63	205	205	629	63	63	629	63	63
min. $cost_{ads,FF}$ [€/hL]	38.48	3.85	12.54	12.54	7.70	0.77	0.77	3.85	0.39	0.39

It is obvious that only the options where the adsorbent is regenerated and operated in a packed bed are economically feasible. It should be kept in mind that economics can drastically change if the regenerability is different in reality. Nonetheless, for the next selection step only options 6, 7, 9 and 10 are considered.

The second step considers mass transfer constraints. Because the intraparticle mass transfer is slow and rate-limiting [27], it is expected that granular material will have a lower adsorbent utilization and higher residence times are required to ensure binding during the adsorptive capturing step. To determine the column volume required to achieve binding and good productivity, the adsorptive capture step is simulated in Aspen Chromatography V8.8 for option 6 and 9. The feed flow rate is 40 hL/h, processing the batch of 800 hL within 20 hours. This leaves approximately 4 hours for desorption and cleaning of the column until the next batch. The prerequisite is that desorption is relatively fast compared to adsorption, an assumption that will be investigated in the following in detail.

As expected, the required residence time in the column for option 6 is significantly lower than the residence time required for option 9 (15 minutes versus nearly 10 hours) and hence the required column volume is more than 40 times larger. As a result, the material requirements are also significantly higher than calculated from the equilibrium relation. To make the process feasible, that is, reduce the material cost price below 1.50 €/hL, the overall batch time of the adsorptive capturing step needs to be extended. In the case of option 6, the column can be operated for the duration of 8 batches until the concentration in the last batch exceeds the required 90% reduction threshold. This has the advantage that if against expectations, desorption is time-consuming, it can be planned in as a bi-monthly activity. Nonetheless, frequent cleaning would be necessary to avoid microbial contamination and fouling.

Since the column volume of option 9 is much larger, it can be operated for up to 56 batches, which is equivalent to 56 operation days, until breakthrough occurs. Only then, the column needs to be regenerated. In principle the consumption of adsorbent per volume unit of product could be optimized, but, due to the enormous column volume, a batch cycle would last for 56 days, which is 64 % of the annual production days. This is highly unacceptable from a quality control point of view. Frequent cleaning steps are mandatory to guarantee food safety. If, as a consequence, the regenerability is impaired, the process can quickly become infeasible.

The (semi-) continuous process mode employed in option 7 and 10 optimize adsorbent utilization. Table 7.4 makes it clear that these systems have a high potential to reduce material costs. Nonetheless, their implementation in the brewery is more complex; at least two columns are required for this system as well as a flexible valve system to switch inlets as well as good process control, which makes their capital investment costs greater. Overall, these short

estimate calculations lead to the overview of bare equipment costs and annual costs for the adsorbent as depicted in Table 7.5.

Table 7.4: Benchmark data for synthesized design options

Design option	6	7	9	10 ¹
V_{col} [m ³]	0.98	0.98	39.76	39.76
No of batches	8	11	56	228
m_{ads} [kg]	657	657	25492	25492
Adsorbent utilisation FF [%]	68	94	12	50

It is obvious that option 9 and 10 are technically not feasible and economically unattractive with the currently considered material. Due to their faster mass transfer, the powder-like material requires option 6 and option 7 are superior. Comparing the simple-packed bed operation with the semi-continuous SMB, option 7 is slightly more economic. However, considering that in this calculation 94% adsorbent utilization is assumed and that the flexible valve system may cause additional costs, this difference might become smaller and cannot outweigh the fact that the operation of such a semi-continuous system is more complex and requires well-trained staff. Hence, overall, the granular filled packed bed in batch most is chosen as the most viable option to scale up.

Table 7.5: Evaluation matrix for option selection

	6	7	9	10
Equipment cost estimate [k€]	122	2x122	419	2x419
Estimated capital cost [k€]	732	1464	2515	5030
Material cost final product [€/hL]	1.24	0.90	3.46	0.85
Annual material costs [k€/a]	287	209	799	196
Annual total costs	361	355	1051	699
Easiness to integrate into brewing process and complexity in process control	moderate	moderate to difficult	easy to moderate	moderate to difficult
Technical difficulties	clogging fouling novel material decrease in capacity	clogging fouling novel material decrease in capacity	(microbial) fouling	(microbial) fouling

It should, however, be kept in mind that more suitable, pellet- or granule-shaped zeolites with improvement in mass transfer could outperform the powder-like material since they are easier to handle and often exhibit a better regenerability. Since the size distribution of powder-like material is very broad and lots of small particles may result in high back pressure and eventually

clogging of the column or cause issues during the subsequent filtration. It has also been shown that the column utilization of such materials decreases over time by the effects of packing compaction and resulting blockage of whole channels [28]. Furthermore, lower operating pressures are possible for option 8-10, which might lower the cost for steel. Another factor related to higher operating pressure is gas solubility. Gasses such as CO₂ might saturate in the liquid and disturb the adsorptive process. Based on this argumentation packed beds filled with granular material may outperform packed beds with powder-like material (option 6) in the future.

7.4.2. Design of unit operation

In previous paragraphs, packed bed adsorption column filled with powder-like material was identified as the most promising unit operation design. To enable binding of target compounds, a residence time of 14.7 min is required, resulting in a column volume of 982 L. The designed column has a diameter of 50 cm and a bed length of 5 meters, resulting in an aspect ratio of H/D of 10. Since this is a capturing process, the process efficiency is not dependant on the aspect ratio, as long as the minimal column length is satisfied. The adsorption column model is set up in the simulation environment of Aspen Chromatography V8.8 as described in section 7.3.1 passing through a complete cycle, consisting of the steps listed below:

1. Loading (20 h) at 4 m³/h and T = 4°C of interconnected columns
2. Washing with one column volume water T = 4°C (4 h)
3. Repetition of step 1 and 2 for another 7 batches
4. Regeneration at 8 m³/h and T = 145°C (3.5 h, \equiv 28 column volumes)
5. Cooling for 0.5 h at 4 m³/h and T = 4°C (\equiv 2 column volumes)

The breakthrough curve and the resulting column profile at saturation as well as the bed concentration profile during the regeneration phase are shown in Figure 7.3 and Figure 7.4.. Since 2- and 3-MB have a very low mass transfer coefficient, they are determining for the column size and show a very broad mass transfer zone. This is why they are present at the process outlet already during the first loading step. The further increase in concentration is, however, not steep and hence none of them is capacity limiting. On the contrary, furfural diffuses rather quickly into the particles but exhibits a much lower isotherm affinity constant. Thus, when its average concentration exceeds 10% of the feed concentration in one batch, the column has to be regenerated. The small jumps depicted in the breakthrough curve of Figure 7.3 are due to the intermediate washing steps of 4 hours, causing a momentary drop in the outlet

concentration of each component. In between the loading steps, the column is washed with process water to avoid product loss. This step could also be carried out as a back-wash step to further increase the column capacity. To counteract microbial growth, washing could also be carried out with hot water to pasteurize the equipment or with a suitable chemical that does not impair the adsorbent's structure. Consequently, after 8 batches the column is regenerated with hot water at a temperature of 145°C, as it was calculated that the isotherm affinity constant is nearly zero in this range and mass transfer is hence considerably faster. By increasing the flow rate by factor 2, a fast regeneration process of a couple of hours can be achieved. The column is consequently cooled down, to prepare for the following adsorption cycle. Since the desorption step is based on parameters calculated from correlations and assumptions, this step needs to be verified. Possibly, a higher temperature is required to desorb the flavours completely. Other desorption fluids, such as steam or hot gas could be considered, but this is outside of the scope of this work.

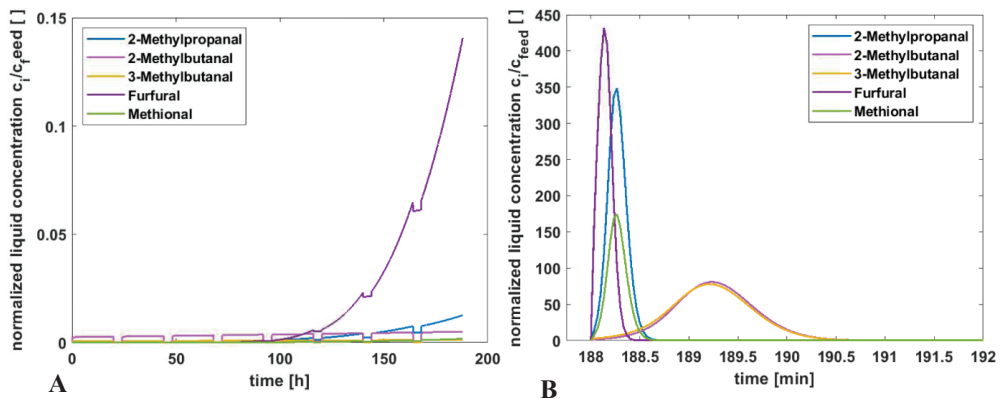


Figure 7.3: (A) Breakthrough curve (B) Concentration profile at outlet during regeneration of the column

Because the flavour compounds are considered as a waste stream, extending the column length is not desirable, as the cycle duration would increase even further. The aspect ratio may be varied without affecting the capacity, as long as the minimum residence time is ensured and other limitations, such as the building height are considered.

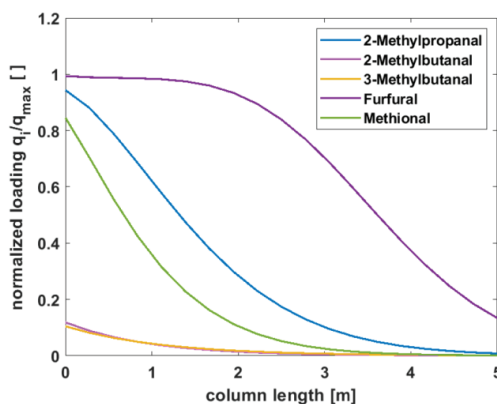


Figure 7.4: Bed profile of solid loading at $t=188$ h

7.4.3. Estimation of costs

To understand, whether the production of flavour-improved AFB is economically feasible, an estimation of the bare equipment and capital costs, as well as the operational expenses, is made. Because the boundary conditions for the unit operation design are very defined and specialized, indirect costs for the plant overhead, taxes or general expenses for research and development or sales are not taken into account. The aim is not to provide a full economic analysis, but to indicate the feasibility and identify the major cost drivers. This information, together with the feasibility study will give direction to future research. Table 7.6 summarizes for capital and operational costs based on rough estimates. Overall, the ball-park figure for the minimal production cost amounts to 1.91 €/hL. In comparison, thermal dealcoholisation production costs amount to 3.27 €/hL [29, 30].

Table 7.6: Estimates of capital and operational costs

Category	Estimate This work	Estimate thermal dealcoholisation
Bare equipment costs [k€]	122	445 ⁹ [29]
Capital costs [k€]	732	2670
Raw material costs [k€/a]	287	n/a
Utility costs [k€/a]	39	328
Min. direct production costs [k€/a]	369	488
Min. overall production costs [€/hL]	1.91	3.27

The assumed plant utilization is with 2100 h/a relatively low; if the plant utilization and hence the capacity is increased, the production cost per volume unit can be lowered. In previous paragraphs, the focus was given to equipment sizing and consumption of adsorbent, and indeed,

⁹ equipment cost from Liguori et al. (2015) and adjusted with an inflation rate of 2.13 % to 2020 prices

the first estimation of the utility costs (see Appendix Table 7.7), confirms that the utilities, only minorly contribute to the overall operational costs. In the current scenario, it is assumed that washes in between cycles are performed with cold water and regeneration at 145°C is sufficient. However, if regeneration requires activation at 500°C, and thus a complete drying of the material, this could increase operational costs significantly and this factor might become relevant for the economic feasibility.

While this estimation is very rough and incomplete, it shows that the newly developed process may reduce production costs as much as 40% when compared to current commercial dealcoholisation techniques. It is also clear that the adsorbent costs and hence the regenerability is crucial for the economic viability. Thus, in the following paragraph, the sensitivity of the design is assessed.

7.4.4. Sensitivity study

Isotherm constants and mass transfer coefficients

Considering the data provided in Table 7.2, the error associated with the isotherm constants is relatively small, however, composition fluctuations in the feed stream may cause a deviation and hence the sensitivity of the design towards this factor is tested. Also and more importantly, the zeolite capacity can be reduced due to incomplete regeneration. As a rather conservative scenario, the impact of 20 % lower isotherm constants is tested. Here, the effect on mass transfer parameters is neglected, but solely the effect on capacity observed. Since furfural is the capacity limiting target molecule, the number of loading steps per cycle reduces from 8 to 7. This results in an increase in material cost to 1.42 €/hL. Overall, this affects the production costs only marginally, i.e. an increase of 10% to 2.10 €/hL and hence it is concluded that the feasibility is not strongly depended on this parameter.

Furthermore, the effect of the mass transfer coefficient one order of magnitude lower was tested, to understand the impact on the economic feasibility. As a result of the worsened mass transport, the number of batches per cycle decreases to 6, causing higher production costs of 2.40 €/hL, which is about 27% higher than in the base scenario. This is a considerable additional cost factor hence, breakthrough column experiments are recommended to verify the regressed parameters from the batch uptake system.

Regenerability & material costs

The above unit adsorption design and economic calculations are based on several the assumption of a moderate regenerability of the material as well as the material cost price. To approximate the impact of these parameters, economic estimates were recalculated for more conservative scenarios. The accessibility of the packed bed for the regeneration fluid might be impaired during operation, resulting in dead zones and fouling. The dependency of the minimal production cost price on the regenerability is depicted in Figure 7.5. In the case that the regenerability is limited to 3 instead of 5 cycles, due to effects such as coking or deterioration of the adsorbent structure, the production costs increase by 43% to 2.73 €/hL. This factor is very critical for the economic viability of the process, and if N is lower than 3, this may become a knock-out criterion for the feasibility. Moreover, as already discussed in previous paragraphs, regeneration might require re-activation at around 500°C. If this is the case, the energy consumption of the process will become decisive for the process feasibility. Alternatively, desorption with eluents such as ethanol that are easier to evaporate and recycle could be considered. Similarly, an increase of the material pricing to 300 €/kg is also of significant influence, raising the overall production costs by 47%.

On the contrary, the regenerability could also be better than assumed. If the material could be used for about ten cycles overall production costs would be reduced by 36 %, making the process economically even more attractive.

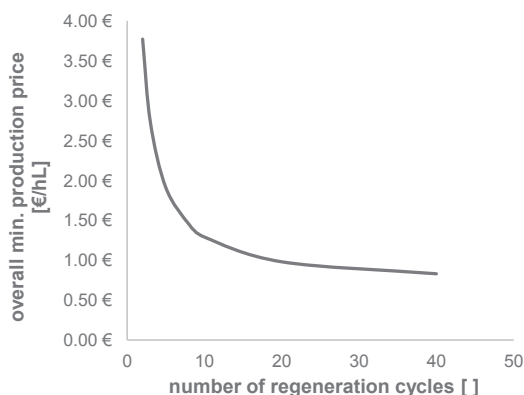


Figure 7.5: Dependency of adsorbent regenerability on overall minimal production costs per volume unit

Furthermore, parameters for desorption are determined from correlations but might differ in reality. Both desorption dynamics, as well as the dependency of the isotherm constant on

temperature, may prolong the regeneration procedure, resulting in higher cycle times and/or costs for energy. Since the boundaries are unknown, this question is left for future research.

7.4.5. Capital cost

In the current estimation of capital expenses, a rather conservative Lang factor of 6.0 is used, resulting in overall capital costs of 732 k€. Considering that only one unit operation is studied, this might be overestimated. If the Lang factor is halved (3.0) overall production costs decrease to 1.66€/hL.

7.5. Conclusion

The above process synthesis and analysis indicates that the flavour optimisation technology developed in previous publications is technically and economically feasible. The analysis also demonstrates that accurate data for the regenerability of the material and the desorption procedure are required. To scale up the process to commercial application, several other factors need to be taken into account, i.e. chemical and thermal stability and solubility in contacting fluids, as well as hardness and mechanical strength [31]. Furthermore, since the taste of an AFB product in a batch and a packed bed operation may differ, the improved product taste should be verified with a trained panel. Another aspect to address is the assurance of product safety and integrity. Additional washes with hot water or antimicrobial agents in between batches should prevent microbial infection. Furthermore, the raw material safety should be checked on regularly.

If the regenerability is undesirable and or technical issues, such as clogging or mechanical instability cannot be prevented, the optimal options selected under paragraph 7.4.1 should be reassessed. New developments in material science on granular or pelleted zeolitic materials could enable the use of pellets and make them economically more viable. A higher number of cycles and a better mass transfer would reduce required column volumes and decrease material costs, and also reduce the environmental footprint of this process as in the current investigation waste costs were not included.

Overall, our work shows the high potential of this flavour removal step. This technology may be able to replace energy-intense and high CAPEX thermal dealcoholisation technologies and have hence a high cost reduction prospect. Future research will show if the last hurdles can be overcome.

7.6.Acknowledgements

The authors acknowledge Heineken Supply Chain B.V. for the funding provided for this project.

7.7.Nomenclature

Symbol	Meaning SI units
c	Concentration in the bulk liquid [kg/m^3]
d_p	Particle diameter [m]
D_{eff}	Effective intraparticle diffusivity [m^2/s]
D_L	Axial dispersion [m^2/s]
D_m	Molecular diffusivity in water [m^2/s]
D_p	Intraparticle diffusivity [m^2/s]
ΔH	Enthalpy [$\text{kg} \cdot \text{m}^2/(\text{mol} \cdot \text{s}^2)$]
k_{ov}	Overall mass transfer coefficient [$1/\text{s}$]
k_f	Film mass transfer coefficient [m/s]
K	Adsorption equilibrium constant linear model [m^3/kg]
M	Molecular weight [kg/mol]
p	Pressure [$\text{kg}/(\text{m} \cdot \text{s}^2)$]
q	Loading of adsorbent [kg/kg]
R	Gas constant [$\text{kg} \cdot \text{m}^2/(\text{K} \cdot \text{mol} \cdot \text{s}^2)$]
r_p	Radius of particle [m]
ΔS	Entropy [$\text{kg} \cdot \text{m}^2/(\text{K} \cdot \text{mol} \cdot \text{s}^2)$]
t	Time [s]
T	Temperature [K]
u	Interstitial velocity [m/s]
V_m	Molecular volume [m^3]
z/x	Abscissa or distance along column length

Symbol	Explanation
ε_p	Particle porosity []
ε_b	Bed porosity []
η	Viscosity [$\text{kg}/(\text{m} \cdot \text{s}^2)$]
ρ	Density [kg/m^3]
Φ	Sphericity of particles in the packed bed []
v	Superficial velocity [m/s]
τ	Tortuosity []
ψ	Constant solute-solvent interaction []

Abbreviations

AFB	Alcohol-free beer
FF	Furfural
2-MB	2-Methylbutanal
3-MB	3-Methylbutanal
2-MP	2-Methylpropanal
Met	Methional
R ²	Coefficient of determination
ZSM-5	Zeolite Socony Mobil-5

7.8. References

1. Brányik, T., et al., *A review of methods of low alcohol and alcohol-free beer production*. Journal of Food Engineering, 2012. 108(4): p. 493-506.
2. Sohrabvandi, S., et al., *Alcohol-free beer: Methods of production, sensorial defects, and healthful effects*. Food Reviews International, 2010. 26(4): p. 335-352.
3. Liguori, L., et al., *Chapter 12 - Production of Low-Alcohol Beverages: Current Status and Perspectives*, in *Food Processing for Increased Quality and Consumption*, A.M. Grumezescu and A.M. Holban, Editors. 2018, Academic Press. p. 347-382.
4. Meilgaard, M.C., *Flavor chemistry in beer: Part II: Flavor and flavor threshold of 239 aroma volatiles*. Master Brewers Association of the Americas, 1975. 12: p. 151-168.
5. Piornos, J.A., et al., *Orthonasal and retronasal detection thresholds of 26 aroma compounds in a model alcohol-free beer: Effect of threshold calculation method*. Food Res Int, 2019. 123: p. 317-326.
6. Perpète, P. and S. Collin, *Contribution of 3-methylthiopropionaldehyde to the worty flavor of Alcohol-free beers*. Journal of Agricultural and Food Chemistry, 1999. 47(6): p. 2374-2378.
7. Andrés-Iglesias, C., et al., *Comparison of carbonyl profiles from Czech and Spanish lagers: Traditional and modern technology*. LWT - Food Science and Technology, 2016. 66: p. 390-397.
8. Gernat, D.C., et al., *Selective off-flavor reduction by adsorption: A case study in alcohol-free beer*. Food and Bioproducts Processing, 2020. 121: p. 91-104.
9. Gernat, D.C., Brouwer, E.R., Faber-Zirkzee, R.C., Ottens, M., *Flavour-improved alcohol-free beer - quality traits, ageing and sensory perception*, s.t.f.a.B. Processing, Editor. 2020.
10. Gernat, D.C., et al., *Mass transfer limitations in binderless ZSM-5 zeolite granules during adsorption of flavour compounds from aqueous streams*. Journal of Chemical Technology & Biotechnology. n/a(n/a).

11. Nederlandse-Brouwers, *Kerncijfers*. 2019.
12. Guiochon, G., *Fundamentals of preparative and nonlinear chromatography*. 2nd ed. ed. 2006, Boston: Elsevier.
13. Felinger, A. and G. Guiochon, *Comparison of the Kinetic Models of Linear Chromatography*. *Chromatographia*, 2004. 60(1): p. S175-S180.
14. McCabe, W.L., J.C. Smith, and P. Harriott, *Unit operations of chemical engineering*. Vol. 5. 1993: McGraw-hill New York.
15. Penning, M.M., *Process development for selective wort flavour adsorption from alcohol-free beer using column adsorption*, in *Bioprocess Engineering*. 2018, Delft University of Technology: Delft.
16. Chung, S.F. and C.Y. Wen, *Longitudinal dispersion of liquid flowing through fixed and fluidized beds*. *AIChE Journal*, 1968. 14(6): p. 857-866.
17. Ruthven, D.M., *Principles of Adsorption and Adsorption Processes*. 1984, USA: John Wiley & Sons Inc.
18. Nfor, B.K., et al., *Model-based rational strategy for chromatographic resin selection*. *Biotechnology Progress*, 2011. 27(6): p. 1629-1643.
19. Pushnov, A.S., *Calculation of average bed porosity*. *Chemical and Petroleum Engineering*, 2006. 42(1): p. 14-17.
20. Hoff, J.H.v.t., *Die Rolle des osmotischen Druckes in der Analogie zwischen Lösungen und Gasen*. 1887. 1U(1): p. 481.
21. Millot, B., et al., *Adsorption of Branched Alkanes in Silicalite-1: A Temperature-Programmed-Equilibration Study*. *Langmuir*, 1999. 15(7): p. 2534-2539.
22. Towler, G. and R. Sinnott, *Chemical Engineering Design : Principles, Practice and Economics of Plant and Process Design*. 2012, Oxford, UNITED KINGDOM: Elsevier Science & Technology.
23. Materials, A. *ZSM-5 Adsorbent Series*. 2020; Available from: acsmaterial.com/zsm-5-adsorbent-series.html.
24. Holtkamp, M., *Optimierte Produktgewinnung und Regeneration bei der reaktionsintegrierten Adsorption*, in *Institut für chemische und thermische Verfahrenstechnik*. 2010, TU Braunschweig.
25. Holtkamp, M. and S. Scholl, *Downstream Processing for Isomaltose following a Reaction Integrated Adsorption*. *Chemie Ingenieur Technik*, 2011. 83(1-2): p. 191-194.
26. *DACE price booklet*. 33 ed. 2018: The Dutch network and knowledge center for cost engineering and value management.

27. Gernat, D.C., Brouwer, E., Ottens, E., *Aldehydes as Wort Off-Flavours in Alcohol-Free Beers - Origin and Control*. Food and Bioprocess Technology, in press.
28. Hartig, D., *Charakterisierung von Adsorbentien in der Flüssigphase mittels dynamischer Methoden*, in *Institut für chemische und thermische Verfahrenstechnik*. 2019, TU Braunschweig.
29. Liguori, L., et al., *Production and characterization of alcohol-free beer by membrane process*. Food and Bioprocess Technology, 2015. 94: p. 158-168.
30. Gernat, D.C., *Process Design of Flavour Controlled Beer Process*. 2016, Delft University of Technology.
31. Seader, J.D.H., E.J., *Separation Process Principles*. 1998, United States of America: John Wiley & Son, Inc.

7.9. Appendix

Table 7.7: Estimates of utility costs

Utility	Cost per unit	Amount	Annual costs [k€/a]
Process water	1.50 [€/m ³]	16 408 [m ³ /a]	24.6
Steam for heating	25.00 [€/ton]	485 [ton/a]	12.2
Electric power	0.15 [€/kWh]	11 934[kWh/a]	1.8
Total			38.6



Chapter 8

Conclusion and Outlook

In this thesis, a technology to produce an alcohol-free beer (AFB) with an improved taste has been developed. After defining and studying the origin of wort off-flavours, a broad screening of existing technologies in literature was done (chapter 2). Process innovation in the often rather traditional food industry with its high standards and regulations has been limited so far. Until now, the beverage industry has focussed on conventional approaches to reducing wort off-flavours that either lack effectiveness or selectivity. Thus, the novel technology should enable the production of an AFB with an improved flavour profile, i.e. reduced wortiness, but at the same time preserve the original characteristics of a beer, such as colour, pH or bitterness. Adsorptive flavour removal was concluded as a promising route to be explored further. As a benchmark, a commercially employed thermal dealcoholisation unit (spinning cone column) was studied at pilot scale (chapter 3). Through this technique, removal of 92-95 % of volatile wort flavours was achieved, however, methional, accepted as one of the most dominant wort flavours in AFB, could not be removed efficiently, due to its higher boiling point. Furthermore, a significant impact of the applied energy in the form of heat was confirmed as well as a residual concentration of all wort flavours as a result of the simultaneous formation and evaporation of them. As a consequence, thermal dealcoholisation technologies are not best suited to decrease wort flavour in AFBs.

Thus, a systematic study of potential adsorbents was performed, with the result that molecular sieves, and in particular hydrophobic zeolites of the ZSM-5 type, are the most selective separation medium to facilitate efficient off-flavour reduction. The choice of the micropore diameter and the $\text{SiO}_2/\text{Al}_2\text{O}_3$ proved crucial. The approach taken in chapter 4 to assess the impact of the multicomponent system on the regressed isotherm parameters is thereby transferrable to other complex systems, where trace compounds are to be removed. To take this one step further, the flavour-improved AFB was produced at pilot scale. An assessment of its chemical compositions as well as sensory characteristics proved that a superior product in terms of wort flavour was obtained by the novel process. The study of ageing behaviour also gives indications to solve the old puzzle of the origin of ageing in beer.

The subsequent study of the material structure and mass transfer in granular ZSM-5 zeolite in a model solution showed that intraparticle transport is the bottleneck and both, macro- as well as micropore transport, may be mutually limiting. Since the diffusivities are very low, adapting the material structure to liquid adsorption processes is crucial. The major conclusion here is that improvements of the material morphology are required and both, crystal (agglomerate) size and overall particle size should be reduced. Interestingly, a correlation of hydrophobicity, the isotherm affinity constant and the diffusivity was found in chapter 4 and 6. This indicates that the molecular size has a subordinate role in the molecular processes – as a sieve – and the chemical interactions between adsorbent and adsorbate dominate.

Combining all the above findings, the conceptual process design (chapter 7) gives insight into the technical and economic feasibility, and most importantly, emphasized which steps are crucial to bring this technology forward. The newly developed process can indeed be economically advantageous when compared to commercial dealcoholisation systems and furthermore if optimized, be more sustainable due to lower consumption of energy and other resources. The most critical parameters still to be investigated are regenerability and the desorption procedure. Moreover, factors such as chemical and mechanical stability as well as product safety and integrity need to be considered, as they may affect the overall feasibility to a large extent.

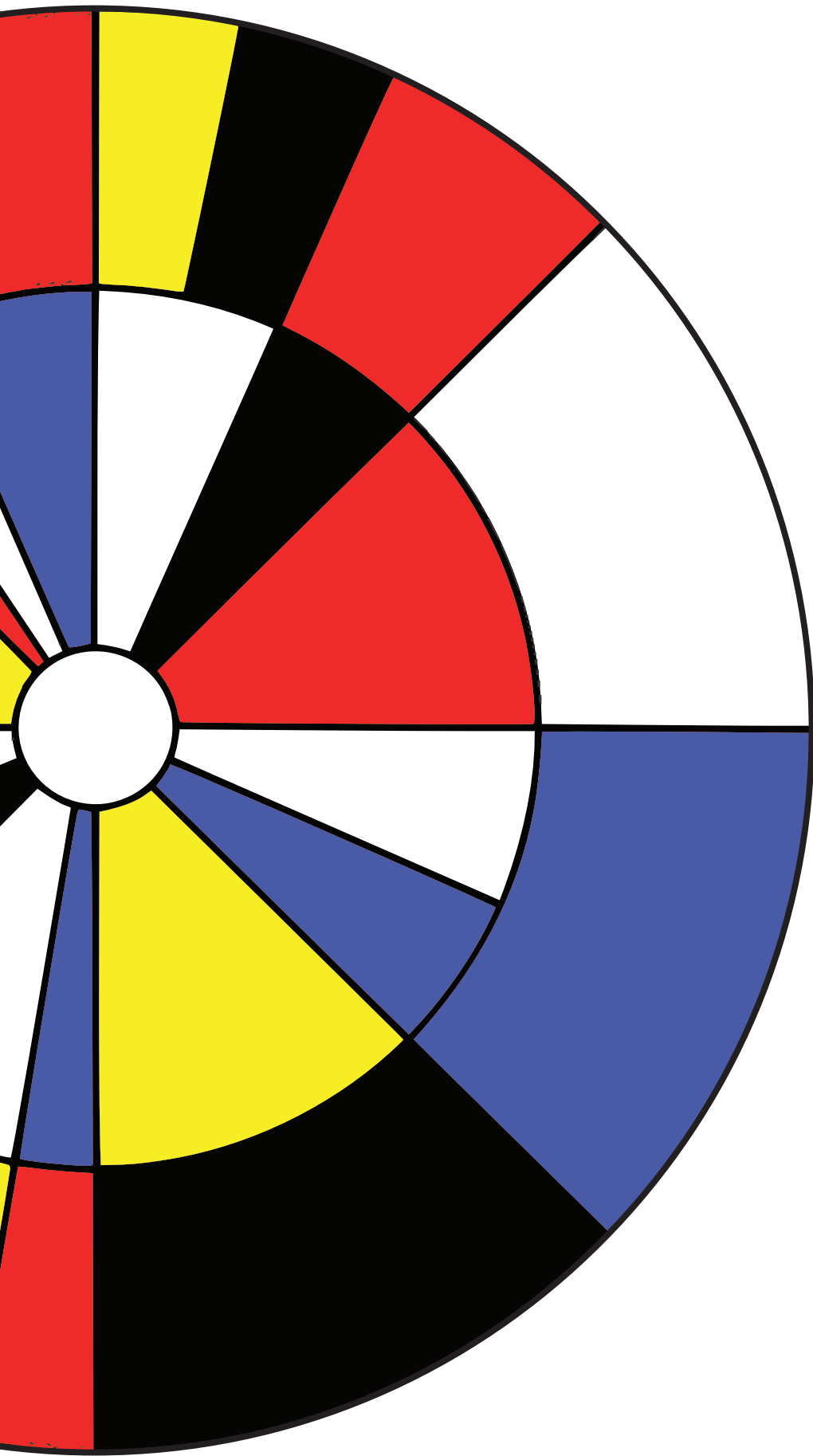
Newer developments in material science, such as the availability of smaller pellets (<1.2 mm in diameter) or granules with good mechanical strength, could also bring advantages with regard to the practical handling in the brewery.

In terms of product development, the flavour-improved beer produced by this novel process can be further optimized with regard to the overall balance in taste, and the addition of a fruit flavour mix adjusted to the novel beer composition. Furthermore, more detailed investigations of the ageing behaviour for instance with hopped AFB are necessary to improve the understanding of the involved mechanisms.

In a broader view, zeolites should be considered as promising candidates for the treatment of waste streams, for instance to de-odourise and valorise aqueous streams from the food industry. Another interesting topic for further research is the correlation of the isotherm adsorbent constant, hydrophobicity and effective intraparticle diffusivity. If such a correlation is generalizable to other molecular groups and materials, it could be used to predict the adsorption behaviour on complex aqueous streams with a minimal amount of experimental effort. If

suitably shaped zeolites are available, one could use this technique also to fine-tune flavour profiles through chromatographic separation.

Overall, this thesis highlights the great potential of microporous adsorbents in the food industry. A novel technology has been developed from just an idea, through laboratory experiments, up to the production of the novel product at pilot scale and verification of the flavour improvement with a sensory panel. Despite the fact that there are still some hurdles to overcome, this novel technology has the potential to compete or even replace established dealcoholisation systems.



Acknowledgments, List of publications & Curriculum Vitae

Acknowledgements

Another journey has ended – my time at the TU Delft. The last six years have formed me, not only professionally, but also very personally – thanks to the many people, but also cultures, experiences and places I was able to get to know.

Dear Marcel, thank you so much for giving me the opportunity to work in not only one, but two projects with you. If it was not for you, I would have not ended up making my hobby (home brewing) my profession. Thank you also for your guidance and for letting me discover the wide world of bioprocess engineering all across the world. I really appreciate the liberty and trust you have put in me. I hope that we will have even more projects together in the future - I will always have a special connection with our group.

Eric, without you there would not be a thesis! Thank you for all the support, enthusiasm, reading through all the papers and technical discussions. Thank you also for your confidence in me with the responsibility of a full two-week pilot-scale study across two countries right at the beginning of my PhD. I am looking forward to being your colleague in the future.

Of course, also many thanks to Luuk for all your input and the inspiring talks, that were not limited to the technical content and, in particular, thank you for the challenging feedback you can give to the point.

Thank you to my students. Fiona, you were the best first student I could have asked for and you set the ground for my thesis. Thank you, Maxime, your great eye for detail, Jonathan, your perseverance and diligence and Renzo, for your great energy and enthusiasm – you all worked very hard and achieved great results.

A big thank you also to my paranymphs! Rita, thank you for always being there and caring, for all your encouraging words, but also the fun times whenever possible. Thanks for making time, with two children and a full-time job to still be my paranymph. You are incredible.

Meine liebe Sammy - du bist die beste Schwester, die man haben kann, denn du hast das ganze Paket: beste Freundin, Life-Coach, Sekretärin, Shoppingberater und Kulturvermittlerin. Du bist wirklich meine zweite Hälfte und die beste Person, um meine Trauzeugin für die Verteidigung zu sein. Danke Timo, dass du sie mir so oft ausleihst.

Thank you to all the BPE members: to my PDEng family: Trinath, André and Kalpana – you are such a positive and supportive persons. I have learned so much from you and hope to do so in the future as well. Thank you to the GoT group: Silvi-Meisje, my PhD sister, I will never forget our awesome trip to the US. Thanks for introducing me to the conference world ☺ Pontibär, MJ, Diogolindo, SarJan (ok that I just made up), Marcelinho, Ana, Joana and of course little Pedro ;). I am still waiting for serious night – it never happened. Monica, thanks for all the fruitful discussion on our topic and being so helpful in general. Bianca, you are an inspiration for your beautiful mind-set. Vic, thanks for all the beers we had at the conferences. I could always count on you during happy hour. Marina, BIOPRO would have been a completely different experience without you, let's go for that trip to Thailand next! Chema, I will miss your *Heinz, Cola* and especially your cow sounds - and by the way, you still have to put some coins in the jerk jaw. Song, thanks for all your patience and not giving up until we have a solution. A big hug of appreciation also to David and Alex, our PhD parents and a reliable source of wisdom.

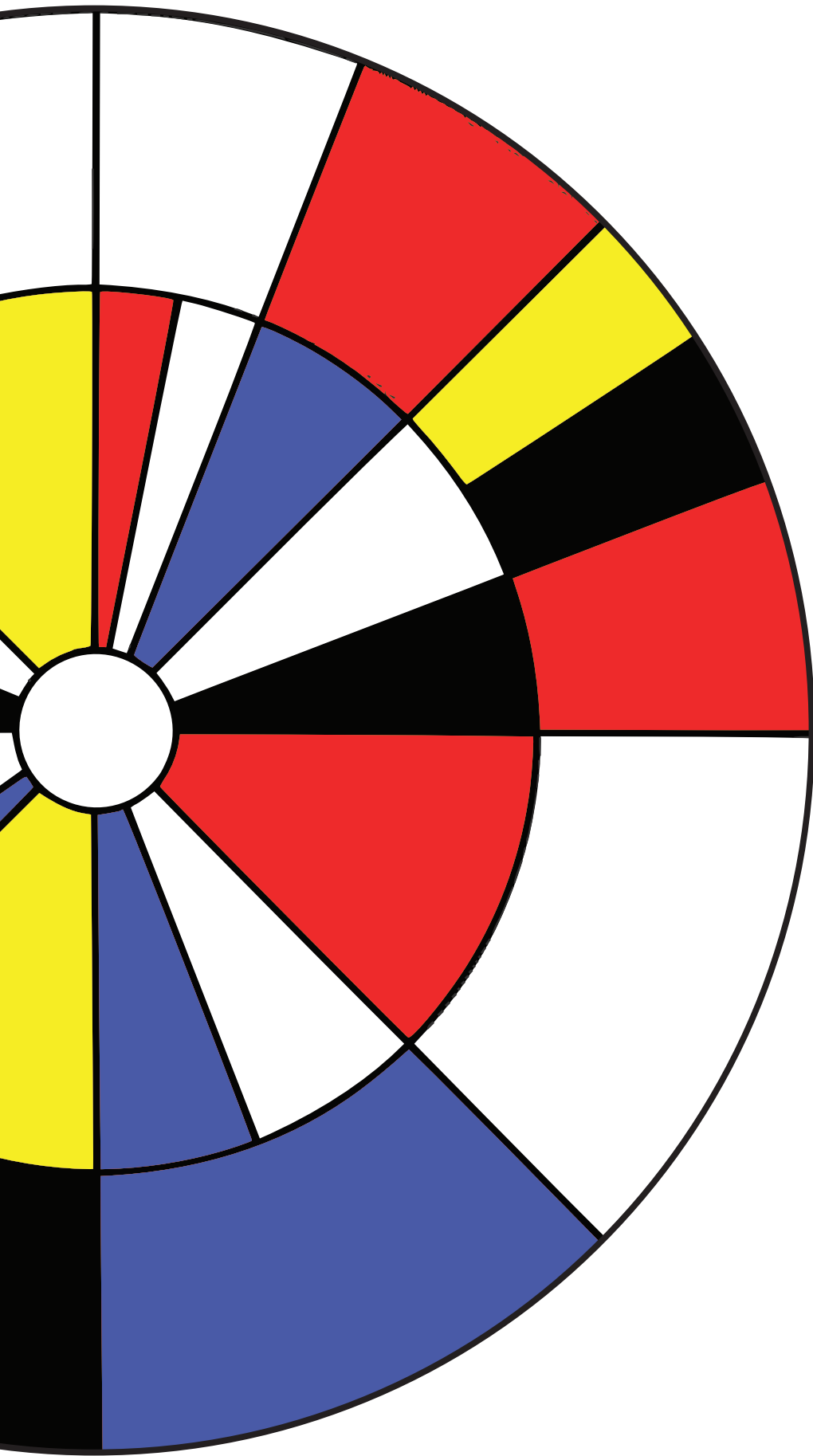
Thanks to the newbies, Tiago, Daphne, Roxana, Mariana, my office mates, Oriol & Marijn for making me feel old, but still young at the same time. And, of course, thank you also to Susanna, Carlos and Shima for all the good office talks. Kawieta, Maria, Adrie, Stef and Max – you are just amazing, we are so lucky to have you - the coffee breaks would not have been the same without you.

Thank you of course also to the Global I&R group. A big thanks especially also to Fred, the GC whisperer and Marcel for all your help in the lab. Sabine, Hannelize, Marion, Tinne, Elizabeth, Elena, Suzanna, Paulien, Ike, Hilda, Yvonne, Hubert, August, Niels, Tom, Thadgh, Petra, Victor, Jan Pieter, Kees, Marlies, Bart and all the people from the pilot brewery as well as the sensory group, Roy, Bianca and Debbie. You always included me and showed how my work actually contributes, which was very encouraging. Thank you also for all the inspiration

and support you gave during the last four years. I am looking forward to (finally) joining the HEINEKEN family as well.

„Dankbarkeit ist das Gedächtnis des Herzens“ (Jean-Baptiste Massillon). Die letzten Worte meiner Doktorarbeit sind für meine Familie. Liebe Großeltern, ich habe euch sehr lieb. Daniel, dank je dat je altijd naar me luistert, ook wil ik de oplossing van het probleem niet horen. Dank je dat je zo een lieve en positieve partner bent en nooit gefrustreerd raakt. Je bent toch onze natuurlijke Yogi! Je was ook een enorm behulpzame office-mate voor de laatste maanden. Door jou heb ik ook een tweede familie en vriendenkring in Rotterdam en Dordrecht gevonden, wat me veel steun geeft.

Liebe Eltern - alles was ich erreicht habe verdanke ich euch. Ich war mir nicht nur immer eurer bedingungslosen Unterstützung bewusst, aber auch eurer Liebe und eures Vertrauens in mich. Letztendlich hat mich dies befähigt und bestärkt die Person zu werden, die ich heute bin.



List of publications

Journal Publications

Gernat, D.C., Brouwer, E.R., Faber-Zirkzee, R.C., Ottens, M., Flavour-improved alcohol-free beer – quality traits, ageing and sensory perception (2020). Food and Bioproducts Processing, 123, pp. 450-458.

Gernat, D.C., Rozenbroek, R., Brouwer, E., van der Wielen, L. and Ottens, M., Mass transfer limitations in binderless ZSM -5 zeolite granules during adsorption of flavour compounds from aqueous streams (2020) J Chem Technol Biotechnol., 95 (12), pp.3134-3148.

Gernat, D.C., Penning, M.M., Swinkels, F.M., Brouwer, E.R., Ottens, M.; Selective off-flavor reduction by adsorption: A case study in alcohol-free beer (2020) Food and Bioproducts Processing, 121, pp. 91-104.

Gernat, D.C., Brouwer, E.R., Ottens, M.; Aldehydes as Wort Off-Flavours in Alcohol-Free Beers—Origin and Control (2020) Food and Bioprocess Technology, 13 (2), pp. 195-216.

Günther, S., Gernat, D., Overbeck, A., Kampen, I., Kwade, A. Micromechanical Properties and Energy Requirements of the Microalgae *Chlorella vulgaris* for Cell Disruption (2016) Chemical Engineering Technology, 39 (9), pp. 1693-1699.

Patents

Gernat, D.C., Brouwer, E.R., Ottens, M. (2020). Non-alcoholic Fermented Beer having improved Flavour (WO2020055233-A1)

Conference contributions

Gernat, D.C., Brouwer, E.R., Ottens, M. Zeolites as selective adsorbents in multicomponent food systems (2019) 16th Netherlands Process Technology Symposium, Eindhoven, The Netherlands (oral presentation)

Khan, A., Momin, B., Gernat, D., Nieto, M., Monje, V. Optimizing Pectin production at industrial scale (2019) BIOPRO World Talent Campus 2019, Copenhagen, Denmark (oral presentation)

Gernat, D.C., Brouwer, E.R., Ottens, M. Zeolites as selective adsorbents in multicomponent food systems – A case study for aroma profile optimization in alcohol-free beer (2019) 13th International Conference on Fundamentals of Adsorption, Cairns, Australia (poster presentation)

Gernat, D.C., Brouwer, E.R., Ottens, M. Off-flavor reduction in multicomponent aqueous food streams with zeolites: Selective Strecker aldehyde removal from alcohol-free beer (2019) 15th International PhD Seminar on Chromatographic Separation Science, Quedlinburg, Germany (oral presentation)

Gernat, D.C., Swinkels, F., Penning, M., Brouwer, E.R., Ottens, M., Optimization of Aroma Profiles through Selective Removal of Off-Flavors: An Exemplary Study in Alcohol-Free Beers (2018) 18th Annual Meeting of the American Institute of Chemical Engineers, Pittsburgh, United States (oral presentation)

Gernat, D.C., Swinkels, F., Penning, M., Brouwer, E.R., Ottens, M., Selective off-flavour reduction:

A case study in malt-based, alcohol-free beverages (2018) 12th European Symposium on Biochemical Engineering Science, Lisbon, Portugal (oral presentation)

Gernat, D.C., Brouwer, E.R., Ottens, M. Aroma optimisation of alcohol-free beverages (2018) 15th International PhD Seminar on Chromatographic Separation Science, Burghausen, Germany (oral presentation)

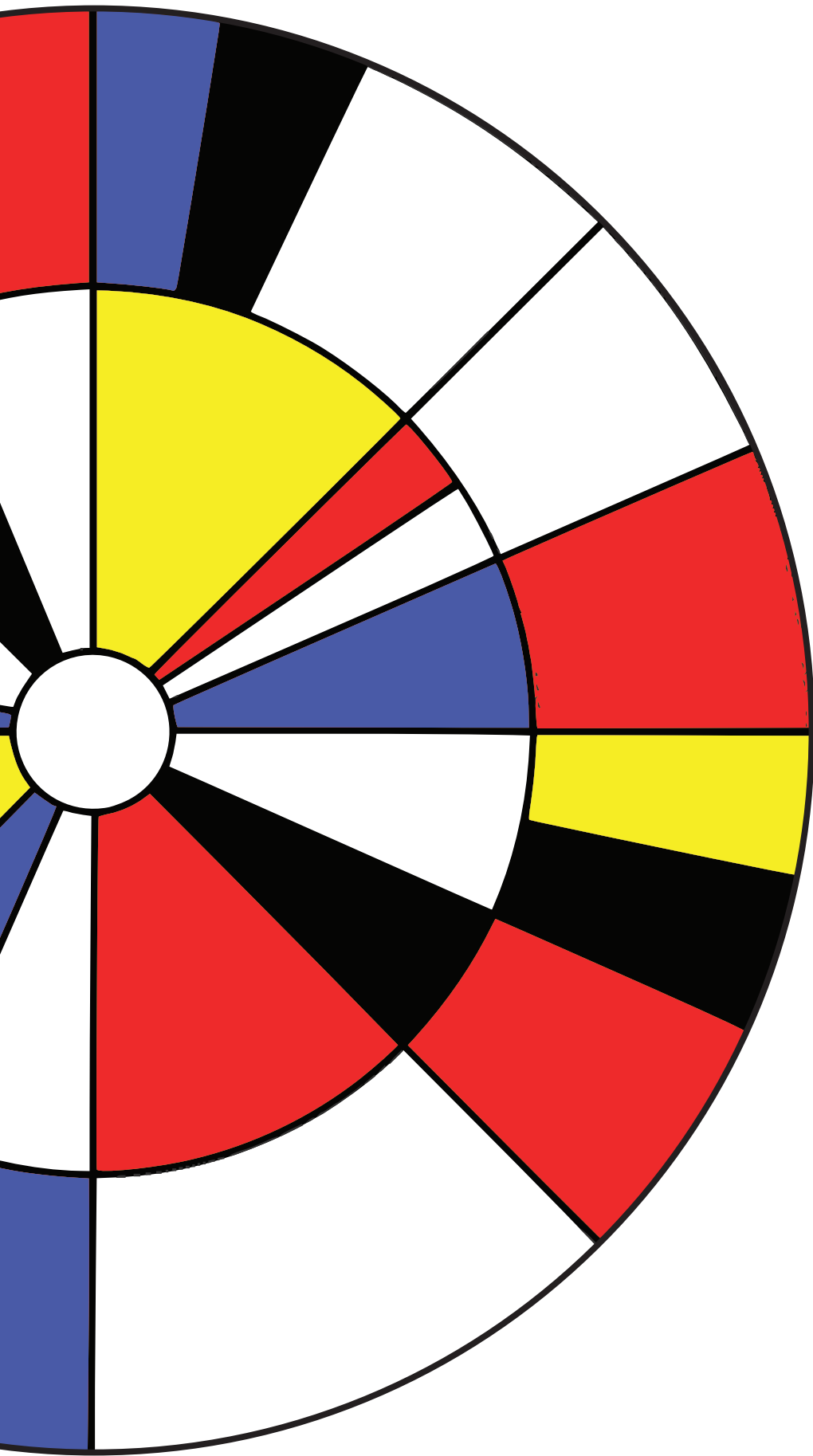
Gernat, D.C., Swinkels, F., Brouwer, E.R., Ottens, M., Selective off-flavour removal for aroma optimisation of malt-based, alcohol-free beverages (2017) 10th World Congress of Chemical Engineering, Barcelona, Spain (poster presentation)

Gernat, D.C., Brouwer, E.R., Ottens, M. Aroma optimization in low caloric, alcohol-free beverages (2017) 253rd American Chemical Society National Meeting, San Francisco, United States (poster presentation)

Curriculum Vitae

Deborah C. Gernat was born on the 18th February 1989 in Berlin, Germany. Early on, she discovered her fascination for science and engineering. After receiving the Abitur at the Hans-Carossa-Gymnasium in Berlin-Spandau in 2007, she began her studies of Biotechnology at the Technical University of Braunschweig. During her Bachelor, she worked as a research assistant at the Fraunhofer Institute for Surface Engineering and Thin Films and found a particular interest in process engineering. Her Bachelor thesis investigated the productivity and morphology of *A. niger* at different growth conditions. She was then selected for a scholarship to study at the University of Waterloo, Canada, during the first year of her Masters in Biotechnology. On her return, while working at the Institute of Chemical and Thermal Process Engineering, she finalized her studies at the Technical University of Braunschweig with her thesis on the characterization of cell disruption and micromechanical properties of *C. vulgaris*. She graduated in 2012 with honours and accepted a yearlong traineeship position at the European Space Research and Technology Centre of the European Space Agency in Noordwijk, The Netherlands. Within the project “Micro-ecological Life Support System Alternative” (MELiSSA), she designed and set-up a test facility for higher plant characterization and modelling of this compartment. To further deepen her knowledge and skills in process engineering, she joined the post-graduate programme Professional Doctorate in Engineering at the Delft University of Technology in 2014. Within this programme, she became a trainee in the Product Development team at the Global Innovation and Research Department at Heineken, where she developed and optimized a conceptual process design for the production of malt-based beverages with focus on flavour separation and flavour profile tuning. In 2016, she became a PhD candidate at the Bioprocess Engineering group at TU Delft under the supervision of Prof. Marcel Ottens, Dr Eric Brouwer and Prof. Luuk van der Wielen to continue her collaboration with Heineken to develop a novel downstream technology to tailor the flavour profile of alcohol-free beer, with particular focus on wort flavour reduction. From August 2020, she joined the Global Innovation & Research department of Heineken as a scientist.





Appendix

Patent application



(51) International Patent Classification:

C12C 12/04 (2006.01) C12H 3/00 (2019.01)

Published:

— with international search report (Art. 21(3))

(21) International Application Number:

PCT/NL2018/050585

(22) International Filing Date:

10 September 2018 (10.09.2018)

(25) Filing Language:

English

(26) Publication Language:

English

(71) Applicant: **HEINEKEN SUPPLY CHAIN B.V.**
[NL/NL]; Burgemeester Smeetsweg 1, 2382 PH Zoeter-
woude (NL).

(72) Inventors: **GERNAT, Deborah Casandra**; Building 58,
Van der Maasweg 9, 2629 HZ Delft (NL). **BROUWER,
Eric Richard**; c/o Burgemeester Smeetsweg 1, 2382 PH
Zoeterwoude (NL). **OTTENS, Marcel**; Building 58, Van
der Maasweg 9, 2629 HZ Delft (NL).

(74) Agent: **NEDERLANDSCH OCTROOIBUREAU**; P.O.
Box 29720, 2502 LS The Hague (NL).

(81) Designated States (*unless otherwise indicated, for every
kind of national protection available*): AE, AG, AL, AM,
AO, AT, AU, AZ, BA, BB, BG, BH, BN, BR, BW, BY, BZ,
CA, CH, CL, CN, CO, CR, CU, CZ, DE, DJ, DK, DM, DO,
DZ, EC, EE, EG, ES, FI, GB, GD, GE, GH, GM, GT, HN,
HR, HU, ID, IL, IN, IR, IS, JO, JP, KE, KG, KH, KN, KP,
KR, KW, KZ, LA, LC, LK, LR, LS, LU, LY, MA, MD, ME,
MG, MK, MN, MW, MX, MY, MZ, NA, NG, NI, NO, NZ,
OM, PA, PE, PG, PH, PL, PT, QA, RO, RS, RU, RW, SA,
SC, SD, SE, SG, SK, SL, SM, ST, SV, SY, TH, TJ, TM, TN,
TR, TT, TZ, UA, UG, US, UZ, VC, VN, ZA, ZM, ZW.

(84) Designated States (*unless otherwise indicated, for every
kind of regional protection available*): ARIPO (BW, GH,
GM, KE, LR, LS, MW, MZ, NA, RW, SD, SL, ST, SZ, TZ,
UG, ZM, ZW), Eurasian (AM, AZ, BY, KG, KZ, RU, TJ,
TM), European (AL, AT, BE, BG, CH, CY, CZ, DE, DK,
EE, ES, FI, FR, GB, GR, HR, HU, IE, IS, IT, LT, LU, LV,
MC, MK, MT, NL, NO, PL, PT, RO, RS, SE, SI, SK, SM,
TR), OAPI (BF, BJ, CF, CG, CI, CM, GA, GN, GQ, GW,
KM, ML, MR, NE, SN, TD, TG).

(54) Title: NON-ALCOHOLIC FERMENTED BEER HAVING IMPROVED FLAVOUR

(57) Abstract: The invention provides a process of producing a non-alcoholic beer comprising the steps of: • fermenting the wort with live yeast to produce a fermented wort; · subjecting the fermented wort to one or more further process steps to produce a non-alcoholic beer; and • introducing the non-alcoholic beer in a sealed container; wherein either the fermentation produces a non-alcoholic fermented wort or wherein the fermentation produces an alcoholic fermented wort and alcohol is subsequently removed to produce a non-alcoholic fermented wort or a non-alcoholic beer; and wherein the heated wort, the non-alcoholic fermented wort and/or the non-alcoholic beer is contacted with a hydrophobic silicate-based molecular sieve. Flavour substances contributing to undesirable flavour notes in non-alcoholic beer can be removed effectively during production by contacting wort before or after fermentation with a hydrophobic silicate-based molecular sieve, provided the wort contains virtually no alcohol.

